

Table of Contents

2.0	SITE CHARACTERIZATION.....	2-1
2.1	Geology.....	2-11
2.1.1	Data Sources.....	2-12
2.1.2	Geologic History.....	2-14
2.1.3	Stratigraphy and Lithology in the Vicinity of the WIPP Site	2-17
2.1.3.1	General Stratigraphy and Lithology below the Bell Canyon	2-21
2.1.3.2	The Bell Canyon Formation	2-22
2.1.3.3	The Castile Formation	2-24
2.1.3.4	The Salado.....	2-28
2.1.3.5	The Rustler	2-36
2.1.3.6	The Dewey Lake Redbeds Formation.....	2-50
2.1.3.7	The Santa Rosa.....	2-53
2.1.3.8	The Gatuña Formation.....	2-53
2.1.3.9	Mescalero Caliche	2-55
2.1.3.10	Surficial Sediments.....	2-57
2.1.3.11	Summary	2-58
2.1.4	Physiography and Geomorphology.....	2-58
2.1.4.1	Regional Physiography and Geomorphology.....	2-59
2.1.4.2	Site Physiography and Geomorphology.....	2-59
2.1.5	Tectonic Setting and Site Structural Features	2-63
2.1.5.1	Tectonics	2-63
2.1.5.2	Loading and Unloading.....	2-66
2.1.5.3	Faulting.....	2-69
2.1.5.4	Igneous Activity	2-69
2.1.6	Nontectonic Processes and Features	2-71
2.1.6.1	Evaporite Deformation.....	2-71
2.1.6.2	Evaporite Dissolution.....	2-76
2.2	Surface Water and Groundwater Hydrology	2-81
2.2.1	Groundwater Hydrology	2-83
2.2.1.1	Conceptual Models of Groundwater Flow	2-89
2.2.1.2	Units Below the Salado	2-91
2.2.1.3	Hydrology of the Salado.....	2-95
2.2.1.4	Units Above the Salado.....	2-99
2.2.1.5	Hydrology of Other Groundwater Zones of Regional Importance	2-123
2.2.2	Surface-Water Hydrology	2-128
2.3	Resources	2-134
2.3.1	Extractable Resources	2-135
2.3.1.1	Potash Resources at the WIPP Site	2-135
2.3.1.2	Hydrocarbon Resources at the WIPP Site.....	2-136
2.3.1.3	Other Resources	2-140
2.3.2	Cultural and Economic Resources	2-140
2.3.2.1	Demographics.....	2-140
2.3.2.2	Land Use.....	2-143
2.3.2.3	History and Archaeology.....	2-144

1	2.4 Background Environmental Conditions.....	2-147
2	2.4.1 Terrestrial and Aquatic Ecology	2-148
3	2.4.1.1 Vegetation	2-149
4	2.4.1.2 Mammals	2-150
5	2.4.1.3 Reptiles and Amphibians.....	2-150
6	2.4.1.4 Birds	2-150
7	2.4.1.5 Arthropods.....	2-151
8	2.4.1.6 Aquatic Ecology.....	2-151
9	2.4.1.7 Endangered Species.....	2-151
10	2.4.2 Water Quality	2-152
11	2.4.2.1 Groundwater Quality.....	2-152
12	2.4.2.2 Surface Water Quality.....	2-154
13	2.4.3 Air Quality	2-154
14	2.4.4 Environmental Radioactivity	2-155
15	2.4.4.1 Atmospheric Radiation Baseline.....	2-155
16	2.4.4.2 Ambient Radiation Baseline.....	2-156
17	2.4.4.3 Terrestrial Baseline.....	2-156
18	2.4.4.4 Hydrologic Radioactivity.....	2-156
19	2.4.4.5 Biotic Baseline	2-159
20	2.5 Climate and Meteorological Conditions	2-159
21	2.5.1 Historic Climatic Conditions.....	2-160
22	2.5.2 Recent Climatic Conditions	2-162
23	2.5.2.1 General Climatic Conditions.....	2-162
24	2.5.2.2 Temperature Summary	2-163
25	2.5.2.3 Precipitation Summary	2-163
26	2.5.2.4 Wind Speed and Wind Direction Summary	2-163
27	2.6 Seismology.....	2-164
28	2.6.1 Seismic History	2-180
29	2.6.2 Seismic Risk.....	2-182
30	2.6.2.1 Acceleration Attenuation.....	2-182
31	2.6.2.2 Seismic Source Zones	2-183
32	2.6.2.3 Source Zone Recurrence Formulas and Maximum	
33	Magnitudes.....	2-183
34	2.6.2.4 Design Basis Earthquake.....	2-186
35	REFERENCES	2-188

List of Figures

37	Figure 2-1.	WIPP Site Location in Southeastern New Mexico.....	2-3
38	Figure 2-2.	WIPP Site and Vicinity Borehole Location Map (partial).....	2-15
39	Figure 2-3.	<i>Locations of Culebra Monitoring Wells Inside the WIPP Site Boundary</i> ...	2-16
40	Figure 2-4.	<i>Locations of Culebra Monitoring Wells Located Outside the WIPP Site</i>	
41		<i>Boundary</i>	2-16
42	Figure 2-5.	<i>Locations of Magenta Monitoring Wells</i>	2-17

1	Figure 2-6.	<i>Locations of Monitoring Wells Completed to Hydrostratigraphic Units</i>	
2		<i>Other Than the Culebra and Magenta Dolomite Members (See also</i>	
3		<i>Figure 2-39).</i>	2-18
4	Figure 2-37.	Major Geologic Events - Southeast New Mexico Region	2-19
5	Figure 2-8.	<i>Partial Site Geologic Column</i>	2-20
6	Figure 2-59.	Schematic Cross-Section from Delaware Basin (southeast) through	
7		Marginal Reef Rocks to Back-Reef Facies (based on King, P.B., 1948)	2-23
8	Figure 2-610.	Structure Contour Map of Top of Bell Canyon	2-25
9	Figure 2-711.	Generalized Stratigraphic Cross Section above Bell Canyon Formation at	
10		WIPP Site	2-26
11	Figure 2-812.	Salado Stratigraphy <i>in the Vicinity of the WIPP Disposal Zone</i>	2-30
12	Figure 2-13.	<i>Dissolution Margin for the Upper Salado</i>	2-34
13	Figure 2-9.	Rustler Stratigraphy (From Appendix FAC, Figure 3-2)	2-37
14	Figure 2-14.	<i>Rustler Stratigraphy</i>	2-38
15	Figure 2-10.	Halite Margins in the Rustler	2-40
16	Figure 2-15.	<i>Halite Margins for the Rustler Formation Members</i>	2-41
17	Figure 2-1116.	Isopach Map of the Entire Rustler	2-43
18	Figure 2-1217.	Percentage of Natural Fractures in the Culebra Filled with Gypsum	2-46
19	Figure 2-1318.	Log Character of the Rustler Emphasizing Mudstone-Halite Lateral	
20		Relationships.	2-49
21	Figure 2-1419.	Isopach of the Dewey Lake.	2-52
22	Figure 2-1520.	Isopach of the Santa Rosa	2-54
23	Figure 2-1621.	Isopach of the Gatuña	2-56
24	Figure 2-1722.	Physiographic Provinces and Sections.	2-60
25	Figure 2-2325.	<i>Topographic Map of the Area Around the WIPP Site</i>	2-61
26	Figure 2-18.	Topographic Map of the Area Around the WIPP Site	2-62
27	Figure 2-1924.	Structural Provinces of the Permian Basin Region.	2-64
28	Figure 2-2025.	Loading and Unloading History Estimated to the Base of the Culebra.	2-67
29	Figure 2-2126.	Regional Structures.	2-70
30	Figure 2-2227.	Igneous Dike in the Vicinity of the WIPP Site	2-72
31	Figure 2-28.	<i>Elevations of the Top of the Culebra Dolomite Member</i>	2-75
32	Figure 2-2329.	Isopach from the Base of MB 103 to the Top of the Salado.	2-79
33	Figure 2-24.	Structure Contour Map of Culebra Dolomite Base.	2-82
34	Figure 2-25.	Drainage Pattern in the Vicinity of the WIPP Facility	2-84
35	Figure 2-2630.	Schematic West-East Cross Section through the North Delaware Basin	2-86
36	Figure 2-2731.	Schematic North-South Cross Section through the North Delaware Basin.	2-87
37	Figure 2-2832.	Recent Occurrences of Pressurized Brine in the Castile.	2-94
38	Figure 2-2933.	Outline of the Groundwater Basin Model Domain on a Topographic Map	2-100
39	Figure 2-3034.	Transmissivities of the Culebra	2-106
40	Figure 2-35.	<i>Correlation Between Culebra Transmissivity ($\log T$ (m^2/s)) and</i>	
41		<i>Overburden Thickness for Different Geologic Environments (after Holt</i>	
42		<i>and Yarbrough 2002)</i>	2-108
43	Figure 2-36.	<i>Water-level Trends in Nash Draw Wells and at P-14 (see Figure 2-2 for</i>	
44		<i>well locations).</i>	2-111
45	Figure 2-31.	Hydraulic Heads in the Culebra	2-113
46	Figure 2-37.	<i>Hydraulic Heads in the Culebra</i>	2-114

1	Figure 2-32 38 .	Hydraulic Heads in the Magenta (1980s)	2-118
2	Figure 2-33.	Interpreted Water Table Surface	2-122
3	Figure 2-39.	Site Map of WIPP Surface Structures Area Showing Location of Wells	
4		(e.g., C-2505) and Piezometers (e.g., PZ-1) (after INTERA 1997)	2-124
5	Figure 2-40.	Santa Rosa Potentiometric Surface Map	2-125
6	Figure 2-34 41 .	Brine Aquifer in the Nash Draw (Redrawn from CCA Appendix	
7		HYDRO, Figure 14).....	2-127
8	Figure 2-35.	Measured Water Levels of the Unnamed Lower Member and Rustler-	
9		Salado Contact Zone	2-129
10	Figure 2-42.	Measured Water Levels of the Los Medaños and Rustler-Salado	
11		Contact Zone (1980s)	2-130
12	Figure 2-36 43 .	Location of Reservoirs and Gauging Stations in the Pecos River Drainage	
13		Area.....	2-132
14	Figure 2-37 44 .	Known Potash Leases Within the Delaware Basin.....	2-137
15	Figure 2-38 45 .	Extent of Economically Mineable Reserves Inside the Site Boundary	
16		(Based on NMBMMR Report)	2-138
17	Figure 2-39 46 .	Delaware Basin Boundary	2-141
18	Figure 2-47.	Distribution of Existing Petroleum Industry Boreholes Within Two	
19		Miles of the WIPP Site.....	2-142
20	Figure 2-40.	Hydrochemical Zones of the Culebra	2-153
21	Figure 2-41.	Monthly Precipitation for the WIPP Site from 1990 through 1994	2-165
22	Figure 2-48.	Monthly Precipitation for the WIPP Site from 1990-2002.....	2-166
23	Figure 2-42.	1991 Annual Windrose WIPP Site	2-167
24	Figure 2-43.	1992 Annual Windrose WIPP Site	2-168
25	Figure 2-44.	1993 Annual Windrose WIPP Site	2-169
26	Figure 2-45.	1994 Annual Windrose WIPP Site	2-170
27	Figure 2-49.	1995 Annual Wind Rose at 10-m (33-ft.) Height at WIPP Site.....	2-171
28	Figure 2-50.	1996 Annual Wind Rose at 10-m (33-ft.) Height at WIPP Site.....	2-172
29	Figure 2-51.	1997 Annual Wind Rose at 10-m (33-ft.) Height at WIPP Site.....	2-173
30	Figure 2-52.	1998 Annual Wind Rose at 10-m (33-ft.) Height at WIPP Site.....	2-174
31	Figure 2-53.	1999 Annual Wind Rose at 10-m (33-ft.) Height at WIPP Site.....	2-175
32	Figure 2-54.	2000 Annual Wind Rose at 10-m (33-ft.) Height at WIPP Site.....	2-176
33	Figure 2-55.	2001 Annual Wind Rose at 10-m (33-ft.) Height at WIPP Site.....	2-177
34	Figure 2-56.	2002 Annual Wind Rose at 10-m (33-ft.) Height at WIPP Site.....	2-178
35	Figure 2-46.	1994 Annual Wind Rose Carlsbad, NM	2-179
36	Figure 2-47 57 .	Regional Earthquake Epicenters Occurring between 1961 and 2002.....	2-181
37	Figure 2-48 58 .	Seismic Source Zones	2-184
38	Figure 2-49 59 .	Alternate Source Geometries	2-185
39	Figure 2-50 60 .	Total WIPP Facility Risk Curve Extrema.....	2-187

List of Tables

41	Table 2-1.	Issues Related to the Natural Environment That Were Evaluated for the	
42		WIPP Performance Assessment Scenario Screening	2-4
43	Table 2-1.	Issues Related to the Natural Environment That Were Evaluated for	
44		the WIPP PA Scenario Screening	2-7

1	Table 2-2.	Chemical Formulas, Distributions, and Relative Abundances of Minerals	
2		in the Castile, Salado, and Rustler Formations	2-31
3	Table 2-3.	Culebra Thickness Data Sets	2-47
4	Table 2-4.	Hydrologic Characteristics of the Rustler at the WIPP and in Nash Draw	2-88
5	Table 2-5.	<i>Depth Intervals of the Injection Zones of Six Salt-Water Injection Wells</i>	
6		<i>Located Near Well H-9 (after SNL 2003a)</i>	2-93
7	Table 2-56.	WIPP Salado and Castile Brine Compositions	2-96
8	Table 2-7.	<i>Estimates of Culebra Transmissivity Model Coefficients</i>	2-108
9	Table 2-8.	<i>Ninety-Five Percent Confidence Intervals for Culebra Water-Quality</i>	
10		<i>Baseline</i>	2-110
11	Table 2-9.	<i>Ninety-Five Percent Confidence Intervals for Dewey Lake Water-</i>	
12		<i>Quality Baseline</i>	2-120
13	Table 2-6 10.	Capacities of Reservoirs in the Pecos River Drainage.....	2-133
14	Table 2-7 11.	Current Estimates of Potash Resources at the WIPP Site.....	2-136
15	Table 2-8 12.	In-Place Oil within Study Area.....	2-139
16	Table 2-9 13.	In-Place Gas within Study Area.....	2-139
17	Table 2-10.	Ranges of Mean Values Measured for Radioactive Isotopes In Soils at	
18		WIPP Site, 5 Miles from WIPP, and beyond 5 Miles from WIPP	2-157
19	Table 2-11.	Mean Values Measured for Radionuclides in Water Wells around the	
20		WIPP Site.....	2-159
21	Table 2-12.	Annual Average, Maximum, and Minimum Temperatures.....	2-163
22	Table 2-14.	<i>Annual Average, Maximum, and Minimum Temperatures</i>	2-164
23			

This page intentionally left blank

2.0 SITE CHARACTERIZATION

The U.S. Department of Energy (DOE) uses the performance assessment (*PA*) methodology described in ~~Section 6.4~~ *Chapter 6.0* to demonstrate that the Waste Isolation Pilot Plant (WIPP) disposal system will meet the environmental performance standards of Title 40 of the Code of Federal Regulations (CFR) Part 191 Subparts B and C. In order to effectively use *PA*, three inputs are necessary: What can happen to the disposal system? What are the chances of it happening? What are the consequences if it happens? The answers to these questions are derived from many sources, including field studies, laboratory evaluations, experiments, and, in the case of some features not amenable to direct characterization, professional judgment. The information used in *PA* is described in terms of features of the disposal system that can be used to describe its isolation capability, events that can affect the disposal system, and processes that are reasonably expected to act on the disposal system.

The DOE selected the Los Medaños region and present site for the WIPP based on certain defined siting criteria. The site selection process, which was focused on sites that contained certain favorable features while other unfavorable features were excluded, was applied by the DOE with the intent of finding the area that best met the siting criteria. The siting process is discussed in this application in *CCA* Appendix GCR. ~~See Table 1-2 in Chapter 1.0 for a list of appendices that~~ *Chapters 3.0, 4.0, and 6.0 and several appendices* provide additional information supporting this chapter.

Conceptual models of the WIPP disposal system simulate the interaction between the natural environment (described in this chapter), the engineered structures (described in Chapter 3.0) and the waste (described in Chapter 4.0). One starting point in developing conceptual models of the WIPP disposal system is an understanding of the natural characteristics of the site and of the region around the site. Site characterization and model development is an interactive process that the DOE has used for many years. Basic site information leads to initial models. Initial model sensitivity studies indicate the need for more detailed information. More site characterization then leads to improved models. In addition, an assessment of the impacts of uncertainty inherent in the parameters used to numerically simulate geological features and processes has also led the DOE to conduct more in-depth investigations of the natural system. These investigations generally proceeded until uncertainty was sufficiently reduced or to the point where no further information could be reasonably obtained.

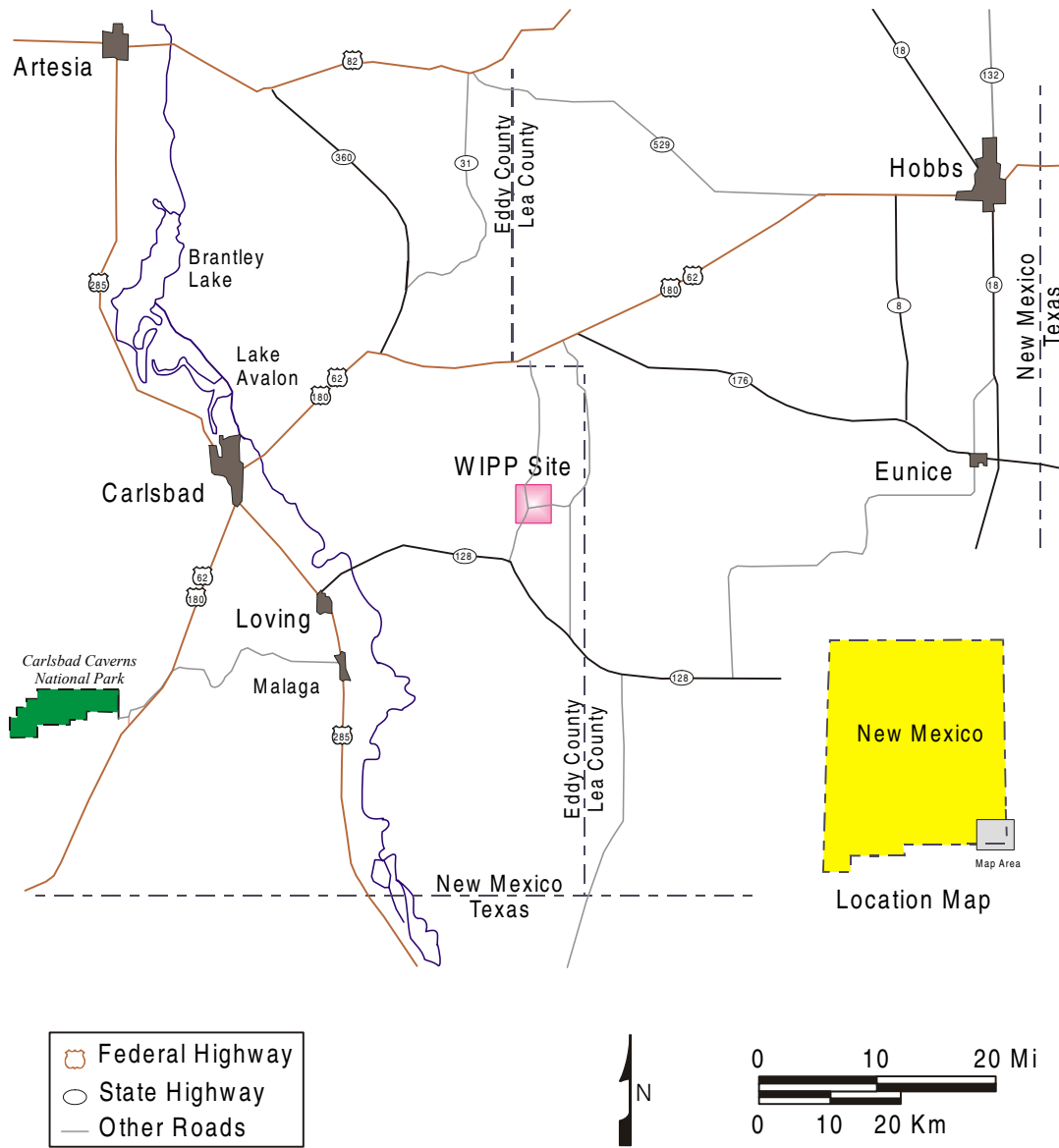
The discussion of conceptual models and initial and boundary conditions is in Section 6.4 and Appendix *PA, Attachment MASS* (~~Sections MASS.2 and MASS.4 through MASS.18~~). Conceptual models implement scenarios about the future. Scenario development is discussed in Section 6.3. Scenario development requires as inputs information about the natural features, events, and processes (FEPs) that can reasonably be expected to act on the disposal system. While the list of possible FEPs is derived independently of the disposal system, their screening (in Section 6.2 ~~Appendix SCR~~ and *Appendix PA, Attachment SCR*) is based on a ~~basic~~ *an* understanding of the geology, hydrology, and climatology of the region and the site in particular. The screening methodology follows U.S. Environmental Protection Agency (EPA) criteria on the Scope of Performance Assessments (40 CFR § 191.32). This basic understanding is provided in this chapter and its associated appendices.

Table 2-1 shows the tie between the list of natural FEPs that were identified and screened for the WIPP and the sections of this chapter or Appendix *PA, Attachment SCR*. Those FEPs that have been retained for inclusion in the modeling are shown in bold in Table 2-1. These generally receive a greater level of detail in the following discussions and are supported by additional discussion in Chapter 6.0, Appendix *PA, Attachments MASS and SCR*, and Appendix *MASS*. In addition, parameter values that have been derived for these FEPs are included in Appendix *PAR*. ~~Appendix PA, Attachment PAR.~~

In this chapter, the DOE describes the WIPP site geology, hydrology, climatology, air quality, ecology, and cultural and natural resources. This chapter's purpose is to (1) explain characteristics of the site, (2) describe background environmental quality, and (3) discuss features of the site that might be important for inclusion in a quantitative *PA*. The DOE has used this information to develop and screen FEPs and to develop conceptual, mathematical, and computational models to evaluate the efficacy of natural and engineered barriers in meeting environmental performance standards (Chapter 6.0). Results of these predictive models are used by the DOE to demonstrate that the DOE has a reasonable expectation that compliance with applicable regulations will be achieved. This chapter has been prepared to describe the site prior to excavating the repository. Excavation of the repository and its associated effects, such as the disturbed rock zone (DRZ), are discussed in Chapter 3.0.

The DOE located the WIPP site 42 km (26 mi) east of Carlsbad, New Mexico, in Eddy County (Figure 2-1). Additional details related to the location of the WIPP site can be found in Section 2.1.4.2 and in Figure 3-1 (see Chapter 3.0). The latitude of the WIPP site center is 32°22' 11" N and the longitude is 103°47' 30" W. The region surrounding the WIPP site has been studied for many years, and exploration of both potash and hydrocarbon deposits has provided extensive knowledge of the geology of the region. Two exploratory holes were drilled by the federal government in 1974 at a location northeast of the present site; that location was abandoned in 1975 as a possible repository site after U.S. Energy Research and Development Administration (ERDA)-6 borehole was drilled and unacceptable structure and pressurized brine were encountered. The results of these investigations are reported in Powers et al. (1978, 2 – 6; included in this document as *CCA* Appendix GCR). During late 1975 and early 1976, the ERDA identified the current site, and an initial exploratory hole (ERDA-9) was drilled. By the time an initial phase of site characterization was completed in August 1978, 47 holes had been or were being drilled for various hydrologic and geologic purposes. Geophysical techniques were applied to augment data collected from boreholes. Since 1978, the DOE has drilled additional holes to support hydrologic studies, geologic studies, and facility design. Geophysical logs, cores, basic data reports, geochemical sampling and testing, and hydrological testing and analyses are reported by the DOE and its scientific advisor, Sandia National Laboratories (SNL), in numerous public documents. Many of those documents form the basis for the DOE's positions in this application. As necessary, specific references from these documents are cited to reinforce statements being made.

Biological studies of the site began in 1975 to gather information for the Environmental Impact Statement (*DOE 1980*). Meteorological studies began in 1976, and economic studies were initiated in 1977. Baseline environmental data were initially reported in 1977 and are now updated annually by the DOE.



CCA-021-2

Figure 2-1. WIPP Site Location in Southeastern New Mexico

Table 2-1. Issues Related to the Natural Environment That Were Evaluated for the WIPP Performance Assessment Scenario Screening

Features, Events, and Processes (FEPs) —	Discussion
NATURAL FEPs	
— Stratigraphy	
— Stratigraphy	Section 2.1.3
— Brine reservoirs	Section 2.2.1.2.2
— Tectonics	
— Changes in regional stress	Section 2.1.5.1
— Regional tectonics	Section 2.1.5.1
— Regional uplift and subsidence	Section 2.1.5.1
— Structural FEPs	
— Deformation	
— Salt deformation	Section 2.1.6.1
— Diapirism	Appendix SCR, Section SCR.1.1.3.1
— Fracture development	
— Formation of fractures	Section 2.1.5
— Changes in fracture properties	Section 2.1.5
— Fault movement	
— Formation of new faults	Section 2.1.5
— Fault movement	Section 2.1.5.4
— Seismic activity	
— Seismic activity	Section 2.6
Crustal processes	
— Igneous activity	
— Volcanic activity	Section 2.1.5.4
— Magmatic activity	Appendix SCR, Section SCR.1.1.4.1.2
— Metamorphic activity	
— Metamorphism	Appendix SCR, Section SCR.1.1.4.2
Geochemical FEPs	
— Dissolution	
— Shallow dissolution	Section 2.1.6.2
— Lateral dissolution	Section 2.1.6.2
— Deep dissolution	Section 2.1.6.2
— Solution chimneys	Section 2.1.6.2
— Breccia pipes	Section 2.1.6.2
— Collapse breccias	Section 2.1.6.2
— Mineralization	
— Fracture infills	Section 2.1.3.5.2
SUBSURFACE HYDROLOGICAL FEPs	
— Groundwater characteristics	
— Saturated groundwater flow	Section 2.2.1

Table 2-1. Issues Related to the Natural Environment That Were Evaluated for the WIPP Performance Assessment Scenario Screening (Continued)

Features, Events, and Processes (FEPs)	Discussion
— Unsaturated groundwater flow	Section 2.2.1
— Fracture flow	Section 2.2.1
— Density effects on groundwater flow	Section 2.2.1
— Effects of preferential pathways	Section 2.2.1
— Changes in groundwater flow	
— Thermal effects on groundwater flow	Appendix SCR, Section SCR.1.2.2.3
— Saline water intrusion	Appendix SCR, Section SCR.1.2.2.1
— Freshwater intrusion	Appendix SCR, Section SCR.1.2.2.2
— Hydrological effects of seismic activity	Appendix SCR, Section SCR.1.2.2.5
— Natural gas intrusion	Appendix SCR, Section SCR.1.2.2.4
SUBSURFACE GEOCHEMICAL FEPs	
— Groundwater geochemistry	Section 2.4.2.1
— Groundwater geochemistry	
— Changes in groundwater geochemistry	
— Saline water intrusion	Appendix SCR, Section SCR.1.2.2.1
— Freshwater intrusion	Appendix SCR, Section SCR.1.2.2.2
— Changes in groundwater Eh	Appendix SCR, Section SCR.1.3.2
— Changes in groundwater pH	Appendix SCR, Section SCR.1.3.2
— Effects of dissolution	Appendix SCR, Section SCR.1.3.2
GEOMORPHOLOGICAL FEPs	
— Physiography	
— Physiography	Section 2.1.4
— Meteorite impact	
— Impact of a large meteorite	Appendix SCR, Section SCR.1.4.2
— Denudation	
— Weathering	
— Mechanical weathering	Appendix SCR, Section SCR.1.4.3.1
— Chemical weathering	Appendix SCR, Section SCR.1.4.3.1
— Erosion	
— Eolian erosion	Section 2.1.3.10
— Fluvial erosion	Section 2.2.2

Table 2-1. Issues Related to the Natural Environment That Were Evaluated for the WIPP Performance Assessment Scenario Screening (Continued)

Features, Events, and Processes (FEPs)	Discussion
— Mass wasting	Appendix SCR, Section SCR.1.4.3.2
— Sedimentation	
— Eolian deposition	Appendix SCR, Section SCR.1.4.3.3
— Fluvial deposition	Appendix SCR, Section SCR.1.4.3.3
— Lacustrine deposition	Appendix SCR, Section SCR.1.4.3.3
— Mass wasting	Appendix SCR, Section SCR.1.4.3.3
— Soil development	
— Soil development	Section 2.1.3.10
SURFACE HYDROLOGICAL FEPs	
— Fluvial	
— Stream and river flow	Section 2.2.2
— Lacustrine	
— Surface water bodies	Section 2.2.2
— Groundwater recharge and discharge	
— Groundwater discharge	Section 2.2.1
— Groundwater recharge	Section 2.2.1
— Infiltration	Section 2.1.4.2
— Changes in surface hydrology	
— Changes in groundwater recharge and discharge	Section 2.2.1
— Lake formation	Section 2.2.2
— River flooding	Section 2.2.2
CLIMATIC FEPs	
— Climate	
— Precipitation (for example, rainfall)	Section 2.5.2.3
— Temperature	Section 2.5.2.2
— Climate change	
— Meteorological	
— Climate change	Section 2.5.1
— Glaciation	
— Glaciation	Section 2.5.1
— Permafrost	Appendix SCR, Section SCR.1.6.2.2
MARINE FEPs	
— Seas	
— Seas and oceans	Appendix SCR, Section SCR.1.7.1

Table 2-1. Issues Related to the Natural Environment That Were Evaluated for the WIPP Performance Assessment Scenario Screening (Continued)

Features, Events, and Processes (FEPs)	Discussion
— Estuaries	Appendix SCR, Section SCR.1.7.1
— Marine sedimentology	
— Coastal erosion	Appendix SCR, Section SCR.1.7.2
— Marine sediment transport and deposition	Appendix SCR, Section SCR.1.7.2
— Sea level changes	
— Sea level changes	Appendix SCR, Section SCR.1.7.3
ECOLOGICAL FEPs	
— Flora & fauna	
— Plants	Section 2.4.1
— Animals	Section 2.4.1
— Microbes	Appendix SCR, Section SCR.1.8.1
— Changes in flora & fauna	
— Natural ecological development	Section 2.4.1

1

Table 2-1. Issues Related to the Natural Environment That Were Evaluated for the WIPP PA Scenario Screening

Features, Events, and Processes (FEPs)	EPA FEP No.	Discussion
NATURAL FEPs		
<i>Stratigraphy</i>		
<i>Stratigraphy</i>	<i>N1</i>	<i>Section 2.1.3</i>
<i>Brine reservoirs</i>	<i>N2</i>	<i>Section 2.2.1.2.2</i>
<i>Tectonics</i>		
<i>Changes in regional stress</i>	<i>N3</i>	<i>Section 2.1.5.1</i>
<i>Regional tectonics</i>	<i>N4</i>	<i>Section 2.1.5.1</i>
<i>Regional uplift and subsidence</i>	<i>N5</i>	<i>Section 2.1.5.1</i>
<i>Structural FEPs</i>		
<i>Deformation</i>		
<i>Salt deformation</i>	<i>N6</i>	<i>Section 2.1.6.1</i>
<i>Diapirism</i>	<i>N7</i>	<i>Appendix PA, Attachment SCR</i>
<i>Fracture development</i>		
<i>Formation of fractures</i>	<i>N8</i>	<i>Section 2.1.5</i>
<i>Changes in fracture properties</i>	<i>N9</i>	<i>Section 2.1.5</i>
<i>Fault movement</i>		
<i>Formation of new faults</i>	<i>N10</i>	<i>Section 2.1.5</i>
<i>Fault movement</i>	<i>N11</i>	<i>Section 2.1.5.3</i>
<i>Seismic activity</i>		
<i>Seismic activity</i>	<i>N12</i>	<i>Section 2.6</i>
<i>Crustal processes</i>		
<i>Igneous activity</i>		

2

Table 2-1. Issues Related to the Natural Environment That Were Evaluated for the WIPP PA Scenario Screening — Continued

<i>Features, Events, and Processes (FEPs)</i>	<i>EPA FEP No.</i>	<i>Discussion</i>
<i>Volcanic activity</i>	<i>N13</i>	<i>Section 2.1.5.4</i>
<i>Magmatic activity</i>	<i>N14</i>	<i>Appendix PA, Attachment SCR</i>
<i>Metamorphic activity</i>		
<i>Metamorphism</i>	<i>N15</i>	<i>Appendix PA, Attachment SCR</i>
<i>Geochemical FEPs</i>		
<i>Dissolution</i>		
<i>Shallow dissolution</i>	<i>N16</i>	<i>Section 2.1.6.2</i>
<i>Lateral dissolution</i>	<i>N17</i>	<i>Section 2.1.6.2</i>
<i>Deep dissolution</i>	<i>N18</i>	<i>Section 2.1.6.2</i>
<i>Solution chimneys</i>	<i>N19</i>	<i>Section 2.1.6.2</i>
<i>Breccia pipes</i>	<i>N20</i>	<i>Section 2.1.6.2</i>
<i>Collapse breccias</i>	<i>N21</i>	<i>Section 2.1.6.2</i>
<i>Mineralization</i>		
<i>Fracture infills</i>	<i>N22</i>	<i>Section 2.1.3.5.2</i>
<i>SUBSURFACE HYDROLOGICAL FEPs</i>		
<i>Groundwater characteristics</i>		
<i>Saturated groundwater flow</i>	<i>N23</i>	<i>Section 2.2.1</i>
<i>Unsaturated groundwater flow</i>	<i>N24</i>	<i>Section 2.2.1</i>
<i>Fracture flow</i>	<i>N25</i>	<i>Section 2.2.1</i>
<i>Density effects on groundwater flow</i>	<i>N26</i>	<i>Section 2.2.1</i>
<i>Effects of preferential pathways</i>	<i>N27</i>	<i>Section 2.2.1</i>
<i>Changes in groundwater flow</i>		
<i>Thermal effects on groundwater flow</i>	<i>N28</i>	<i>Appendix PA, Attachment SCR</i>
<i>Saline water intrusion</i>	<i>N29</i>	<i>Appendix PA, Attachment SCR</i>
<i>Freshwater intrusion</i>	<i>N30</i>	<i>Appendix PA, Attachment SCR</i>
<i>Hydrological effects of seismic activity</i>	<i>N31</i>	<i>Appendix PA, Attachment SCR</i>
<i>Natural gas intrusion</i>	<i>N32</i>	<i>Appendix PA, Attachment SCR</i>
<i>SUBSURFACE GEOCHEMICAL FEPs</i>		
<i>Groundwater geochemistry</i>		
<i>Groundwater geochemistry</i>	<i>N33</i>	<i>Section 2.2.1.4.1.2</i>
<i>Changes in groundwater geochemistry</i>		
<i>Saline water intrusion</i>	<i>N34</i>	<i>Appendix PA, Attachment SCR</i>
<i>Freshwater intrusion</i>	<i>N35</i>	<i>Appendix PA, Attachment SCR</i>
<i>Changes in groundwater Eh</i>	<i>N36</i>	<i>Appendix PA, Attachment SCR</i>
<i>Changes in groundwater pH</i>	<i>N37</i>	<i>Appendix PA, Attachment SCR</i>

Table 2-1. Issues Related to the Natural Environment That Were Evaluated for the WIPP PA Scenario Screening — Continued

<i>Features, Events, and Processes (FEPs)</i>	<i>EPA FEP No.</i>	<i>Discussion</i>
<i>Effects of dissolution</i>	<i>N38</i>	<i>Appendix PA, Attachment SCR</i>
GEOMORPHOLOGICAL FEPs		
<i>Physiography</i>		
<i>Physiography</i>	<i>N39</i>	<i>Section 2.1.4</i>
<i>Meteorite impact</i>		
<i>Impact of a large meteorite</i>	<i>N40</i>	<i>Appendix PA, Attachment SCR</i>
Denudation		
<i>Weathering</i>		
<i>Mechanical weathering</i>	<i>N41</i>	<i>Appendix PA, Attachment SCR</i>
<i>Chemical weathering</i>	<i>N42</i>	<i>Appendix PA, Attachment SCR</i>
<i>Erosion</i>		
<i>Eolian erosion</i>	<i>N43</i>	<i>Section 2.1.3.10</i>
<i>Fluvial erosion</i>	<i>N44</i>	<i>Section 2.1.3.6</i>
<i>Mass wasting</i>	<i>N45</i>	<i>Appendix PA, Attachment SCR</i>
<i>Sedimentation</i>		
<i>Eolian deposition</i>	<i>N46</i>	<i>Appendix PA, Attachment SCR</i>
<i>Fluvial deposition</i>	<i>N47</i>	<i>Appendix PA, Attachment SCR</i>
<i>Lacustrine deposition</i>	<i>N48</i>	<i>Appendix PA, Attachment SCR</i>
<i>Mass wasting (deposition)</i>	<i>N49</i>	<i>Appendix PA, Attachment SCR</i>
<i>Soil development</i>		
<i>Soil development</i>	<i>N50</i>	<i>Section 2.1.3.10</i>
SURFACE HYDROLOGICAL FEPs		
<i>Fluvial</i>		
<i>Stream and river flow</i>	<i>N51</i>	<i>Section 2.2.2</i>
<i>Lacustrine</i>		
<i>Surface water bodies</i>	<i>N52</i>	<i>Section 2.2.2</i>
<i>Groundwater recharge and discharge</i>		
<i>Groundwater discharge</i>	<i>N53</i>	<i>Section 2.2.1</i>
<i>Groundwater recharge</i>	<i>N54</i>	<i>Section 2.2.1</i>
<i>Infiltration</i>	<i>N55</i>	<i>Section 2.1.3 Section 2.2.1</i>
<i>Changes in surface hydrology</i>		
<i>Changes in groundwater recharge and discharge</i>	<i>N56</i>	<i>Section 2.2.1</i>
<i>Lake formation</i>	<i>N57</i>	<i>Section 2.2.2</i>
<i>River flooding</i>	<i>N58</i>	<i>Section 2.2.2</i>

Table 2-1. Issues Related to the Natural Environment That Were Evaluated for the WIPP PA Scenario Screening — Continued

<i>Features, Events, and Processes (FEPs)</i>	<i>EPA FEP No.</i>	<i>Discussion</i>
CLIMATIC FEPs		
<i>Climate</i>		
<i>Precipitation (for example, rainfall)</i>	<i>N59</i>	<i>Section 2.5.2.3</i>
<i>Temperature</i>	<i>N60</i>	<i>Section 2.5.2.2</i>
<i>Climate change</i>		
<i>Meteorological</i>		
<i>Climate change</i>	<i>N61</i>	<i>Section 2.5</i>
<i>Glaciation</i>		
<i>Glaciation</i>	<i>N62</i>	<i>Section 2.5.1</i>
<i>Permafrost</i>	<i>N63</i>	<i>Appendix PA, Attachment SCR</i>
MARINE FEPs		
<i>Seas</i>		
<i>Seas and oceans</i>	<i>N64</i>	<i>Appendix PA, Attachment SCR</i>
<i>Estuaries</i>	<i>N65</i>	<i>Appendix PA, Attachment SCR</i>
<i>Marine sedimentology</i>		
<i>Coastal erosion</i>	<i>N66</i>	<i>Appendix PA, Attachment SCR</i>
<i>Marine sediment transport and deposition</i>	<i>N67</i>	<i>Appendix PA, Attachment SCR</i>
<i>Sea level changes</i>		
<i>Sea level changes</i>	<i>N68</i>	<i>Appendix PA, Attachment SCR</i>
ECOLOGICAL FEPs		
<i>Flora and fauna</i>		
<i>Plants</i>	<i>N69</i>	<i>Section 2.4.1</i>
<i>Animals</i>	<i>N70</i>	<i>Section 2.4.1</i>
<i>Microbes</i>	<i>N71</i>	<i>Appendix PA, Attachment SCR</i>
<i>Changes in flora and fauna</i>		
<i>Natural ecological development</i>	<i>N72</i>	<i>Section 2.4.1</i>

**NOTE: Additional information for FEPs N1-N72 is located in Appendix PA, Attachment SCR.*

The DOE located the WIPP disposal horizon within a rock salt deposit known as the Salado Formation (hereafter referred to as the Salado) at a depth of 650 m (2,150 ft) below the ground surface. The Salado is regionally extensive, includes continuous beds of salt without complicated structure, is deep with little potential for dissolution in the immediate vicinity of the WIPP, and is near enough to the surface to make access reasonable. Particular site selection criteria narrowed the choices when the present site was located during 1975 and 1976, as is discussed in [CCA](#) Appendix GCR (2-10 to 2-27) and summarized by Weart (1983).

2.1 Geology

The DOE and its predecessor agencies determined at the outset of the geological disposal program that the geological characteristics of the disposal system are extremely important because the natural barriers provided by the geological units have a significant impact on the performance of the disposal system. Among the DOE's site selection criteria was the intent to maximize the beneficial impacts of the geology. This was accomplished when the DOE selected (1) a host formation that behaves plastically, thereby creeping closed to encapsulate buried waste, (2) a location where the effects of dissolution are minimal and predictable, (3) an area where deformation of the rocks is low, (4) an area where excavation is relatively easy, (5) an area where future resource development is predictable and minimal, and (6) a repository host rock that is relatively uncomplicated lithologically and structurally. Therefore, a thorough and accurate description of the WIPP facility's natural environmental setting is considered crucial by the DOE for a demonstration of compliance with the disposal standards and is an EPA certification ~~criteria~~ **criterion** in 40 CFR § 191.14(a). The DOE is providing the detail necessary to assess the achievable degree of waste isolation. In this chapter, the DOE addresses environmental factors and long-term environmental changes that are important for assessing the waste isolation potential of the disposal system. The first of these environmental factors is geology.

Geological data have been collected from the WIPP site and surrounding area to evaluate the site's suitability as a radioactive waste repository. These data have been collected principally by the DOE, the DOE's predecessor agencies, the United States Geological Survey (USGS), the New Mexico Bureau of Mines and Mineral Resources (NMBMMR), and private organizations engaged in natural resource exploration and extraction. The DOE has analyzed the data and has determined that the data support the DOE's position that the WIPP site is suitable for the long-term isolation of radioactive waste.

Many issues have been discussed, investigated, and resolved in order for the DOE to conclude that the site is suitable. The DOE discusses these issues in the following sections. Most of the data collected have been reported or summarized in **CCA** Appendices GCR, SUM, HYDRO, and FAC. These appendices represent the majority of the site characterization results for the WIPP site which ended in 1988. A number of more focused geological and hydrological studies continued after this date. These latter studies, ~~many of which were only recently concluded,~~ provided detailed information needed to construct the conceptual models for disposal system performance that are discussed in Section 6.4. An example of these studies is the H-19 multiwell tracer test that was completed in early 1996. Results of this test ~~were have been~~ incorporated into the discussions in this chapter and into the conceptual models described in Section 6.4.6. Model parameters derived from the ~~results~~ **data** are displayed in Appendix ~~PAR~~ **PA, Attachment PAR**. A discussion of the ~~test results~~ **data** is included in **CCA** Appendix MASS; (~~Section MASS.15~~) and **Appendix PA, Attachment MASS**.

Geological field studies designed to collect data pertinent to the WIPP PA continue. The Culebra Dolomite Member and Magenta Dolomite Members are the two carbonates in the Rustler Formation, the youngest evaporite-bearing formation in the Delaware Basin. Geologic data related to the Culebra and Magenta remain of particular interest, as these members are the most significant transmissive units at the WIPP site.

The EPA's December 19, 1996 letter (A-93-02, Docket II-I-01) made a request to the DOE for recent studies that had provided detailed information used in developing conceptual models for disposal system performance. In a response letter to EPA dated February 26, 1997 (Docket A-93-02, Item II-I-10), the DOE cited Holt (1997) for detailed information on the recent enhancement of the conceptual model for transport in the Culebra. Holt (1997) discusses interpretation and conceptual insights obtained from field and laboratory tracer tests and core studies that support the double-porosity conceptual model of the Culebra, in which Culebra porosity is divided into advective and diffusive components.

Geological data provide the basis for a different approach to estimating the transmissivity field for modeling fluid flow and transport in the Culebra (Beauheim 2002). Geological data correlate strongly with Culebra transmissivity (Holt and Yarbrough 2002), and they are available from many more locations, such as industry (oil, gas, potash) drillholes, than are transmissivity data. With this correlation, Culebra properties can be inferred over a wide area, leading to an improved computational model of the spatial distribution of Culebra transmissivity. Initial results from this computational model of the spatial distribution of Culebra transmissivity have been incorporated in the PA; they are discussed in more detail in Section 2.2.1.4.1.2, and are incorporated in Appendix PA, Attachment TFIELD. Additional data in support of this modeling are being collected through field activities, including drilling and testing of new wells, to improve understanding of the Culebra and to assess the causes(s) of rising water levels (see Section 2.2.1.4.1.2).

2.1.1 Data Sources

The geology of southeastern New Mexico has been of great interest for more than a century. The Guadalupe Mountains have become a common visiting and research point for geologists because of the spectacular exposures of Permian-age reef rocks and related facies (see Shumard 1858, Crandall 1929, Newell et al. 1953, and Dunham 1972 in the [CCA](#) bibliography). Because of intense interest in both hydrocarbon and potash resources in the region, a large volume of data exists as background information for the WIPP site, though some data are proprietary. Finally, there is the geological information developed directly and indirectly by studies sponsored by the DOE for the WIPP project; it ranges from raw data to interpretive reports.

Elements of the geology of southeastern New Mexico have been discussed or described in professional journals or technical documents from many different sources. These types of articles are an important source of information, and where there is consistency among the technical community, the information in these articles is referenced when subject material is relevant. Implicit rules of professional conduct for research and reporting have been assumed, as have journal and editorial review. Elements of the geology presented in such sources have been deemed critical to the WIPP and have been the subject of specific DOE-sponsored WIPP studies.

The geological data that the DOE has developed explicitly for the WIPP project have been produced over a 25-year period by different organizations and contractors using applicable national standards (Quality Assurance Program history is described in Section 5.1.2). During a rulemaking in 1988 related to the underground injection of hazardous wastes, the EPA addressed the use of older geological data in making a long-term demonstration of repository performance. In response to comments on a proposed rule regarding the permitting of underground injection

1 wells, the EPA concluded that “[e]xcluding historical data or information which might have been
 2 gathered off-site by methods not consistent with certain prescribed procedures may be
 3 counterproductive.” The EPA further stated that such data should be used as long as their
 4 limitations are accounted for. In the final rule, the EPA stipulated “that only measurements
 5 pertaining to the waste or that result from testing performed to gather data for the petition
 6 demonstration comply with prescribed procedures.” Further, the EPA stated that “the concerns
 7 about the accuracy of geologic data are addressed more appropriately by requiring that the
 8 demonstration identify and account for the limits on data quality rather than by excluding data
 9 from consideration” (EPA 1988).

10 As site characterization activities progressed, the DOE, along with independent review groups
 11 such as the National Academy of Sciences (NAS), the Environmental Evaluation Group (EEG),
 12 and the state of New Mexico acting through the Governor’s Radioactive Waste Consultation
 13 Task Force, identified natural FEPs that required additional detailed investigation. Because
 14 these investigations, in many cases, were to gather data that would either be used in developing
 15 conceptual models or in the prediction of disposal system performance, the quality assurance
 16 (QA) standards applied to these investigations were more stringent, thereby ensuring accuracy
 17 and repeatability to the extent possible for geologic investigations.

18 Geological data from site characterization have been developed by the DOE through a variety of
 19 WIPP-sponsored studies using drilling, mapping or other direct observation, geophysical
 20 techniques, and laboratory work. Most of the techniques and statistics of data acquisition will be
 21 incorporated by specific discussion. The processes used in deriving modeling parameters from
 22 field and laboratory data are discussed in records packages which support the conceptual models
 23 in Section 6.4 and the parameters in Appendix ~~PAR~~ *PA, Attachment PAR*. Pointers to these
 24 records packages are provided principally in Appendix ~~PAR~~ *PA, Attachment PAR*. Records
 25 packages are stored in the Sandia WIPP Central Files (SWCF) in Albuquerque *Records Center*
 26 *in Carlsbad*. Access to review of these records packages can be obtained by contacting the
 27 person designated in Table 1-10. Borehole investigations are a major source of geological data
 28 for the WIPP and surrounding area. Borehole studies provide raw data (for example, depth
 29 measurements, amount of core, geophysical logs) that support point data and interpreted data
 30 sets. These data sets are used in developing other analysis tools such as structure maps for
 31 selected stratigraphic horizons or isopachs (thicknesses) of selected stratigraphic intervals.

32 The borehole data sets that ~~were~~ *was* used specifically for obtaining ~~Waste Isolation Pilot Plant~~
 33 (WIPP) geologic information *is* included as reference information in *CCA* Appendix BH. This
 34 ~~appendix provides some summary information and is a pointer for data reports that contain more~~
 35 ~~detailed results.~~ A map of some borehole locations in the data set is provided in Figure 2-2.

36 *Figure 2-3 shows Culebra monitoring wells within the site boundary as of December 2002,*
 37 *including well C-2737, which was drilled and completed in 2001 (Powers 2002c). Figure 2-4*
 38 *shows Culebra monitoring wells outside the WIPP site as of December 2002; plugged and*
 39 *abandoned wells formerly monitored are not included in this figure. Figure 2-5 shows the*
 40 *locations of wells configured to monitor the Magenta, including well C-2737. Other*
 41 *hydrostratigraphic units are monitored in wells shown in Figure 2-6, including well C-2811,*
 42 *which was drilled and completed in 2001 to monitor a shallow saturated zone developed since*
 43 *the WIPP surface structures were constructed (Powers and Stensrud 2003).* Other holes are
 44 not shown because they were not of sufficient depth, were not cored, or were not drilled for

purposes of site characterization. A more comprehensive drillhole database of the entire Delaware Basin is addressed in Section 2.3.1.2 and is presented in [Appendix DATA Appendix DEL \(Figure DEL-4\)](#). This database includes all drillholes used in evaluating human intrusion rates for the WIPP [PA](#).

2.1.2 Geologic History

In this section, the DOE summarizes the more important points of the area's geologic history within about 320 km (200 mi) of the WIPP site, with emphasis on more recent or nearby events. Figure 2-37 shows the major elements of the area's geological history from the end of the Precambrian Period.

The geologic time scale that the DOE uses for WIPP is based on the compilation by Palmer (1983, [pp.](#) 503 – 504) for *The Decade of North American Geology* (DNAG). There are several compiled sources of chronologic data related to different reference sections or methods (see, for example, Harland et al. 1989 and Salvador 1985 in the bibliography). Although most of these sources show generally similar ages for chronostratigraphic boundaries, there is no consensus on either reference boundaries or most-representative ages. The DNAG scale is accepted by the DOE as a standard that is useful and sufficient for WIPP purposes, as no known critical performance assessment parameters require more accurate or precise dates.

The geologic history in this region can be conveniently subdivided into three general phases:

- A Precambrian Period, represented by metamorphic and igneous rocks ranging in age from about 1.5 to 1.1 billion years;
- A period from about 1.1 to 0.6 billion years ago, from which no rocks are preserved. Erosion may have been the dominant process during much of this period; [and](#)
- An interval from 0.6 billion years ago to the present represented by a more complex set of mainly sedimentary rocks and shorter periods of erosion and dissolution.

This latter phase is the main subject of the DOE's detailed discussion in this text.

Only a few boreholes in the WIPP region have bored deep enough to penetrate Precambrian crystalline rocks, and, therefore, relatively little petrological information is available. Foster (1974, Figure 3) extrapolated the elevation of the Precambrian surface under the area of WIPP as being between 4.42 km (14,500 ft) and 4.57 km (15,000 ft) below sea level; the site surface at WIPP is about 1,036 m (3,400 ft) above sea level. Keesey (1976, Vol. II, Exhibit No. 2) projected a depth of about 5,545 m (18,200 ft) from the surface to the top of Precambrian rocks in the vicinity of the WIPP. The depth projection is based on the geology of the nearby borehole in Section 15, T22S, R31E.

Precambrian rocks of several types crop out in the following locations: the Sacramento Mountains northwest of WIPP; around the Sierra Diablo and Baylor Mountains near Van Horn, Texas; west of the Guadalupe Mountains at Pump Station Hills; and in the Franklin Mountains

1N



Figure 2-2. WIPP Site and Vicinity Borehole Location Map (partial)

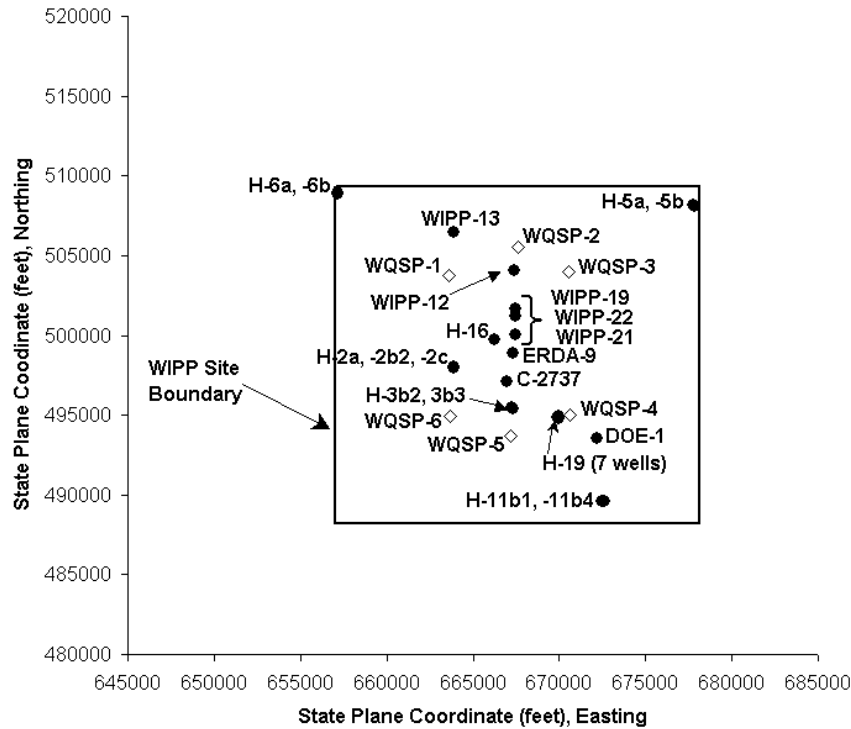


Figure 2-3. Locations of Culebra Monitoring Wells Inside the WIPP Site Boundary

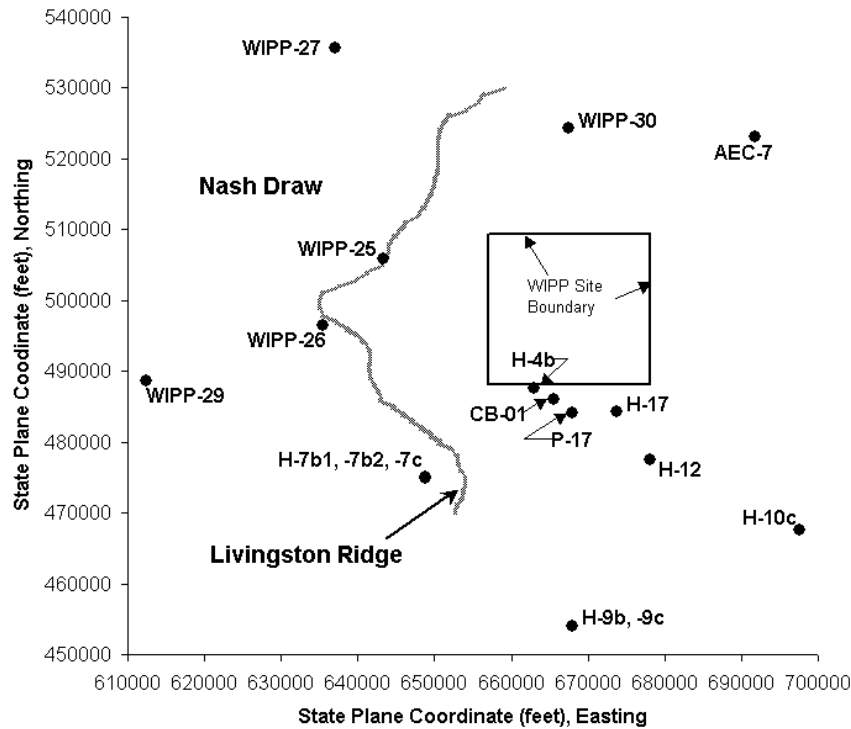


Figure 2-4. Locations of Culebra Monitoring Wells Located Outside the WIPP Site Boundary

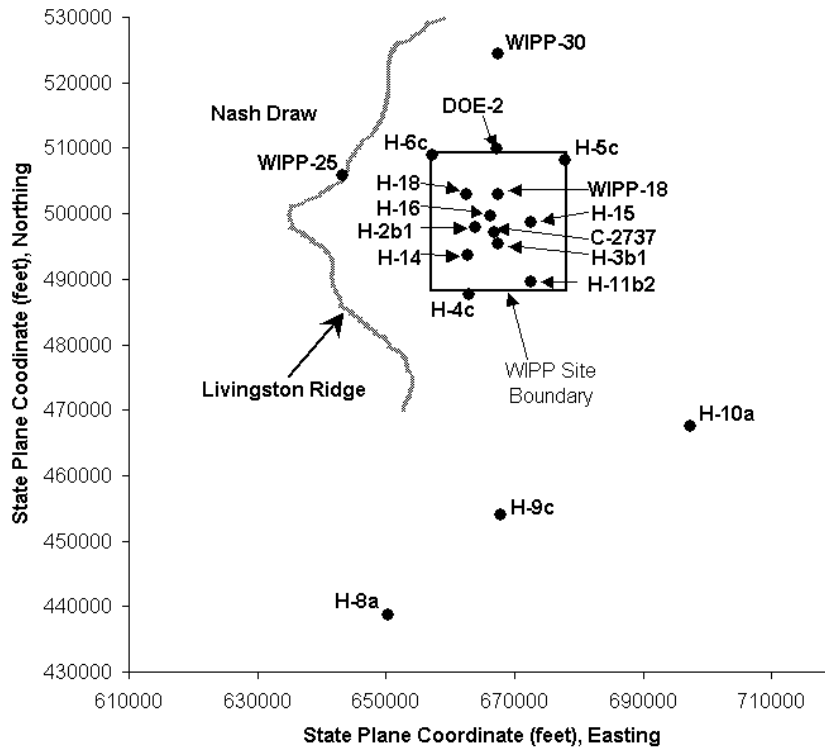


Figure 2-5. Locations of Magenta Monitoring Wells

near El Paso, Texas. East of the WIPP, a relatively large number of boreholes on the Central Basin Platform have penetrated the top of the Precambrian (Foster 1974, Figure 3). As summarized by Foster (1974, 10), Precambrian rocks in the area considered similar to those in the vicinity of the site range in age from about 1.14 to 1.35 billion years.

For about 500 million years (1.1 to 0.6 billion years ago), there is no certain rock record in the region around the WIPP. The most likely rock record for this period may be the Van Horn sandstone (McGowan and Groat 1971), but there is no conclusive evidence that it represents part of this time period (CCA Appendix GCR, Section 3.3.1). The region is generally thought to have been subject to erosion for much of the period until the Bliss sandstone began to accumulate during the Cambrian.

There is additional geologic history information contained in the EPA Technical Support Document for Section 194.14: Content of Compliance Certification Application, Section IV (Docket A-93-02, Item V-B-3).

2.1.3 Stratigraphy and Lithology in the Vicinity of the WIPP Site

The conceptual model of the disposal system uses information about the geometry of the various rock layers as a model input as described in Section 6.4.2.1. This means that stratigraphic information (thickness and lateral extent) provided in the following sections are important inputs.

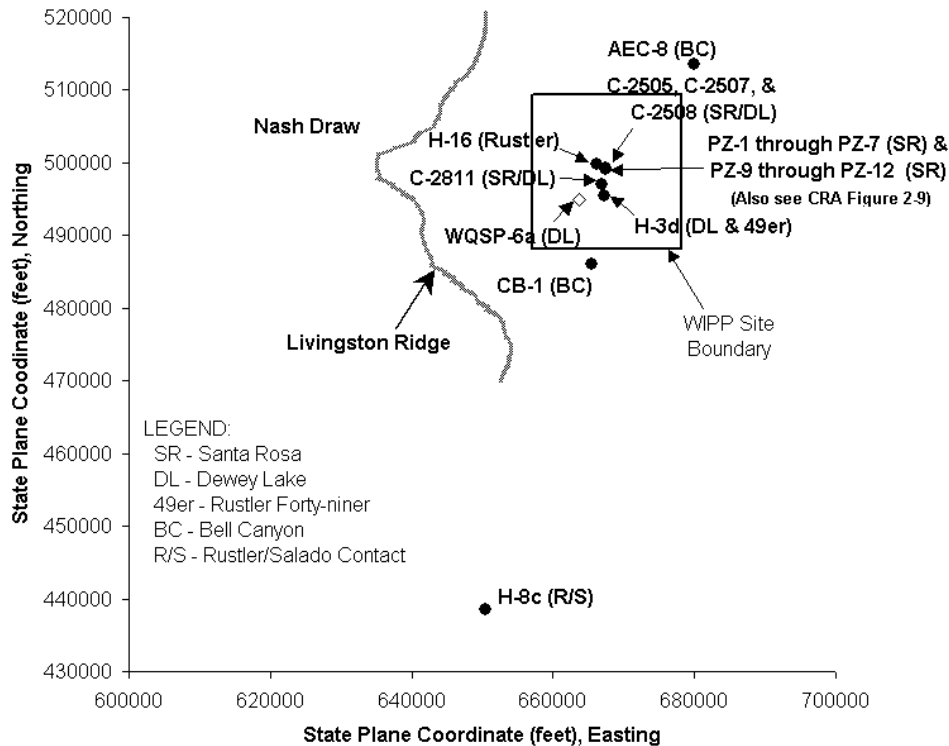


Figure 2-6. Locations of Monitoring Wells Completed to Hydrostratigraphic Units Other Than the Culebra and Magenta Dolomite Members (See also Figure 2-39).

In addition, less important features such as the lithology and the presence of geochemically significant minerals are provided to support screening arguments in Appendix PA, Attachment SCR. Consequently, this discussion has focused on the general properties of the various rock units as determined from field studies. Specific parameters used in the modeling described in Sections 6.4.5 and 6.4.6 are summarized in Appendix PAR (Tables PAR-25 to PAR-32 and PAR-34 to PAR-36) Appendix PA, Attachment PAR. Stratigraphy-related parameters are input as constants. Stratigraphic thicknesses of units considered in modeling are compiled in Appendix PA, Attachment PAR, Table PAR-5749.

This section describes the stratigraphy and lithology of the Paleozoic and younger rocks underlying the WIPP site and vicinity (Figure 2-48), emphasizing the units nearer the surface. After briefly describing pre-Permian rocks, the section provides detailed information on the Permian (Guadalupian) Bell Canyon Formation (hereafter referred to as the Bell Canyon)—the upper unit of the Delaware Mountain Group—because this is the uppermost transmissive formation below the evaporites. The principal stratigraphic data are the chronologic sequence, age, and extent of rock units, including some of the nearby relevant facies changes. For deeper rocks, characteristics such as thickness and depth are summarized from published sources, and for shallower rocks, they are mainly based on data sets presented in CCA Appendix BH (above the Bell Canyon). The lithologies of upper formations and some formation members are described. A comprehensive discussion of stratigraphy in the WIPP area is presented in this application in CCA Appendix GCR. Detailed referencing to original investigations by the USGS and others is included.

E R A	PERIOD	EPOCH	YEARS		MAJOR GEOLOGIC EVENTS - SOUTHEAST NEW MEXICO REGION
			DURATION	BEFORE PRESENT	
C E N O Z O I C	Quaternary	Holocene	10,000	1,600,000	Eolian and erosion/solution activity. Development of present landscape.
		Pleistocene	1,590,000		Continued deposition of Gatuña sediments.
	Tertiary	Pliocene	3,700,000	66,400,000	Deposition of Gatuña sediments. Formation of caliche caprock. Regional uplift and east-southeastward tilting; Basin-Range uplift of Sacramento and Guadalupe-Delaware Mountains.
		Miocene	18,400,000		Erosion dominant. No Early to Mid-Tertiary rocks present.
		Oligocene	12,900,000		Laramide revolution. Uplift of Rocky Mountains. Mild tectonism and igneous activity to west and north.
		Eocene	21,200,000		
		Paleocene	8,600,000		
M E S O Z O I C	Cretaceous		77,600,000	144,000,000	Submergence. Intermittent shallow seas. Thin limestone and clastics deposited.
	Jurassic		64,000,000	208,000,000	Emergent conditions. Erosion, formation of rolling terrain.
	Triassic		37,000,000	245,000,000	Deposition of fluvial clastics. Erosion. Broad flood plain develops.
P A L E O Z O I C	Permian		41,000,000	286,000,000	Deposition of evaporite sequence followed by continental redbeds. Sedimentation continuous in Delaware, Midland, Val Verde basins and shelf areas.
	Pennsylvanian		34,000,000	320,000,000	Massive deposition of clastics. Shelf, margin, basin pattern of deposition develops.
	Mississippian		40,000,000	360,000,000	Regional tectonic activity accelerates, folding up Central Basin platform. Matador arch, ancestral Rockies. Regional erosion. Deep, broad basins to east and west of platform develop.
	Devonian		48,000,000	408,000,000	Renewed submergence. Shallow sea retreats from New Mexico; erosion. Mild epeirogenic movements. Tobosa basin subsiding. Pedernal landmass and Texas Peninsula emergent until Middle Mississippian.
	Silurian		30,000,000	438,000,000	
	Ordovician		67,000,000	505,000,000	Marathon-Quachita geosyncline, to south, begins subsiding. Deepening of Tobosa basin area; shelf deposition of clastics, derived partly from ancestral Central Basin platform and carbonates.
	Cambrian		65,000,000	570,000,000	Clastic sedimentation - Bliss sandstone.
	PRECAMBRIAN				Erosion to a nearly level plain. Mountain building, igneous activity, metamorphism, erosional cycles.

Figure 2-37. Major Geologic Events - Southeast New Mexico Region


SYSTEM/ Series		Group	Formation	Members
QUATER- NARY	Holocene		surficial deposits	
TERTIARY	Pleisto- cene		Mescalero caliche	
	Pliocene		Gatuña	
	Miocene			
TRIASSIC		Dockum	 Santa Rosa	
			Dewey Lake	
PERMIAN	Ochoan		Rustler	<i>Forty-niner</i> <i>Magenta Dolomite</i> <i>Tamarisk</i> <i>Culebra Dolomite</i> <i>Los Medaños</i>
			Salado	<i>upper</i> <i>Vaca Triste Sandstone</i> <i>McNutt potash zone</i> <i>lower</i>
			Castile	
	Guadalupian	Delaware Mountain	Bell Canyon	
			Cherry Canyon	
Brushy Canyon				

Figure 2-8. Partial Site Geologic Column

2.1.3.1 General Stratigraphy and Lithology below the Bell Canyon

As stated previously, the Precambrian basement near the site is projected to be about 5,545 m (18,200 ft) below the surface (Keesey 1976, Vol. II, Exhibit No. 2), consistent with information presented by Foster in 1974. Ages of similar rock suites in the region range from about 1.14 to 1.35 billion years.

A detailed discussion of the distribution of Precambrian rocks in southeastern New Mexico and Texas can be found in this application in CCA Appendix GCR (Section 3.3.1). Figure 3.4-2 in CCA Appendix GCR provides a structure contour map of the Precambrian. The basal Paleozoic units overlying Precambrian rocks are clastic rocks commonly attributed either to the Cambrian Bliss sandstone or the Ellenberger Group (Foster 1974, p. 10), considered most likely to be Ordovician in age in this area. The Ordovician System comprises the Ellenberger, Simpson, and Montoya Groups in the northern Delaware Basin. Carbonates are predominant in these groups, with sandstones and shales common in the Simpson Group. Foster (1974, Figure 4) reported 297 m (975 ft) of Ordovician-age rocks north of the site area and extrapolated a thicker section of about 396 m (1,300 ft) at the present site (Foster 1974, Figure 5). Keesey (1976, Vol. II, Exhibit No. 2) projected a thickness of 366 m (1,200 ft) for the Ordovician System within the site boundaries.

Silurian-Devonian rocks in the Delaware Basin are not stratigraphically well defined, and there are various notions for extending nomenclature into the basin. Common drilling practice is not to differentiate, though the Upper Devonian Woodford shale at the top of the sequence is frequently distinguished from the underlying dolomite and limestone (Foster 1974, p. 18). Foster (1974, Figure 6) showed a reference thickness of 384 and 49 m (1,260 and 160 ft) for the carbonates and the Woodford shale, respectively; he estimated thickness of these units at the present WIPP site to be about 351 m (1,150 ft) (Foster 1974, Figure 7) and 52 m (170 ft) (Foster 1974, Figure 8), respectively. Keesey (1976, Vol. II, Exhibit No. 2) projected 381 m (1,250 ft) of carbonate and showed 25 m (82 ft) of the Woodford shale.

The Mississippian System in the northern Delaware Basin is commonly attributed to Mississippian limestone and the overlying Barnett shale (Foster 1974, p. 24), but the nomenclature is not consistently used. At the reference well used by Foster (1974, 25), the limestone is 165 m (540 ft) thick and the shale is 24 m (80 ft); isopachs at the WIPP are 146 m (480 ft) (Foster 1974, Figure 10) and less than 61 m (200 ft). Keesey (1976, Vol. II, Exhibit No. 2) indicates 156 m (511 ft) and 50 m (164 ft), respectively, within the site boundaries.

The nomenclature of the Pennsylvanian System applied within the Delaware Basin is both varied and commonly inconsistent with accepted stratigraphic rules. Chronostratigraphic, or time-stratigraphic, names are applied from base to top of these lithologic units: the Morrow, Atoka, and Strawn (Foster 1974, p. 31). Foster (1974, Figure 13) extrapolated thicknesses of about 671 m (2,200 ft) for the Pennsylvanian at the WIPP site. Keesey (1976, Vol. II, Exhibit No. 2) reports 636 m (2,088 ft) for these units. The Pennsylvanian rocks in this area are mixed clastics and carbonates, with carbonates more abundant in the upper half of the sequence.

The Permian is the thickest system in the northern Delaware Basin, and it is divided into four series from the base to top: Wolfcampian, Leonardian, Guadalupian, and Ochoan. According to

1 Keesey (1976, Vol. II, Exhibit No. 2), the three lower series total 2,647 m (8,684 ft) near the site.
 2 Foster (1974, Figures 14, 16, and 18) indicates a total thickness for the lower three series of
 3 2,336 m (7,665 ft) for a reference well north of WIPP. Foster's isopach maps of these series
 4 (Foster 1974, Figures 15, 17, and 19) indicate about 2,591 m (8,500 ft) for the WIPP site area.
 5 The Ochoan Series at the top of the Permian is considered in more detail later because the
 6 formations host and surround the WIPP repository horizon. Its thickness at DOE-2, about 3.2
 7 km (2 mi) north of the site center, is 1,200 m (3,938 ft), according to Mercer et al. (1987, *p.* 23).

8 The Wolfcampian Series is also referred to as the Wolfcamp Formation (hereafter referred to as
 9 the Wolfcamp) in the Delaware Basin. In the site area, the lower part of the Wolfcamp is
 10 dominantly shale with carbonate and some sandstone, according to Foster (1974, Figure 14);
 11 carbonate increases to the north (Foster 1974, *p.* 36). Clastics increase to the east toward the
 12 margin of the Central Basin Platform. Keesey (1976, Vol. II, Exhibit No. 2) reports the
 13 Wolfcamp to be 455 m (1,493 ft) thick at a well near the WIPP site.

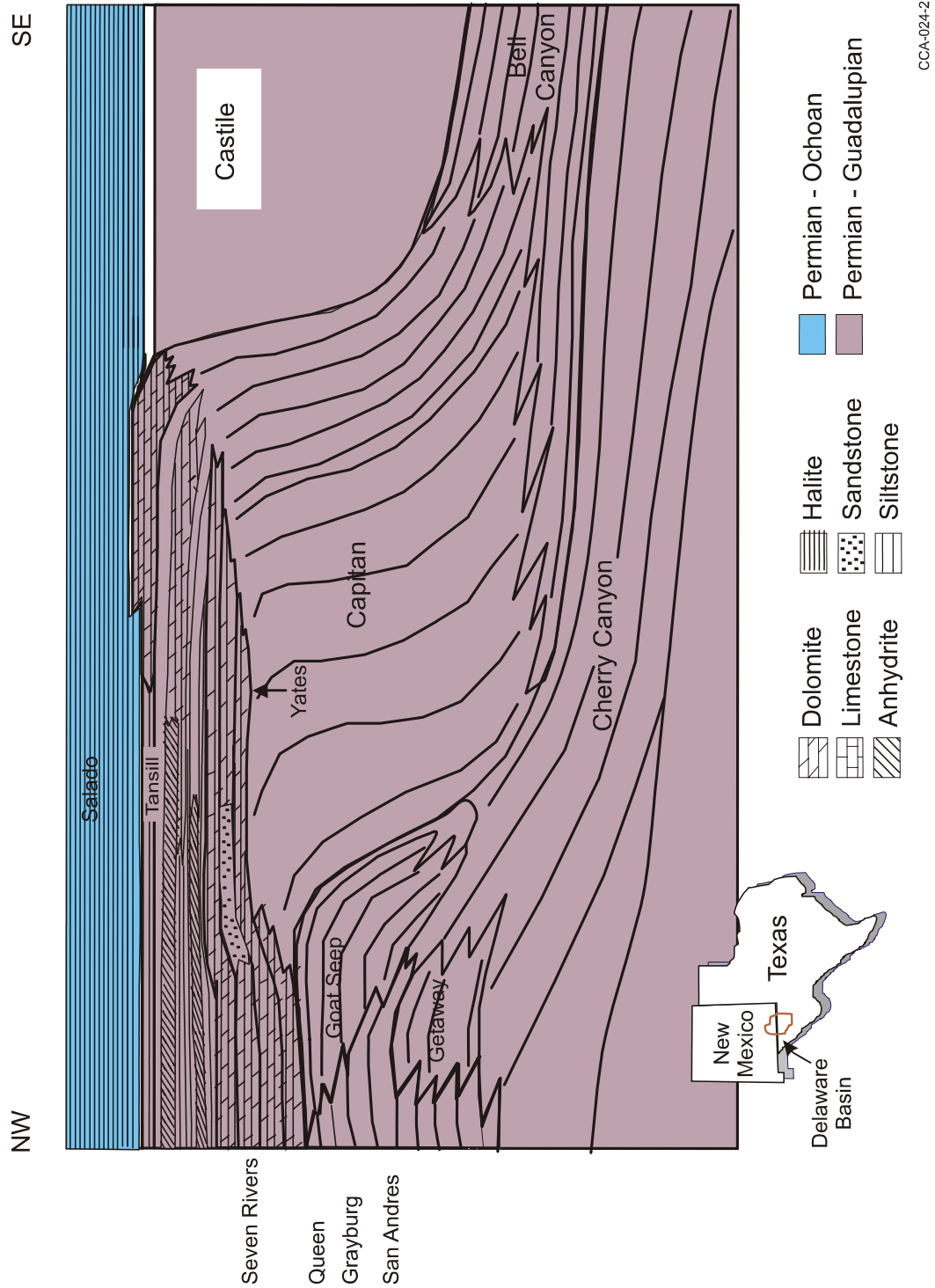
14 The Leonardian Series is represented by the Bone Spring Limestone *or* Formation (hereafter
 15 referred to as the Bone Spring). According to Foster (1974, *pp.* 35 - 36), the lower part of the
 16 formation is commonly interbedded carbonate, sandstone, and some shale, while the upper part is
 17 dominantly carbonate. Near the site the Bone Spring is 990 m (3,247 ft) thick, according to
 18 Keesey (1976, Vol. II, Exhibit No. 2).

19 The Guadalupian Series is represented in the general area of the site by a number of formations
 20 exhibiting complex facies relationships (Figure 2-59). The Guadalupian Series is known in
 21 considerable detail west of the site from outcrops in the Guadalupe Mountains, where numerous
 22 outcrops *are present* and subsurface studies have been undertaken. (See, for example, *P.B.* King
 23 1948, Newell et al. 1953, and Dunham 1972 in the *CCA* bibliography.)

24 Within the Delaware Basin, the Guadalupian Series, known as the Delaware Mountain Group,
 25 comprises three formations: Brushy Canyon, Cherry Canyon, and Bell Canyon, from base to
 26 top. These formations are dominated by submarine channel sandstones with interbedded
 27 limestone and some shale. The Lamar limestone generally tops the series, immediately
 28 underneath the Castile Formation (hereafter referred to as the Castile). Around the margin of the
 29 Delaware Basin, reefs developed when the Cherry Canyon and Bell Canyon were being
 30 deposited. These massive reef limestones, the Goat Seep and Capitan Limestones, are equivalent
 31 in time to the basin sandstone formations but were developed topographically much higher
 32 around the basin margin. A complex set of limestone-to-sandstone and evaporite beds was
 33 deposited further away from the basin, behind the reef limestones. The Capitan ~~re~~ reef and back-
 34 reef limestones are well known because numerous caves, including the Carlsbad Caverns, are
 35 partially developed in these rocks.

36 2.1.3.2 The Bell Canyon

37 As will be discussed in Section 2.1.3.3, the Castile is a 427-to-487-meter(1,400-to-1,600-~~feet~~)
 38 thick layer of nearly impermeable anhydrites and halites that isolate the Salado from the



CCA-024-2

Figure 2-59. Schematic Cross-Section from Delaware Basin (southeast) through Marginal Reef Rocks to Back-Reef Facies (based on King, P.B., 1948)

1
2
3
4

deeper water-bearing rocks. This notwithstanding, the DOE is interested in the Bell Canyon because it is the first laterally continuous transmissive unit below the WIPP repository. The significance of this unit is related to the FEP in Table 2-1 for deep dissolution. In evaluating this FEP, the DOE considers the potential for groundwater to migrate from the Bell Canyon or lower units into the repository and cause dissolution. The following discussion summarizes the basic understanding of the Bell Canyon lithology. Dissolution is discussed in Section 2.1.6. Bell Canyon hydrology is presented in Section 2.2.1.2. A thorough discussion of dissolution is in [CCA Appendix DEF](#)(~~Section DEF-3.1~~).

The Bell Canyon is known from outcrops on the west side of the Delaware Basin and from subsurface intercepts for oil and gas drilling. Several informal lithologic units are commonly named during such drilling. Mercer et al. (1987, [p. 28](#)) stated that DOE-2 penetrated the Lamar limestone, the Ramsey sand, the Ford shale, the Olds sand, and the Hays sand. This informal nomenclature is used for the Bell Canyon in some other WIPP reports.

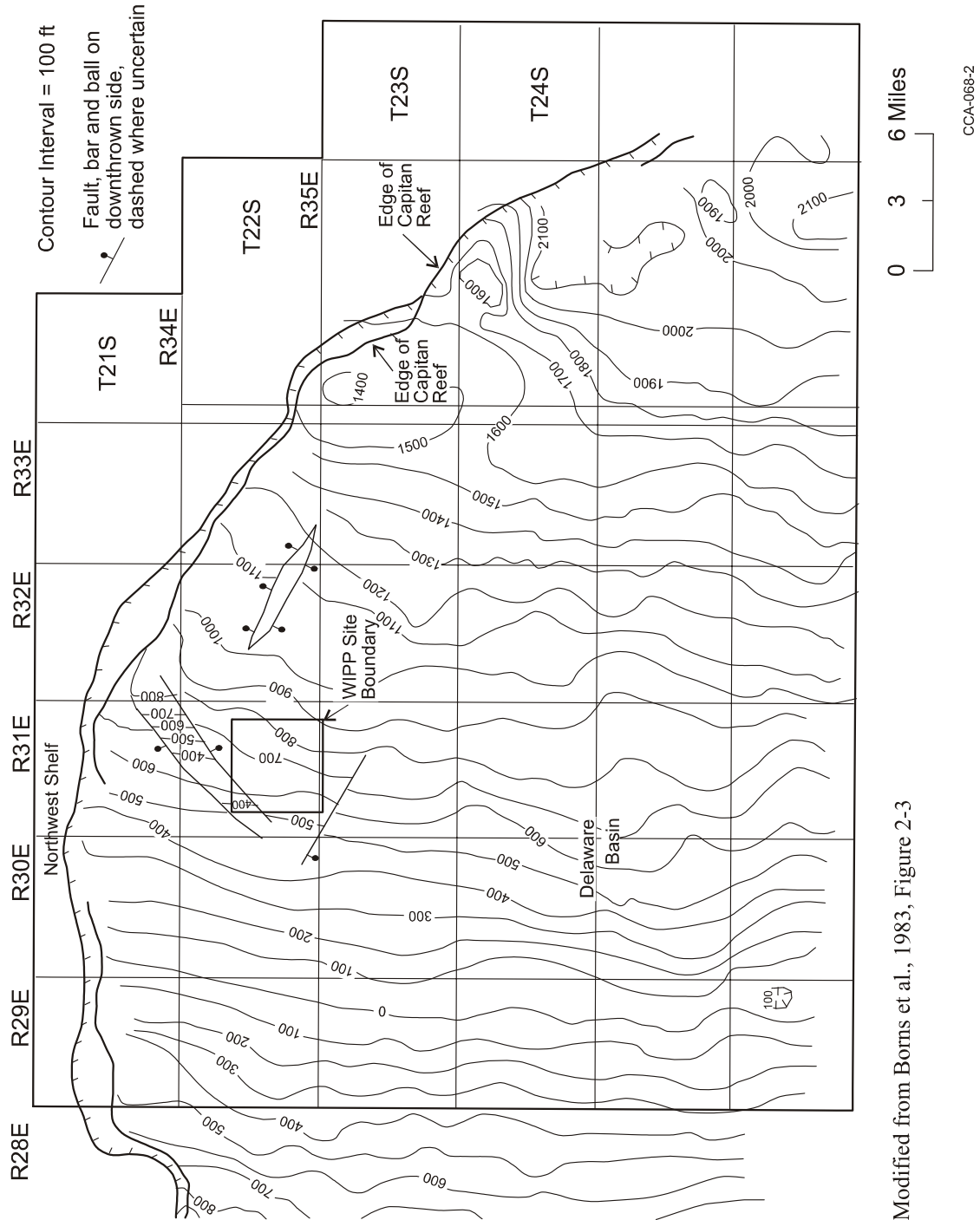
The Clayton Williams Badger Federal borehole (Section 15, T22S, R31E) intercepted 961 feet (293 meters) of Bell Canyon, including the Lamar limestone, according to Keesey (1976, Vol. II, Exhibit No. 2). Reservoir sandstones of the Bell Canyon were deposited in channels that are straight to slightly sinuous. In their 1988 paper, Harms and Williamson proposed that density currents flowed from shelf regions, cutting channels and depositing the sands.

Within the basin, the Bell Canyon- (Lamar limestone-) Castile contact is distinctive on geophysical logs because of the contrast in low natural gamma of the basal Castile anhydrite compared to the underlying limestone. Density or acoustic logs are also distinctive because of the massive and uniform lithology of the anhydrite compared to the underlying beds. In cores, the transition is sharp, as described by Mercer et al. (1987, 312) for DOE-2. A structure contour map of the top of the Bell Canyon is shown in Figure 2-6~~10~~. Also see [CCA Appendix MASS](#), ~~Section MASS-18~~, MASS Attachment 18-6, Figure 5.3-3. According to Powers et al. (1978) ([CCA Appendix GCR, 4-59](#)), this structure does not reflect the structure of deeper formations, suggesting different deformation histories. The rootless character of at least some of the normal faulting in the lower Permian suggests these are shallow-seated features.

2.1.3.3 The Castile

The Castile is the lowermost lithostratigraphic unit of the Late Permian Ochoan Series (Figure 2-7~~11~~) and is part of the thick layer of evaporites within the WIPP disposal system. It was originally named by Richardson (1904, [p. 43](#)) for outcrops in Culberson County, Texas.

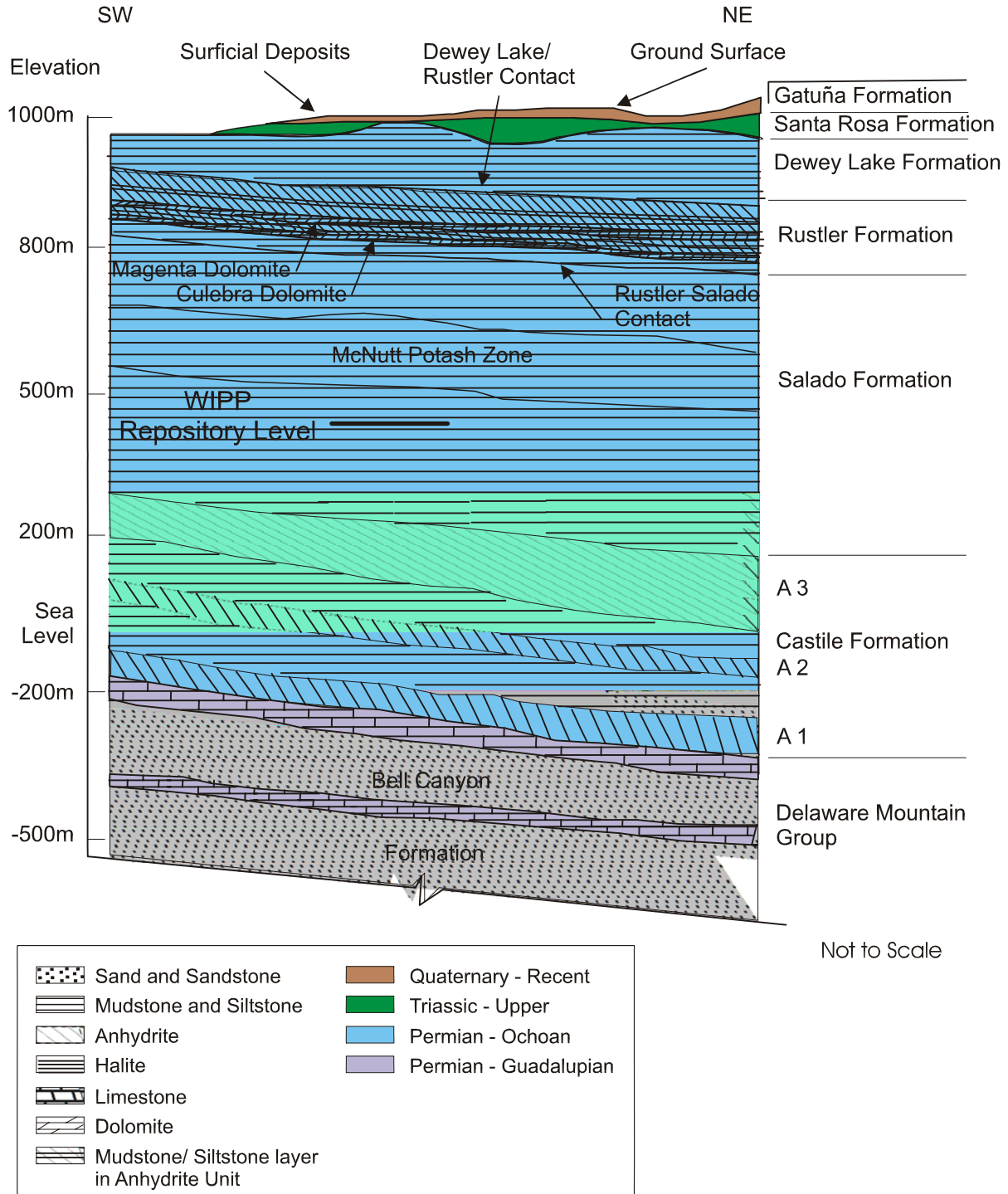
The Castile crops out along a lengthy area of the western side of the Delaware Basin. The two distinctive lithologic sequences now known as the Castile and the Salado were separated into the Upper and Lower Castile by Cartwright (1930). Lang in (1939) clarified the nomenclature by restricting the Castile to the lower unit and naming the upper unit the Salado. By defining an anhydrite resting on the marginal Capitan limestone as part of the Salado, Lang in 1939 effectively restricted the Castile to the Delaware Basin inside the reef rocks.



Modified from Borns et al., 1983, Figure 2-3

Figure 2-610. Structure Contour Map of Top of Bell Canyon

1
2
3



CCA-025-2

Figure 2-711. Generalized Stratigraphic Cross Section above Bell Canyon Formation at WIPP Site

Through detailed studies of the Castile, Anderson et al. (1972) introduced an informal system of names that is widely used and included in many WIPP reports. The units are named from the base as anhydrite I (A1), halite I (H1), anhydrite II (A2), etc. The informal nomenclature varies through the basin from A3 up because of complexity of the depositional system. The Castile consists almost entirely of thick beds of two lithologies: (1) interlaminated carbonate and anhydrite, and (2) high-purity halite.

In the eastern part of the Delaware basin, the Castile thickness is commonly *ranges from about 427-299 to 487-616 m meters (1,400-980 to 1,600-2,022 ft) thick* (derived from *Powers et al. 1996, Figure 5.3-1; see also* Borns and Shaffer 1985, Figures 9, 11, *and 16 for an earlier range based on fewer drillholes*). *At DOE-2, the Castile is 301 m (989 ft) thick.* The Castile is thinner in the western part of the Delaware Basin, and it lacks halite units.

Anderson et al. (1978) and Anderson (1978, Figures 1, 3, 4, *and 5*) correlated geophysical logs throughout the WIPP region, interpreting thin zones equivalent to halite units as dissolution residues. Anderson et al. (1972, *p.* 81) further attributed the lack of halite in the basin to its removal by dissolution. A structure contour map of the top of the Castile is reported in Figure 4.4-6, *CCA* Appendix GCR based on seismic data gathered for site characterization. In addition, Borns et al. (1983) prepared a seismic time structure of the middle Castile for identifying deformation. This map is shown in Figure DEF-2.2 in *CCA* Appendix DEF. *Powers et al. (1996; Figures 5.2-1, 5.2-2, and 5.2-3) provide comparative figures of the elevations of the top of the Bell Canyon, top of Anhydrite 2 (of the Castile), and top of Anhydrite 3 (of the Castile), respectively, based on geophysical log data from oil and gas wells.*

For borehole DOE-2, a primary objective was to ascertain whether a series of depressions in the Salado ~~2 miles (3.3 kilometers)~~ *3.3 km (2 mi)* north of the site *center* was from dissolution in the Castile and related processes, as proposed by Davies (1984, *p.* 175) in his doctoral thesis (1984, 175). Studies have suggested that these depressions were not from dissolution but from halokinesis in the Castile (see, for example, Borns 1987). Robinson and Powers (1987, *pp.* 22 and 78) interpreted one deformed zone in the Castile *in the western part of the Delaware Basin* as partly caused by synsedimentary, gravity-driven, clastic deposition and suggested that the extent of dissolution may have been overestimated by previous workers. No Castile dissolution is known to be present in the immediate vicinity of the WIPP site. The process of dissolution and the resulting features are discussed later in this chapter. See *CCA* Appendix DEF, Section DEF.3 for a more in-depth discussion of the study of dissolution in the Castile.

In Culberson County, Texas, the Castile hosts major native sulfur deposits. The outcrops of Castile on the Gypsum Plain south of White's City, New Mexico, have been explored for native sulfur without success, and there is no reported indication of native sulfur anywhere in the vicinity of the WIPP.

In part of the area around the WIPP, the Castile has been significantly deformed and there are pressurized brines associated with the deformed areas; borehole ERDA-6 encountered both deformation and pressurized brine. WIPP-12, 1.6 km (1 mi) north of the site center, revealed lesser Castile structure, but it also encountered a zone of pressurized brine within the Castile. Castile deformation is described and discussed in Section 2.1.5 and in *CCA* Appendix DEF,

which detail structural features. Pressurized brine is described in Section 2.2.1, which details the area's hydrology.

Where they exist, Castile brine reservoirs in the northern Delaware Basin are believed to be fractured systems, with high-angle fractures spaced widely enough that a borehole can penetrate through a volume of rock containing a brine reservoir without intersecting any fractures and therefore not produce brine. They occur in the upper portion of the Castile (Popielak et al. 1983). Appreciable volumes of brine have been produced from several reservoirs in the Delaware Basin, but there is little direct information on the areal extent of the reservoirs or the interconnection between them. The presence of a pressurized brine pocket is treated in the conceptual model of WIPP as discussed in Section 6.4.8.

The Castile continues to be an object of research interest unrelated to the WIPP program as an example of evaporites supposedly deposited in deep water. Anderson (1993, pp. 12-13) discusses alternatives and contradictory evidence. *Becker et al. (2002) presented a data set yielding a total Pb/U isochron age of 251.5 ± 2.8 million years (Ma) for calcite from the Castile and inferred that the Permo-Triassic boundary could be younger than this date. This discussion contrasts with other data regarding age of the Salado, Rustler, and Dewey Lake Formations (see later sections), including evidence that later formations yield slightly older radiometric ages.* Although these discussions and a resolution might eventually affect some concepts of Castile deposition and dissolution, this issue is largely of academic interest and bears no impact on the suitability of the Los Medaños region for the WIPP site. Additional discussion of Castile deformation and the associated WIPP studies appears in Section 2.1.6.1 and CCA Appendix DEF. The Castile is included in the conceptual model as described in Section 6.4.8. As shown in Appendix PA, Attachment PAR, in Table PAR-4943, no stratigraphic or lithologic parameters are of importance for this unit. Important hydrological parameters are discussed subsequently.

The EPA questioned DOE's geologic and geophysical basis for the probability (i.e., eight percent probability) of intercepting pressurized brine in the Castile Formation beneath the WIPP disposal panels, and therefore required this distribution to be revised (to a uniform distribution with a range of 0.01 to 0.6) in Performance Assessment Verification Testing (PAVT) (Docket A-93-02, Item II-I-25). The formation of Castile brine pockets as a result of Castile deformation was described in the CCA, and although DOE's discussion of the distribution and nature of fractures in the Castile was limited, parameters were modified to include larger Castile brine pockets in the PAVT. Further information on this topic is contained in EPA Technical Support Document for Section 194.14: Content of Compliance Certification Application, Section IV.C (Docket A-93-02, Item V-B-3), EPA Technical Support Document for Section 194.23: Parameter Justification Report (Docket A-93-02, Item V-B-14), and EPA Technical Support Document for Section 194.23: Review of TDEM Analysis of WIPP Brine Pockets (Docket A-93-02, Item V-B-30).

2.1.3.4 The Salado

The Salado is of interest because it contains the repository horizon and provides the primary natural barrier for the long-term containment of radionuclides. The following section provides basic information regarding the genesis and lithology of the Salado. Subsequent sections discuss

Salado deformation, Salado dissolution, and Salado hydrology. [CCA](#) Appendix GCR provides detailed information about the Salado from early site characterization studies.

The Salado is dominated by halite, in contrast to the underlying Castile. The Salado extends well beyond the Delaware Basin, and Lowenstein (1988, [p. 592](#)) has termed the Salado a saline “giant.”

While the Fletcher Anhydrite Member, which is deposited on the Capitan [Reef](#) rocks, is defined by Lang (1939; 1942) as the base of the Salado, some investigators consider that the Fletcher Anhydrite Member may interfinger with anhydrites normally considered part of the Castile. The Castile-Salado contact is not uniform across the basin, and whether it is conformable is unresolved. Around the WIPP site, the Castile-Salado contact is commonly placed at the top of a thick anhydrite informally designated A3; the overlying halite is called the infra-Cowden salt and is included within the Salado. Bodine (1978, [pp. 28 - 29](#)) suggests that the clay mineralogy of the infra-Cowden in ERDA-9 cores changes at about 4.6 m (15 ft) above the lowermost Salado and that the lowermost clays are more like Castile clays. At the WIPP site, the DOE recognizes the top of the thick A3 anhydrite as the local contact for differentiating the Salado from the Castile and notes that the distinction is related only to nomenclature and has no relevance to the performance of the WIPP disposal system.

The Salado in the northern Delaware Basin is broadly divided into three informal members. The middle member is known locally as the McNutt Potash Zone (hereafter referred to as McNutt) or [Member](#), and it includes 11 defined potash zones, 10 of which are of economic significance in the Carlsbad Potash District. The lower member and the upper member remain unnamed. The WIPP repository level is located below the McNutt in the lower member. Figure 2-8[12](#) shows details of the Salado stratigraphy near the excavated regions. Elements of this stratigraphy are important to the conceptual model. The conceptual model for the Salado is discussed in Section 6.4.5. The thicknesses used in the model are given in Appendix [PA, Attachment PAR](#), Table [PAR-5749](#).

Within the Delaware Basin, a system is used for numbering the more significant sulfate beds within the Salado, designating these beds as marker beds (MBs) from ~~MB 100~~ [MB 100](#) (near the top of the formation) to ~~MB 144~~ [MB 144](#) (near the base). The system is generally used within the Carlsbad Potash District as well as at and around the WIPP site. The repository is located between MB 139 and MB 138.

In the central and eastern part of the Delaware Basin, the Salado is at its thickest, ranging up to about 600 m (2,000 ft) thick and consisting mainly of interbeds of sulfate minerals and halite, with halite dominating. The thinnest portions of the Salado consist of a brecciated residue of insoluble material a few tens-of-feet thick, which is exposed in parts of the western Delaware Basin. The common sulfate minerals are anhydrite (CaSO_4), gypsum ($\text{CaSO}_4 \cdot 2\text{H}_2\text{O}$) near the surface, and polyhalite ($\text{K}_2\text{SO}_4 \cdot \text{MgSO}_4 \cdot 2\text{CaSO}_4 \cdot 2\text{H}_2\text{O}$). They form interbeds and are also found along halite grain boundaries. Isopach maps of various intervals of the Salado above the repository horizon have been provided to assist in understanding regional structure. These are Figures 4.3-4 to 4.3-7 in [CCA](#) Appendix GCR. A structure contour map of the Salado can be found in [CCA](#) Appendix GCR (Figure 4.4-10).

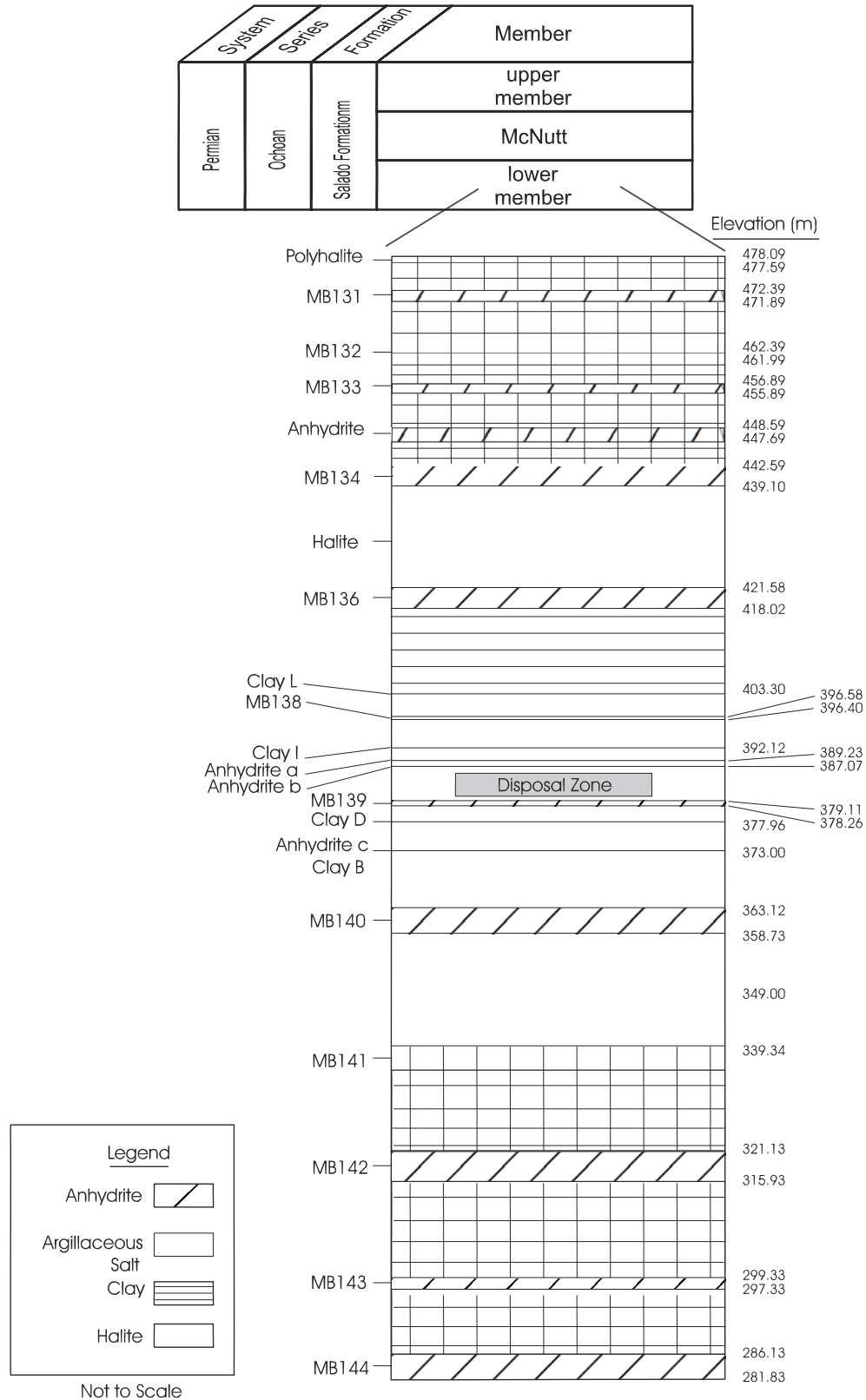


Figure 2-812. Salado Stratigraphy in the Vicinity of the WIPP Disposal Zone

Table 2-2. Chemical Formulas, Distributions, and Relative Abundances of Minerals in the Castile, Salado, and Rustler Formations

Mineral	Formula	Occurrence and Abundance
Amesite	$(\text{Mg}_4\text{Al}_2)(\text{Si}_2\text{Al}_2)\text{O}_{10}(\text{OH})_8$	S, R
Anhydrite	CaSO_4	CCC, SSS, RRR (rarely near surface)
Calcite	CaCO_3	S, RR
Carnallite	$\text{KMgCl}_3 \cdot 6\text{H}_2\text{O}$	SS
Chlorite	$(\text{Mg}, \text{Al}, \text{Fe})_{12}(\text{Si}, \text{Al})_8\text{O}_{20}(\text{OH})_{16}$	S, R
Corrensite	mixed-layer chlorite and smectite	S, R
Dolomite	$\text{CaMg}(\text{CO}_3)_2$	RR
Feldspar	$(\text{K}, \text{Na}, \text{Ca})(\text{Si}, \text{Al})_4\text{O}_8$	C, S, R
Glauberite	$\text{Na}_2\text{Ca}(\text{SO}_4)_2$	C, S (never near surface)
Gypsum	$\text{CaSO}_4 \cdot 2\text{H}_2\text{O}$	CCC (only near surface), S, RRR
Halite	NaCl	CCC, SSS, RRR (rarely near surface)
Illite	$\text{K}_{1-1.5}\text{Al}_4[\text{Si}_{7-6.5}\text{Al}_{1-1.5}\text{O}_{20}](\text{OH})_4$	S, R
Kainite	$\text{KMgClSO}_4 \cdot 3\text{H}_2\text{O}$	SS
Kieserite	$\text{MgSO}_4 \cdot \text{H}_2\text{O}$	SS
Langbeinite	$\text{K}_2\text{Mg}_2(\text{SO}_4)_3$	S
Magnesite	MgCO_3	C, S, R
Polyhalite	$\text{K}_2\text{Ca}_2\text{Mg}(\text{SO}_4)_4 \cdot 2\text{H}_2\text{O}$	SS, R (never near surface)
Pyrite	FeS_2	C, S, R
Quartz	SiO_2	C, S, R
Serpentine	$\text{Mg}_3\text{Si}_2\text{O}_5(\text{OH})_4$	S, R
Smectite	$(\text{Ca}_{1/2}, \text{Na})_{0.7}(\text{Al}, \text{Mg}, \text{Fe})_4(\text{Si}, \text{Al})_8\text{O}_{20}(\text{OH})_4 \cdot n\text{H}_2\text{O}$	S, R
Sylvite	KCl	SS

Legend:

C = Castile
 S = Salado
 R = Rustler
 3 letters = abundant
 2 letters = common
 1 letter = rare or accessory

In the vicinity of the repository, authigenic quartz (SiO_2) and magnesite (MgCO_3) are also present as accessory minerals. Interbeds in the salt are predominantly anhydrite with seams of clay. The clays within the Salado are enriched in magnesium and depleted in aluminum (Bodine 1978, *p.* 1). The magnesium enrichment probably reflects the intimate contact of the clays with brines derived from evaporating sea water, which are relatively high in magnesium.

Powers et al. (*Chapter 7 of CCA* Appendix GCR, ~~Chapter 7~~) studied the geochemistry of the rocks in the vicinity of the disposal system. A partial list of minerals found in the Delaware Basin evaporites, together with their chemical formulas, is given in Table 2-2. The table also indicates the relative abundances of the minerals in the evaporite rocks of the Castile, Salado, and Rustler. Minerals found either only at depth, removed from influence of weathering, or only near the surface, as weathering products, are also identified.

Although the most common Delaware Basin evaporite mineral is halite, the presence of less soluble interbeds (dominantly anhydrite, polyhalite, and claystone) and more soluble admixtures (for example, sylvite, glauberite, kainite) has resulted in chemical and physical properties of the bulk Salado that are significantly different from those of pure halite layers contained within it. In particular, the McNutt, between MB116 *MB 116* and MB126 *MB 126*, is locally explored and mined for potassium-bearing minerals of economic interest. Under differential stress, interbeds (anhydrite, polyhalite, magnesite, dolomite) may fracture while, under the same stress regime, pure halite would undergo plastic deformation. Fracturing of relatively brittle beds, for example, has locally enhanced the permeability, allowing otherwise nonporous rock to carry groundwater. Some soluble minerals incorporated in the rock salt can be radiometrically dated, and their dates indicate the time of their formation. The survival of such minerals is significant, in that such dating is impossible in pure halite or anhydrite.

Liquids were collected from fluid inclusions *in the Salado halite* and from seeps and boreholes within the WIPP drifts. Analysis of these samples indicated that there is compositional variability in the fluids that shows the effects of various phase transformations on brine composition. The fluid inclusions belong to a different chemical population than do the fluids emanating from the walls. It was concluded that much of the brine is completely immobilized within the salt and that the free liquid emanating from the walls is present as a fluid film along intergranular boundaries, mainly in clays and in fractures in anhydrites. Additional information can be found in *CCA* Appendix GCR, Sections 7.5 and 7.6.

Early investigators of the Salado recognized a repetitious vertical succession or cycle of beds in the Salado: clay - anhydrite - polyhalite - halite and minor polyhalite - halite. Later investigators described the cyclical units as clay - magnesite - anhydrite or polyhalite or glauberite - halite - argillaceous halite capped by mudstone. Lowenstein (1988, *pp.* 592 - 608) defined a depositional cycle (Type I) consisting of (1) basal mixed siliciclastic and carbonate (magnesite) mudstone, (2) laminated to massive anhydrite or polyhalite, (3) halite, and (4) halite with mud. Lowenstein also recognized repetitious sequences of halite and halite with mud as incomplete Type I cycles and termed them Type II cycles. Lowenstein (1988, *pp.* 592 - 608) interpreted the Type I cycles as having formed in a shallowing upward, desiccating basin beginning with a perennial lake or lagoon of marine origin and evaporating to saline lagoon and salt pan environments. Type II cycles are differentiated because they do not exhibit features of prolonged subaqueous deposition and also have more siliciclastic influx than do Type I cycles.

From detailed mapping of the Salado in the air intake shaft (AIS) at WIPP, Holt and Powers (1990a, *pp.* 2-26) ~~constructed~~ *interpreted depositional cycles of the Salado* ~~a more detailed sedimentological analysis of Salado depositional cycles, similar in broad aspects to the Type I cycle of Lowenstein. Argillaceous halites and halitic mudstone at the top of many depositional cycles were interpreted by Holt and Powers (1990a, 3—26) in terms of modern features such as those at Devil's Golf Course at Death Valley National Monument, California. The evaporative basin was desiccated, and varying amounts of insoluble residues had collected on the surface through surficial dissolution, eolian sedimentation, and some clastic sedimentation from temporary flooding caused from surrounding areas. The surface developed local relief that could be mapped in some cycles, while the action of continuing desiccation and exposure increasingly concentrated insoluble residues. Flooding, most commonly from marine sources, reset the sedimentary cycle by depositing a sulfate bed.~~

The details available from the shaft demonstrated the important role of syndepositional water level to water table changes that created solution pits and pipes within the halitic beds while they were at the surface. Holt and Powers (1990a, Appendix F) concluded that passive halite cements filled the pits and pipes, as well as less dramatic voids, as the water table rose. Early diagenetic to synsedimentary cements filled the porosity early and rather completely with commonly clear and coarsely crystalline halite, reducing the porosity to a very small volume according to Casas and Lowenstein (1989).

Although Holt and Powers (1990a) found no evidence for postdepositional halite dissolution in the AIS, dissolution of the upper Salado halite has occurred west of the WIPP. Effects of dissolution are visible in Nash Draw and at other localities where gypsum karst has formed, where units above the Salado such as the Rustler Formation (hereafter referred to as the Rustler), Dewey Lake Redbeds (hereafter referred to as the Dewey Lake), and post-Permian rocks have subsided. Dissolution studies are summarized in CCA Appendix DEF, Section DEF.3. *The dissolution margin of upper Salado halite (see Figure 2-13), based on changes in thickness of the interval from the Culebra dolomite to the Vaca Triste Sandstone Member of the Salado, has been interpreted in detail by Powers (2002a, 2002b, 2003a), Holt and Powers (2002), and Powers et al. (2003). Powers (2002a, 2002b, 2003a) examined data from additional drillholes and noted that the upper Salado dissolution margin appears relatively narrow in many areas, and it directly underlies much of Livingston Ridge. The hydraulic properties of the Culebra correlate in part with dissolution of halite from the upper Salado (Holt and Yarbrough 2002; Powers et al. 2003), and the relationships are further described in Section 2.2.1.4.1.2.*

Within Nash Draw, Robinson and Lang (1938, pp. 87-88) recognized a zone equivalent to the upper Salado but lacking halite. Test wells in southern Nash Draw produced brine from this interval, and it has become known as the brine aquifer. Robinson and Lang (1938) considered this zone a residuum from dissolution of Salado halite (see Section 2.1.6.2). Jones et al. (1960) remarked that the residuum should be considered part of the Salado, though in geophysical logs it may resemble the Lower ~~Lower~~ Rustler. The approximate eastern limit of the residuum and brine aquifer lies near Livingston Ridge (the eastward margin of Nash Draw) and is marked by a thickening of the Salado (see Section 2.1.6.2.2).

At the center of the site, Holt and Powers (1984, pp. 4-9) recognized clasts of fossil fragments and mapped channeling in siltstones and mudstones above the halite; they considered these beds to be a normal part of the transition from the shallow evaporative lagoons and desiccated salt pans of the Salado to the saline lagoon of the lower Rustler. Although some Salado halite dissolution at the WIPP may have occurred before deposition of the Rustler clastics, this process was quite different from the subsurface removal of salt from the Salado in more recent time that caused the residuum and associated brine aquifer in Nash Draw. ~~Where the Salado halite is buried at depths greater than about 1,000 feet (approximately 300 meters), physical evidence for large-scale dissolution (for example, postdepositional accumulation of insoluble residues, brecciation from differential collapse, and mass removal) is not observed.~~

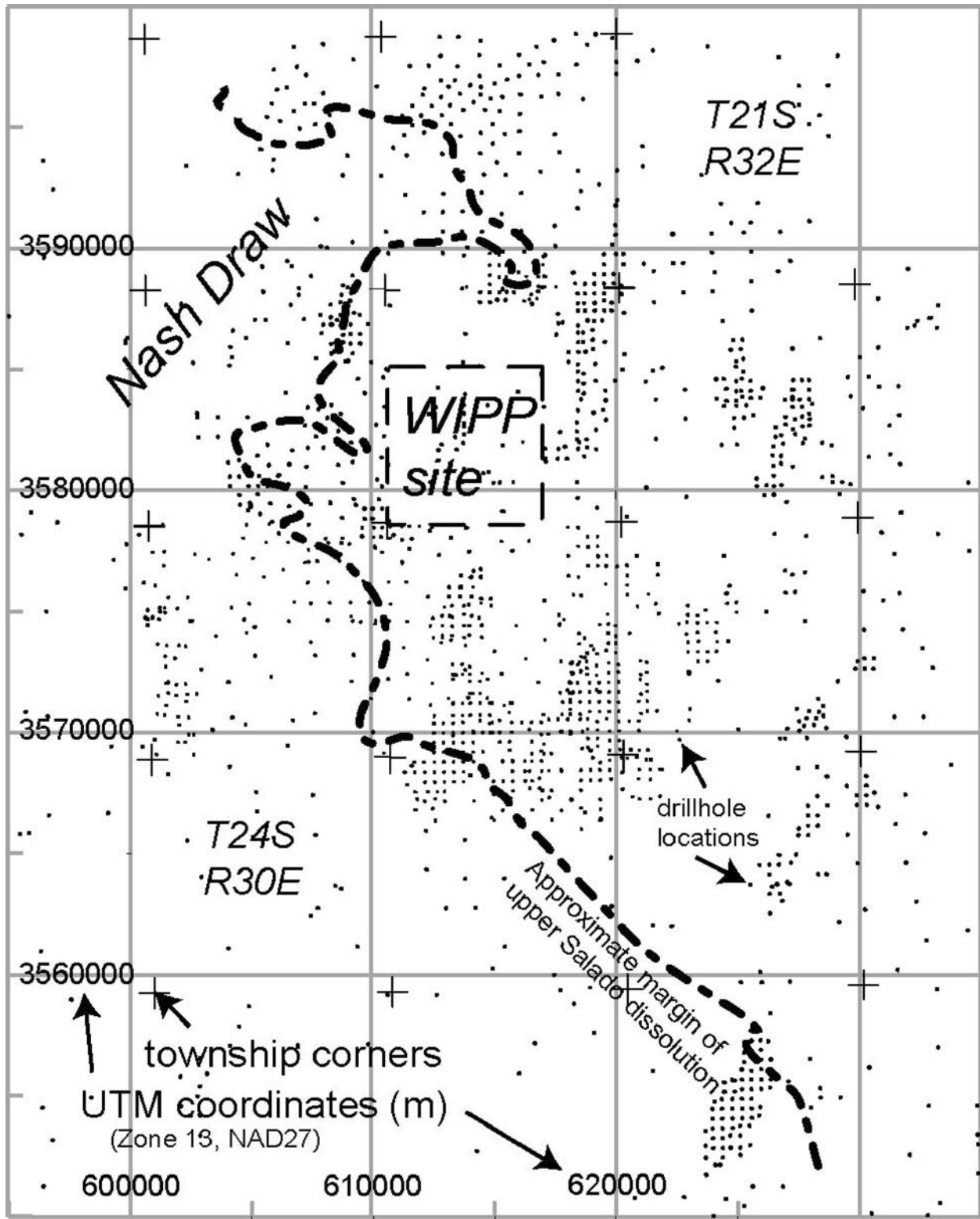


Figure 2-13. Dissolution Margin for the Upper Salado

Geochronological investigations provide a means to confirm the physical evidence indicating that little or no rock-water interactions have occurred in the Salado at the WIPP since the Late Permian Period. Radiometric techniques provide a means of determining the approximate time of the latest episode of regional recrystallization of evaporite minerals, which can be inferred as the approximate time of the latest episode of freely circulating groundwater. Radiometric dates for minerals of the Salado are available from mines and boreholes in the vicinity of the WIPP (Register and Brookins, 1980, pp. 30-42; Brookins, 1980, pp. 29-31; Brookins, et al. 1980, pp. 635-637; Brookins, 1981; and Brookins and Lambert, 1987, pp. 771-780). The distribution of dates shows that many of the rubidium-strontium (Rb-Sr) isochron determinations on evaporite minerals, largely sylvite (214 ± 14 million years ago), are in good agreement with potassium-argon (K-Ar) determinations on pure polyhalites (198 to 216 million years ago). (Potassium-argon ages for sylvite are significantly younger than Rb-Sr ages for the same rocks because of the loss of radiogenic argon. Radiogenic strontium, as a solid, is less mobile than argon and therefore the Rb-Sr isochron method is preferred for sylvite.) *Renne et al. (1998) sampled langbeinite crystals from the Salado and obtained Ar-39/Ar-40 plateau ages of 251 ± 0.2 Ma and 251 ± 0.4 Ma.* Clay minerals have both Rb-Sr and K-Ar ages significantly older (390 ± 77 million years [Register, 1981]) than the evaporite minerals, presumably reflecting the detrital origin of the clays.

One significantly younger recrystallization event has been identified in evaporites in the WIPP region and is a contact phenomenon associated with the emplacement of an Oligocene igneous dike (see Section 2.1.5.4). Polyhalite near the dike yields a radiometric age of 21 million years, compared to the 32- to 34-million-year age determined for the dike (Brookins, 1980, pp. 29-31; and Calzia and Hiss, 1978, p. 44) (this number was recalculated to 34.8 ± 0.8 million years; CCA Appendix GCR, pp. 3 - 80). This exception notwithstanding, the results of radiometric determinations argue for the absence of pervasive recrystallization of the evaporites in the Salado in the last 200 million years. This conclusion is supported by the number of replicate determinations, the wide distribution of similarly dated minerals throughout the Delaware Basin, and the concordance of dates obtained by various radiometric methods.

The notion of extensive recrystallization of Salado evaporites has been raised again since the CCA was submitted. Hazen and Roedder (2001), reiterating some arguments presented by Roedder (1984) and O'Neill et al. (1986), suggested that halite has been extensively recrystallized by water moving through the Salado at unknown times. Stable isotope data from fluid inclusions within coarse, clear halite crystals were interpreted as signifying that modern meteoric water constituted part of the fluid inclusion. O'Neill et al. (1986) noted as well that the stable isotope data are consistent with meteoric water falling on a desiccated Salado salt pan surface. Powers and Hassinger (1985) and Holt and Powers (1990a, 1990b) interpret syndepositional dissolution pipes as a common feature of the Salado, with coarse, clear halite with large fluid inclusions formed on a desiccated salt pan. Powers et al. (2001) summarized the arguments against extensive recrystallization of Salado halite. Stein and Krumhansl (1988) found variable compositions of large fluid inclusions, and show that inclusion chemistry differs significantly from intercrystalline brines, indicating that fluid movement is very limited. Satterfield et al. (2002) also concluded that the coarse halite cements found in certain beds of the Salado are syndepositional, based on ionic concentrations in fluid inclusions. Moreover, Beauheim and Roberts (2002) find extremely low permeability in Salado halite, showing that fluid movement, especially vertically, through the Salado is too

limited and slow to create the purported recrystallization. These findings are also consistent with indications that salt pan deposits are cemented quickly and thoroughly at shallow depths of burial (Casas and Lowenstein 1989). The conclusion that Salado halite has not been pervasively recrystallized remains sound.

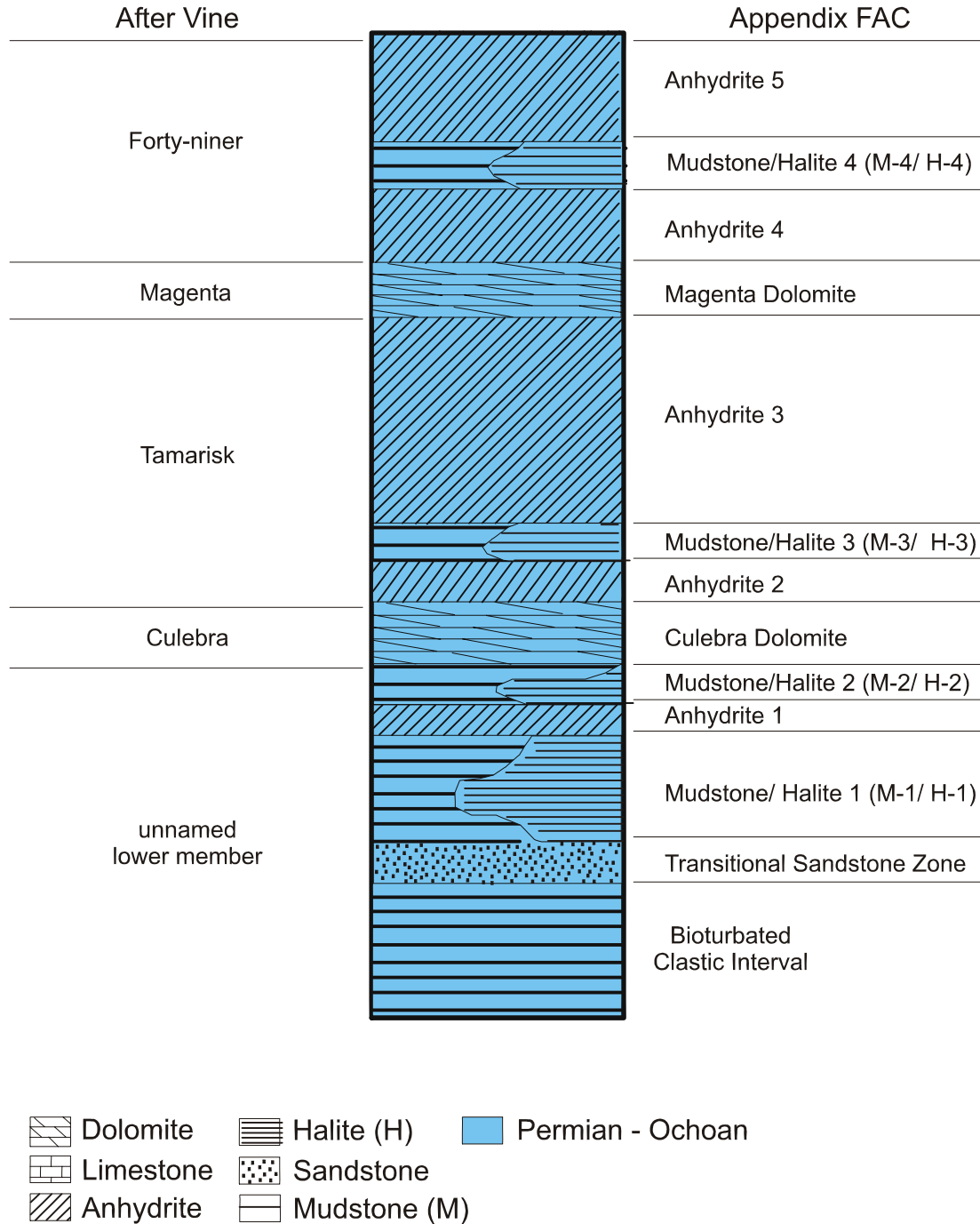
The Salado is of primary importance to the containment of waste. Because it is the principal natural barrier, many of the properties of the Salado have been characterized by the DOE, and numerical codes are used by the DOE to simulate the natural processes within the Salado that affect the disposal system performance.

Two conceptual models of the Salado are used in the performance assessment. One models the creep closure properties of the Salado and the other, the hydrological properties. The creep closure of the Salado is discussed in *Appendix PA, Attachment Appendix* ~~Appendix~~ *PORSURF*. This model uses key parameters derived from both in-situ measurements and laboratory testing on Salado core samples. Summaries of these parameters are in *Butcher (1997)*. Appendix *PORSURF* Attachment 1, Table 2.

The second conceptual model is titled the Salado conceptual model and is discussed in Section 6.4.5. This model divides the Salado into two lithologic units: impure halite and Salado interbeds. The impure halite in this conceptual model is characterized entirely by its hydrological parameters as shown in Table 6-16. The interbeds are characterized by both hydrological parameters in Table 6-17 and fracture properties in Table 6-19. This latter information is needed since the model in Section 6.4.5.2 incorporates the possibility of interbed fracturing should pressures in the repository become high enough. The modeling assumptions surrounding the fracturing model are discussed in Appendix *PA, Attachment* *MASS*, Section ~~MASS-13.3~~.

2.1.3.5 The Rustler

The Rustler is the youngest evaporite-bearing formation in the Delaware Basin. It was originally named by Richardson in 1904 for outcrops in the Rustler Hills of Culberson County, Texas. Adams (1944, p. 1614) first used the names Culebra Member and Magenta Member to describe the two carbonates in the formation, indicating that Lang favored the names, although Lang did not use these names to subdivide the Rustler in his 1942 publication. Vine (1963, p. B1) extensively described the Rustler in Nash Draw and proposed the four formal names and one informal term that ~~are still~~ *were* used for the stratigraphic subdivisions of the Rustler. These are as follows (from the base): unnamed lower member, Culebra Dolomite Member, Tamarisk Member, Magenta Dolomite Member, and Forty-niner Member (~~Figure 2-9~~ *Figure 2-14*). ~~Though it has been suggested by some investigators that the unnamed lower member might be named the Los Medaños Member, this nomenclature has not been formalized and is not adopted here.~~ *Powers and Holt (1999) formalized the nomenclature for the lower Rustler, naming the Los Medaños Member for the exposures of the former "unnamed lower member" in the WIPP shafts and in boreholes in the vicinity of Los Medaños near the WIPP site. Four* ~~Two~~ studies of the Rustler since Vine's 1963 work contribute important information about the stratigraphy, sedimentology, and regional relationships while examining more local details as well. Eager (1983) published a report on relationships of the Rustler observed in the southern Delaware Basin as part of sulfur exploration in the area. Holt and Powers (1988, Section 5.0), reproduced



CCA-027-2

Figure 2-9. Rustler Stratigraphy (From Appendix FAC, Figure 3.2)

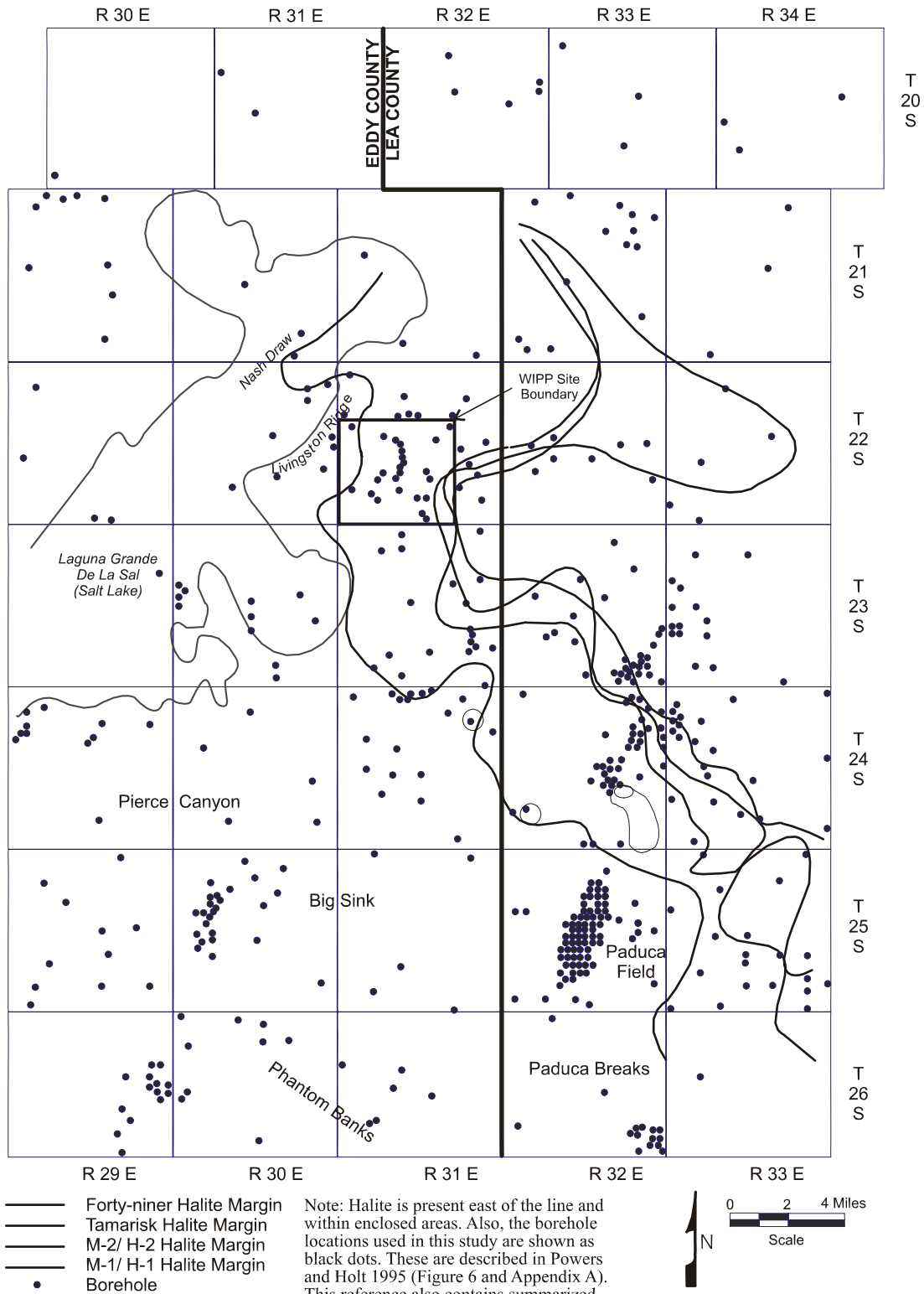
in this application as *CCA Appendix FAC, reported the details of sedimentologic and stratigraphic studies of WIPP shafts and cores as well as of geophysical logs from about 600 boreholes in southeastern New Mexico. Their work resulted in the more detailed subdivisions of the Rustler indicated in the right-hand column of Figure 2-14.*

The Rustler is regionally extensive; a similar unit in the Texas panhandle is also called the Rustler. Within the area around WIPP, evaporite units of the Rustler are interbedded with significant siliciclastic beds and the carbonates. Both the Magenta and the Culebra extend regionally beyond areas of direct interest to the WIPP. In the general area of the WIPP, both the Tamarisk and the Forty-niner have similar lithologies: lower and upper sulfate beds and a middle unit that varies principally from mudstone to halite from west to east (~~Figure 2-9~~) (*Figure 2-14*). In a general sense, halite in the ~~unnamed lower member~~ *Los Medaños* broadly persists to the west of the WIPP site, and halite is found east of the center of the WIPP in the Tamarisk and the Forty-niner (~~Figure 2-10~~) (*Figure 2-15*).

~~Two different explanations have been used to account for the halite distribution. An implicit assumption in many documents is that halite was originally deposited relatively uniformly in the noncarbonate members across southeastern New Mexico, including the WIPP site. The modern distribution resulted from dissolution of Rustler halite to the west of the site. As shown in Appendix FAC, sedimentary features and textures within WIPP shafts and cores led Holt and Powers to propose an alternative interpretation of depositional facies for the mudstone-halite units: halite was dissolved syndepositionally from mudflat facies, especially to the west, and was redeposited in a halite pan to the east.~~ *Two different explanations have been proposed over the history of the project to account for the observed distribution of halite in the non-dolomite members of the Rustler. The earliest researchers (e.g., Bachman [1985] and Snyder [1985]) assumed that halite had originally been present in all the non-sulfate intervals of the Forty-niner, Tamarisk, and Los Medaños Members, and that its present-day absence reflected post-depositional dissolution.*

An alternative interpretation was presented by Holt and Powers (1988) following detailed mapping of the Rustler exposed in the WIPP ventilation (now waste) and exhaust shafts in 1984. Fossils, sedimentological features, and bedding relationships were identified in units that had previously been interpreted from boreholes as dissolution residues. Cores from existing boreholes, outcrops, geophysical logs, and petrographic data were also reexamined to establish facies variability across the area.

As a result of these studies, the Rustler was interpreted to have formed in variable depositional environments, including lagoon and saline playas, with two major episodes of marine flooding which produced the carbonate units. Sedimentary structures were interpreted to indicate syndepositional dissolution of halite from halitic mudstones around a saline playa and fluvial transport of more distal clastic sediments. The halite in the Rustler, by this interpretation, has a present-day distribution similar to that at the time the unit was deposited. Some localized dissolution of halite may have occurred along the depositional margins, but not over large areas. Hence, the absence of halite in Rustler members at the WIPP site more generally reflects non-deposition than dissolution.



CCA-028-2

Figure 2-10. Halite Margins in the Rustler

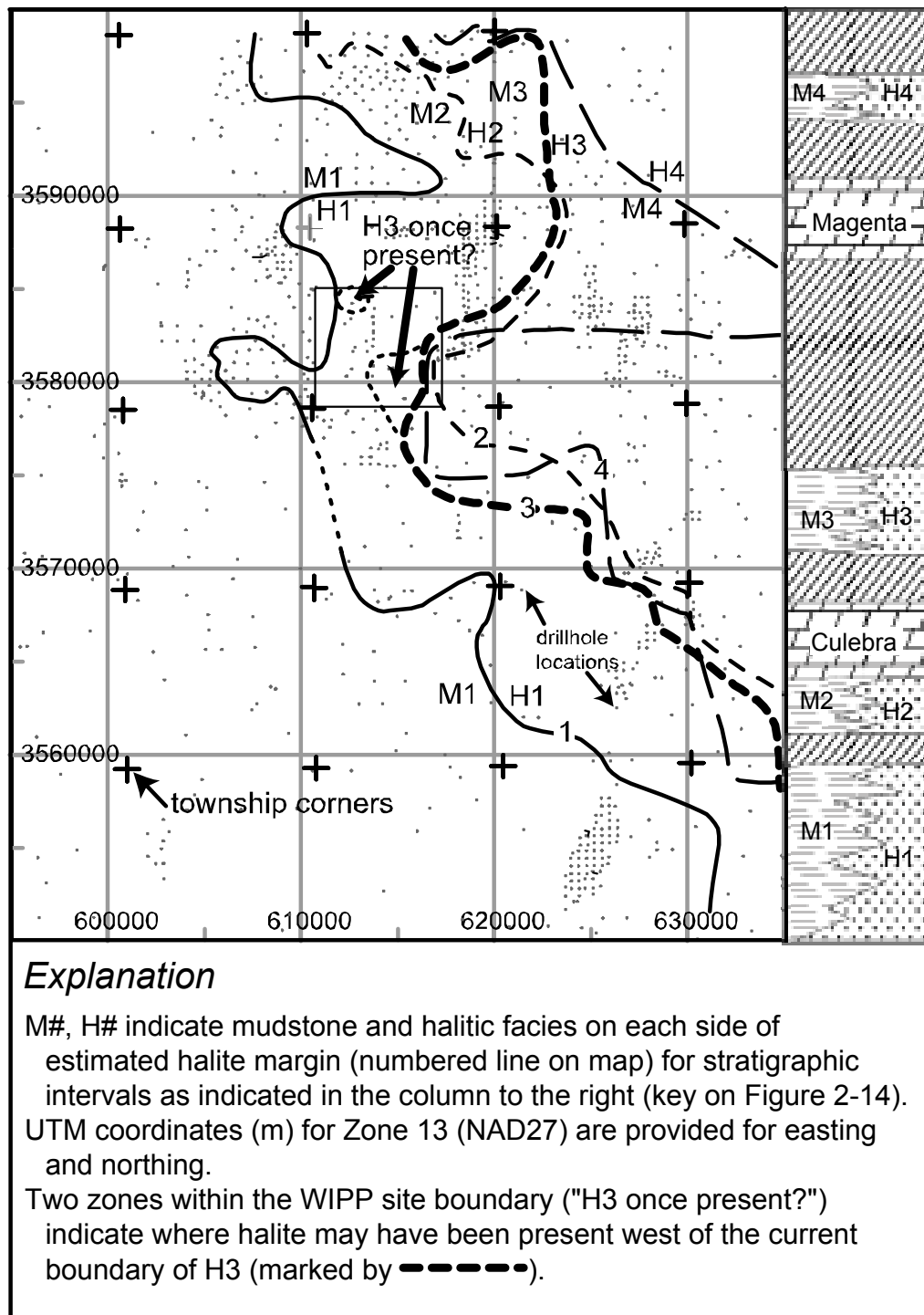


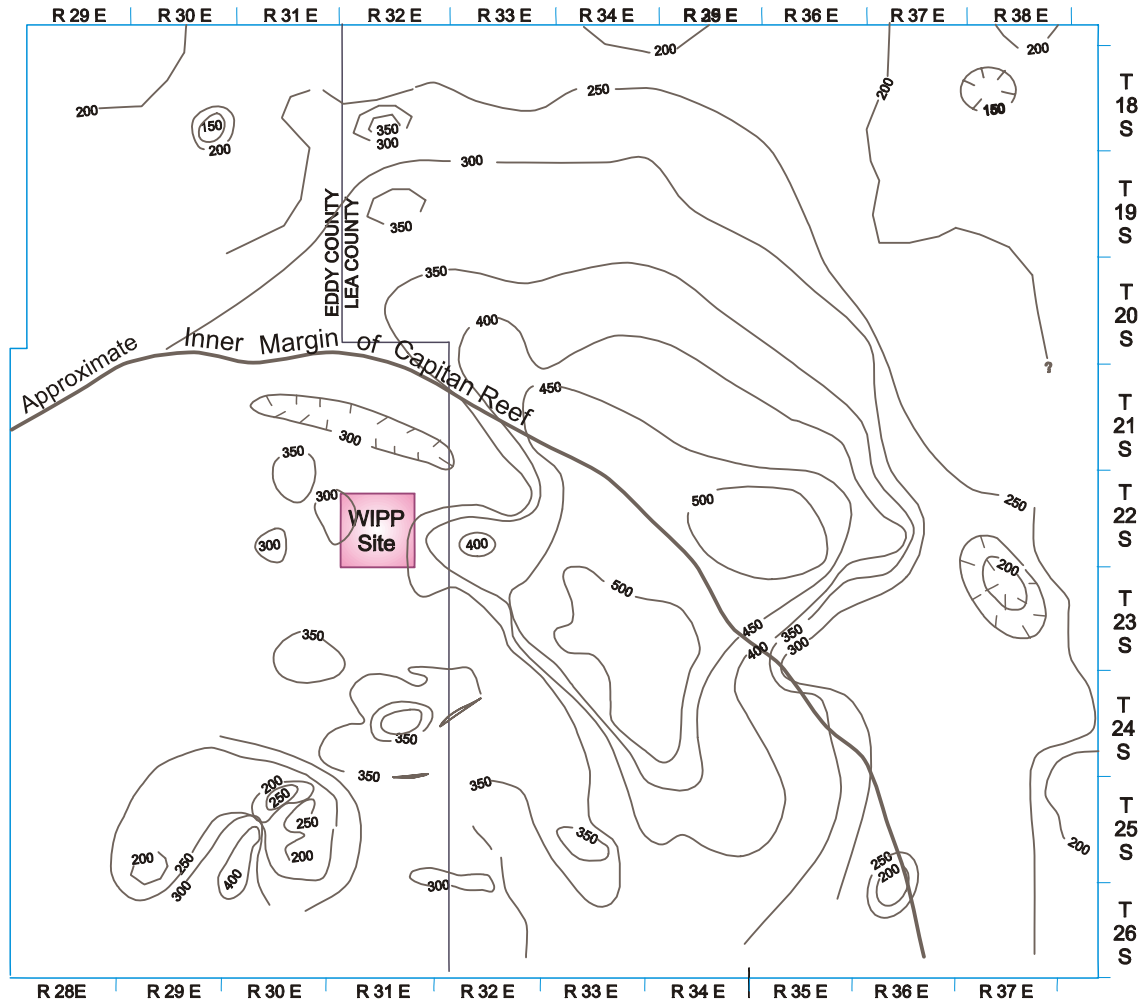
Figure 2-15. Halite Margins for the Rustler Formation Members

This hypothesis was tested and refined by subsequent investigations (e.g., Powers and Holt 1990, 1999, 2000; Holt and Powers 1990a) and is now considered the accepted explanation for the present-day distribution of halite in the Rustler. Powers and Holt (1999) thoroughly described the sedimentary structures and stratigraphy of the Los Medaños as part of the procedure for naming the unit. This shows the basis for interpreting the depositional history of the member and for rejecting significant post-burial dissolution of halite in that unit. Powers and Holt (2000) further describe the lateral facies relationships in other Rustler units, especially the Tamarisk, developed on sedimentologic grounds, and rejected the concept of broad, lateral dissolution of halite from the Rustler across the WIPP site area.

As discussed in Section 2.2.1.4, regional Culebra transmissivity shows about six orders of magnitude variation across the area around the site and about three orders of magnitude across the site itself. Although some investigators have called attention to the ~~correlation~~ **broad relationship** between the distribution of halite in the Rustler and variations in Culebra transmissivity and have attributed the variation to fracturing resulting from postdepositional dissolution of Rustler halite (see, for example, Snyder, 1985, p. 10; and **CCA** Appendix DEF, Section DEF-3.2), ~~Holt and Powers' work~~ **CCA** Appendix FAC **and Powers and Holt 1990, 1999, 2000**) largely rule out this explanation. Variations in transmissivity of the Culebra ~~(Beauheim and Holt 1990) have also been~~ were correlated qualitatively to the thickness of overburden above the Culebra (see discussion in Section 2.1.5.2), the amount of dissolution of the upper Salado, and the distribution of gypsum fillings in fractures in the Culebra **(Beauheim and Holt 1990). Subsequently, Holt and Yarbrough (2002) and Powers et al. (2003) related the variation in Culebra transmissivity more quantitatively to overburden thickness and dissolution of upper Salado halite.** The DOE believes that variations in Culebra transmissivity are primarily caused by the relative abundance of open fractures in the unit, which may be related to each of these factors. As discussed in Section 6.4.6.2 and Appendix **PA, Attachment** TFIELD, uncertainty in spatial variability in the transmissivity of the Culebra has been incorporated in the PA.

In the region around the WIPP, the Rustler reaches a maximum thickness of more than 152 m (500 ft) (Figure 2-44**16**), while it is about 91 to 107 m (300 to 350 ft) thick within most of the WIPP site. Much of the difference in Rustler thickness can be attributed to variations in the amount of halite contained in the formation. Variation in Tamarisk thickness accounts for a larger part of thickness changes than do variations in either the ~~unnamed lower member~~ **Los Medaños** or the Forty-niner. Details of the Rustler thickness can be found in **CCA** Appendix GCR, 4-39 to 4-42 and Figure 4.3-8. See also **CCA** Appendix FAC.

Much project-specific information about the Rustler is contained in **CCA** Appendix FAC. The WIPP shafts were a crucial element in Holt and Powers' 1988 study, exposing features not previously reported. Cores were available from several WIPP boreholes, and their lithologies were matched to geophysical log signatures to extend the interpretation throughout a larger area in southeastern New Mexico. These data are included in ~~Appendix II to~~ **CCA** Appendix FAC, **Appendix II.**



Contour Interval = 50 feet

Source: Powers and Holt (1990)

CCA-029-2

Figure 2-11. Isopach Map of the Entire Rustler

2.1.3.5.1 ~~Unnamed Lower Member~~ *Los Medaños Member*

The unit formerly referred to as the unnamed lower member has been named the Los Medaños Member. The ~~unnamed lower member~~ *Los Medaños* rests on the Salado with apparent conformity at the WIPP site. It consists of significant proportions of bedded and burrowed siliciclastic sedimentary rocks with cross-bedding and fossil remains. These beds record the transition from strongly evaporative environments of the Salado to saline lagoonal environments. The upper part of the ~~unnamed lower member~~ *Los Medaños* includes halitic and sulfatic beds within clastics. Holt and Powers (*CCA Appendix FAC*, pp. 6-8) *and Powers and Holt (1999)* interpret these as facies changes within a saline playa or lagoon environment, not dissolution residues from postdepositional dissolution.

According to ~~Holt and Powers (CCA Appendix FAC~~, Figure 4-4, the ~~unnamed lower member~~ *Los Medaños* ranges in thickness from about 29 to 38 m (96 to 126 ft) within the site boundaries. The maximum thickness recorded during that study was 63 m (208 ft) southeast of the WIPP site. An isopach of the ~~unnamed lower member~~ *Los Medaños* is shown as Figure 4-7 in *CCA Appendix FAC*.

Halite is present in the M1/H1 unit of the ~~unnamed lower member~~ *Los Medaños* west of most of the site area (see ~~Figure 2-10~~ *Figure 2-15* for an illustration of the halite margins). *The drilling initiated during CRA-2004 preparation to investigate Culebra transmissivity variations based on overburden and Salado dissolution will develop additional detailed information about distribution of halite in the Los Medaños.* Cross-sections based on geophysical log interpretations by Holt and Powers (*CCA Appendix FAC*) *and Powers and Holt (2000)* show that the unit is thicker to the east where the halite is more abundant. The ~~unnamed lower member~~ *Los Medaños* is incorporated into the conceptual model as described in Section 6.4.6.1. Model parameters are in Appendix *PA, Attachment PAR*, Table ~~PAR-34~~ *27*.

2.1.3.5.2 The Culebra *Dolomite Member*

The Culebra rests with apparent conformity on the ~~unnamed lower member~~, *Los Medaños*, though the underlying unit ranges from claystone to its lateral halitic equivalent in the site area. West of the WIPP site, in Nash Draw, the Culebra is disrupted from dissolution of underlying halite. Holt and Powers (*CCA Appendix FAC*, Section 8.9.3) principally attribute this to dissolution of Salado halite, *noting the presence of sedimentologic features in the lower Rustler (see also Powers and Holt 1999).* while Snyder (1985, 6) indicates that salt was dissolved postdepositionally from the ~~unnamed lower member~~. These alternative interpretations offer differing explanations of how the existing Rustler hydrologic system developed and might continue to develop. Culebra hydrology and its significance to disposal system performance are discussed in detail in Section 2.2.1.4.1.2.

The Culebra was described by Robinson and Lang (1938, *p.* 83) as a dolomite 11 meters (35 feet *ft*) in thickness. The Culebra is generally brown, finely crystalline, locally argillaceous and arenaceous dolomite with rare to abundant vugs with variable gypsum and anhydrite filling; Adams (1944, *p.* 1614) noted that oölites are present in some outcrops as well. Holt and Powers (*CCA Appendix FAC*, *pp.* 5 - 11) describe the Culebra features in detail, noting that most of the Culebra is microlaminated to thinly laminated, while some zones display no depositional fabric.

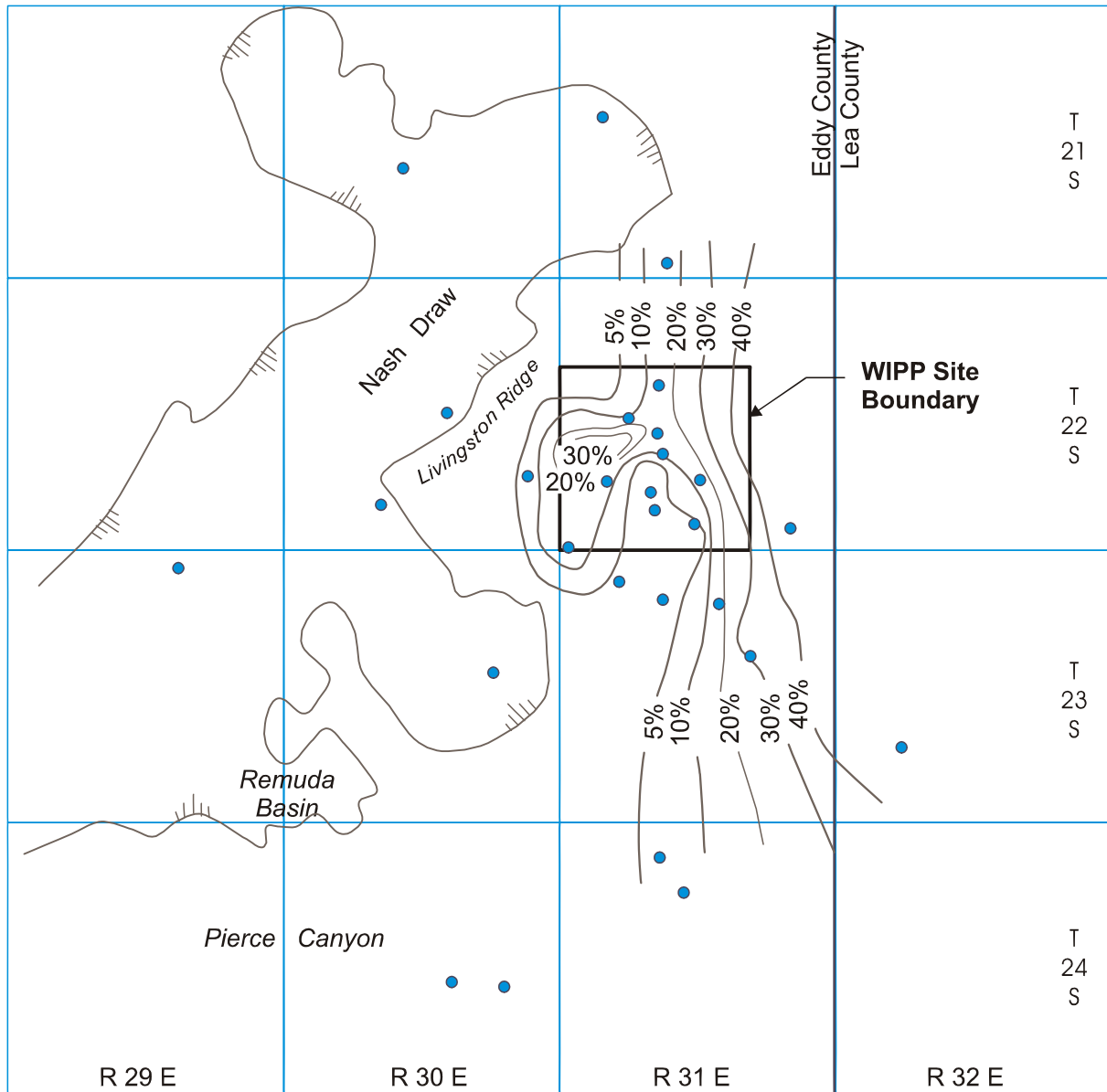
Holt and Powers (1984) described an upper interval of the Culebra consisting of medium brown, microlaminated carbonate that thickens up to 0.6 m (2 ft) in the vicinity of dome structures and is of probable algal origin. This is underlain by a 0.64-to-2.56 m (2.1-to-8.4-ft) thick bed of cohesive black claystone. Because of the unique organic composition of this thin layer, Holt and Powers (1988) did not include it in the Culebra for thickness computations, and this will be factored into discussions of Culebra thickness. Based on core descriptions from the WIPP project, Holt and Powers (CCA Appendix FAC) concluded that there is very little variation of depositional sedimentary features throughout the Culebra.

Vugs are an important part of Culebra porosity. They are commonly zoned parallel to bedding. In outcrop, vugs are commonly empty. In the subsurface, vugs range from open to partially filled or filled with anhydrite, gypsum, or clay (Holt and Powers 1990a, pp. 3-18 to 3-20). Lowenstein (1987, pp. 19 - 20) noted similar features. Holt and Powers (CCA Appendix FAC) attributed vugs partly to syndepositional growth as nodules and partly as later replacive textures. Lowenstein (1987, pp. 29 - 31) also described textures related to later replacement and alteration of sulfates. Vug or pore fillings vary across the WIPP site and contribute to the porosity structure of the Culebra. As pointed out by Holt and Powers (see CCA Appendix FAC, Section 8.8), natural fractures filled with gypsum are common east of the WIPP site center and in a smaller area west of the site center (Figure 2-12). Section 2.1.5.2 discusses Culebra fracture mechanisms. Additional discussion of Culebra fractures and their role in groundwater flow and transport is in Section 2.2.1.4.1.1, Appendix PA, Attachment MASS, Sections MASS.14.24 and MASS.15.

Holt (1997) reexamined geological and hydrological data for the Culebra and developed a conceptual model for transport processes. In this document, Holt (1997) recognized several porosity types for the Culebra, and separated four Culebra units (CU) informally designated CU-1 through CU-4 from top to bottom. CU-1 differs from underlying units because it has been disrupted very little by syndepositional processes. Microvugs and interbeds provide most of the porosity, and the permeability of CU-1 is relatively limited. CU-2 and CU-3 likely contribute most of the flow in the Culebra, and the significant difference is that CU-2 includes more persistent silty dolomite interbeds. CU-2 and CU-3 include "small-scale bedding-plane fractures, networks of randomly oriented small-scale fractures and microfractures, discontinuous silty dolomite interbeds, large vugs hydraulically connected with microfractures and small-scale fractures, microvugs hydraulically connected with microfractures and intercrystalline porosity, blebs of silty dolomite interconnected with microfractures and intercrystalline porosity, and intercrystalline porosity" (Holt 1997, p. 2-19). Bedding-plane fractures dominate CU-4 at the base of the Culebra, and the unit shows some brittle deformation. CU-4 has not been isolated for hydraulic testing.

Holt (1997, p. 1) also related porosity and solute transport, conceptualizing the medium "as consisting of advective porosity, where solutes are carried by the groundwater flow, and fracture-bounded zones of diffusive porosity, where solutes move through slow advection or diffusion." Holt (1997) noted that length or time scales will govern how each porosity type will contribute to solute transport.

Sewards et al. (1991, pp. IX-1) report that the Culebra is primarily dolomite with some quartz and clay. Clay minerals include corrensite, illite, serpentine, and chlorite. Clay occurs in bulk



● Boreholes Examined
Contour Interval = 10%
5% Line Shown for Clarity



0 2 4 Miles

CCA-030-2

1 Source: Beauheim and Holt (1990)

2 **Figure 2-1217. Percentage of Natural Fractures in the Culebra Filled with Gypsum**

3

rock and on fracture surfaces. Even though these clays occur, the conceptual model discussed in Section 6.4.6.2.1 takes no credit for their presence.

In the WIPP area, the Culebra varies in thickness. Depending on the area considered and the horizons chosen for the upper and lower boundaries of the Culebra, different data sources provide varying estimates (Table 2-3). Holt and Powers ([CCA Appendix FAC, p. 4-4](#)) considered the organic-rich layer at the Culebra-Tamarisk contact separately from the Culebra in interpreting geophysical logs.

Comparing data sets, Holt and Powers ([CCA Appendix FAC](#)) typically interpret the Culebra as being about 1 m (about 3 ft) thinner than do other interpretations. In general, this reflects the difference between including or excluding the unit at the Culebra-Tamarisk contact. ~~Holt and Powers~~ The isopach of the Culebra is shown as Figure 4.8 in [CCA Appendix FAC](#).

LaVenue et al. (1988, Table B.1) calculated a mean thickness of 7.7 meters (25 feet [ft](#)) for the Culebra within their model domain based on thicknesses measured in 78 boreholes. Mercer (1983, reproduced here as [CCA Appendix HYDRO](#)) reported a data set similar to that of LaVenue et al. ([Table 1 of Appendix HYDRO](#)). The borehole database for the region of interest is provided in [CCA Appendix BH](#).

The treatment of the Culebra in the conceptual model is discussed in Section 6.4.6.2 and associated parameter values in Table 6-20. A more thorough discussion of Culebra features, such as fractures, is provided in Appendix [PA, Attachment MASS](#), Section MASS.15.

Table 2-3. Culebra Thickness Data Sets

Source	Data Set Location								
	T22S, R31E			T21-23S, R30-32E			Entire Set		
	n	ave	std dev	n	ave	std dev	n	ave	std dev
Richey (1989)	7	7.5 m	1.04 m	115	7.9 m	1.45 m	633	7.7 m	1.65 m
CCA Appendix FAC	35	6.4 m	0.59 m	122	7.0 m	1.26 m	508	6.5 m	1.89 m
LaVenue et al. (1988)							78	7.7 m	
Source	WIPP Potash Drillholes								
Jones (1978)				21	7.5 m	0.70 m			
CCA Appendix FAC				21	6.3 m	0.50 m			

Legend:

n number of boreholes or data points
ave average or mean
std dev standard deviation
m meters

2.1.3.5.3 The Tamarisk [Member](#)

Vine (1963, B14) named the Tamarisk for outcrops near Tamarisk Flat in Nash Draw. Outcrops of the Tamarisk are distorted, and subsurface information was used to establish member

characteristics. Vine reported two sulfate units separated by a siltstone, about 1.5 m (5 ft) thick, interpreted by Jones et al. in 1960 as a dissolution residue.

The Tamarisk is generally conformable with the underlying Culebra. The transition is marked by an organic-rich unit interpreted as being present over most of southeastern New Mexico. The Tamarisk around the WIPP site consists of lower and upper sulfate units separated by a unit that varies from mudstone (generally to the west) to mainly halite (to the east). Near the center of the WIPP site, the lower anhydrite was partially eroded during deposition of the middle mudstone unit, as observed in the WIPP waste-handling and exhaust shafts. The lower anhydrite was completely eroded at WIPP-19. Before shaft exposures were available, the lack of the Lower Tamarisk anhydrite at WIPP-19 was interpreted as the result of dissolution and the mudstone was considered a cave filling.

Jones (1978) interprets halite to be present east of the center of the WIPP site based on geophysical logs and drill cuttings. Based mainly on cores and cuttings records from the WIPP potash drilling program, Snyder prepared a map in 1985 showing the halitic areas of each of the noncarbonate members of the Rustler (Snyder 1985, Figure 4). A very similar map based on geophysical log characteristics was prepared by Holt and Powers (1988).

~~Holt and Powers (CCA Appendix FAC) describes the mudstones and halitic facies in the middle of the Tamarisk and postulate that the unit formed in a salt-pan-to-mudflat system. Holt and Powers Powers and Holt (2000) cited sedimentary features and the lateral relationships as evidence of syndepositional dissolution of halite in the marginal mudflat areas. In contrast, other investigators interpreted the lateral decrease in thickness and absence of halite to the west as evidence of postdepositional dissolution (see, for example, Jones et al. 1960, Jones 1978, and Snyder 1985).~~

The Tamarisk thickness varies greatly in southeastern New Mexico, principally as a function of the thickness of halite in the middle unit. Within T22S, R31E, the thickness ranges from 26 to 56 m (84 to 184 ft) for the entire Tamarisk and from 2 to 34 m (6 to 110 ft) for the interval of mudstone-halite between lower and upper anhydrites (CCA Appendix FAC, Figures 4-9 and 4-11). Expanded geophysical logs with corresponding lithology illustrate some of the lateral relationships for this interval (Figure 2-18; see also Powers and Holt 2000).

The Tamarisk is modeled as discussed in Section 6.4.6.3. Tamarisk parameter values are given in Appendix PA, Attachment PAR, Table PAR-24.

2.1.3.5.4 The Magenta Dolomite Member

Adams (1944, p. 1614) attributes the name Magenta Member to Lang, based on a feature named Magenta Point north of Laguna Grande de la Sal. According to ~~Holt and Powers~~ CCA (Appendix FAC), the Magenta is a gypsiferous dolomite with abundant primary sedimentary structures and well-developed algal features. It does not vary greatly in sedimentary features

1
2
3

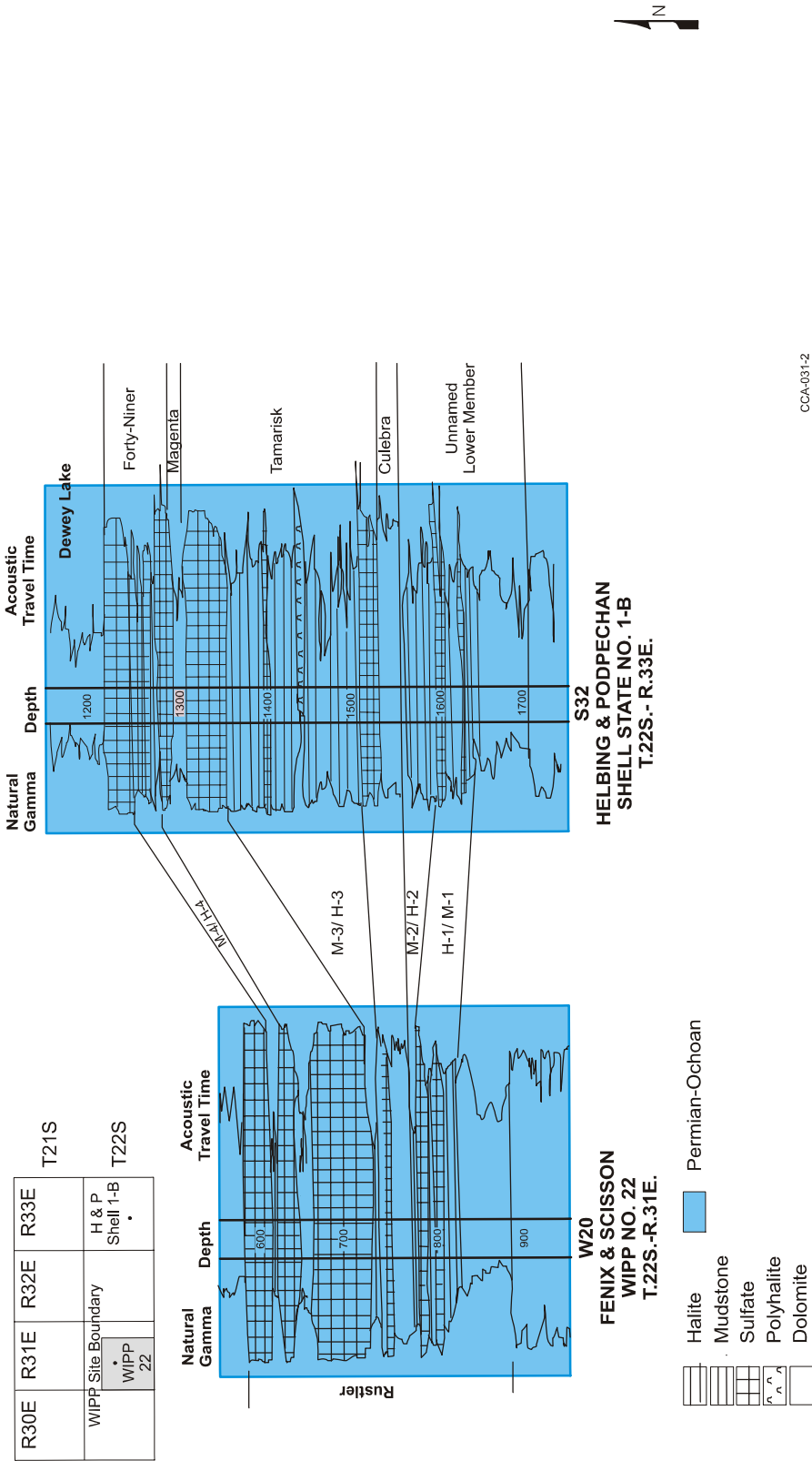


Figure 2-4318. Log Character of the Rustler Emphasizing Mudstone-Halite Lateral Relationships

across the site area. ~~Holt and Powers~~ (CCA Appendix FAC, 5-22) reported that the Magenta varies from 7.0 to 8.5 m (23 to 28 ft) around the WIPP site. ~~Holt and Powers~~ CCA Appendix FAC did not ~~prepare~~ include a regional Magenta isopach. Additional detail on the Magenta can be found in Section 4.3.2 of CCA Appendix GCR and in Sections 4.1.4, 4.2.4, and 5.4 of CCA Appendix FAC. The Magenta is included in the conceptual model as discussed in Section 6.4.6.4. Modeling values are in Table 6-24.

2.1.3.5.5 The Forty-niner Member

Vine (1963) named the Forty-niner for outcrops at Forty-niner Ridge in eastern Nash Draw, but the unit is poorly exposed there. In the subsurface around the WIPP, the Forty-niner consists of basal and upper sulfates separated by a mudstone. It is conformable with the underlying Magenta. As with other members of the Rustler, geophysical log characteristics can be correlated with core and shaft descriptions to extend geological inferences across a large area (Holt and Powers 1988).

The Forty-niner varies from 13 to 23 m (43 to 77 ft) thick within T22S, R31E. East and southeast of the WIPP, the Forty-niner exceeds 24 m (80 ft), and some of the geophysical logs from this area indicate that halite is present in the beds between the sulfates. A regional isopach map of the Forty-niner is in CCA Appendix FAC (Figure 4-13). See also Powers and Holt (2000).

Within the waste-handling shaft, the Forty-niner mudstone displayed sedimentary features and bedding relationships indicating sedimentary transport. ~~The mudstone has commonly been interpreted as a residue from the dissolution of halitic beds because it is thinner where there is no halite.~~ These beds are not known to have been described in detail prior to mapping in the waste-handling shaft at WIPP, and the features found there led Holt and Powers (CCA Appendix FAC) to reexamine the available evidence for, and interpretations of, dissolution of halite in Rustler units.

The inclusion of the Forty-niner in the conceptual model is discussed in Section 6.4.6.5.

2.1.3.6 The Dewey Lake Redbeds

The nomenclature for rocks included in the Dewey Lake Formation was introduced during the 1960s to clarify relationships between these rocks assigned to the Upper Permian and the Cenozoic Gatuña Formation ~~(hereafter referred to as the Gatuña).~~

There are three main sources of data about the Dewey Lake in the area around WIPP. Miller reported the petrology of the unit in 1955 and 1966. Schiel (1988) described outcrops in the Nash Draw areas and interpreted geophysical logs of the unit in southeastern New Mexico and west Texas to infer the depositional environments and stratigraphic relationships in 1988 and 1994. Holt and Powers (1990a) were able to describe the Dewey Lake in detail at the AIS for WIPP in 1990, confirming much of Schiel's (1988) information and adding data regarding the Lower Dewey Lake.

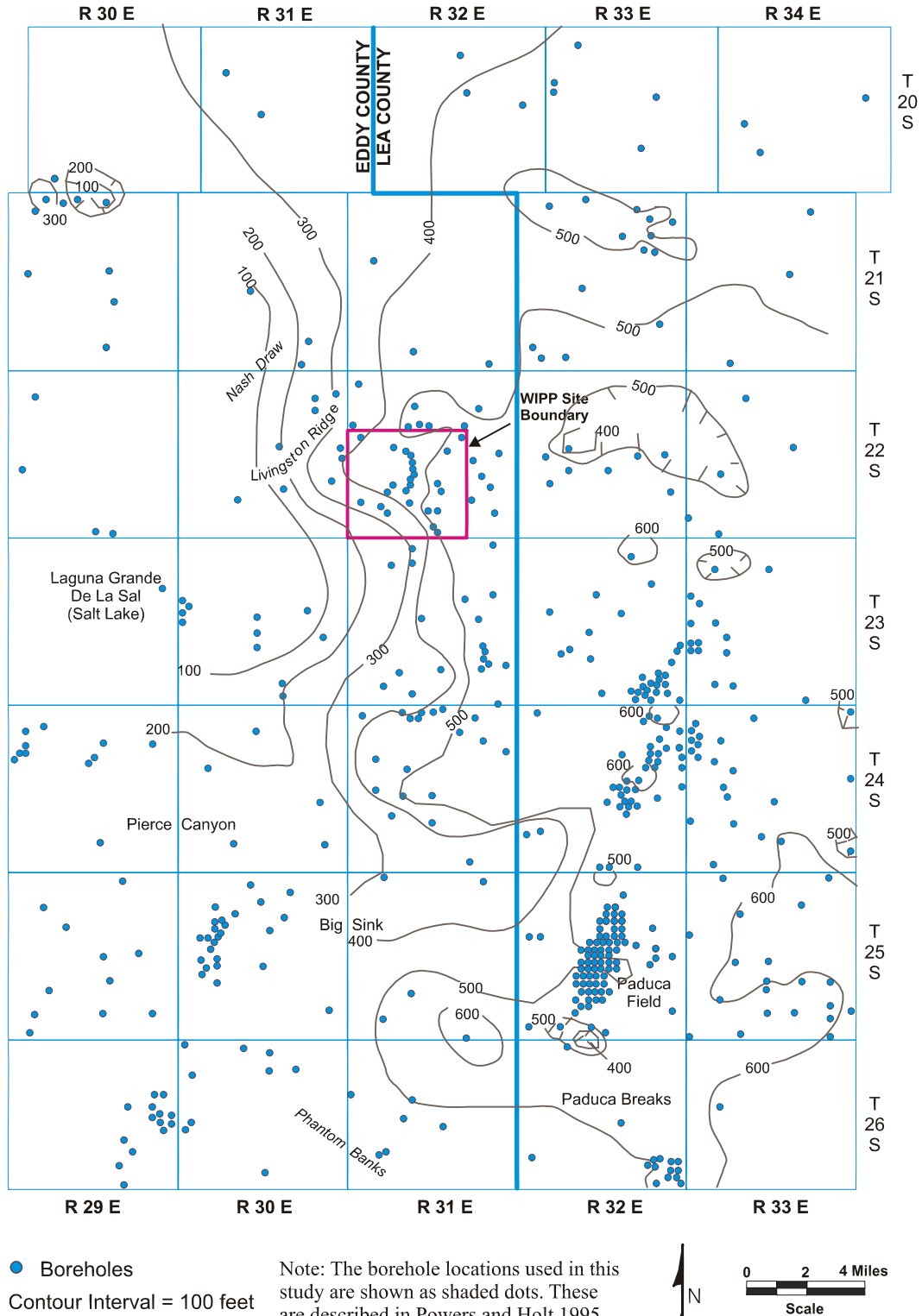
The Dewey Lake overlies the Rustler conformably, though local examples of the contact (for example, the AIS described by Holt and Powers in (1990a) show minor disruption by dissolution

of some of the upper Rustler sulfate. The formation is predominantly reddish-brown fine sandstone to siltstone or silty claystone with greenish-gray reduction spots. Thin bedding, ripple cross-bedding, and larger channeling are common features in outcrops, and additional soft sediment deformation features and early fracturing from the lower part of the formation are described by Holt and Powers (1990a). Schiel (1988, p. 143; 1994, p. 9) attributed the Dewey Lake to deposition on “a large, arid fluvial plain subject to ephemeral flood events.”

There is ~~little~~**no** direct faunal or radiometric evidence of the age of the Dewey Lake **in the vicinity of the WIPP site**. It is assigned to the Ochoan Series, **considered historically to be of** Late Permian **in** age, and it is regionally correlated with units of similar lithology and stratigraphic position. Schiel (1988, 1994) reviewed the limited radiometric data from lithologically similar rocks (Quartermaster Formation) and concluded that much of the unit could be Early Triassic in age. ***Renne et al. (1996) resampled tephra from the Quartermaster in the Texas panhandle area and found that radiometric data support the idea that the Quartermaster is mainly Triassic in age rather than Permian. Others have begun to infer as well that the Dewey Lake in the vicinity of the WIPP may be mostly Triassic (e.g., Powers and Holt 1999). These age relationships continue to be of academic interest because of the geologic significance of the Permo-Triassic boundary, but there is no significance for waste isolation at the WIPP.***

Near the center of the WIPP site, Holt and Powers (1990a, Figure 5) mapped 152 m (498 ft) of the Dewey Lake (Figure 2-14**19**). The formation is thicker to the east (Schiel 1994, Figure 2) of the WIPP site, in part because western areas were eroded before the overlying Triassic rocks were deposited.

The Dewey Lake contains fractures, which are filled with minerals to varying degrees. Both cements and fracture fillings have been examined and used to infer groundwater infiltration. Holt and Powers (1990a, pp. 3-10) described the Dewey Lake as cemented by carbonate above 50 m (164.5 ft) in the AIS; some fractures in the lower part of this interval were also filled with carbonate, and the entire interval surface was commonly moist. Below this point, the cement is harder **and more commonly anhydrite (Powers 2003b)**, the shaft is dry, and fractures are filled with gypsum. ***Powers (2002c; 2003b) reports core and geophysical log data supporting these vertical changes in natural mineral cements in the Dewey Lake over a larger region at a horizon that is believed to underlie known natural groundwater occurrences in the Dewey Lake. In areas where the Dewey Lake has been exposed to weathering after erosion of the overlying Santa Rosa, this cement boundary tends to generally parallel the eroded upper surface of the Dewey Lake, suggesting that weathering has affected the location of the boundary. Where the Dewey Lake has been protected by overlying rocks of the Santa Rosa, the cement change appears to be stratigraphically controlled but the data points are too few to be certain.*** Holt and Powers (1990a, pp. 3 - 11, Figure 16) suggested that the cement change might be related to infiltration of meteoric water. They also determined that some of the gypsum-filled fractures are syndepositional. Dewey Lake fractures include horizontal to subvertical trends, some of which were mapped in detail (Holt and Powers 1986, Figures 6, 7, and 8).



CCA-032-2

Figure 2-14/19. Isopach of the Dewey Lake

Lambert (~~in Siegel et al.~~ (1991, *pp.* 5 - 65) analyzed the deuterium/hydrogen (D/H) ratios of gypsum in the Rustler and gypsum veins in the Dewey Lake. He suggests that none of the gypsum formed from evaporitic fluid such as Permian seawater but that the D/H ratios all show influence of meteoric water. Furthermore, Lambert (~~in Siegel et al.~~ 1991, 5 – 66) infers that the gypsum D/H ratio is not consistent with modern meteoric water; it may, however, be consistent with older meteoric fluids. There is no obvious correlation with depth to indicate infiltration. Strontium isotope ratios ($^{87}\text{Sr}/^{86}\text{Sr}$) indicate no intermixing or homogenization of fluids between the Rustler and the Dewey Lake, but there may have been lateral movement of water within the Dewey Lake (~~Lambert Siegel et al.~~ 1991, *pp.* 5 - 54). Dewey Lake carbonate-vein material shows a broader range of strontium ratios than does surface caliche, and the ratios barely overlap.

The treatment of the Dewey Lake in the conceptual model can be found in Section 6.4.6.6. Dewey Lake parameter values are in Table 6-25.

2.1.3.7 The Santa Rosa

There have been different approaches to the nomenclature of rocks of Triassic age in southeastern New Mexico. Bachman (1974) generally described the units ~~in 1974~~ as “Triassic, undivided” or as the Dockum Group, without dividing it. Vine ~~in~~ (1963) used “Santa Rosa Sandstone,” and Santa Rosa has become common usage. Lucas and Anderson (1993a, 1993b) import other formation names that are unlikely to be useful for WIPP.

The Santa Rosa has been called disconformable over the Dewey Lake by Vine (1963, B25). These rocks have more variegated hues than the underlying uniformly colored Dewey Lake. Coarse-grained rocks, including conglomerates, are common, and the formation includes a variety of cross-bedding and sedimentary features (Lucas and Anderson 1993a, *pp.* 231 - 235).

Within the WIPP site boundary, the Santa Rosa is relatively thin to absent (Figure 2-45~~20~~). At the AIS, Holt and Powers (1990a, Figure 5) attributed about 0.6 m (2 ft) of rock to the Santa Rosa. The Santa Rosa is a maximum of 78 m (255 ft) thick in potash holes drilled for WIPP east of the site boundary. The Santa Rosa is thicker to the east. *The geologic data from design studies (Sergent et al. 1979) were incorporated with data from drilling to investigate shallow subsurface water in the Santa Rosa to provide structure and thickness maps of the Santa Rosa in the vicinity of the WIPP surface structures area (Powers 1997). These results are consistent with the broader regional distribution of the Santa Rosa.*

The Santa Rosa and younger rocks are modeled in the WIPP *PA* as a single region as discussed in Section 6.4.6.7. The model parameters for this supra-Dewey Lake region are given in Table 6-26.

2.1.3.8 The Gatuña Formation

Lang (in Robinson and Lang 1938, *p.* 84) named the Gatuña for outcrops in the vicinity of Gatuña Canyon in the Clayton Basin. Rocks now attributed to the Gatuña in Pierce Canyon were once included in the Pierce Canyon Formation with rocks now assigned to the Dewey Lake. The

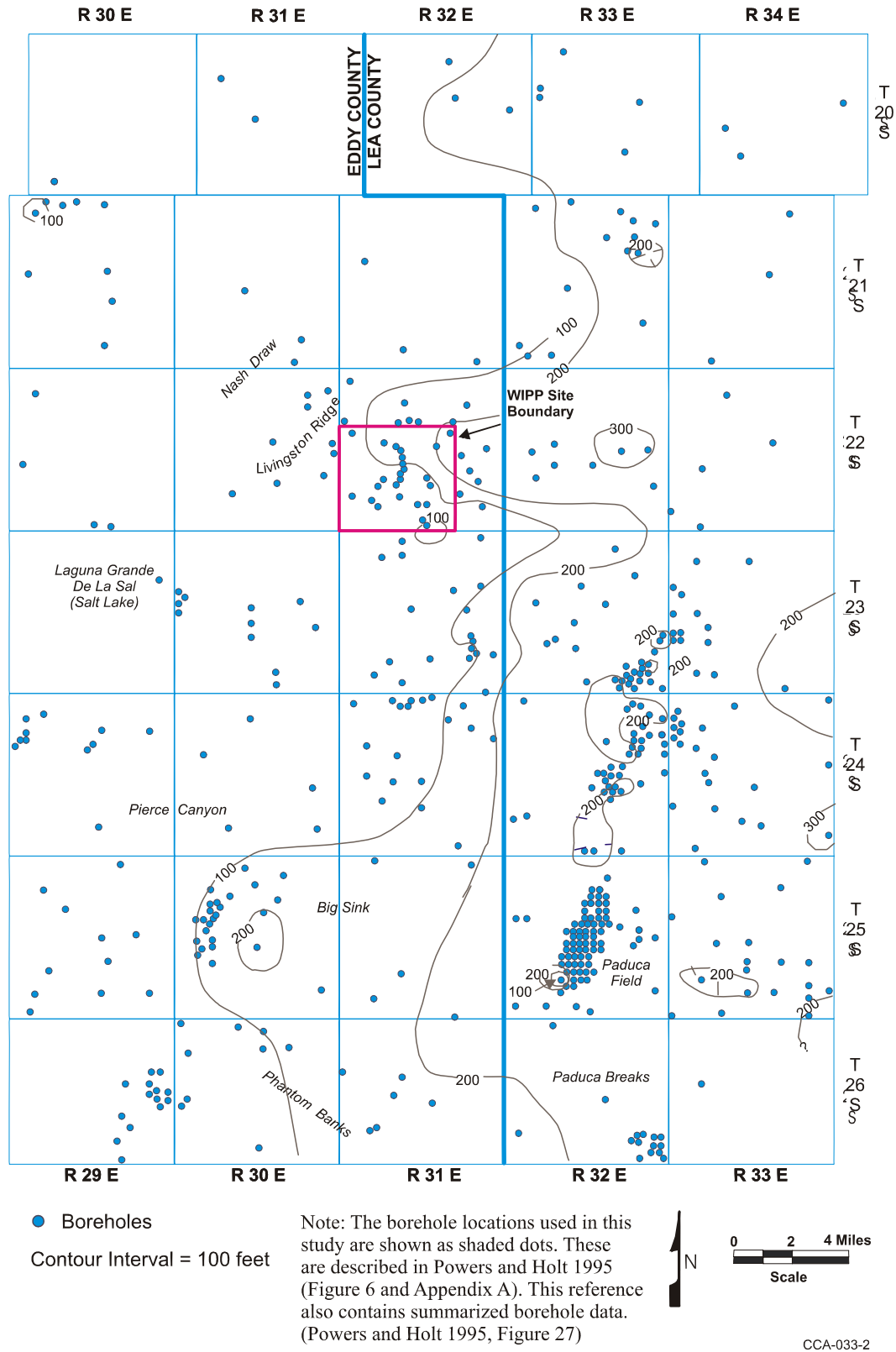


Figure 2-4520. Isopach of the Santa Rosa

formation has been mapped from the Santa Rosa, New Mexico, area south to the vicinity of Pecos, Texas. It is unconformable with underlying units.

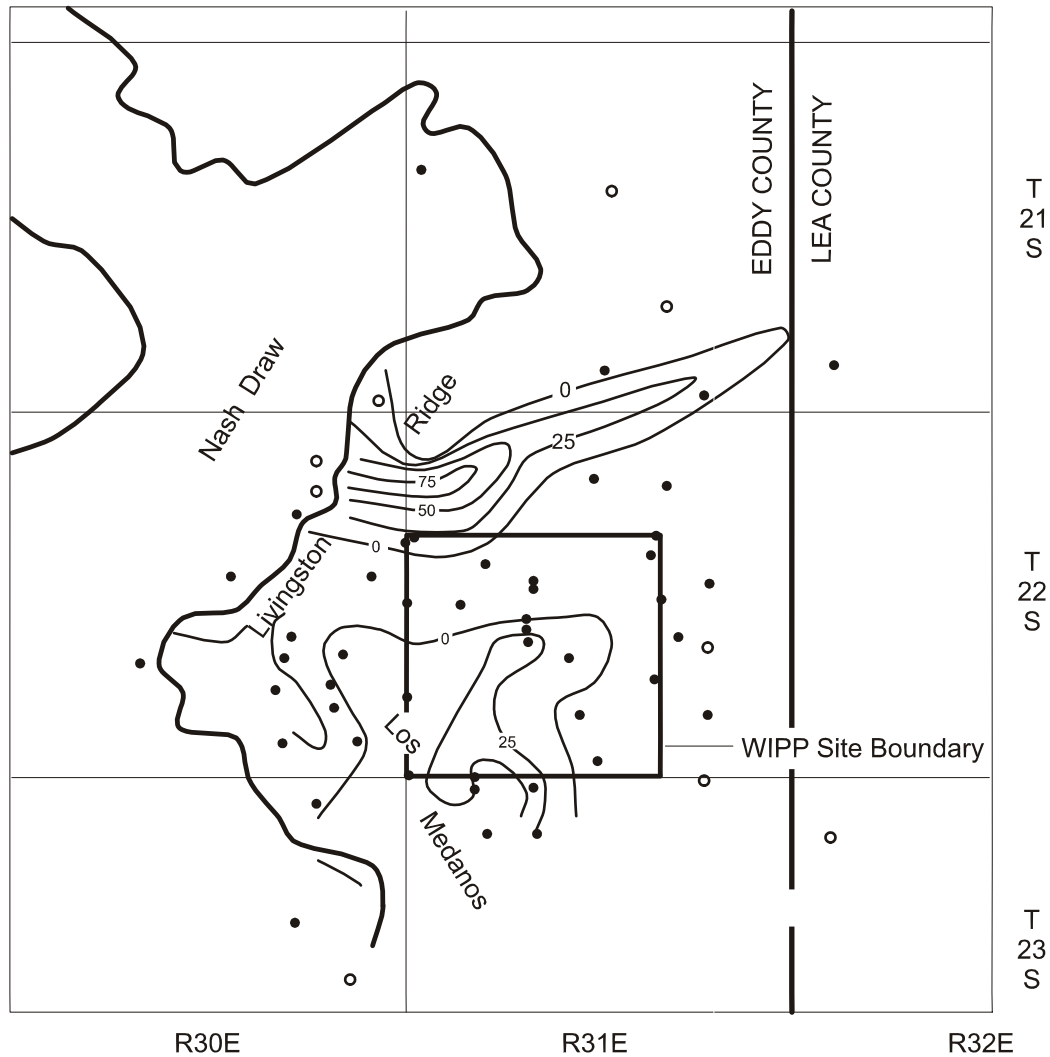
Vine (1963) and Bachman (1974) provided some limited description of the Gatuña. The most comprehensive study of the Gatuña is based on WIPP investigations and landfill studies for the City of Carlsbad and Eddy County (Powers and Holt 1993). Much of the formation is colored light reddish-brown. It is broadly similar to the Dewey Lake and the Santa Rosa, though the older units have more intense hues. The formation is highly variable, ranging from coarse conglomerates to claystones with some highly gypsiferous sections. Sedimentary structures are abundant. Analysis of lithofacies indicates that the formation is dominantly fluvial in origin with areas of low-energy deposits and evaporitic minerals.

The thickness of the Gatuña is not very consistent regionally, as shown in Figure 2-46. ~~Thicknesses range up to about 300 feet (91 meters) at Pierce Canyon, with thicker areas generally subparallel to the Pecos River.~~ *The thickness of the Gatuña ranges up to 91 m (300 ft) at Pierce Canyon, with thicker areas generally subparallel to the Pecos River.* To the east, the Gatuña is thin or absent. Holt and Powers (1990a) reported about 2.7 m (9 ft) of undisturbed Gatuña in the AIS at WIPP. *Powers (1997) integrated data from facility design geotechnical work (Sergent et al. 1979) and drilling to investigate shallow water to develop maps of the Gatuña in the vicinity of the WIPP surface facility. These maps are consistent with the broader regional view of the distribution of the Gatuña.*

The Gatuña has been considered Pleistocene in age based on a volcanic glass in the Upper Gatuña along the eastern margin of Nash Draw that has been identified as the Lava Creek B ash, dated at 0.6 million years by Izett and Wilcox (1982). This upper-limit age is corroborated by the age determinations from the Mescalero caliche (hereafter referred to as the Mescalero) that overlies the Gatuña (see Section 2.1.3.9). An additional volcanic ash from the Gatuña in Texas yields consistent K-Ar and geochemical data, indicating that it is about 13 million years old at that location (Powers and Holt 1993, p. 271). Thus, the Gatuña ranges in age over a period of time that may be greater than that spanned by the Ogallala Formation (hereafter referred to as the Ogallala) on the High Plains east of WIPP.

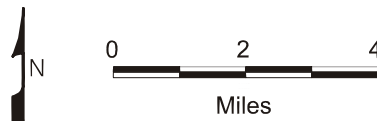
2.1.3.9 Mescalero Caliche

The Mescalero caliche is an informal stratigraphic unit apparently first differentiated by Bachman in 1974, though Bachman (1973, p. 17, p. 27) described the caliche on the Mescalero Plain. He differentiated the Mescalero from the older, widespread Ogallala caliche or caprock on the basis of textures, noting that breccia and pisolitic textures are much more common in the Ogallala caliche. The Mescalero has been noted over significant areas in the Pecos drainage, including the WIPP area, and it has been formed over a variety of substrates. Bachman (1973) described the Mescalero as a two-part unit: (1) an upper dense laminar caprock and (2) a basal, earthy-to-firm, nodular calcareous deposit. Machette (1985, p. 5) classified the Mescalero as having Stage V morphologies of a calcic soil (the more mature Ogallala caprock that occurs east of the WIPP site reaches Stage VI).



Modified from Mercer, J. W., 1983, Figure 1a

- Test Hole for Oil and Gas
 - Test Hole for Basic Data or Potash
- Contour Interval = 25 feet



CCA-071-2

Figure 2-1621. Isopach of the Gatuña

Bachman (1976, Figure 8) provided structure contours on the Mescalero caliche for a large area of southeastern New Mexico, including the WIPP site. From the contours and Bachman's discussion of the Mescalero as a soil, it is clear that the Mescalero is expected to be continuous over large areas. Explicit WIPP data are limited mainly to boreholes, though some borehole reports do not mention the Mescalero. The unit may be as much as 3 m (10 ft) thick.

1 The Mescalero overlies the Gatuña and was interpreted by Bachman (1976) on basic
2 stratigraphic grounds as having accumulated during the early-to-middle Pleistocene. Samples of
3 the Mescalero from the vicinity of the WIPP were studied using uranium-trend methods.

4 Based on early written communication from Rosholt, Bachman (1985, *p.* 20) reports that the
5 basal Mescalero began to form about 510,000 years ago and the upper part began to form about
6 410,000 years ago; these ages are commonly cited in WIPP literature. The samples are
7 interpreted by Rosholt and McKinney (1980, Table 5) in the formal report as indicating ages of
8 $570,000 \pm 110,000$ years for the lower part of the Mescalero and $420,000 \pm 60,000$ years for the
9 upper part.

10 According to Bachman (1985, *p.* 19), where the Mescalero is flat-lying and not breached by
11 erosion, it is an indicator of stability or integrity of the land surface over the last 500,000 years.
12 An additional discussion of the Mescalero caliche can be found in *CCA* Appendix GCR, Section
13 4.2.2.

14 2.1.3.10 Surficial Sediments

15 Soils of the region have developed mainly from Quaternary and Permian parent material. Parent
16 material from the Quaternary System is represented by alluvial deposits of major streams, dune
17 sand, and other surface deposits. These are mostly loamy and sandy sediments containing some
18 coarse fragments. Parent material from the Permian System is represented by limestone,
19 dolomite, and gypsum bedrock. Soils of the region have developed in a semiarid, continental
20 climate with abundant sunshine, low relative humidity, erratic and low rainfall, and a wide
21 variation in daily and seasonal temperatures. Subsoil colors are normally light brown to reddish
22 brown but are often mixed with lime accumulations (caliche) that result from limited, erratic
23 rainfall and insufficient leaching.

24 A soil association is a landscape with a distinctive pattern of soil types (series). It normally
25 consists of one or more major soils and at least one minor soil. There are three soil associations
26 within 8.3 km (5 mi) of the WIPP site: the Kermit-Berino, the Simona-Pajarito, and the Pyote-
27 Maljamar-Kermit. Of these three associations, only the Kermit-Berino soil series has been
28 mapped across the WIPP site by Chugg et al. (1952, Sheet No. 113). These are sandy soils
29 developed on eolian material. The Kermit-Berino soils include active dune areas. The Berino
30 soil has a sandy A horizon; the B horizons include more argillaceous material and weak-to-
31 moderate soil structures. A and B horizons are described as noncalcareous, and the underlying C
32 horizon is commonly caliche. Bachman (1980, *p.* 44) interpreted the Berino soil as a paleosol
33 that is a remnant B horizon of the underlying Mescalero. Rosholt and McKinney (1980, Table 5)
34 applied uranium-trend methods to samples of the Berino soil from the WIPP site area. ~~They~~
35 *Rosholt and McKinney (1980)* interpreted the age of formation of the Berino soil as $330,000 \pm$
36 $75,000$ years.

37 Generally, the Berino Series, which covers about 50 percent of the site, consists of deep,
38 noncalcareous, yellow-red to red sandy soils that developed from wind-worked material of
39 mixed origin. These soils are described as undulating to hummocky and gently sloping (*zero to*
40 *three* percent slopes). The soils are the most extensive of the deep, sandy soils in the Eddy
41 County area. Berino soils are subject to continuing wind and water erosion. If the vegetative

cover is seriously depleted, the water-erosion potential is slight, but the wind-erosion potential is very high. These soils are particularly sensitive to wind erosion in the months of March, April, and May, when rainfall is minimal and winds are highest. These soil characteristics are a consideration for the design of long-term passive controls such as monuments and markers (see [CCA Appendix PIC, Section III](#)).

The Kermit Series consists of deep, light-colored, noncalcareous, excessively drained loose sands, typically yellowish-red fine sand. The surface is undulating to billowy (from 0 to 3 percent slopes) and consists mostly of stabilized sand dunes. Kermit soils are slightly to moderately eroded. Permeability is very high, and, if vegetative cover is removed, the water-erosion potential is slight, but the wind-erosion potential is very high.

Surface soils appear to play a role in the infiltration of precipitation. Mercer ([CCA Appendix HYDRO](#)) points out that where surface deposits are thickest, they may contain localized perched zones of groundwater. A more thorough discussion of this topic can be found in [CCA Appendix HYDRO](#).

2.1.3.11 Summary

The stratigraphy and lithology at the WIPP site has been summarized from the lowermost pre-Cambrian units to the surface soils. While these are important for an understanding of the site and its stability, not all of these units are important to the performance of the disposal system. As a result, the DOE has developed a conceptual model that describes the lithology as [13](#) discrete model regions ranging from the Castile to a region that generally includes units above the Dewey Lake. In this model, emphasis is placed on the Castile, the Salado, the five members of the Rustler, the Dewey Lake, and the supra-Dewey Lake units. The Salado is divided into five stratigraphic units to capture the variations in properties near the horizon of the repository (see [Section 6.4.2.1 Figure 6-14](#)). The identification and definition of the appropriate modeling units is based on the identification of FEPs that can impact the performance of the disposal system. Details of the conceptual model can be found in Section 6.4.2.

2.1.4 *Physiography and Geomorphology*

In this section, the DOE presents a discussion of the physiography and geomorphology of the WIPP site and surrounding area. This information is taken from DOE 1980 ([pp. 7-21 to 7-23](#)). Geomorphology and physiography are determined by the DOE ([1980](#)) to be features that are potentially important to disposal system performance. They are included in the consequence analysis through consideration of the topography and its influence on the regional water table. (See discussion of regional water table characteristics in Section 2.2.1.) Consequently, topographic information is presented in this section. In addition, several geomorphological processes have been screened out on the basis of either low consequence or low probability, as discussed in Appendix [PA, Attachment SCR](#). These include weathering, erosion, sedimentation, and soil development. Information is presented in this section to support this screening. In order to perform this screening, such factors as slopes, proximity to watercourses, dissection, and historic and existing processes are important. These are presented in this section in terms of the regional and local physiographic and geomorphological characteristics. Tectonic processes that may alter the physiography of the region or site area are discussed in Section 2.1.5. In addition,

Section 2.1.6 presents more specific details on nontectonic processes identified during site characterization as having the potential for affecting the repository over the longer term and as requiring detailed investigation. These include halite deformation and dissolution.

2.1.4.1 Regional Physiography and Geomorphology

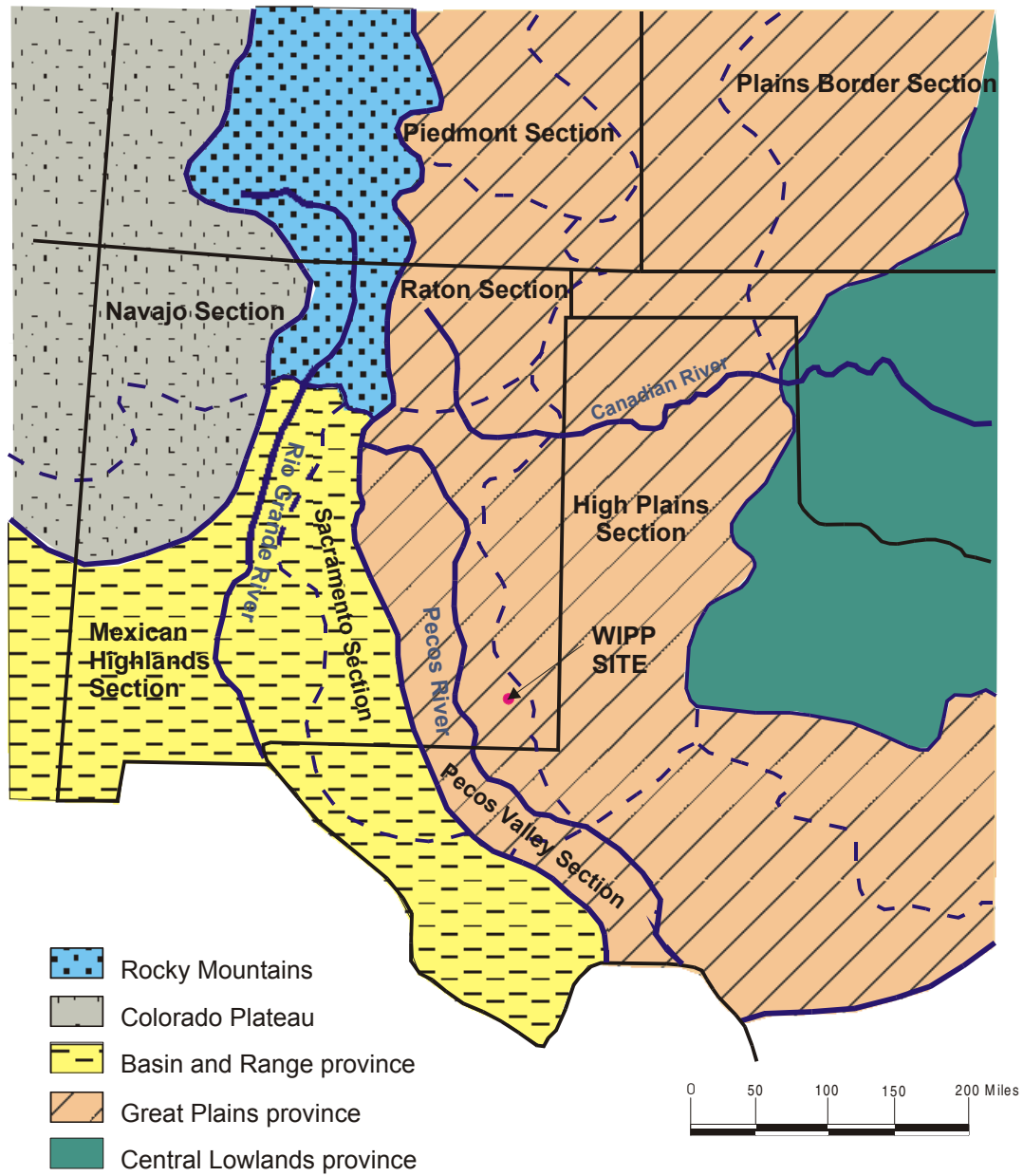
The WIPP site is in the Pecos Valley section of the southern Great Plains physiographic province (Figure 2-47~~22~~), a broad, highland belt sloping gently eastward from the Rocky Mountains and the Basin and Range Province to the Central Lowlands Province. The Pecos Valley section itself is dominated by the Pecos River Valley, a long north-south trough that is from 8.3 to 50 km (5 to 30 mi) wide and as much as 305 m (1,000 ft) deep in the north. The Pecos River System has evolved from the south, cutting headward through the Ogallala sediments and becoming entrenched some time after the Middle Pleistocene. It receives almost all the surface and subsurface drainage of the region; most of its tributaries are intermittent because of the semiarid climate. The surface locally has a karst terrain containing sinkholes, dolines, and solution-subsidence troughs from both surface erosion and subsurface dissolution. The valley has an uneven rock- and alluvium-covered floor with widespread solution-subsidence features, the result of dissolution in the underlying Upper Permian rocks. The terrain varies from plains and lowlands to rugged canyonlands, and contains such erosional features as scarps, cuestas, terraces, and mesas. The surface slopes gently eastward, reflecting the underlying rock strata. Elevations vary from more than 1,829 m (6,000 ft) in the northwest to about 610 m (2,000 ft) in the south.

The Pecos Valley section is bordered on the east by the virtually uneroded plain of the Llano Estacado. The Llano Estacado is part of the High Plains section of the Great Plains physiographic province and is a poorly drained eastward-sloping surface covered by gravels, wind-blown sand, and caliche that has developed since early-to-middle Pleistocene time. Few and minor topographic features are present in the High Plains section, formed when more than 152 m (500 ft) of Tertiary silts, gravels, and sands were laid down in alluvial fans by streams draining the Rocky Mountains. In many areas, the nearly flat surface is cemented by a hard caliche layer.

To the west of the Pecos Valley section are the Sacramento Mountains and the Guadalupe Mountains, part of the Sacramento section of the Basin and Range Province. The Capitan escarpment along the southeastern side of the Guadalupe Mountains marks the boundary between the Basin and Range and the Great Plains provinces. The Sacramento section has large basinal areas and a series of intervening mountain ranges (DOE 1980).

2.1.4.2 Site Physiography and Geomorphology

The land surface in the area of the WIPP site is a semiarid, wind-blown plain sloping gently to the west and southwest, and is hummocky with sand ridges and dunes. A hard caliche layer (Mescalero rocks) is typically present beneath the sand blanket and on the surface of the underlying Gatuña. Figure 2-48~~23~~ is a topographic map of the area. ~~Detailed topographic maps are attached at the end of this volume.~~ Elevations at the site range from 1,088 m (3,570 ft) in the east to 990 m (3,250 ft) in the west. The average east-to-west slope is 9.4 meters per kilometer (50 ft/mi).



CCA-034-2

Figure 2-1722. Physiographic Provinces and Sections

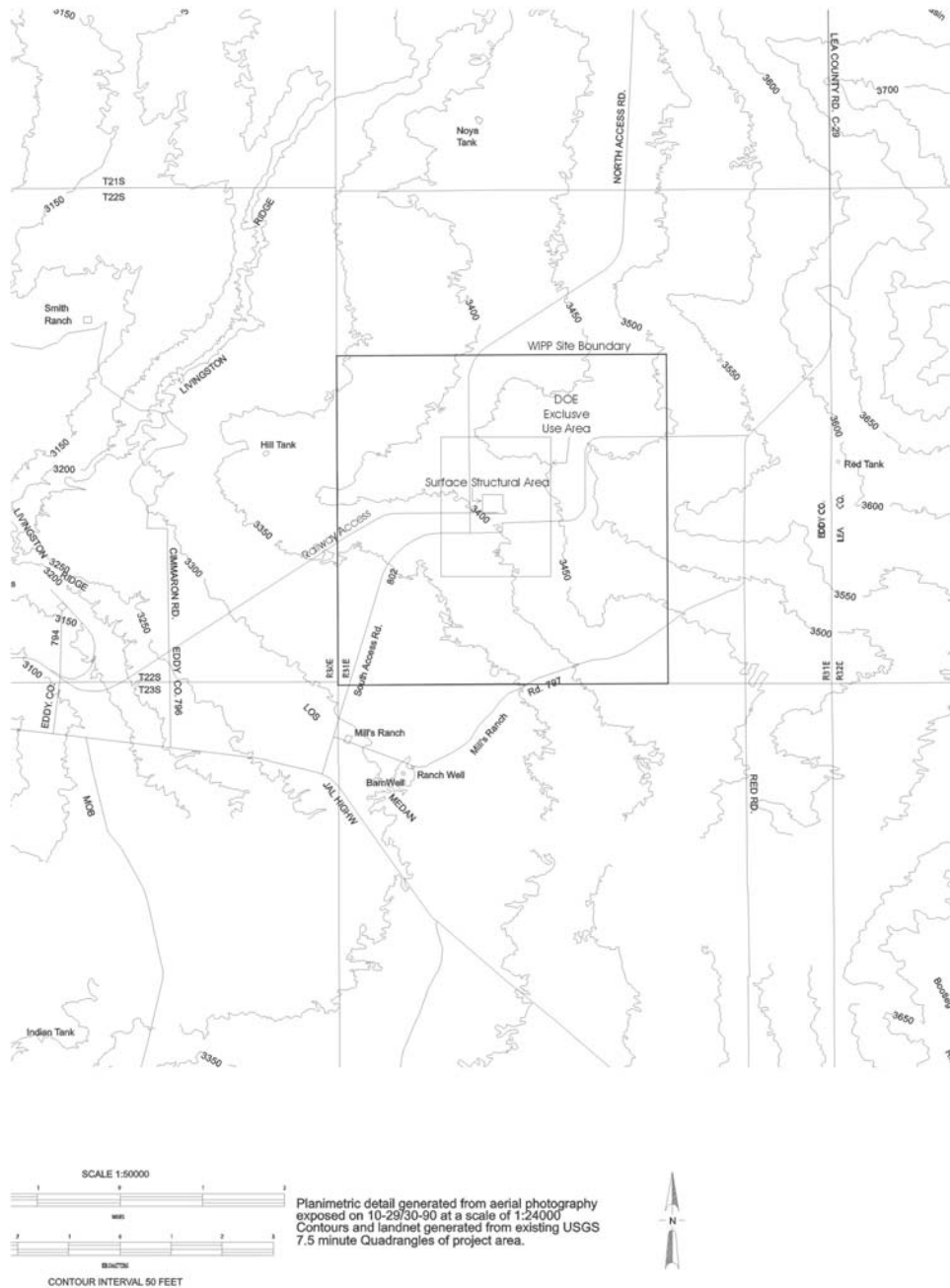


Figure 2-2325. Topographic Map of the Area Around the WIPP Site

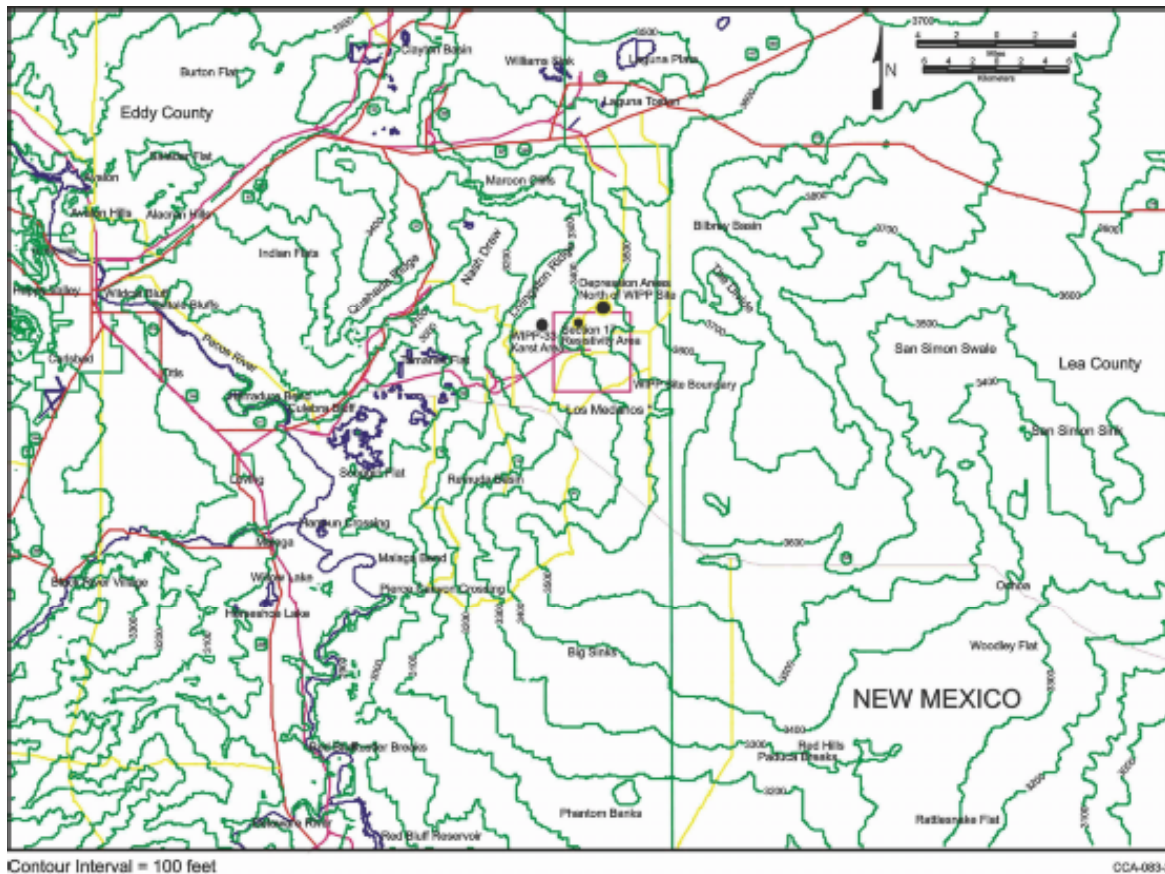


Figure 2-18. Topographic Map of the Area Around the WIPP Site

Livingston Ridge is the most prominent physiographic feature near the site. It is a west-facing escarpment that has about 23 m (75 ft) of topographic relief and marks the eastern edge of Nash Draw, the drainage course nearest to the site (see Figure 2-18²³). Nash Draw is a shallow 8-km-wide (5-mi-wide) basin, 61 to 91 m (200 to 300 ft) deep and open to the southwest. It was caused, at least in part, by subsurface dissolution and the accompanying subsidence of overlying sediments. Livingston Ridge is the approximate boundary between terrain that has undergone erosion and/or solution collapse to the west and terrain that has been little affected to the east.

About 24 km (15 mi) east of the site is the southeast-trending San Simon Swale, a depression caused, at least in part, by subsurface dissolution. Between San Simon Swale and the site is a broad, low mesa named the Divide. Lying about 9.7 km (6 mi) east of the site and about 30 m (100 ft) above the surrounding terrain, it is a boundary between southwest drainage toward Nash Draw and southeast drainage toward San Simon Swale. The Divide is capped by the Ogallala and the overlying caliche, upon which have formed small, elongated depressions similar to those in the adjacent High Plains section to the east.

Surface drainage is intermittent; the nearest perennial stream is the Pecos River, 19 km (12 mi) southwest of the WIPP site boundary. The site's location near a natural divide protects it from

flooding and serious erosion caused by heavy runoff. Should the climate become more humid, any perennial streams should follow the present basins, and Nash Draw and San Simon Swale would be the most eroded, leaving the area of the Divide relatively intact.

2.1.5 *Tectonic Setting and Site Structural Features*

The DOE has screened out, on the basis of either probability or consequence or both, all tectonic, magmatic, and structural related processes. The screening discussions can be found in Appendix *PA, Attachment* SCR. The information needed for this screening is included here and covers regional tectonic processes such as subsidence and uplift and basin tilting, magmatic processes such as igneous intrusion and events such as volcanism, and structural processes such as faulting and loading and unloading of the rocks because of long-term sedimentation or erosion. Discussions of structural events, such as earthquakes, are considered to the extent that they may create new faults or activate old faults. The seismicity of the area is considered in Section 2.6 for the purposes of determining seismic design parameters for the facility.

2.1.5.1 Tectonics

The processes and features included in this section are those more traditionally considered part of tectonics, processes that develop the broad-scale features of the earth. Salt dissolution is a different process that can develop some features resembling those of tectonics.

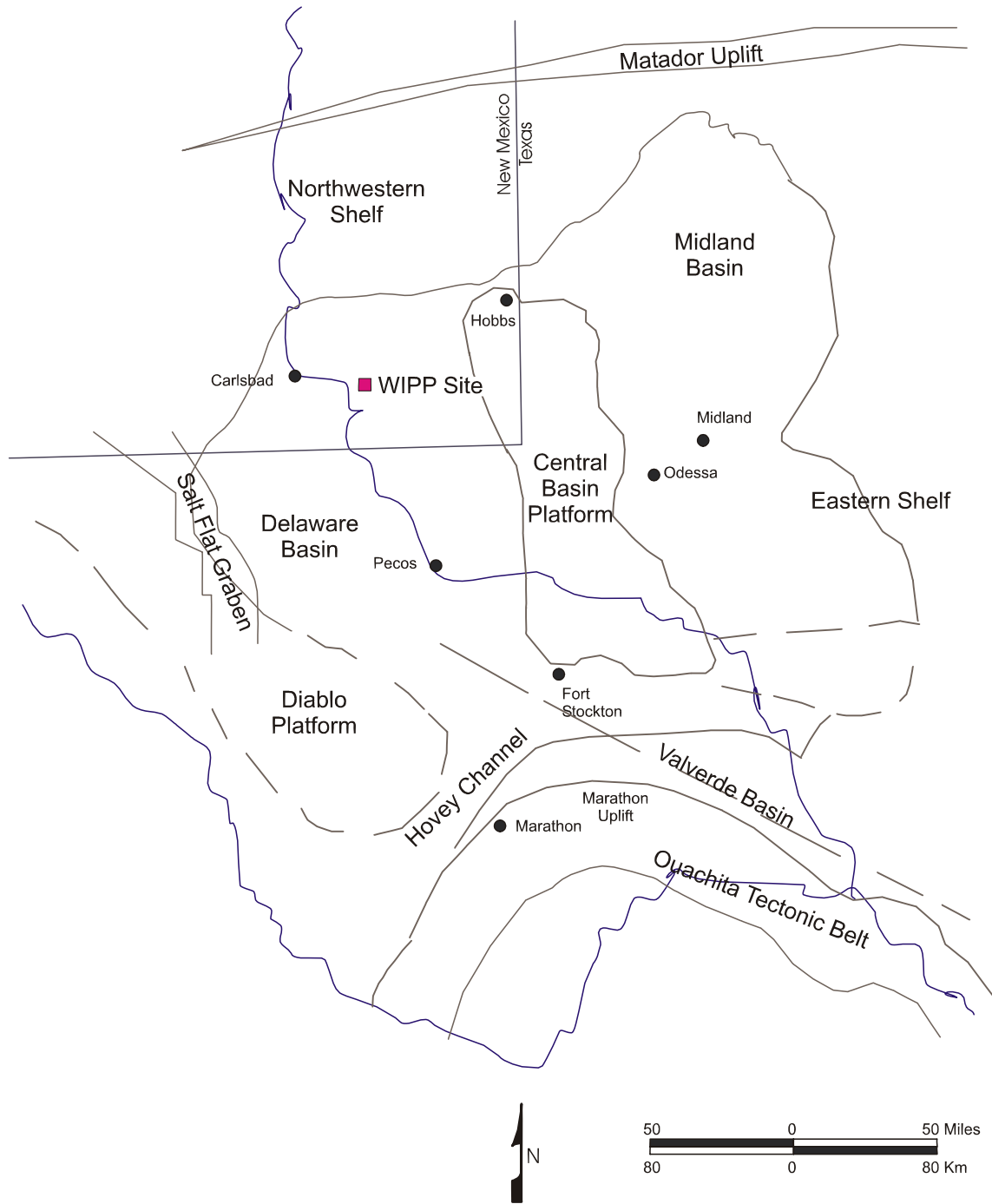
Most broad-scale structural elements of the area around the WIPP developed during the Late Paleozoic (*CCA* Appendix GCR, *pp.* 3-58 to 3-77). There is little historical or geological evidence of significant tectonic activity in the vicinity, and the level of stress in the region is low. The entire region tilted slightly during the Tertiary, and activity related to Basin and Range tectonics formed major structures southwest of the area. Seismic activity is specifically addressed in a separate section.

Broad subsidence began in the area as early as the Ordovician, developing a sag called the Tobosa Basin. By Late Pennsylvanian to Early Permian time, the Central Basin Platform developed (Figure 2-49~~24~~), separating the Tobosa Basin into two parts: the Delaware Basin to the west and the Midland Basin to the east. The Permian Basin refers to the collective set of depositional basins in the area during the Permian Period. Southwest of the Delaware Basin, the Diablo Platform began developing either in the Late Pennsylvanian or Early Permian. The Marathon Uplift and Ouachita tectonic belt limited the southern extent of the Delaware Basin.

According to Brokaw et al. (1972, *p.* 30), pre-Ochoan sedimentary rocks in the Delaware Basin show evidence of gentle downwarping during deposition, while Ochoan and younger rocks do not. A relatively uniform eastward tilt, generally from about 14 to 19 m/*per* km (75 to 100 ft/mi), has been superimposed on the sedimentary sequence.¹ ~~P.B.~~ King (1948, *pp.* 108 and 121) generally attributes the uplift of the Guadalupe and Delaware mountains along the west side of the Delaware Basin to the later Cenozoic, though he also notes that some faults along the west margin of the Guadalupe Mountains have displaced Quaternary gravels.

¹ Local dip of the Salado has been determined by mapping in the WIPP underground excavations. This dip is modeled as one degree to the south, as discussed in Section 6.4.2.1.

1



CCA-036-2

2

3

Figure 2-1924. Structural Provinces of the Permian Basin Region

4

1 ~~P.B.~~ King (1948, [p. 144](#)) also infers the uplift from the Pliocene-age deposits of the Llano
2 Estacado. Subsequent studies of the Ogallala of the Llano Estacado show that it varies in age
3 from Miocene (about 12 million years before present) to Pliocene (Hawley 1993). This is the
4 most likely range for uplift of the Guadalupe Mountains and broad tilting to the east of the
5 Delaware Basin sequence.

6 Analysis of the present regional stress field indicates that the Delaware Basin lies within the
7 Southern Great Plains stress province. This province is a transition zone between the extensional
8 stress regime to the west and the region of compressive stress to the east. An interpretation by
9 Zoback and Zoback (1991, [p. 350](#)) of the available data indicates that the level of stress in the
10 Southern Great Plains stress province is low. Changes to the tectonic setting, such as the
11 development of subduction zones and a consequent change in the driving forces, would take
12 much longer than 10,000 years to occur.

13 To the west of the Southern Great Plains province is the Basin and Range province, or
14 Cordilleran Extension province, where according to Zoback and Zoback (1991, [pp. 348 - 351](#)),
15 normal faulting is the characteristic style of deformation. The eastern boundary of the Basin and
16 Range province is marked by the Rio Grande Rift. Sanford et al. (1991, [p. 230](#)) note that, as a
17 geological structure, the [rift](#) extends beyond the relatively narrow geomorphological feature seen
18 at the surface, with a magnetic anomaly at least 500 km (300 mi) wide. On this basis, the Rio
19 Grande Rift can be regarded as a system of axial grabens along a major north-south trending
20 structural uplift (a continuation of the Southern Rocky Mountains). The magnetic anomaly
21 extends beneath the Southern Great Plains stress province, and regional-scale uplift of about
22 1,000 m (3,300 ft) over the past 10 million years also extends into eastern New Mexico.

23 To the east of the Southern Great Plains province is the large Mid-Plate province that
24 encompasses central and eastern regions of the conterminous United States and the Atlantic
25 basin west of the Mid-Atlantic Ridge. The Mid-Plate province is characterized by low levels of
26 paleo- and historic seismicity. Where Quaternary faulting has occurred, it is generally strike-slip
27 and appears to be associated with the reactivation of older structural elements.

28 Zoback et al. (1991) report no stress measurements from the Delaware Basin. The stress field in
29 the Southern Great Plains stress province has been defined from borehole measurements in west
30 Texas and from volcanic lineaments in northern New Mexico. These measurements were
31 interpreted by Zoback and Zoback (1991, [p. 353](#)) to indicate that the least principal horizontal
32 stress is oriented north-northeast and south-southwest and that most of the province is
33 characterized by an extensional stress regime.

34 There is an abrupt change between the orientation of the least principal horizontal stress in the
35 Southern Great Plains and the west-northwest orientation of the least principal horizontal stress
36 characteristic of the Rio Grande Rift. In addition to the geological indications of a transition
37 zone as described above, Zoback and Zoback (1980, [p. 6134](#)) point out that there is also evidence
38 for a sharp boundary between these two provinces. This is reinforced by the change in crustal
39 thickness from about 40 km (24 mi) beneath the Colorado Plateau to about 50 km (30 mi) or
40 more beneath the Southern Great Plains east of the Rio Grande Rift. The base of the crust within
41 the Rio Grande Rift is poorly defined but is shallower than that of the Colorado Plateau
42 (Thompson and Zoback 1979, [p. 152](#)). There is also markedly lower heat flow in the Southern

Great Plains (typically $< 60 \text{ mWm}^{-2}$) reported by Blackwell et al. (1991, [p. 428](#)) compared with that in the Rio Grande Rift (typically $> 80 \text{ mWm}^{-2}$) reported by Reiter et al. (1991, [p. 463](#)).

On the eastern boundary of the Southern Great Plains province, there is only a small rotation in the direction of the least principal horizontal stress. There is, however, a change from an extensional, normal faulting regime to a compressive, strike-slip faulting regime in the Mid-Plate province. According to Zoback and Zoback (1980, [p. 6134](#)), the available data indicate that this change is not abrupt and that the Southern Great Plains province can be viewed as a marginal part of the Mid-Plate province.

2.1.5.2 Loading and Unloading

Loading and unloading during the geological history since deposition is considered an influence on the hydrology of the Permian units because of its possible effect on the development of fractures.

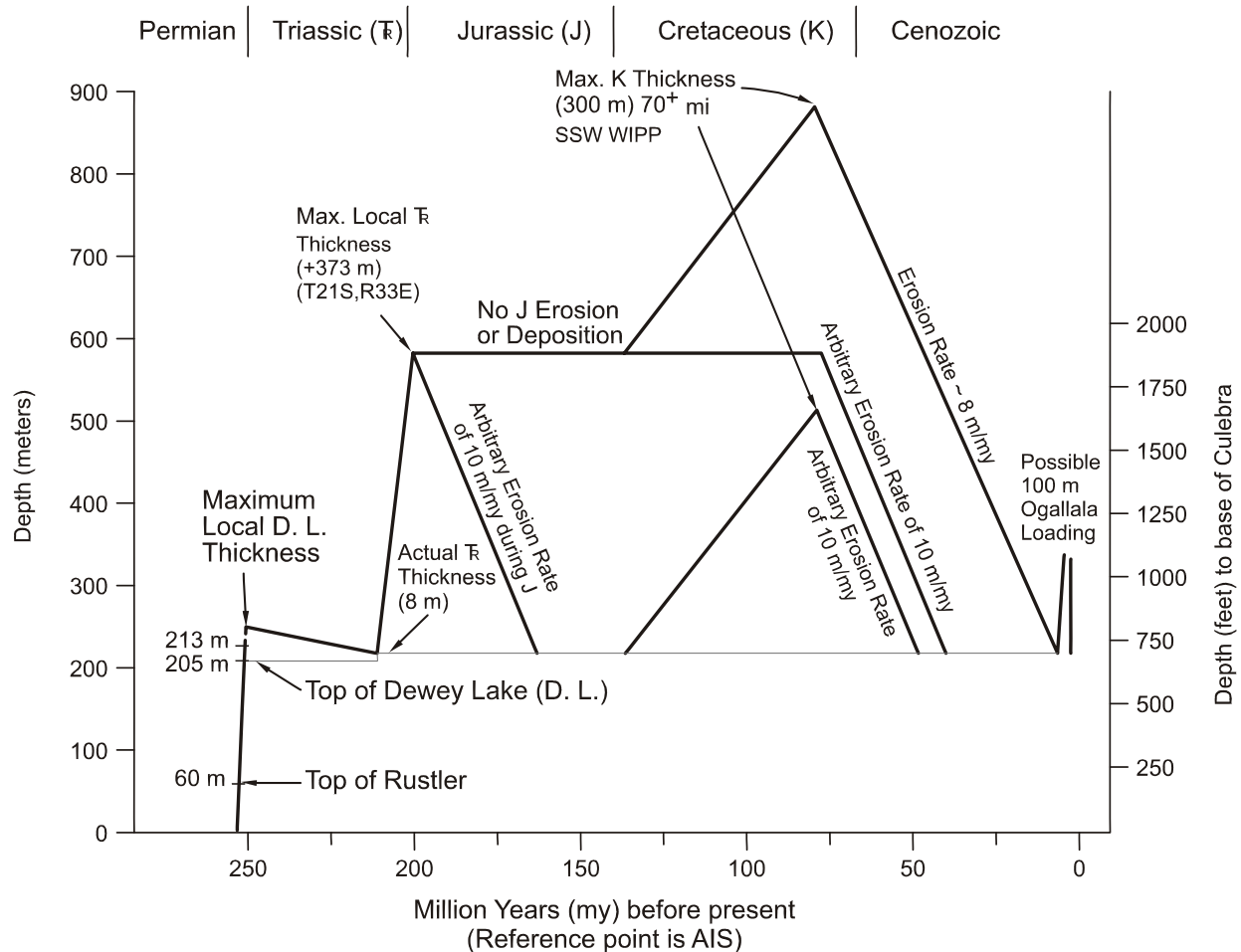
The sedimentary loading, depth of total burial, and erosion events combine in a complex history reconstructed here from regional geological trends and local data. The history is presented in Figure 2-2025 with several alternatives, depending on the inferences that are drawn, ranging from minimal to upper-bound estimates (Powers and Holt 1995, Section 5.3). Borns (1987) also made a generalized estimate of loading that is similar. The estimates are made with a reference point and depth to the Culebra at the AIS.

Given the maximum local thickness of the Dewey Lake, the maximum load at the end of the Permian was no more than approximately 240 m (787 ft). Given the present depth to the Culebra from the top of the Dewey Lake in the AIS, approximately 35 m (115 ft) of Dewey Lake might have been eroded during the Early Triassic before additional sediments were deposited. The Triassic thickness at the AIS is approximately 8 m (26 ft). Northeast of the WIPP site (T21S, R33E), Triassic rocks (Dockum Group) have a maximum local thickness of approximately 373 m (1,233 ft). This thickness is a reasonable estimate of the maximum thickness also attained at the WIPP site prior to the Jurassic Period. At the end of the Triassic, the total thickness at the WIPP site may have then attained approximately 586 m (1,863 ft) in two similar loading stages of a few million years each, over a period of approximately 50 million years.

The Jurassic outcrops nearest to the WIPP site are in the Malone Mountains of west Texas. There is no evidence that Jurassic rocks were deposited at or in the vicinity of the WIPP site.

As a consequence, the Jurassic is considered a time of erosion or nondeposition at the site, though erosion is most likely.

Widespread erosion during the Jurassic obviously cannot be broadly inferred for the area or there would not be thick Triassic rocks still preserved. Triassic rocks of this thickness are preserved nearby, indicating either pre-Jurassic tilting or that erosion did not occur until later (but still after tilting to preserve the Triassic rocks near the WIPP site). It is also possible that the immediate site area had little Triassic deposition or erosion, but very limited Triassic deposition (that is, 8 m [26 ft]) at the WIPP site seems unlikely.



Note: The estimates are made with a reference point and depth to the base of the Culebra at the AIS. Source: Powers and Holt 1995, Figure 34.

CCA-037-2

Figure 2-2025. Loading and Unloading History Estimated to the Base of the Culebra

Lang (1947) reported fossils from Lower Cretaceous rocks in the Black River Valley southwest of the WIPP site. Bachman (1980, [p. 28](#)) also reported similar patches of probable Cretaceous rocks near Carlsbad and south of White's City. From these reports, it is likely that some Cretaceous rocks were deposited at the WIPP site. Approximately 110 km (70 mi) south-southwest of the WIPP site, significant Cretaceous outcrops of both Early and Late Cretaceous age have a total maximum thickness of approximately 300 m (1,000 ft). Southeast of the WIPP, the nearest Cretaceous outcrops are thinner and represent only the Lower Cretaceous. Based on outcrops, a maximum thickness of 300 m (1,000 ft) of Cretaceous rocks could be estimated for the WIPP site. Compared to the estimate of Triassic rock thickness, it is less likely that Cretaceous rocks were this thick at the site. The uppermost lines of Figure 2-2025 summarize the assumptions of maximum thickness of these units.

1 A more likely alternative is that virtually no Cretaceous rocks were deposited, followed by
2 erosion of remaining Triassic rocks during the Late Cretaceous to the Late Cenozoic. Such
3 erosion may also have taken place over an even longer period, beginning with the Jurassic
4 Period. Ewing (1993) favors Early Cretaceous uplift and erosion for the Trans-Pecos Texas area,
5 but ~~he~~ does not analyze later uplift and erosional patterns.

6 In the general vicinity of the WIPP site, there are outcrops of Cenozoic rock from the Late
7 Miocene (Gatuña and Ogallala Formations). There is little reason to infer any significant Early
8 Cenozoic sediment accumulation at the WIPP site. Erosion is the main process inferred to have
9 occurred during this period and an average erosion rate of approximately 10 m (33 ft) per million
10 years is sufficient during the Cenozoic to erode the maximum inferred Triassic and Cretaceous
11 thickness prior to Gatuña and Ogallala deposition. Significant thicknesses of Cretaceous rocks
12 may not have been deposited, however, and average erosion rates could have been lower.

13 Maximum-known Gatuña thickness in the area around the WIPP is approximately 100 m
14 (330 ft); at the WIPP site, the Gatuña is very thin to absent. Ogallala deposits are known from
15 the Divide east of the WIPP site, as well as from the High Plains further east and north. On the
16 High Plains northeast of the WIPP, the upper Ogallala surface slopes to the southeast at a rate of
17 approximately 4 m/km (20 feet per mile). A straight projection of the 1,250-m (4,100-ft) contour
18 line from this High Plains surface intersects the site area, which is at an elevation slightly above
19 1,036 m (3,400 ft). This difference in elevation of 213 m (700 ft) represents one estimate,
20 probably near an upper bound, of possible unloading subsequent to deposition of the Ogallala
21 Formation.

22 Alternatively, the loading and unloading of the Ogallala could have been closer to 100 m
23 (330 ft). In any case, it would have occurred as a short-lived pulse over a few million years at
24 most.

25 While the above inferences about greater unit thicknesses and probable occurrence are
26 permissible, a realistic assessment suggests a more modest loading and unloading history
27 (Powers and Holt 1995). It is likely that the Dewey Lake accumulated to near local maximum
28 thickness of approximately 240 m (787 ft) before being slightly eroded prior to the deposition of
29 Triassic rocks. It also is most probable that the Triassic rocks accumulated at the site to near
30 local maximum thickness. In two similar cycles of rapid loading, the Culebra was buried to a
31 depth of approximately 650 m (2,132 ft) by the end of the Triassic.

32 It also seems unlikely that a significant thickness of Cretaceous rock accumulated at the WIPP
33 site. Erosion probably began during the Jurassic, slowed or stopped during the Early Cretaceous
34 as the area was nearer or at base level, and then accelerated during the Cenozoic, especially in
35 response to uplift as Basin and Range tectonics encroached on the area and the basin was tilted
36 more. Erosional beveling of Dewey Lake and Santa Rosa suggest considerable erosion since
37 tilting in the mid-Cenozoic. Erosion rates for this shorter period could have been relatively high,
38 resulting in the greatest stress relief on the Culebra and surrounding units. Some filling occurred
39 during the Late Cenozoic as the uplifted areas to the west formed an apron of Ogallala sediment
40 across much of the area, but it is not clear how much Gatuña or Ogallala sediment was deposited
41 in the site area. From general reconstruction of Gatuña history in the area (Powers and Holt
42 1993, *p.* 281), the DOE infers that Gatuña or Ogallala deposits likely were not much thicker at

the WIPP site than they are now. The loading and unloading spike (Figure 2-2025) representing Ogallala thickness probably did not occur. Cutting and headward erosion by the Pecos River has created local relief and unloading by erosion.

At the WIPP site, this history is a little complicated by dissolution, though locally (for example, Nash Draw) the effects of erosion and dissolution are more significant. The underlying evaporites have responded to foundering of anhydrite in less dense halite beds. These have caused local uplift of the Culebra (as at ERDA 6) but little change in the overburden at the WIPP. Areas east of the WIPP site are likely to have histories similar to that of the site. West of the site, the final unloading is more complicated by dissolution and additional erosion leading to exposure of the Culebra along stretches of the Pecos River Valley.

2.1.5.3 Faulting

Fault zones are well known along the Central Basin Platform, east of WIPP, from extensive drilling for oil and gas, as reported by Hills (1984). Holt and Powers performed a more recent an analysis in 1988 (CCA Appendix FAC, p. 4-14) of geophysical logs from oil and gas wells to examine the regional geology for the Rustler. This analysis showed that faults along the margin of the Central Basin Platform displaced Rustler rocks of at least Late Permian age. The overlying Dewey Lake shows marked thinning along the same trend, according to Schiel (1988, Figure 21), but the structure contours of the top of the Dewey Lake are not clearly offset. Schiel (1988) concluded that the fault was probably reactivated during the Dewey Lake's deposition, but movement ceased at least by the time the Santa Rosa was deposited. No surface displacement or fault has been reported along this trend.

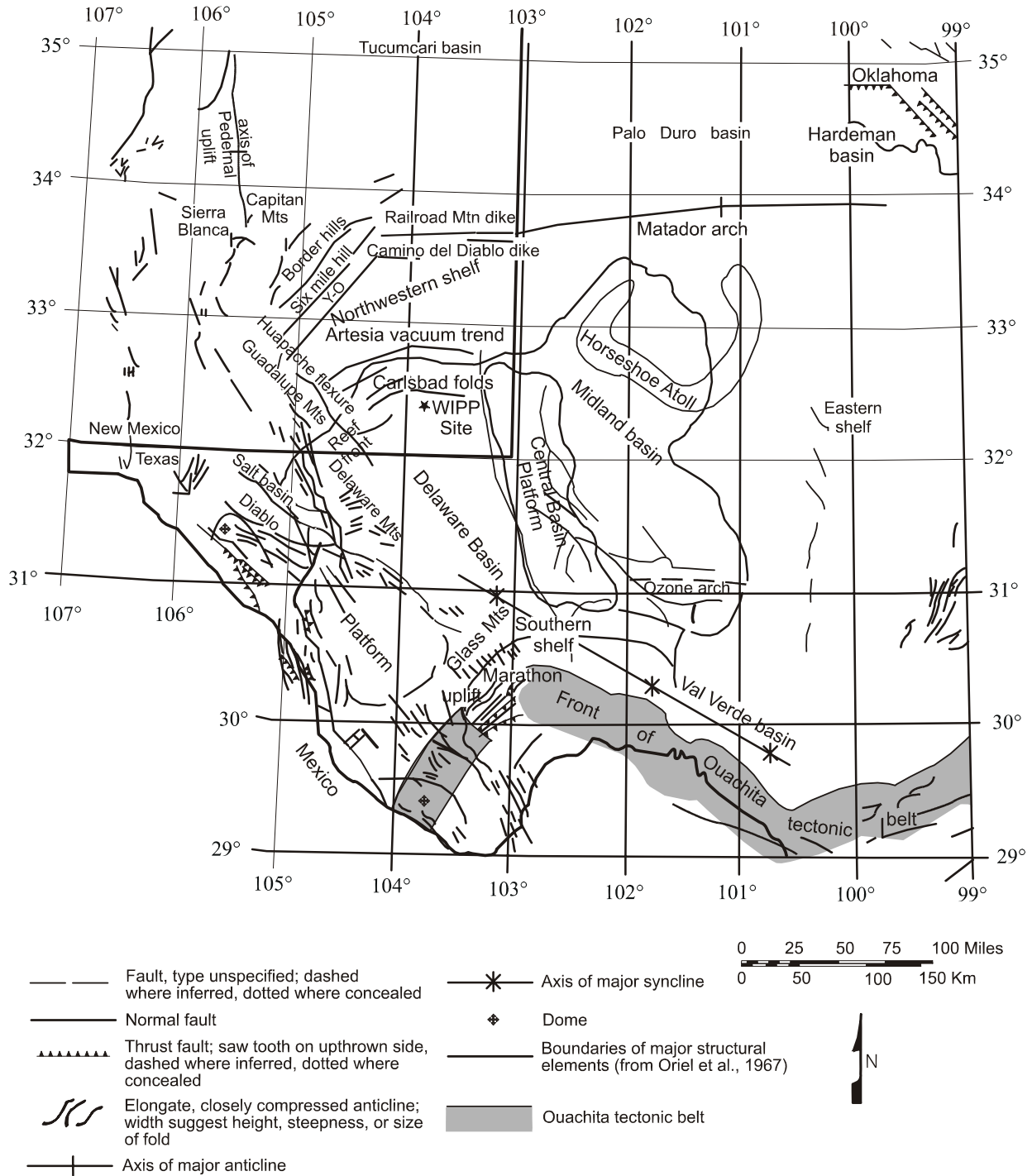
Muehlberger et al. (1978) have mapped Quaternary fault scarps along the Salt Basin graben west of both the Guadalupe and Delaware mountains. These are the nearest known Quaternary faults of tectonic origin to the WIPP. Kelley in (1971) inferred the Carlsbad and Barrera faults along the eastern escarpment of the Guadalupe Mountains based mainly on vegetative lineaments. Hayes and Bachman (1979) reexamined the field evidence for these faults in 1979 and concluded that they were nonexistent. Figure 2-2426 illustrates major regional structures, including faults.

On a national basis, Howard et al. (1971, sheets 1 and 2) assessed the location and potential for activity of young faults. For the region around the WIPP site, Howard et al. (1971, sheet 1) located faults along the western escarpment of the Delaware and Guadalupe mountain trend. These faults were judged to be Late Quaternary (approximately the last 500,000 years) or older.

In summary, there are no known Quaternary or Holocene faults of tectonic origin that offset rocks at the surface nearer to the site than the western escarpment of the Guadalupe Mountains. A significant part of the tilt of basin rocks is attributed to a mid-Miocene to Pliocene uplift trend along the Guadalupe-Sacramento Mountains that is inferred on the basis of High Plains sediments of the Ogallala.

2.1.5.4 Igneous Activity

Within the Delaware Basin, only one feature of igneous origin is known to have formed since the Precambrian. An igneous lamprophyre dike or series of dikes occurs along a linear trace about 120 km (75 mi) long from the Yeso Hills south of White's City to the northeast of the WIPP site



CCA-070-2

Figure 2-2426. Regional Structures

(Elliot Geophysical Company 1976). At its closest, the dike trend passes about 13 km (8 mi) northwest of the WIPP site center, as shown in Figure 2-22~~27~~²⁷. Evidence for the extent of the dike includes outcroppings at Yeso Hills, subsurface intercepts in boreholes and mines, and airborne magnetic responses.

An early radiometric determination for the dike by Urry (1936) yielded an age of 30 ± 1.5 million years. ~~More recent work~~ Work on dike samples by Calzia and Hiss (1978) is consistent with earlier work, indicating an age of 34.8 ± 0.8 million years.² Work by Brookins (1980) on polyhalite samples in contact with the dike indicated an age of about 21.4 million years. Volcanic ashes found in the Gatuña (Section 2.1.3.8) were airborne from distant sources and do not represent volcanic activity at the WIPP site.

2.1.6 *Nontectonic Processes and Features*

Nontectonic processes and features, which include evaporite deformation and dissolution of strata, are known to be active in the Delaware Basin. These processes are of interest because they represent mechanisms that are potentially disruptive to the repository in the long term. Both processes have been investigated extensively. The conclusions from these investigations are summarized in this section.

Halite in evaporite sequences is relatively plastic, which can lead to the process of deformation; it is also highly soluble, which can lead to the process of dissolution. Both processes (deformation and dissolution) can produce structural features similar to those produced by tectonic processes. The features developed by dissolution and deformation can be distinguished from similar-looking tectonic features where the underlying units do not reflect the same feature as do the evaporites. As an example, the evaporite deformation commonly does not affect the underlying Bell Canyon. Beds underlying areas of dissolved salt are not affected, but overlying units to the surface may be affected. The deformation in the Castile and Salado also tends to die out in overlying units, and the Rustler or the Dewey Lake may show little, if any, effects from deformed evaporites.

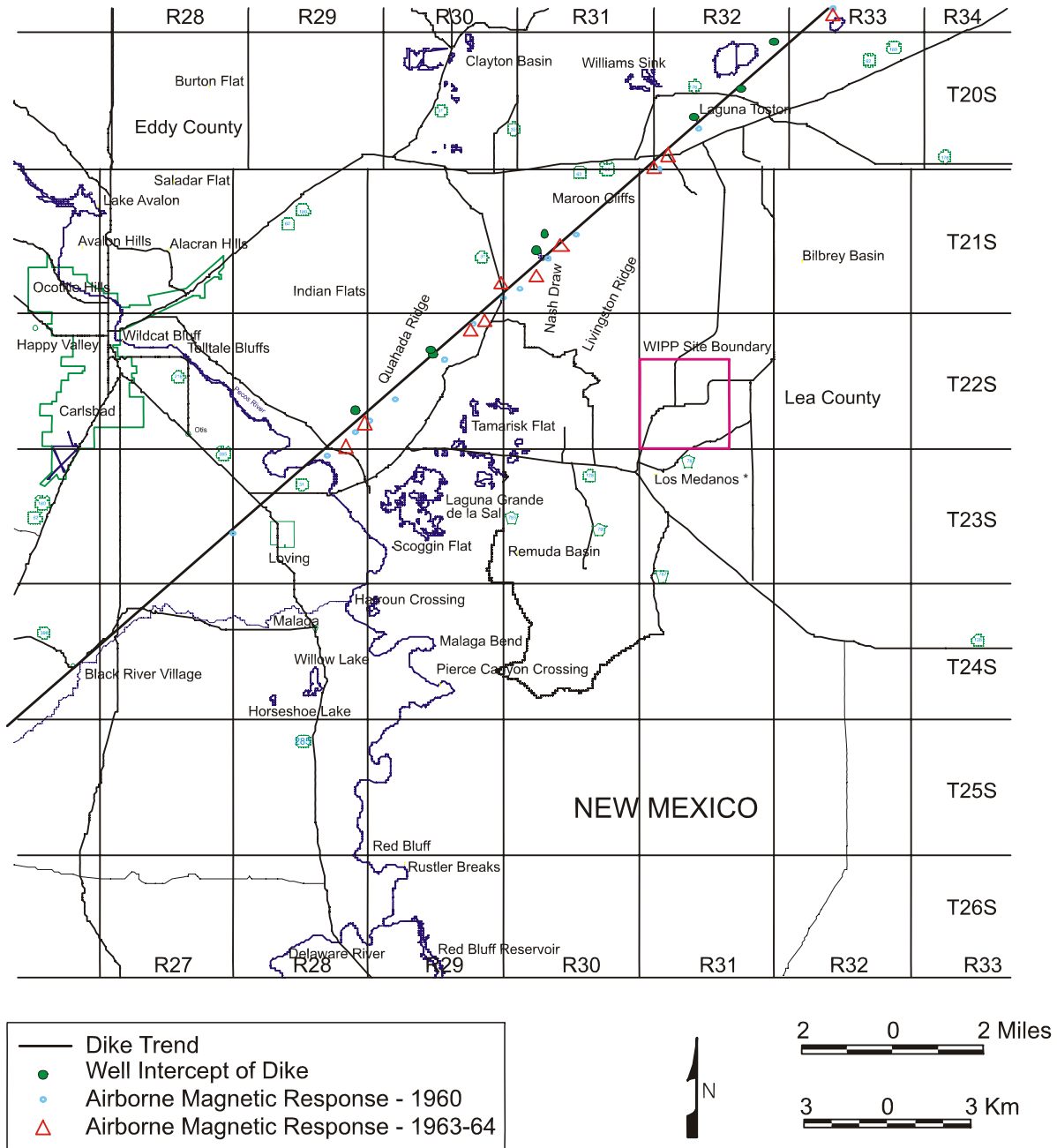
2.1.6.1 Evaporite Deformation

The most recent review of evaporite deformation in the northern Delaware Basin and original work to evaluate deformation is summarized here. More detail is provided in CCA Appendix DEF.

2.1.6.1.1 Basic WIPP History of Deformation Investigations

The Castile has been known for many years to be deformed in parts of the Delaware Basin, especially along the northern margin. Jones et al. in (1973) clearly showed the Castile to be thicker from the northwestern to northern part of the basin margin, just inside the Capitan Reef. A dissertation by Snider (1966, Figures 11 and 14) and a paper by Anderson et al. (1972, Figure 10) also presented maps showing some evidence of thicker sections of Castile next to the

² Calzia and Hiss (1978, p. 44) reported 32.2 to 33.9 million years. However, Powers et al. 1978 (CCA Appendix GCR, p. 3-80) reported a recalculated value of 34.8 ± 0.8 million years based on a change in measured decay constant.



Source: Elliot (1976)

CCA-076-2

Figure 2-2227. Igneous Dike in the Vicinity of the WIPP Site

Capitan. ERDA-6 was drilled during 1975 as part of the program to characterize an initial site for WIPP. The borehole penetrated increasingly deformed beds through the Salado into the Castile, and, at 826 m (2,711 ft) depth, the borehole began to produce pressurized brine and gas. Anderson and Powers (1978, *p.* 79) and Jones (1981a) interpreted beds to have been displaced structurally by as much as 289.5 m (950 ft). Some of the lower beds may have pierced overlying beds. The beds were considered too structurally deformed to mine reasonably along single horizons for a repository. Therefore, the site was abandoned in 1975, and the current site was located in 1976 (CCA Appendix GCR). The deformed beds around ERDA-6 were considered part of a deformed zone within about 10 km (6 mi) of the inner margin of the Capitan Reef. As a consequence, the preliminary selection criteria were revised to prohibit locating a new site within 10 km (6 mi) of the Capitan margin.

General criteria for the present site for the WIPP appeared to be met based on initial data from drilling (ERDA-9) and geophysical surveys. Beginning in 1977, the new site was more intensively characterized through geophysical surveys, including seismic reflection and drilling. Extensive seismic reflection work revealed good reflector quality in the southern part of the site and poor-quality or disturbed reflectors in a sector of the northern part of the site (see CCA Appendix DEF, Figure DEF-2.2). The area of disturbed reflectors became known as the disturbed zone, the area of anomalous seismic reflectors, or the zone of anomalous seismic reflection data. (The disturbed zone based on poor Castile seismic reflectors is completely different from the DRZ that describes the deformation around mined underground openings at the WIPP.)

Powers et al., in CCA Appendix GCR, Figures 4.4, 4.5, and 4.6, generally shows the disturbed zone beginning about 1.6 km (1 mi) north of the WIPP site center. Borns et al., ~~in~~ (1983), included two areas south of the WIPP site as showing the same features of the disturbed zone. Neill et al., ~~also in~~ (1983); summarized the limits of the disturbed zone based on differing interpretations and included the area less than 1.6 km (1 mi) north of the site center, where the dip in the Castile begins to steepen. WIPP-11 was drilled in early 1978 about 5 km (3 mi) north of the site center over part of the disturbed zone where proprietary petroleum company data had also indicated significant seismic anomalies. The borehole encountered highly deformed beds within the Castile and altered thicknesses of halite units, but no pressurized brine and gas were found.

Less than 1.6 km (1 mi) north of the site center, seismic data indicated possible faulting of the upper Salado and the lower Rustler over the area of steepening Castile dips. Four boreholes (WIPP-18, -19, -21, -22) were drilled into the upper Salado and demonstrated neither faulting nor significant deformation of the Rustler-Salado contact. Lateral changes in the seismic velocity of the upper sections contributed to the interpretation of a possible fault and thus complicated interpretations of deeper structure.

WIPP-12 was located about 1.6 km (1 mi) north of the center of the site and drilled during 1978 to a depth of 850 m (2,785 ft) in the upper Castile to determine the significance of structure on possible repository horizons. The top of the Castile was encountered at an elevation about 49 m (160 ft) above the same contact in ERDA-9 at the site center.

WIPP-12 was deepened during late 1981 to a depth of 1,200 m (3,925 ft) to test for possible brine and gas in the deformed Castile. The probability of encountering brine and gas was considered low because ERDA-6 and other known brine reservoirs in the Castile occurred in areas with greater deformation. During drilling, fractured anhydrite in the upper Castile (lower A3) began to yield pressurized brine and gas. The borehole was deepened to the basal anhydrite (A1) of the Castile. Subsequent reservoir testing (Popielak et al. 1983) was conducted to estimate reservoir properties (see Section 2.2.1.2.2 and Section 6.4.8).

As a consequence of discovering pressurized brine and gas in WIPP-12, the EEG recommended that the design of the facility be changed and that proposed waste disposal areas in the north be moved or reoriented to the south. After additional drilling of DOE-1, the DOE concluded that the design change had advantages, and the disposal facilities were placed south of the site center.

A microgravity survey of the site was designed to delineate further the structure within the disturbed zone, based on the large density differences between halite and anhydrite. The gravity survey was unsuccessful in yielding any improved resolution of the Castile structure.

DOE-2 was the last WIPP borehole to examine structure within the Castile. Potash drillhole data suggested a low point in Salado units about 3.3 km (2 mi) north of the site center. It was proposed by Davies (1984, *p.* 175) that the Salado low might indicate deeper dissolution of Castile halite, somewhat similar to the dissolution causing breccia pipes (see Section 2.1.6.2 on evaporite dissolution). The borehole demonstrated considerable Castile deformation, but there was no indication that halite had been removed by dissolution (Mercer et al. 1987; Borns 1987).

2.1.6.1.2 Extent of the Disturbed Zone at the Site

Nearby surface drilling, shafts, and underground drilling during early excavations at WIPP showed that the repository horizon varies modestly from the regional structure over the central part of the site; north of the site center, the beds dip gently to the south. Borns ~~in~~ (1987) suggested that the south dip is probably related to the dip on the underlying Castile.

The upper surface of MB 139, under the repository horizon, exhibited local relief in the exploratory salt-handling shaft. Jarolimek et al. (1983, *pp.* 4 - 6) interpreted the relief as mainly caused by syndepositional growth of gypsum at the water-sediment interface to form mounds and by subsequent partial crushing. Jarolimek et al. (1983) concluded that the MB relief was not caused by deformation because the base of the MB showed no comparable relief. Based on concerns of the EEG, MB 139 was reevaluated. Borns (1985) found less relief on the upper surface of the MB in the areas they examined; he also concluded that depositional processes were responsible for the relief. In both cases, deformation is not thought to have caused the relief on MB 139.

For the investigation of geologic factors related to hydraulic properties of the Culebra, Powers (2002a; 2002b; 2003a) constructed elevation maps of the top of the Culebra for the region around the WIPP site. A simplified version (Figure 2-28) showing the elevations of the top of the Culebra in meters above mean sea level (m amsl) illustrates that deformation of the Castile propagated upward through the Culebra to the northeast of the WIPP site, forming a northwest-southeast trending anticline informally termed "the Divide anticline." Across the

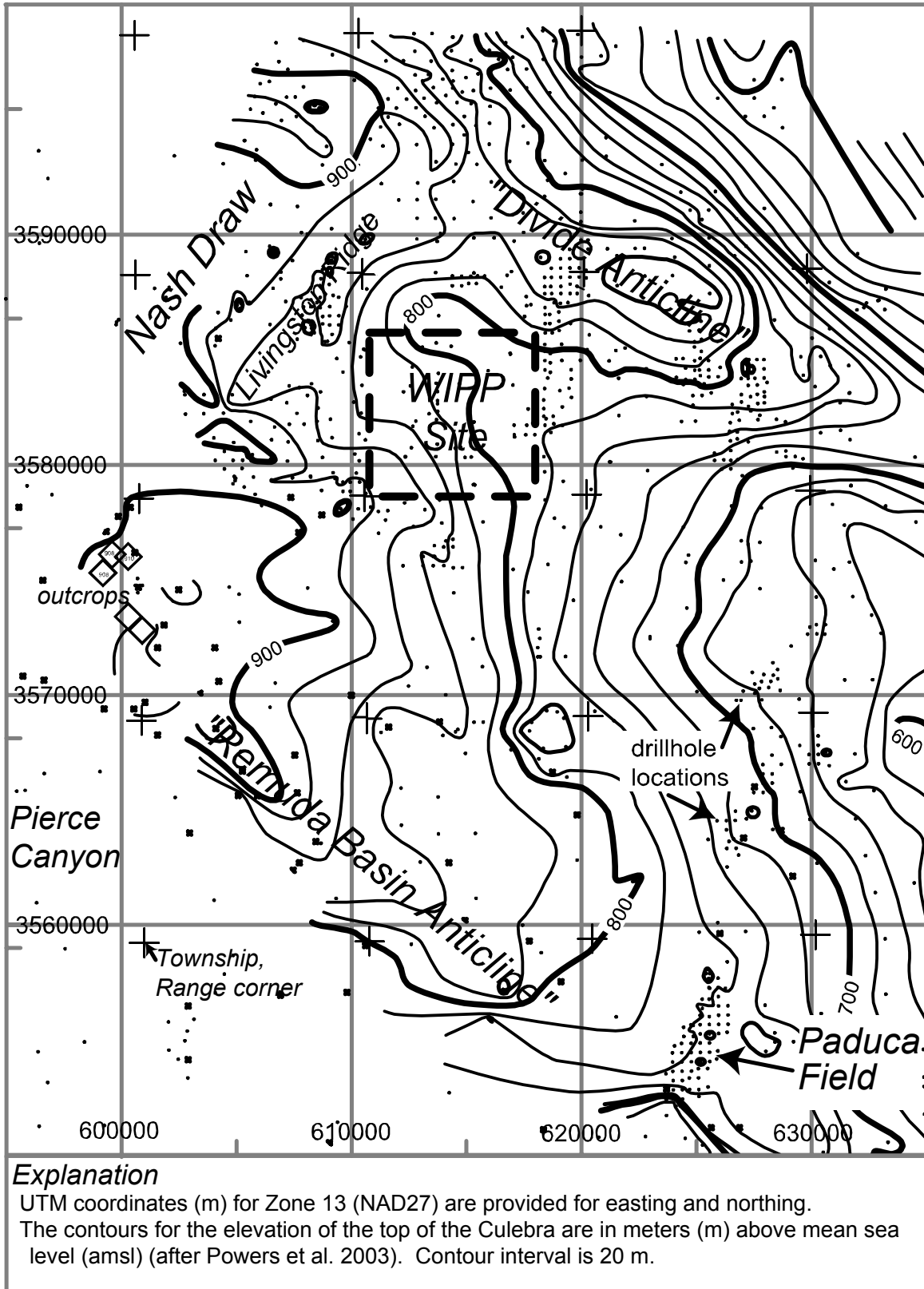


Figure 2-28. Elevations of the Top of the Culebra Dolomite Member

WIPP site, the Culebra is slightly deformed by the deeper deformation, and the “disturbed zone” defined earlier geophysically is slightly evident at this horizon.

2.1.6.1.3 Deformation Mechanisms

In analyzing Castile structure in the northern Delaware Basin, Borns et al. (1983, p. 3) proposed five processes as the principal hypotheses to explain the structure: gravity foundering, dissolution, gravity sliding, gypsum dehydration, and depositional processes. Gravity foundering is the most comprehensive and best-accepted hypothesis of the five. It is based on the fact that anhydrite is much more dense (about 2.9 g/cm³) than halite (about 2.1 g/cm³), and anhydrite beds therefore have a potential for sinking into underlying halite. Regardless of which mechanism caused the disturbed zone, the important consideration is the long-term future effects. To evaluate this, Borns et al. (1983) postulated that both gravity-driven deformation mechanisms could be ongoing. The strain rates from such deformation are such that deformation would progress over the next 250,000 years and that such deformation would not directly jeopardize the disposal system.

2.1.6.1.4 Timing of Deformation of the Disturbed Zone at the Site

Jones (1981a, *p.* 18) estimated that deformation of the Castile and overlying rocks took place before the Ogallala Formation was deposited, as he believes the unit is undeformed. Anderson and Powers (1978, *p.* 79) inferred that data from ERDA-6 indicate that the Castile was deformed after the basin was tilted. Though these lines of evidence could be consistent with mid-Miocene deformation, there are other interpretations consistent with older deformation (Madsen and Raup 1988). There is no known evidence of surface deformation or other features to indicate recent deformation.

2.1.6.2 Evaporite Dissolution

Because evaporites are much more soluble than most other rocks, project investigators have considered it important to understand the dissolution processes and rates that occur within the site being considered for long-term isolation. These dissolution processes and rates constitute the limiting factor in any evaluation of the site. Over the course of the WIPP project, extensive resources have been committed to identify and study a variety of features in southeastern New Mexico interpreted to have been caused by dissolution. The subsurface distribution of halite for various units has been mapped. Several different kinds of surface features have been attributed to dissolution of salt or karst formation. The processes proposed or identified include point-source (brecciation), deep dissolution, shallow dissolution, and karst. These are each discussed in more detail in *CCA* Appendix DEF, Section DEF.3. Screening arguments relative to dissolution are presented in Appendix *PA, Attachment* SCR, *FEPs N17 and N21* (including dissolution associated with abandoned boreholes in Sections SCR.1.2.1 and SCR.3.3.1 *the discussion for FEP H34*). These arguments are based principally on the observed rates and processes in the region. These are described below.

2.1.6.2.1 Brief History of Project Studies

Well before the WIPP project, several geologists recognized that dissolution is an important process in southeastern New Mexico, and that it contributed to the subsurface distribution of

halite and to the surficial features. Early studies include those by Lee (1925), Maley and Huffington (1953), and Olive (1957) ~~(in the Bibliography)~~. Robinson and Lang (1938, *p.* 100) identified an area under Nash Draw where brine occurred at about the stratigraphic position of the upper Salado-basal Rustler and considered that salt had been dissolved to produce a dissolution residue. Vine (1963, *p.* B38 and B40) mapped Nash Draw and surrounding areas. Vine (1963) reported surficial domal structures, later called breccia pipes and identified as deep-seated dissolution and collapse features.

As the USGS and Oak Ridge National Laboratory (ORNL) began to survey southeastern New Mexico as an area in which to locate a repository site in salt, Brokaw et al. ~~in~~ (1972) prepared a summary of the geology that included solution and subsidence as significant processes in creating the features of southeastern New Mexico. Brokaw et al. (1972) also recognized a solution residue at the top of the salt in the Salado in the Nash Draw area, and the unit commonly became known as the brine aquifer because it yielded brine. Brokaw et al. (1972) also interpreted the east-west decrease in thickness of the Rustler to be a consequence of removal by dissolution of halite and other soluble minerals.

During the early 1970s, the basic ideas about shallow dissolution of salt (generally from higher stratigraphic units and within a few hundred feet of the surface) were set out in a series of reports, ~~by Bachman, Jones, and collaborators,~~ as discussed in the following sections. Piper (1973; 1974) independently evaluated the geological survey data for ORNL. Claiborne and Gera (1974) concluded that salt was being dissolved too slowly from the near-surface units to affect a repository for several million years, at least.

By 1978, shallower drilling around the WIPP site to evaluate potash resources was interpreted by Jones (1978, *p.* 9), ~~and he~~ *who* felt that the Rustler included “dissolution debris, convergence of beds, and structural evidence for subsidence.” Halite in the Rustler has been reevaluated by the DOE, but there are only minor differences in inferred distributions among the various investigators. These investigators do have different explanations about how this distribution occurred (see Section 2.1.3.5 on Rustler stratigraphy): (1) through extensive dissolution of the Rustler’s halite after the Rustler was deposited, or (2) through syndepositional dissolution of halite from saline mud flat environments during Rustler deposition.

Anderson (1978) and Anderson et al. (1978) reevaluated halite distribution in deeper units, especially the Castile and Salado formations. ~~He~~ *They* identified local anomalies proposed as features developed after deep dissolution of halite by water flowing upward from the underlying Bell Canyon. Anderson (1978) mapped geophysical log signatures of the Castile and interpreted lateral thinning and change from halite to non-halite lithology as evidence of lateral dissolution of deeper units (part of deep dissolution), and ~~he~~ proposed that deep dissolution might threaten the WIPP site. In response to Anderson’s (1978) developing concepts, ERDA-10 was drilled south of the WIPP area during the latter part of 1977. ERDA-10 intercepted a stratigraphic sequence without evidence of solution residues in the upper Castile.

A set of annular or ring fractures is evident in the surface around San Simon Sink, about 30 km (18 mi) east of the WIPP site. Nicholson and Clebsch (1961, *p.* 14) suggested that San Simon Sink developed as a result of deep-seated collapse. WIPP-15 was drilled at about the center of the sink to a depth of 245 m (811 ft) to obtain samples for paleoclimatic data and stratigraphic

data to interpret collapse. Anderson (1978) and Bachman (1980) both interpret San Simon Sink as dissolution and collapse features, and the annular fractures are not considered evidence of tectonic activity.

Following the work by Anderson, Bachman (1980, 1981) mapped surficial features in the Pecos Valley, especially at Nash Draw, and differentiated between those surface features in the basin that were formed by karst and those that were formed by deep collapse features over the Capitan. WIPP-32, WIPP-33, and two boreholes over the Capitan Reef were eventually drilled. Their data, which demonstrated the concepts proposed by Bachman (1980, 1981), are documented in Snyder, et al. (1982, p. 65).

A final program concerning dissolution and karst was initiated following a microgravity survey of a portion of the site during 1980. Based on localized low-gravity anomalies, Barrows et al. (1983) interpreted several areas within the site as locations of karst. WIPP-14 was drilled during 1981 at a low-gravity anomaly. It revealed normal stratigraphy through the zones proposed to be affected by karst. As a follow-up, in 1985 Bachman (1985) also reexamined surface features around the WIPP and concluded that there was no evidence for active karst within the WIPP site. The nearest karst feature is northwest of the site boundaries at WIPP-33.

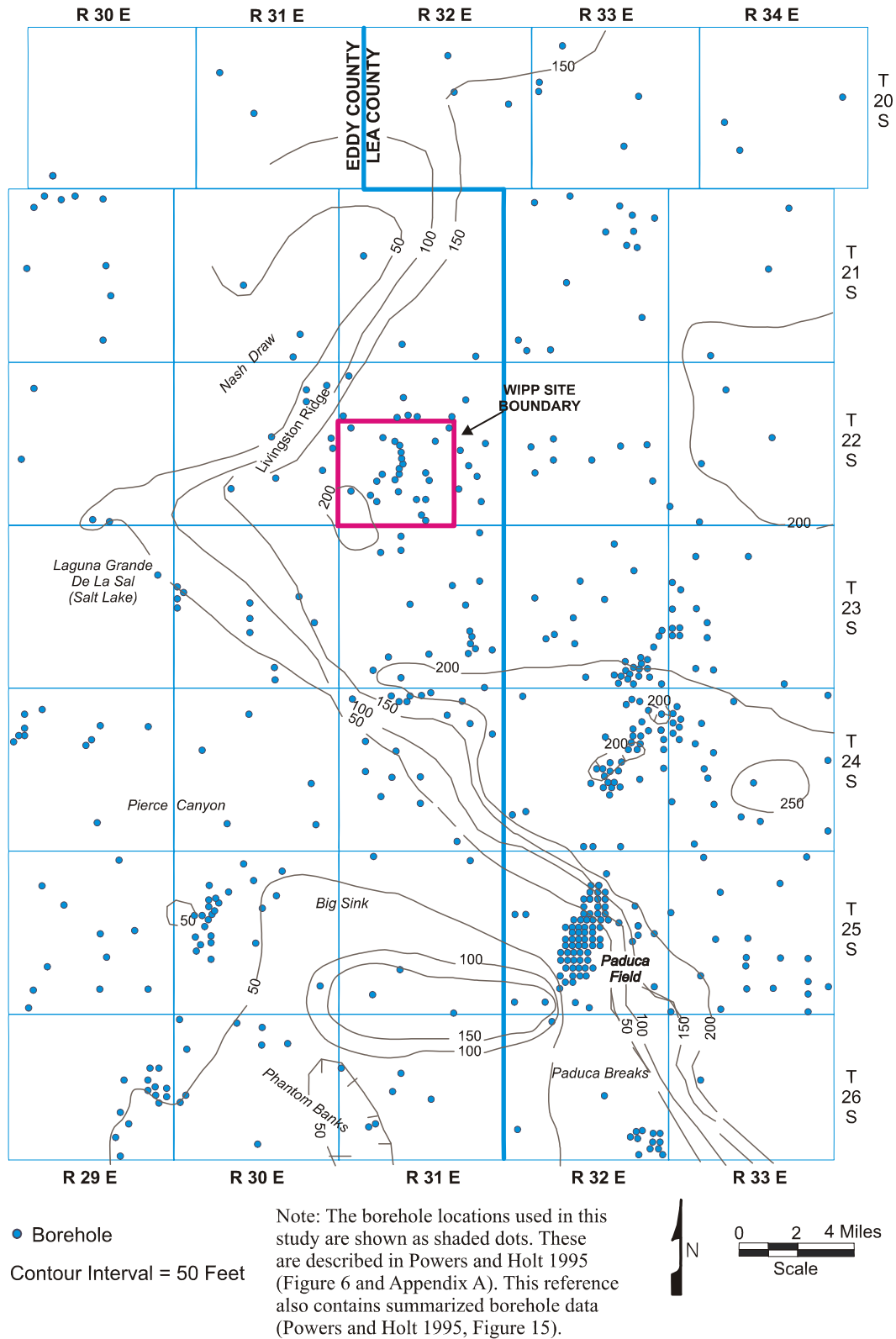
2.1.6.2.2 Extent of Dissolution

~~The margins of halite within the anhydrite and claystone members of the Rustler have been mapped by different methods, the findings of which were consolidated by Beauheim (in 1987a, 131–134). There are few differences in interpretation, despite the different methods used (Figure 2-10). Lower members of the Rustler are halitic west of the site, and higher members generally show halite only further east. Snyder interprets these margins as a consequence of post-depositional dissolution of halite. Holt and Powers (Appendix FAC, 6-29) report and interpret sedimentary structures within the Rustler mudstone equivalent to halite beds, indicating that most halite was removed during the depositional process and redeposited in a salt pan in the eastern part of the depositional basin. *Within the Rustler, dissolution of halite is believed to have occurred only near the depositional margins, as discussed in Section 2.1.3.5. Figure 2-15 shows the only two areas where evidence has been found for halite dissolution from the M3/H3 horizon in the Tamarisk.*~~

Upper intervals of the Salado thin dramatically west and south of the WIPP site (Figure 2-23²⁹) compared to deeper Salado intervals. There are no cores for further consideration of possible depositional variations. As a consequence, this zone of thinning is interpreted by the DOE as the edge of dissolution of the upper Salado.

2.1.6.2.3 Timing of Dissolution

The dissolution of Ochoan evaporites through the near-surface processes of weathering and groundwater recharge has been studied extensively (Anderson 1981; Lambert 1983a; Lambert 1983b; Bachman 1984; and see also CCA Appendix FAC). The work of Lambert (1983a) was specifically mandated by the agreement between the DOE and the state of New Mexico to evaluate in detail the conceptual models of evaporite dissolution proposed by Anderson (1981). There was no clear consensus among investigators on the volume of rock salt removed. Hence,



CCA-039-2

Figure 2-2329. Isopach from the Base of MB 103 to the Top of the Salado

estimates of the instantaneous rate of dissolution vary significantly. Dissolution may have taken place as early as the Ochoan, during or shortly after deposition. For the Delaware Basin as a whole, Anderson (1981) proposed that up to 40 percent of the rock salt in the Castile and Salado formations was dissolved during the past 600,000 years. Lambert (1983b, *p.* 292) suggested that in many places the variations in salt-bed thicknesses inferred from borehole geophysical logs that were the basis for Anderson's (1981) calculation were depositional in origin, compensated by thickening of adjacent nonhalite beds, and were not associated with the characteristic dissolution residues. Borns and Shaffer (1985, *p.* 44 – 45) also suggested in 1985 a depositional origin for many apparent structural features attributed to dissolution.

Snyder (1985, *p.* 8), as well as earlier workers (for example, Vine 1963; Lambert 1983b; and Bachman 1984), attribute the variations in thickness in the Rustler, which crops out in Nash Draw, to postdepositional evaporite dissolution. Holt and Powers (CCA Appendix FAC, *p.* 9-2) have challenged this view and attribute the east-to-west thinning of salt beds in the Rustler to depositional facies variability rather than postdepositional dissolution. Bachman (1974, 1976, and 1980) envisioned several episodes of dissolution since the Triassic, each dominated by greater degrees of evaporite exhumation and a wetter climate, interspersed with episodes of evaporite burial and/or a drier climate. Evidence for dissolution after deposition of the Salado and before deposition of the Rustler along the western part of the Basin was cited by Adams (1944, *p.* 1612). Others have argued that the evaporites in the Delaware Basin were above sea level and therefore potentially subject to dissolution, during the Triassic, Jurassic, Tertiary, and Quaternary periods. Because of discontinuous deposition, not all of these times are separable in the geological record of southeastern New Mexico. Bachman (1980) contends that dissolution was episodic during the past 225 million years as a function of regional base level, climate, and overburden.

There have been several attempts to estimate the rates of shallow dissolution in the basin. Bachman (1974) provided initial estimates of dissolution rates based on a reconstruction of Nash Draw relationships, including the observation that portions of the Gatuña were deposited over areas of active dissolution and subsidence of the underlying evaporites. Though these rates indicate no hazard to the WIPP related to Nash Draw dissolution, Bachman (1980, *p.* 85) later reconsidered the Nash Draw relationships and concluded that pre-Cenozoic dissolution had also contributed to salt removal. Thus, the initial estimated rates were too high.

With regards to deep dissolution, Anderson concluded in 1978 that the integrity of the WIPP to isolate radioactive waste would not be jeopardized by dissolution within about *one* million years. Anderson and Kirkland (1980, *pp.* 66 - 69) expanded on the concept of brine density flow proposed by Anderson in (1978) as a means of dissolving evaporites at a point by circulating water from the underlying Bell Canyon. Wood et al. (1982, *p.* 100) examined the mechanism and concluded that, while it was physically feasible, it would not be effective enough in removing salt to threaten the ability of the WIPP to isolate transuranic (TRU) waste.

2.1.6.2.4 Features Related to Dissolution

Bachman (1980, *p.* 97) separated breccia pipes, formed over the Capitan Reef by dissolution and collapse of a cylindrical mass of rock, from evaporite karst features that appear similar to breccia pipes. There are surficial karst features, including sinks and caves, in large areas of the

basin. Nash Draw is the result of combined dissolution and erosion. Within the site boundaries, there are no known surficial features caused by dissolution or karst.

The subsurface structure of the Culebra is shown in Figure 2-24~~28~~. South of the WIPP site, *an antiformal structure informally called the “Remuda Basin anticline” has been created by dissolution of salt from the underlying Salado to the southwest of the anticline.* ~~between Pierree Canyon and Paduca Breaks there is a relationship between this structure and dissolution. Salt has been removed from the underlying Salado to create a general anticline from near Laguna Grande de la Sal to the southeast of the WIPP site.~~ Beds generally dip to the east, and salt removed to the west created the other limb of the structure. Units below the evaporites apparently do not show the same structure.

2.2 Surface Water and Groundwater Hydrology

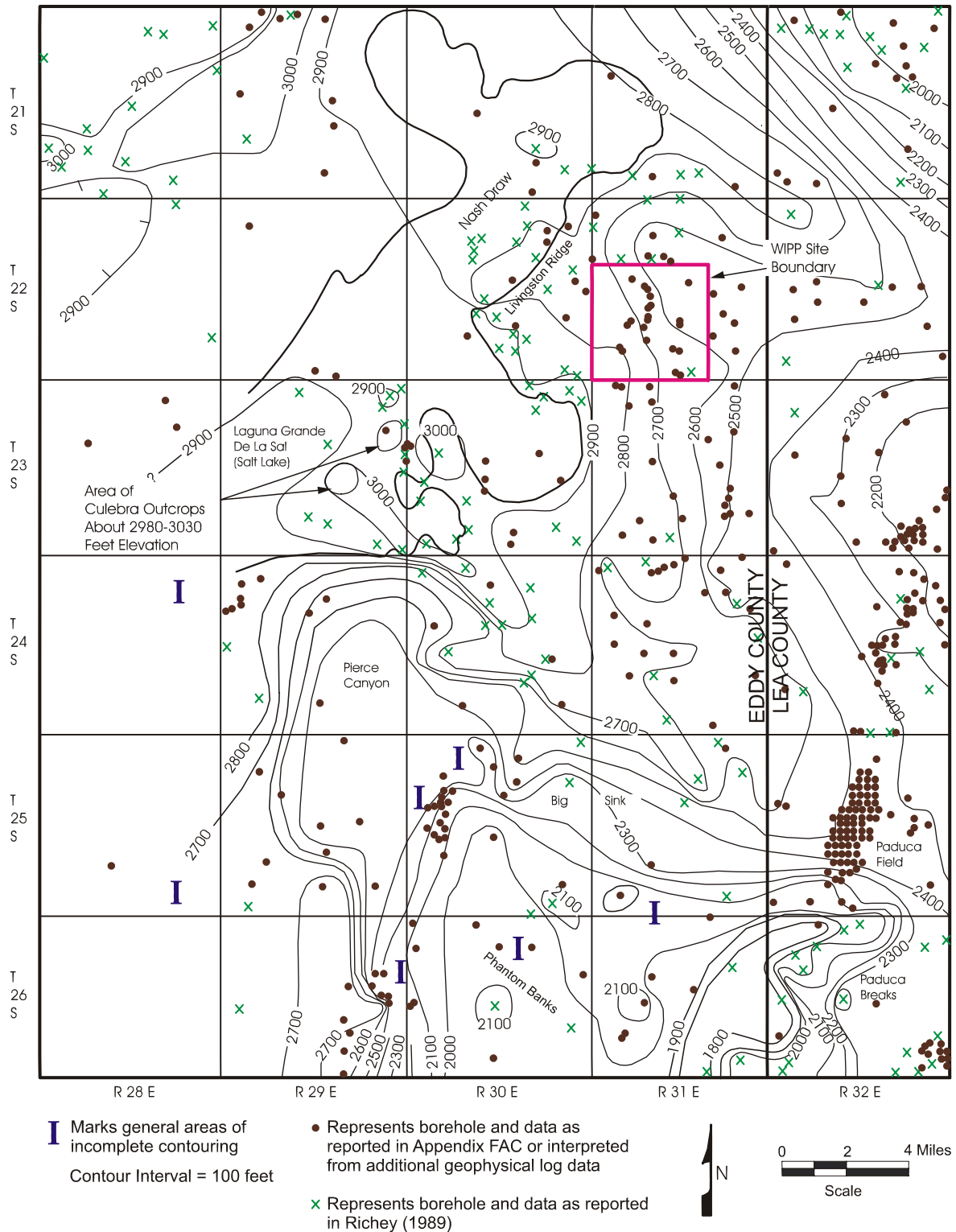
The DOE has determined that the hydrological characteristics of the disposal system are important because contaminant transport via fluid flow has a potential to impact the performance of the disposal system. In addition, the EPA has provided numerous criteria related to groundwater in 40 CFR § 194.14(a). At the WIPP site, one of the DOE’s selection criteria was to choose a location that would minimize this impact. This was accomplished when the DOE selected (1) a host formation that contains little groundwater and transmits it poorly, (2) a location where the effects of groundwater flow are minimal and predictable, (3) an area where groundwater use is low, (4) an area where there are no permanent surface waters, (5) an area where future groundwater use is unlikely, and (6) a repository host rock that will not likely be affected by anticipated possible long-term climate changes within 10,000 years.

The following discussion summarizes the characteristics of the groundwater and surface water at and around the WIPP site. This summary is based on data collection programs that were initiated with the WIPP program and that continue to some extent today. The purpose of these programs was to provide information sufficient for the development and use of predictive models of the groundwater movement at the WIPP site.

For a comprehensive understanding of the impact of groundwater and surface water on the disposal system, the following factors have been evaluated:

Groundwater

- Horizontal and vertical flow fluxes and velocities,
- Hydraulic interconnectivity between rock units,
- Hydraulic parameters (porosity, etc.),
- General groundwater use, and
- Chemistry (including, but not limited to, salinity, mineralization, age, Eh, and pH).



CCA-041-2

Figure 2-24. Structure Contour Map of Culebra Dolomite Base

1 Surface Water

- 2 • Regional precipitation and evapotranspiration rates,
- 3 • Location and size of surface-water bodies,
- 4 • Water volume, flow rate, and direction,
- 5 • Drainage network,
- 6 • Hydraulic connection with groundwater,
- 7 • Soil hydraulic properties (infiltration), and
- 8 • General water chemistry and use.

9 Changes to the hydrological system due to human activity are evaluated in Chapter 6.0.

10 The specifics of groundwater modeling are found in Section 6.4.6, Appendix *PA, Attachment*
 11 MASS, Section MASS.14.2. The hydrological system is divided into four segments for the
 12 discussion in this chapter. These are: (1) the rock units below the Salado, which may impact the
 13 disturbed (human intrusion) performance of the disposal system, (2) the Salado, which mostly
 14 addresses the undisturbed performance of the disposal system, (3) the rock units above the
 15 Salado, which essentially impact only the disturbed (human intrusion) performance of the
 16 disposal system, and (4) the surface waters. The groundwater regime is discussed in
 17 Section 2.2.1, and the surface-water regime in Section 2.2.2.

18 The WIPP site lies within the Pecos River drainage area (Figure 2-25~~23~~²³, see also Section 2.2.2,
 19 Figure 2-36~~43~~⁴³). As discussed in the Final Environmental Impact Statement (FEIS) (DOE 1980,
 20 Section 7.1.1), the climate is semiarid, with a mean annual precipitation of about 0.33 m (13 in.),
 21 a mean annual runoff of 2.5 to 5 mm (0.1 to 0.2 in.), and a mean annual pan evaporation of more
 22 than 2.5 m (100 in.). Runoff is practically nonexistent and the WIPP does not have a well
 23 defined drainage pattern. The general movement of runoff can be inferred from the topography
 24 in Figure 2-25~~23~~²³. Only one stream flow gaging station has been operated in the vicinity. This is
 25 at the location shown as Hill Tank in Figure 2-25~~23~~²³. Observations at Hill Tank are discussed in
 26 Section 2.2.2.

27 Additional information about climatic conditions at the WIPP is given in Section 2.5.2. Brackish
 28 water with total dissolved solids (TDS) concentrations of more than 3,000 parts per million is
 29 common in the shallow wells near the WIPP site. Surface waters typically have high TDS
 30 concentrations, particularly of chloride, sulfate, sodium, magnesium, and calcium. Additional
 31 information about water quality is given in Section 2.4.2.

32 **2.2.1 Groundwater Hydrology**

33 At the WIPP site, the DOE ~~has obtained~~ obtains groundwater hydrologic data from conventional
 34 and special-purpose test configurations in multiple surface boreholes. ~~(Figure 2-2 is a map of~~
 35

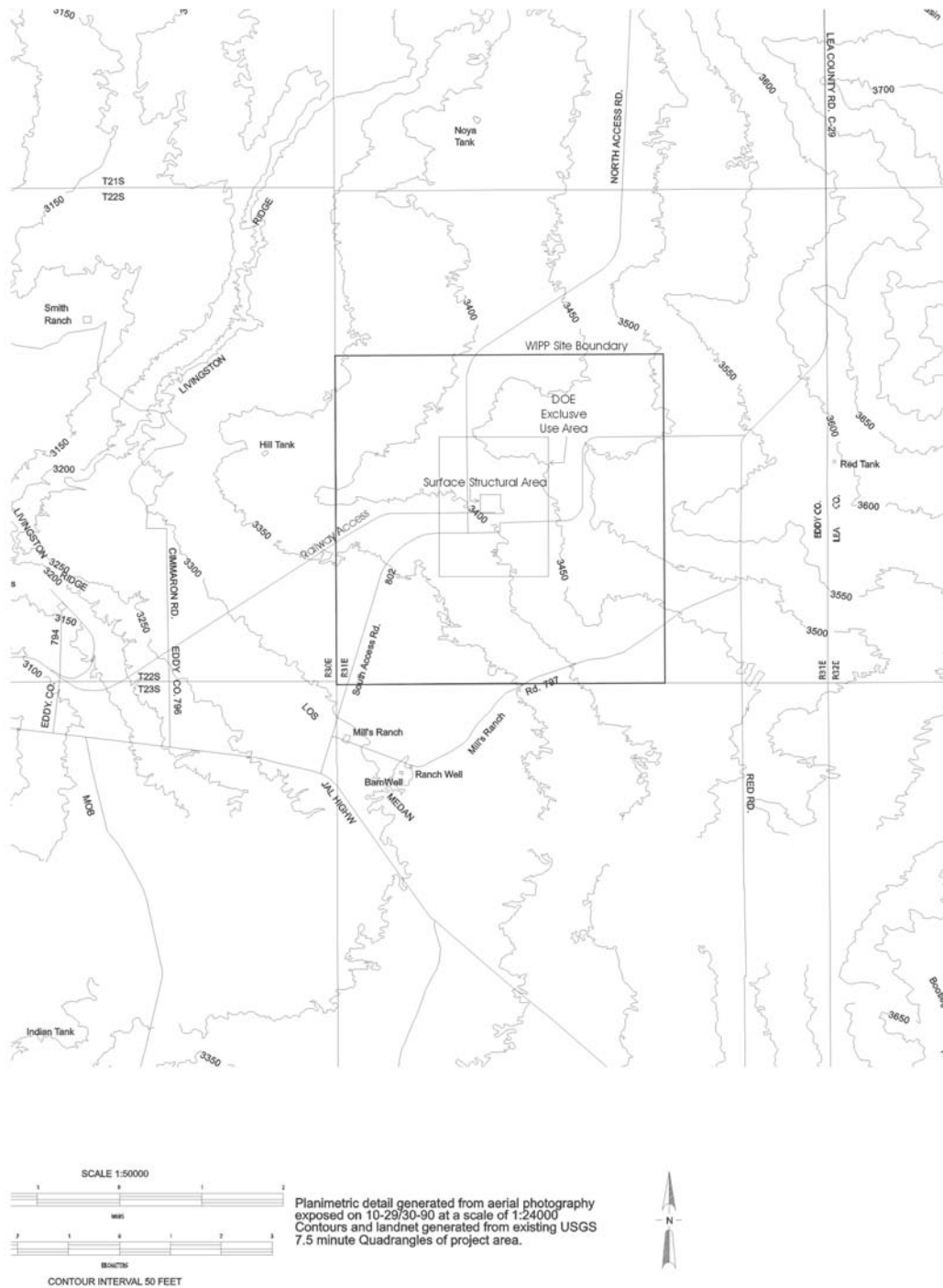


Figure 2-25. Drainage Pattern in the Vicinity of the WIPP Facility

~~borehole locations.~~) Geophysical logging of the boreholes has provided hydrologic information on the rock strata intercepted. Pressure measurements, fluid samples, and ranges of rock permeability have been obtained for selected formations through the use of standard and modified drill-stem tests. Slug injection or withdrawal tests and other flow-rate tests have provided data to aid in the estimation of transmissivity and storage. The hydraulic heads of groundwaters within many water-bearing zones in the region have been mapped from measured depths to water in the boreholes.

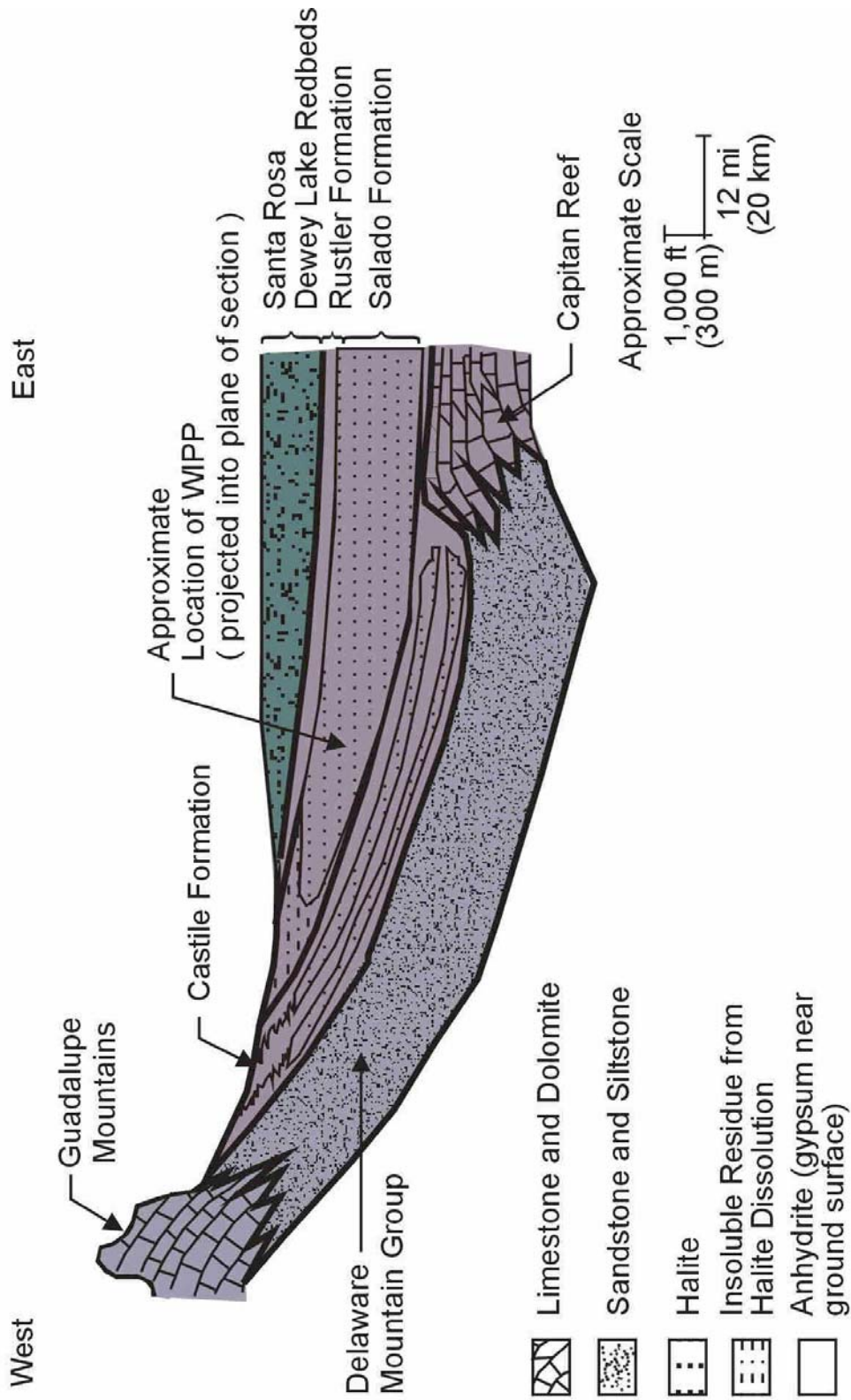
Since the CCA was submitted to the EPA in 1996, the DOE has implemented a number of monitoring programs (see Appendix MON-2004), including the Groundwater Monitoring Program, to meet the assurance requirements of 40 CFR § 191.14(b). In addition to the groundwater monitoring program, other hydrologic data gathered since the CCA come from logging of new or replacement wells, piezometers, special-purpose field investigations, and surveys of drilling practices in the Delaware Basin. A data summary of all these activities is provided in Appendix DATA.

Historically, the DOE has obtained hydrological data principally from a conventional well-monitoring network (Figures 2-3 through 2-6 are maps of the well locations) comprising 71 wells located on 45 separate wellpads (DOE 2003). Most of the 71 wells are completed only to a single hydrologic unit; however, six are multiple-completions to allow monitoring of two or more units in the same well. Hydrologic information (such as hydraulic head) is obtained at 80 completion intervals within the 71 wells. The focus of the hydrological monitoring is the Rustler (comprising 72 of the 80 monitored intervals) because this formation contains two of the most transmissive saturated units, the Culebra and Magenta Dolomites, which are important to the modeling of releases during various human intrusion scenarios. Limited hydrological monitoring of the Bell Canyon, Dewey Lake, and Santa Rosa also occurs.

Rock units that are shown in the conceptual models in Section 6.4 to be important to disposal system performance from a hydrological standpoint are the Castile, the Salado, the Rustler, and the Dewey Lake (Figures 2-26~~30~~ and 2-27~~31~~). However, other units which are discussed due to their significance in screening hydrological processes or because they are less important to the conceptual model include the Bell Canyon, the Capitan, the Rustler-Salado contact zone, and the ~~supra~~-Dewey Lake units. These will also be discussed because they are features of the groundwater flow system of the WIPP region.

The Bell Canyon is of interest to the DOE because it is the first regionally continuous water-bearing unit beneath the WIPP *and is the target stratigraphic horizon for salt-water injection by industry outside of the WIPP site boundary*. The halite and anhydrite layers of the Castile provide a hydrologic barrier between the Salado and the underlying Bell Canyon. The Castile is of interest to *PA* because it contains isolated high-permeability zones containing pressurized brine. As discussed in Section 2.1.6.1, several such zones of pressurized brine have been intercepted by boreholes near the WIPP site, and one or more *of these zones* may exist at the WIPP site.

The Salado comprises low-permeability beds of variable composition. The low permeability of the Salado provides a hydrologic barrier in all directions between the repository and the accessible environment or more transmissive beds. *At the repository horizon, a much higher*



CCA-043-2

Figure 2-26.30. Schematic West-East Cross Section through the North Delaware Basin

1

2

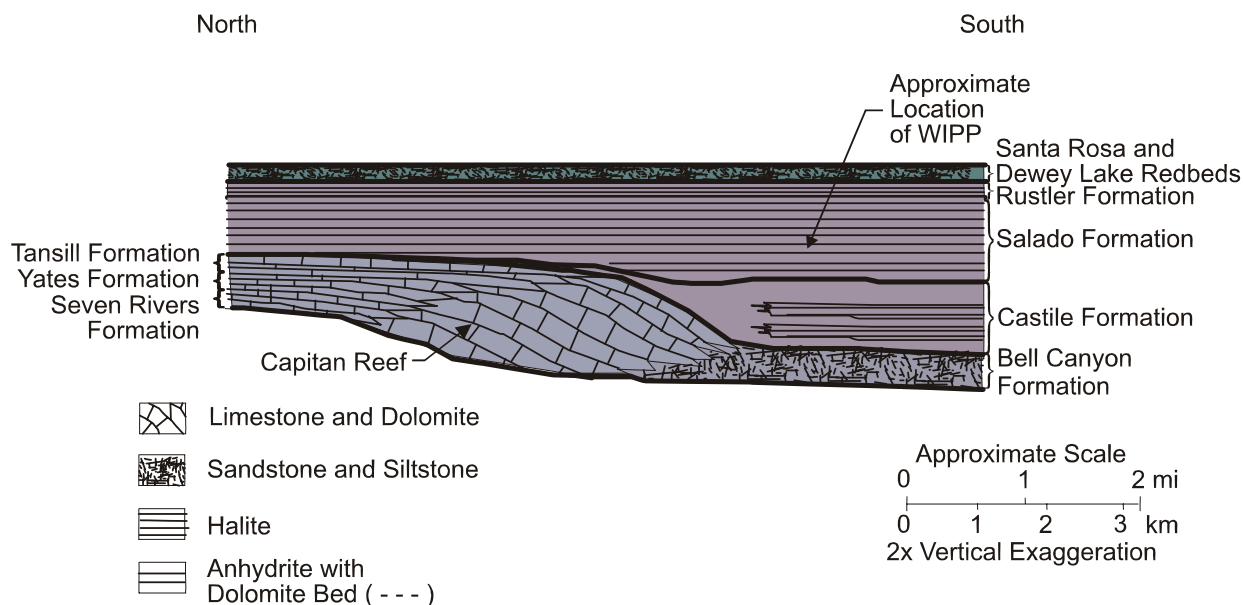


Figure 2-2731. Schematic North-South Cross Section through the North Delaware Basin

permeability DRZ forms locally in the salt around the waste emplacement rooms and operational drifts. As described in Appendix DATA, the DRZ is of limited extent compared to the significant thickness of the Salado low-permeability beds surrounding the repository horizon.

The Rustler contains two laterally transmissive members. The Culebra is the first laterally continuous unit located above the WIPP underground facility to display hydraulic conductivity sufficient to warrant ~~concern about~~ *investigation for* lateral contaminant transport. It is also the most transmissive *continuously saturated* unit above the Salado *WIPP repository* at the WIPP site. Therefore, except for a ~~breach~~ *release* directly to the surface, the Culebra provides the most direct pathway between the WIPP underground and the accessible environment. The hydrology and fluid geochemistry of the Culebra are complex and, as a result, have received a great deal of study (see, for example, LaVenue et al. 1988, 1990; Haug et al. 1987; and Siegel et al. 1991 ~~in the bibliography~~). The Magenta, although more transmissive than the anhydrite and claystone members of the Rustler, has lower transmissivity than the Culebra, and is unfractured at the WIPP.

There was no inflow of water from the Dewey Lake into the WIPP shafts after they were completed and prior to their lining, indicating unsaturated conditions or low transmissivity. ~~Flow from a fractured zone has been observed at Water Quality Sampling Program (WQSP) 6a. The Santa Rosa is shallow and unsaturated at the site, and the only flow through it is infiltration, which likely occurs at low rates because of the evaporative climate.~~ *However, since 1995, routine inspections of the WIPP exhaust shaft have revealed water entering the shaft at a depth of approximately 24 m (80 ft) at a location where no water had been observed during construction (the DOE is investigating the source and extent of this water; see Sections*

2.2.1.4.2.1 and Appendix DATA). The quantity and quality of water in the Dewey Lake is also monitored in a deeper fractured zone in the Dewey Lake at well WQSP-6a (WIPP MOC 1995).

The Santa Rosa is shallow and unsaturated at the site *(with the exception of a perched water table directly below the WIPP surface structures; – see Section 2.2.1.4.2.2 and Appendix DATA), and apparently receives recharge only through infiltration.* ~~and the only flow through it is infiltration, which likely occurs at low rates because of the evaporative climate.~~

In conclusion, at the WIPP site, the DOE recognizes the Salado as the most significant nontransmissive unit and the Culebra and the Magenta as the most significant transmissive units. Other units are considered to have less important roles. The DOE's sampling and analysis of non-Salado groundwater has focused on the Culebra and Magenta, and their hydrologic background, presented here, is more detailed than for other non-Salado rock units. Table 2-4 provides an overview of the hydrologic characteristics of the Rustler rock units at the WIPP site and the Rustler-Salado contact zone in Nash Draw. In developing this position on modeling the hydrology of the WIPP, the DOE considered several modeling approaches. These are summarized in *CCA* Appendix MASS, Section MASS.14.1 *in* general and Section MASS.15.1 for the Culebra. The DOE's conceptual models for hydrology are in Sections 6.4.5 and 6.4.6.

Table 2-4. Hydrologic Characteristics of the Rustler at the WIPP and in Nash Draw

Member	Thickness (meters)		Transmissivity (square meters per second)		Porosity	
	max	min	max	min	max	min
Forty-niner	23	13	8×10^{-8}	3×10^{-9}	—	—
Magenta	8.5	7	4×10^{-4}	1×10^{-9}	0.25	0
Tamarisk	56	26	2.7×10^{-11}	—	—	—
Culebra	11.6	4	1×10^{-3}	1×10^{-9}	0.30	0.03
unnamed lower <i>Los Medaños</i>	38	29	2.9×10^{-10}	2.2×10^{-13}	—	—
Rustler-Salado Contact Zone in Nash Draw	18	3	8.6×10^{-6}	3.2×10^{-11}	0.33	0.15

The EPA sought information supporting the conceptualization of the disposal system and the major site-related characteristics included in the PA modeling during the compliance review process for Section 194.14(a)(3). In general, the EPA concluded that the groundwater hydrology information for the various geologic and hydrostratigraphic units at the WIPP site identified the important characteristics of the PA and was therefore technically sufficient. The EPA also noted that the primary hydrogeologic units of concern relative to containment capability of the WIPP are the Castile, Salado, Rustler, and the Dewey Lake.

The EPA noted that the potential for fluid migration through Salado marker beds and the Culebra were acknowledged by DOE and included in the PA calculations. While the Dewey Lake is a potential underground source of drinking water (Section 8.2.2), DOE's modeling

indicated that radionuclides will not reach the Dewey Lake, thus removing the formation as a unit needing consideration as a pathway (Docket A-93-02, Item II-G-26 and Docket A-93-02, Item II-G-28). The EPA concluded that Salado marker beds, and the Culebra were adequately identified and characterized to the level necessary for PA calculations.

2.2.1.1 Conceptual Models of Groundwater Flow

The DOE addresses issues related to groundwater flow and radionuclide transport within the context of a conceptual model of how the natural hydrologic system works on a large scale. The conceptual model of regional flow around the WIPP that is presented here is based on widely accepted concepts of regional groundwater flow in groundwater basins (see, for example, Hubbert 1940; Tóth 1963; and Freeze and Witherspoon 1967 in the bibliography).

See CCA Appendix MASS, Sections MASS.14.1 and MASS.14.2 for a summary of the DOE's activities leading to the acceptance of the groundwater basin model as a reasonable representation of groundwater flow in the region.

An idealized groundwater basin is a three-dimensional closed hydrologic unit bounded on the bottom by an impermeable rock unit (units with much smaller permeability than the units above), on the top by the ground surface, and on the sides by groundwater divides. The water table is the upper boundary of the region of saturated liquid flow. All rocks in the basin are expected to have finite permeability; in other words, hydraulic continuity exists throughout the basin. This means that the potential for liquid flow from any unit to any other units exists, although the existence of any particular flow path is dependent on a number of conditions related to gradients and permeabilities. All recharge to the basin is by infiltration of precipitation to the water table and all discharge from the basin is by flow across the water table to the land surface.

Differences in elevation of the water table across an idealized basin provide the driving force for groundwater flow. The pattern of groundwater flow depends on the lateral extent of the basin, the shape of the water table, and the heterogeneity of the permeability of the rocks in the basin. Water flows along gradients of hydraulic head from regions of high head to regions of low head. The highest and lowest heads in the basin occur at the water table at its highest and lowest points, respectively. Therefore, groundwater flows from the elevated regions of the water table, downward across confining layers (layers with relatively small permeability), then laterally along more conductive layers, and finally upward to exit the basin in regions where the water table (and by association, the land surface) is at low elevations. Recharge is necessary to maintain relief on the water table, without which flow does not occur.

Groundwater divides are boundaries across which it is assumed that no groundwater flow occurs. In general, these are located in areas where groundwater flow is dominantly downward (recharge areas) or where groundwater flow is upward (discharge areas). Topography and surface-water drainage patterns provide clues to the location of groundwater divides. Ridges between creeks and valleys may serve as recharge-type divides, and rivers, lakes, or topographic depressions may serve as discharge-type divides.

In the groundwater basin model, rocks can be classified into hydrostratigraphic units. A hydrostratigraphic unit is a continuous region of rock across which hydraulic properties are

1 similar or vary within described or stated limits. The definition of hydrostratigraphic units is a
2 practical exercise to separate rock regions with similar hydrologic characteristics from rock
3 regions with dissimilar hydrologic characteristics. Although hydrostratigraphic units often are
4 defined to be similar to stratigraphic units, this need not be the case. Hydrostratigraphic unit
5 boundaries can reflect changes in hydraulic properties related to differences in composition,
6 fracturing, dissolution, or a variety of other factors that may not be reflected in the definition of
7 stratigraphic formations.

8 Confining layers in a groundwater basin model can be characterized as allowing vertical flow
9 only. The amount of vertical flow occurring in a confining layer generally decreases in relation
10 to the depth of the layer. Flow in conductive units is more complicated. In general, flow will be
11 lateral through conductive units. The magnitude (in other words, volume flux) of lateral flow is
12 related to the thickness, conductivity, and gradient present in the unit. Gradients generally
13 decrease in deeper units. The direction of flow is generally related to the distance the unit is
14 from the land surface. Near the land surface, flow directions are influenced primarily by the
15 local slope of the land surface. In deeper conductive units, flow directions are generally oriented
16 parallel to the direction between the highest and lowest points in a groundwater basin. Thus,
17 flow rates, volumes, and directions in conductive units in a groundwater basin are generally not
18 expected to be the same.

19 In the WIPP region, the Salado provides an extremely low-permeability layer that forms the base
20 for a regional groundwater-flow basin in the overlying rocks of the Rustler, Dewey Lake, and
21 Santa Rosa. The Castile and Salado together form their own groundwater system, and they
22 separate flow in units above them from that in units below. Because of the plastic nature of
23 halite and the resulting low permeability, fluid pressures in the evaporites are more related to
24 lithostatic stress than to the shape of the water table in the overlying units, and regionally neither
25 vertical nor horizontal flow will occur as a result of natural pressure gradients in time scales
26 relevant to the disposal system. (On a repository scale, however, the excavations themselves
27 create pressure gradients that may induce flow near the excavated region.) Consistent with the
28 recognition of the Salado as the base of the groundwater basin of primary interest, the following
29 discussion is divided into three sections: hydrology of units below the Salado, hydrology of the
30 Salado, and hydrology of the units above the Salado. The DOE has implemented the
31 groundwater basin model in the conceptual model for groundwater flow within the rocks above
32 the Salado. The details of the model are discussed in Section 6.4.6. Key modeling assumptions
33 associated with the implementation are provided in Appendix *PA, Attachment* MASS, Section
34 MASS.14.2.

35 *Technical issues related to the Castile brine, Salado marker bed permeability, and Culebra*
36 *hydraulic properties (e.g., transmissivity variation) were raised by the EPA in a letter dated*
37 *December 19, 1996 (Docket A-93-02, Item II-I-01). The DOE provided additional information*
38 *regarding these issues in letters dated January 24, 1997; February 7, 1997; April 15, 1997;*
39 *June 13, 1997; June 27, 1997; and July 3, 1997 (Docket A-93-02, Items II-I-03, II-I-07, II-I-*
40 *24, II-H-44, II-H-45, and II-H-46, respectively).*

41 *A request was made in the December 19, 1996 EPA letter (Docket A-93-02, Item II-I-01) that*
42 *DOE provide general hydraulic characteristic information for all geologic units within the*
43 *disposal system by revising a partially complete table included in the letter. The DOE letter,*

dated February 14, 1997 (Docket A-93-02, Item II-I-08), transmitted the summary table providing the EPA with additional groundwater hydrology information related to hydraulic conductivity, storage coefficients, transmissivity, permeability, thickness, matrix and fracture characteristics, and hydraulic gradients for each of the geologic units in the WIPP disposal system. This information was reproduced as Figure IV-10 in EPA Technical Support Document for Section 194.14: Content of Compliance Certification Application (Docket A-93-02, Item V-B-3).

In addition, the EPA in the December 19, 1996 EPA letter (Docket A-93-02, Item II-I-01) required the DOE to include the following in the discussion of conceptual models for groundwater flow: (1) the estimated infiltration at the surface and to the Dewey Lake, and (2) the estimated vertical flow of groundwater into other transmissive units within the area surrounding the WIPP. The DOE provided the estimates in a letter dated February 26, 1997 (Docket A-93-02, Item II-I-10) to EPA.

2.2.1.2 Units Below the Salado

Units of interest to the WIPP project below the Salado are the Bell Canyon and the Castile. These units have quite different hydrologic characteristics. Because of its potential to contain brine reservoirs below the repository, the hydrology of the Castile is regarded as having the most potential of all units below the Salado to impact the performance of the disposal system.

2.2.1.2.1 Hydrology of the Bell Canyon Formation

The Bell Canyon is considered for the purposes of regional groundwater flow to form a single hydrostratigraphic unit about 300 m (1,000 ft) thick. Tests at five boreholes (Atomic Energy Commission [AEC]-7, AEC-8, ERDA-10, DOE-2, and Cabin Baby ~~[CBJ-1]~~ (CCA Appendix HYDRO, pp. 29-31; Beauheim et al. 1983, pp. 4-9 to 4-12; Beauheim 1986, p. 61-1]) indicate a range of hydraulic conductivities for the Bell Canyon from 1.7×10^{-7} to 3.5×10^{-12} m/sec (5×10^{-2} ft/day to 1×10^{-6} ft/day). The pressure measured in the Bell Canyon at the DOE-2 and ~~CB-1 Cabin Baby~~ boreholes *at the time of the CCA ranged* ~~ranges~~ from 12.6 to 13.3 megapascals. *Under the current groundwater-monitoring program, Bell Canyon water levels are measured in only two wells: CB-1 and AEC-8 (see locations in Figure 2-6).*

After recovery from well work in 1999, the Bell Canyon water levels at CB-1 have remained steady for more than three years at 919 m (3,015 ft) above mean sea level (SNL 2003a). In contrast, since the beginning of 1994, the Bell Canyon water levels at AEC-8 have steadily risen by more than 32 m (106 ft) at a rate of approximately 0.5 m/month (1.6 ft/month) and stood at over 933.4 m (3,062 ft) above mean sea level (SNL 2003a) at the end of 2002. This water-level rise is hypothesized to be the result of deterioration of the well and not a response to actual Bell Canyon hydrologic conditions at this location. The well will be inspected and repaired or plugged and abandoned, as necessary, according to the requirements of DOE's groundwater monitoring program (see Appendix MON-2004).

Fluid flow in the Bell Canyon is markedly influenced by the presence of the extremely low-permeability Castile and Salado above it, which effectively isolate ~~it~~ *the Bell Canyon* from interaction with overlying units except where the Castile is absent because of erosion or

nondeposition, such as in the Guadalupe Mountains, or where the Capitan ~~R~~ef is the overlying unit (Figures 2-26~~30~~ and 2-27~~31~~). Because of the isolating nature of the Castile and Salado, fluid flow directions in the Bell Canyon are sensitive only to gradients established over very long distances. At the WIPP, the brines in the Bell Canyon flow northeasterly under an estimated hydraulic gradient of 4.7 to 7.6 m/km (25 to 40 ft/mi) and discharge into the Capitan aquifer. Velocities are on the order of tenths of feet per year, and groundwater yields from wells in the Bell Canyon are 2.3 to 5.8 liters (0.6 to 1.5 gallons) per minute. The fact that flow directions in the Bell Canyon under the WIPP are inferred to be almost opposite to the flow directions in units above the Salado (see Section 2.2.1.4) is not of concern because, as discussed above, the presence of the Castile and Salado makes the flow in the Bell Canyon sensitive to gradients established over long distances, whereas flow in the units above the Salado is sensitive to gradients established by more local variations in water table elevation.

As discussed in Appendix DATA, oil companies are currently involved in deep-well injection at several locations outside of the WIPP site boundary. Specifically, salt water (brine) produced during oil-field exploitation is injected into the Bell Canyon and Brushy Canyon Formations. For nearly four years, the DOE has monitored injection rates and pressures for a cluster of six of these salt water injection wells located approximately 1.6 to 2.4 km (1 to 1.5 mi) northeast of well H-9. Table 2-5 summarizes the depth intervals of the injection zones for each well. The cluster of six wells is currently injecting approximately 800 to 950 m³ per day (5,000 to 6,000 barrels per day) of salt water; however, in previous years, injection has ranged from approximately 480 to 1270 m³ per day (3,000 to 8,000 barrels per day) (SNL 2003a). Wellhead injection pressures typically range between 5.5 to 6.9 MPa (800 to 1,000 psi). Because only two Bell Canyon wells are currently being monitored, the effect of salt-water injection on Bell Canyon water levels is speculative, but water levels in the Bell Canyon monitoring well nearest the cluster (i.e., CB-1, Figure 2-6) indicate no response to the injection. Additional discussion on potential effects of salt-water injection on the WIPP hydrologic setting is provided below in Section 2.2.1.4.

2.2.1.2.2 Castile Hydrology

As described in Section 2.1.3, the Castile is dominated by low-permeability anhydrite and halite zones. However, fracturing in the upper anhydrite has generated isolated regions with much greater permeability than the surrounding intact anhydrite. These regions are located in the area of structural deformation, as discussed in Section 2.1.6.1.1. The higher-permeability regions of the Castile contain brine at pressures greater than hydrostatic and have been referred to as brine reservoirs (see Figure 2-28~~32~~). The fluid pressure measured by Popielak et al. ~~in~~ (1983) in the WIPP-12 borehole (12.7 megapascals) is greater than the nominal hydrostatic pressure for a column of equivalent brine at that depth (11.1 megapascals).

Therefore, under open-hole conditions, brine could flow upward to the surface through a borehole.

Results of hydraulic tests performed in the ERDA-6 and WIPP-12 boreholes suggest that the extent of the highly permeable portions of the Castile is limited. As discussed in Section 2.1.3.3 and modeled in Section 6.4.8, the vast majority of brine is thought to be stored in low-permeability microfractures; about ~~5~~ *five* percent of the overall brine volume is stored in large

Table 2-5. Depth Intervals of the Injection Zones of Six Salt-Water Injection Wells Located Near Well H-9 (after SNL 2003a)

<i>Injection Well</i>	<i>Depth Interval of Injection Zone, feet⁽¹⁾</i>
<i>Cal Mon #5</i>	<i>4,484 – 5,780⁽²⁾</i>
<i>Sand Dunes 28F#1⁽³⁾</i>	<i>4,295 – 5,570⁽²⁾</i>
<i>Pure Gold B F#20⁽³⁾</i>	<i>7,740 – 7,774⁽⁴⁾</i>
<i>Todd 26F#2</i>	<i>4,460 – 5,134⁽²⁾</i>
<i>Todd 26F#3</i>	<i>4,390 – 6,048⁽²⁾</i>
<i>Todd 27F#16</i>	<i>4,694 – 5,284⁽²⁾</i>

⁽¹⁾ *Below ground surface, bgs*

⁽²⁾ *Bell Canyon Formation*

⁽³⁾ *Wells hydraulically connected to same manifold*

⁽⁴⁾ *Brushy Canyon Formation*

open fractures. The volumes of the ERDA-6 and WIPP-12 brine reservoirs were estimated by Popielak et al. in (1983) to be 100,000 m³ (3.5 × 10⁶ ft³) and 2,700,000 m³ (9.5 × 10⁷ ft³), respectively. The conceptual model of the Castile brine region is discussed in Section 6.4.8. The model uses parameter values derived from the ERDA-6 and WIPP-12 tests for quantifying some reservoir characteristics. The derivation of some model parameters in Appendix *PA, Attachment PAR, Table PAR-44* (Tables PAR-49 and PAR-50) from the data discussed here is also given in *CCA* Appendix MASS, Section MASS.18.

A geophysical survey using time-domain electromagnetic (TDEM) methods was completed over the WIPP-12 brine reservoir and the waste disposal panels (The Earth Technology Corporation 1988). The TDEM measurements detected a conductor interpreted to be the WIPP-12 brine reservoir and also indicated that similar brine occurrences may be present within the Castile under a portion of the waste disposal panels. In a recent geostatistical analysis, Powers et al. (1996) used 354 drill holes and 27 Castile brine occurrences to establish that there is an 8 *eight* percent probability of a hole drilled into the waste panel region encountering brine in the Castile. This analysis is *was* included in the application as Attachment 18-6 in *CCA* Appendix MASS, *Attachment 18-6*.

Initially, the EPA found that DOE's discussion of the size, orientation, and repressurization potential of the Castile brine reservoirs was not well supported (Docket A-93-02, Item II-I-27). The EPA required the probability of encountering a brine reservoir to be sampled between a range of 1 and 60 percent in the PAVT (Docket A-93-02, Item II-G-26 and Docket A-93-02, Item II-G-28). In addition, the EPA modified the values for parameters such as bulk compressibility of Castile rock so that the brine reservoir sampling used in the PA would better represent the larger, higher-end possible brine volumes. Further information on the EPA review of these parameters may be found in CARD 23—Models and Computer Codes (EPA 1998f), EPA Technical Support Document for Section 23: Models and Computer Codes (Docket A-93-02, Item V-B-6), and EPA Technical Support Document for Section 23: Ground

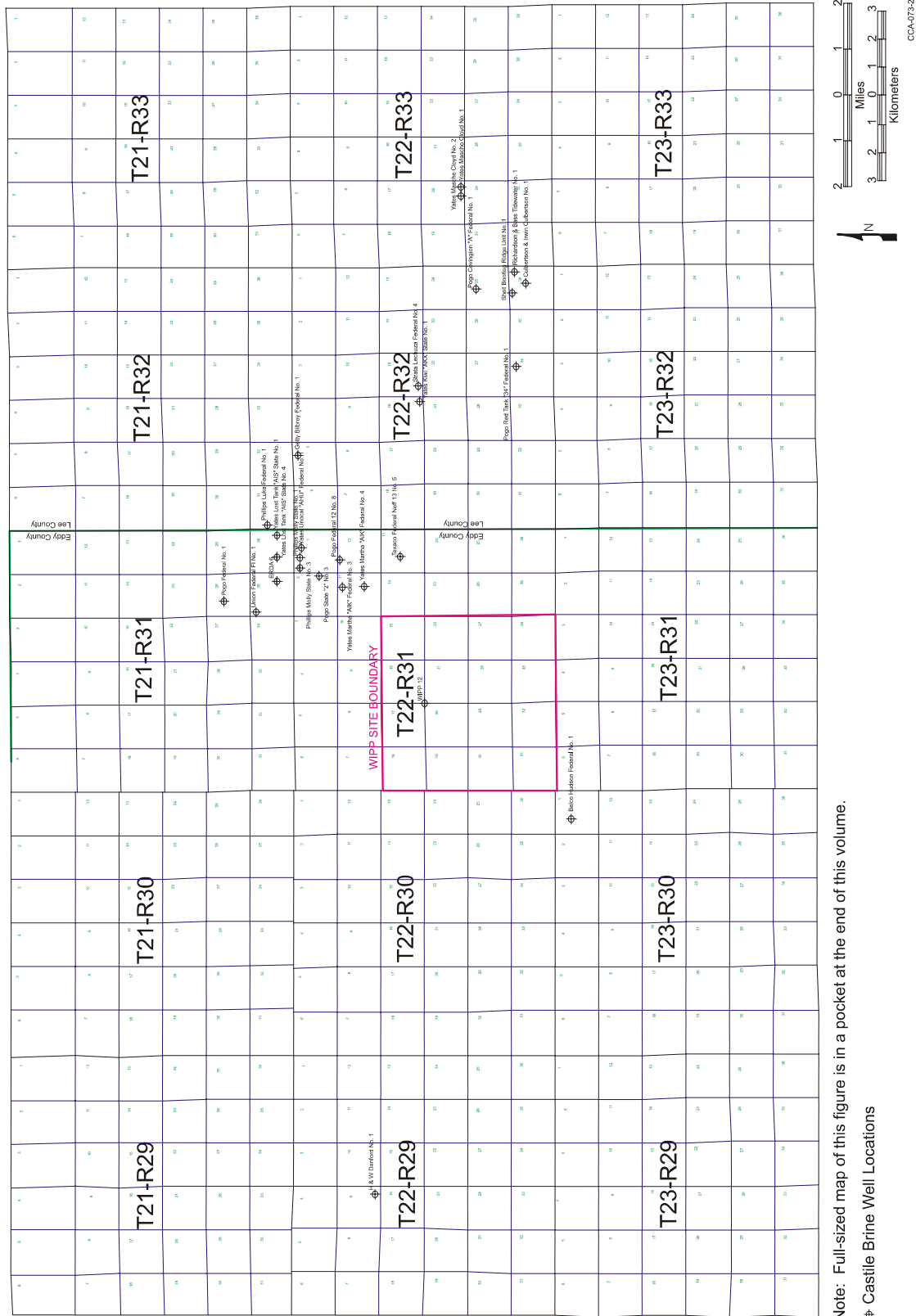


Figure 2-2832. Recent Occurrences of Pressurized Brine in the Castile

Water Flow and Contaminant Transport Modeling at WIPP (Docket A-93-02, Item V-B-7). The PAVT used modified Castile brine reservoir characteristics and showed that the WIPP still meets the containment requirements (Docket A-93-02, Item II-G-26, Figure 7-2).

Based on these analyses, there was no significant impact on releases over the range of probabilities sampled. However, the DOE identified this parameter as a compliance monitoring parameter (see Appendix DATA) and conducts annual surveys as part of the Delaware Basin Monitoring Program (see Appendix MON-2004) to identify Castile brine encounters by drillers in the basin. Since the CCA, these surveys have identified five additional brine encounters. Appendix DATA provides extensive information pertinent to the brine reservoirs. The Delaware Basin Monitoring Annual Report (DOE 2002a), for example, documents three of the five Castile brine encounters. Two were located near well ERDA-6 northeast of the WIPP site and one was located to the southwest of the site. In the two encounters northeast of the site, reports indicated several hundred barrels of brine per hour were produced, but all brine was contained within the pits; thus, it was not necessary to file a report with the New Mexico Oil Conservation Division. In the other encounter, initial flows of from 64 to 79 m³ (400 to 500 barrels) per hour were observed, but flow dissipated within hours of the encounter. Because of the relatively large number of boreholes (345 wells in the nine-township area drilled between 1996 and 2002), the five brine encounters that occurred do not substantially change the probability defined by Powers et al. (1996) and are unlikely to have any significant impact on PA given the large range of probabilities sampled in the PAVT analyses.

The origin of brine in the Castile has been investigated geochemically. Popielak et al. (1983, p. 2) concluded that the ratios of major and minor element concentrations in the brines indicate that these fluids originated from ancient seawater and that no evidence exists for fluid contribution from present meteoric waters. The Castile brine chemistries from the ERDA-6 and WIPP-12 reservoirs are distinctly different from each other and from local groundwaters. These geochemical data indicate that brine in reservoirs has not mixed to any significant extent with other waters and has not circulated. The brines are saturated, or nearly so, with respect to halite and, consequently, have little potential to dissolve halite. The chemical composition of Castile brine is given in Table 2-56. *It's the use of the chemical composition of Castile brine as a parameter model in the conceptual model of repository performance is discussed in the Appendix PA. SOTERM (Section SOTERM.2.2.1).*

2.2.1.3 Hydrology of the Salado

As described in Section 2.1.3, the Salado consists mainly of halite and anhydrite. A considerable amount of information about the hydraulic properties of these rocks has been collected through field and laboratory experiments. ~~Appendices HYDRO (41-42) and Appendix PA PAR~~ summarizes this information.

Hydraulic testing in the Salado in boreholes in the WIPP underground repository provided quantitative estimates of the hydraulic properties controlling brine flow through the Salado (Beauheim et al. 1991a; Beauheim et al. 1993; Domski et al. 1996; *Roberts et al. 1999*). *This work was summarized by Beauheim and Roberts (2002).* The stratigraphic intervals tested

1

Table 2-56. WIPP Salado and Castile Brine Compositions

	Salado Brine Average (n between 82 and 96)		Castile ERDA-6	Castile WIPP-12
Specific Gravity	1.22	± 0.01	1.216	1.215
pH	6.1		6.17	7.06
Sodium	79100	± 2,100	112000	138000
Potassium	15900	± 800	3800	2900
Calcium	282	± 38	490	350
Magnesium	22700	± 1,400	450	1600
Boron	1450	± 120	680	990
Lithium	nd		240	280
Silicon	1.6	± 0.7	21	27
Strontium	1.6	± 0.6	18	19
Ammonium	148	± 16	1119	476
Nitrate	0.8	(median)	2746	2436
Chloride	193000	± 4,000	170000	178000
Sulfate	17000	± 900	16000	18000
Bromide	1500	± 60	880	510
Iodide	14.8	± 3.1	28	24
Alkalinity (as HCO ₃ ⁻ equivalent) ¹	883	± 123	2600	2700
Total Organic Carbon	54	± 50	nd	nd
Total Dissolved Solids	374000	± 13,000	330000	328000

¹ Alkalinity measured to an endpoint pH of 2.5 and expressed as equivalent bicarbonate.

Legend:

nd not determined

Note: All determinands reported in units of milligrams per liter (**mg/L**), except for pH and Specific Gravity. Only determinands with a concentration in excess of 10 **mg/L** in at least one of the brines are shown. Data taken from DOE (1994, Table 3-3) and Popeliak et al. (1983, Table C.2).

2 include both pure and impure halite, *as well as anhydrite*. Tests influence rock as far as 10 m
3 (33 ft) distant from the test zone and therefore provide results *representative of rock beyond the*
4 *zone of mechanical disturbance associated with drilling of the test boreholes* that are not
5 significantly influenced by disturbances associated with the tests themselves. Because tests close
6 to the repository are within the DRZ that surrounds the excavated regions (see Section 3.2),
7 results of the tests farthest from the repository are most representative of undisturbed conditions.

8 *Fifty-nine intervals were isolated and monitored and/or tested in 27 boreholes. Thirty-five of*
9 *the intervals isolated halite beds, and 24 isolated anhydrite beds. Permeability estimates were*

obtained from 14 of the halite intervals and 16 of the anhydrite intervals. ~~Twenty-two~~ hydraulic tests have been performed in impure halite, and two in pure halite. Interpreted permeabilities using a Darcy-flow model vary from 24×10^{-23} to $34 \times 10^{-168} \text{ m}^2$ for impure halite intervals, *with the lower values representing halite with few impurities and the higher values representing intervals within the DRZ of the excavations.* Interpreted formation pore pressures vary from ~~atmospheric~~ 0.3 to 9.87 MPa for impure halite, with the lower pressures believed to show *ing the* effects of the DRZ. Tests in pure halite show no observable response, indicating either extremely low permeability ($<10^{-23} \text{ m}^2$), or no flow whatsoever, even though appreciable pressures are applied to the test intervals.

~~Fourteen hydraulic tests have been performed in anhydrite.~~ Interpreted permeabilities using a Darcy-flow model vary from 2×10^{-20} to $9.7 \times 10^{-18} \text{ m}^2$ for anhydrite intervals. Interpreted formation pore pressures vary from atmospheric to ~~142.85 megapascals~~ 142.85 MPa for anhydrite intervals (Beauheim *and Roberts 2002 p. 82* ~~et al. 1993, 139~~). Lower values are caused by depressurization near the excavation.

As discussed in Beauheim and Roberts (2002), permeabilities of some tested intervals have been found to be dependent on the pressures at which the tests were conducted, which is interpreted as the result of fracture apertures changing in response to changes in effective stress. Flow dimensions inferred from most test responses are subradial, meaning that flow to/from the test boreholes is not radially symmetric but is derived from a subset of the rock volume. The subradial flow dimensions are believed to reflect channeling of flow through fracture networks, or portions of fractures, that occupy a diminishing proportion of the radially available space, or through percolation networks that are not “saturated” (that is, fully interconnected). This is probably related to the directional nature of the permeability created or enhanced by excavation effects. Other test responses indicate flow dimensions between radial and spherical, which may reflect propagation of pressure transients above or below the plane of the test interval or into regions of increased permeability (e.g., closer to an excavation). The variable stress and pore-pressure fields around the WIPP excavations probably contribute to the observed non-radial flow dimensions.

The properties of anhydrite interbeds have also been investigated in the laboratory. Tests were performed on three groups of core samples from MB 139 as part of the Salado Two-Phase Flow Laboratory Program. The laboratory experiments provided porosity, intrinsic permeability, and capillary pressure data. Analysis of capillary pressure test results indicates a threshold pressure of less than 1 MPa . Both laboratory and field data were used to establish hydraulic parameters for the Salado for PA as summarized in *CCA* Appendix PAR (Tables PAR-6 and PAR-7).

The EPA believed the DOE’s initial information on anhydrite characteristics and response to high pressure was unclear. In response, the DOE provided the EPA with data on modeling implementation and anhydrite characterization clarifying DOE’s approach to anhydrite fracture properties under pressurized conditions. The EPA concluded that while fracture distribution and subsequent fluid flow in the Salado marker beds cannot be detailed, the general application of fracturing and subsequent fluid flow appears to be an adequate representation of overall site conditions. The EPA also concluded that DOE’s modeling of fractures within Salado anhydrite marker beds is acceptable. For further discussion on this topic, see CARD 23—Models and Computer Codes, Section 1.3.2.

Fluid pressure above hydrostatic is a hydrologic characteristic of the Salado (and the Castile) that plays a potentially important role in the repository behavior. It is difficult to accurately measure natural pressures in these formations *accurately* because the boreholes or repository excavations required to access the rocks decrease the stress in the region measured. Stress released instantaneously decreases fluid pressure in the pores of the rock, so measured pressures must be considered as a lower bound of the natural pressures. Stress effects related to test location and the difficulty of making long-duration tests in lower-permeability rocks result in higher pore pressures observed to date in anhydrites. The highest observed pore pressures in halite-rich units, near Room Q, *are* is on the order of 9 MPa, whereas the highest pore pressures observed in anhydrite are *approximately* 12.5 MPa (Beauheim et al. 1993, 139; *Beauheim and Roberts 2002, p. 82*). Far-field pore pressures in halite-rich and anhydrite beds in the Salado at the repository level are expected to be similar because the anhydrites are too thin and of too low permeabilities to have liquid pressures much different than those of the surrounding salt. For comparison, the hydrostatic pressure for a column of brine at the depth of the repository is about 7 MPa, and the lithostatic pressure calculated from density measurements in ERDA-9 is about 15 MPa.

Fluid pressures in sedimentary basins that are much higher or much lower than hydrostatic are referred to as abnormal pressures by the petroleum industry, where they have received considerable attention. In the case of the Delaware Basin evaporites, the high pressures are almost certainly maintained because of the large compressibility and plastic nature of the halite and, to a lesser extent, the anhydrite. The lithostatic pressure at a particular horizon must be supported by a combination of the stress felt by both the rock matrix and the pore fluid. In highly deformable rocks, the portion of the stress that must be borne by the fluid exceeds hydrostatic pressure but cannot exceed lithostatic pressure.

Brine content within the Salado is estimated at 1 to 2 percent by weight, although the thin clay seams have been *inferred* ~~observed~~ by Deal et al. (1993, *pp.* 4-3) to contain up to 25 percent brine by volume. Where sufficient permeability exists, this brine will move towards areas of lower hydraulic potential, such as a borehole or mined section of the Salado.

Observation of the response of pore fluids in the Salado to changes in pressure boundary conditions at walls in the repository, in boreholes without packers, in packer-sealed boreholes, or in laboratory experiments is complicated by low permeability and low porosity. Qualitative data on brine flow to underground workings and exploratory boreholes ~~have been~~ *were* collected routinely *between* ~~since~~ 1985 *and 1993* under the Brine Sampling and Evaluation Program (BSEP) and have been documented in a series of reports (Deal and Case 1987; Deal et al. 1987, 1989, 1991a, 1991b, *and 1993, and 1995*). ~~These and other investigations are discussed in Appendix SUM (Section 3.3.1.3).~~ A discussion of alternative conceptual models for Salado fluid flow is given in Appendix *PA, Attachment* MASS, Section MASS.7. Additional data on brine inflow are available from the Large-Scale Brine Inflow Test (Room Q). Flow has been observed to move to walls in the repository, to boreholes without packers, and to packer-sealed boreholes. These qualitative and relatively short-term observations suggest that brine flow in the fractured DRZ is a complex process. In some locations, evidence for flow is no longer observed where it once was; in others, flow has begun where it once was not observed. In many cases, observations and experiments must last for months or years to obtain useful results.

For *PA* modeling, brine flow is a calculated term dependent on local hydraulic gradients and properties of the Salado units. Data on pore pressure and permeability of halite and anhydrite layers are available from the Room Q tests and other borehole tests *as summarized in Beauheim and Roberts (2002)*, and these data form the basis for the quantification of the material properties used in the *PA*. See Section 6.4.3.2 for a description of the repository fluid flow model.

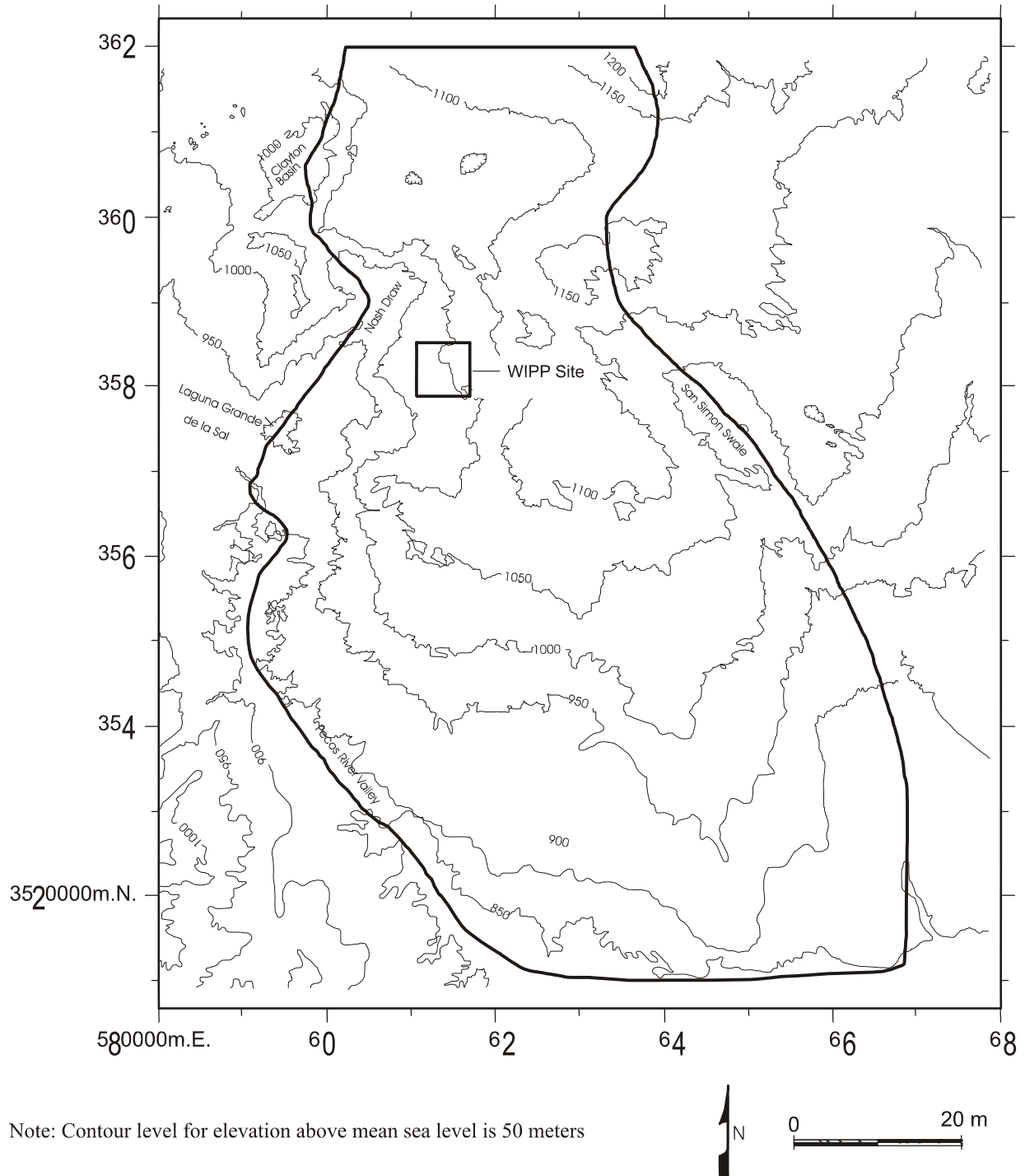
Because brine is an important factor in repository performance, several studies of its chemistry have been conducted. Initial investigations were reported in Powers et al. (*CCA* Appendix GCR, Section 7.5) and were continued once access to the underground was established. The most comprehensive data were developed by the BSEP (Deal and Case 1987; Deal et al. 1987, 1989, 1991a, 1991b, 1993, *1995*). Results are summarized in Table 2-56. *CCA* Appendix SOTERM discusses the role of brine chemistry in the conceptual model for actinide dissolution. The conceptual model is described in Section 6.4.3.5.

2.2.1.4 Units Above the Salado

In evaluating groundwater flow above the Salado, the DOE considers the Rustler, Dewey Lake, Santa Rosa, and overlying units to form a groundwater basin with boundaries coinciding with selected groundwater divides as discussed in Section 2.2.1.1. The model boundary follows Nash Draw and the Pecos River valley to the west and south and the San Simon Swale to the east (Figure 2-29*33*). The boundary continues up drainages and dissects topographic highs along its northern part. These boundaries represent groundwater divides whose positions remain fixed over the past several thousand years and 10,000 years into the future. For reasons described in Section 2.2.1.2.1, the lower boundary of the groundwater basin is the upper surface of the Salado. Nash Draw and the Pecos River are areas where discharge to the surface occurs. Hunter ~~in~~ (1985) described discharge at Surprise Spring and into saline lakes in Nash Draw. She reported groundwater discharge into the Pecos River between Avalon Dam north of Carlsbad and a point south of Malaga Bend as approximately 0.92 m³/see (32.5 ft³/see), mostly in the region near Malaga Bend.

Within this groundwater basin, hydrostratigraphic units with relatively high permeability are called conductive units, and those with relatively low permeability are called confining layers. The confining layers consist of halite and anhydrite and are perhaps five orders of magnitude less permeable than conductive units.

In a groundwater basin, the position of the water table moves up and down in response to changes in recharge. The amount of recharge is generally a very small fraction of the amount of rainfall; this condition is expected for the WIPP. Modeling of recharge changes within the groundwater basin as a function of climate variation is discussed in Section 6.4.9. The water table would stabilize at a particular position if the pattern of recharge remained constant for a long time. The equilibrated position depends, in part, on the distribution of hydraulic conductivity in all hydrostratigraphic units in the groundwater basin. However, the position of the water table depends mainly on the topography and geometry of the groundwater basin and the hydraulic conductivity of the uppermost strata. The position of the water table can adjust slowly to changes in recharge. Consequently, the water table can be at a position that is very much different from its equilibrium position at any given time. Generally, the water table drops



CCA-045-2

Figure 2-2933. Outline of the Groundwater Basin Model Domain on a Topographic Map

1 very slowly in response to decreasing recharge but might rise rapidly in times of increasing
2 recharge.

3 The asymmetry of response occurs because the rate at which the water table drops is limited by
4 the rate at which water flows through the entire basin. In contrast, the rate at which the water
5 table rises depends mainly on the recharge rate and the porosity of the uppermost strata. From
6 groundwater basin modeling, the head distribution in the groundwater basin appears to
7 equilibrate rapidly with the position of the water table.

8 The groundwater basin conceptual model (Corbet and Knupp 1996) described above has been
9 implemented in a numerical model, as described in ~~Section 6.4.6.2 and~~ **CCA** Appendix MASS,
10 Section MASS.14.2. This model has been used to simulate the interactive nature of flow through
11 conductive layers and confining units for a variety of possible rock properties and climate
12 futures. Thus, this model has allowed insight into the magnitude of flow through various units.
13 The DOE has used this insight as a basis for model simplifications used in **PA** that are described
14 here and in Chapter 6.0.

15 One conclusion from the regional groundwater basin modeling is pertinent here. In general,
16 vertical leakage through confining layers is directed downward over all of the controlled area.
17 This downward leakage uniformly over the WIPP site is the result of a well-developed discharge
18 area, Nash Draw and the Pecos River, along the western and southern boundaries of the
19 groundwater basin. This area acts as a drain for the laterally conductive units in the groundwater
20 basin, causing most vertical leakage in the groundwater basin to occur in a downward direction.
21 This conclusion is important in **PA** simplifications related to the relative importance of lateral
22 flow in the Magenta versus the Culebra, which will be discussed later in this chapter and in
23 Section 6.4.6.

24 *Public concern was expressed that groundwater flow to the spring supplying brine to Laguna*
25 *Grande de la Sal could be related to the presence of karst features. The EPA examined*
26 *information regarding the hydrology of the units above the Salado and DOE's*
27 *conceptualization of the groundwater flow model, including supplementary information*
28 *submitted in letters dated May 2, 1997 (Docket A-93-02, Item V-B-6 (6)), and May 14, 1997*
29 *(Docket A-93-02, Item II-I-31), and the EPA concluded that the information was adequate.*

30 *The EPA concluded, based on WIPP field observations and site-specific hydrologic*
31 *information, there is no indication that any cavernous or other karst-related flow is present*
32 *within the WIPP site boundary. The EPA concurred with DOE's conceptualization of*
33 *groundwater flow in the Culebra, which includes the presence of fractures within the Culebra*
34 *and recharge and discharge areas for groundwater that are more consistent with potential*
35 *discharge to areas south and west of the WIPP.*

36 2.2.1.4.1 Hydrology of the Rustler Formation

37 The Rustler is of particular importance for WIPP because it contains the most transmissive units
38 above the repository. Fluid flow in the Rustler is characterized by very slow rates of vertical
39 leakage through confining layers and faster lateral flow in conductive units. To illustrate this
40 point, regional modeling with the groundwater basin model indicates that lateral specific

discharges in the Culebra, for example, are perhaps two to three orders of magnitude greater than the vertical specific discharges across the top of the Culebra.

Because of its importance, the Rustler continues to be the focus of studies to understand better the complex relationship between hydrologic properties and geology, particularly in view of water-level rises observed in the Culebra and Magenta (e.g., SNL 2003a; also see Appendix DATA). An example of the complex nature of Rustler hydrology is the variation in Culebra transmissivity (T). Culebra T varies over three orders of magnitude on the WIPP site itself and over six orders of magnitude on the scale of the regional groundwater basin model with lower T east of the site and higher T west of the site in Nash Draw (e.g., Beauheim and Ruskauff 1998). As discussed below, site investigations and studies (e.g., Holt and Powers 1988; Beauheim and Holt 1990; Powers and Holt 1995; Holt 1997; Holt and Yarbrough 2002; Powers et al. 2003) suggest that the variability in Culebra T can be explained largely by the thickness of Culebra overburden, the location and extent of upper Salado dissolution, and the occurrence of halite in the mudstone units bounding the Culebra (see Section 2.1.3.5).

2.2.1.4.1.1 ~~Unnamed Lower Member~~ *Los Medaños*

The unnamed lower member was named the Los Medaños by Powers and Holt (1999). ~~The unnamed lower member makes up~~ *The Los Medaños is treated as* a single hydrostratigraphic unit in WIPP models of the Rustler, although its composition varies. Overall, it acts as a confining layer. The basal interval of the *Los Medaños* ~~unnamed lower member~~, approximately 19.5 m (64 ft) thick, is composed of siltstone, mudstone, and claystone and contains the water-producing zones of the lowermost Rustler. Transmissivities of 2.9×10^{-10} m²/sec (2.7×10^{-4} ft²/day) and 2.4×10^{-10} m²/sec (2.2×10^{-4} ft²/day) were reported by Beauheim (1987a, p. 50) from tests at well H-16 that included this interval. The porosity of the ~~unnamed lower member~~ *Los Medaños* was measured in 1995 as part of testing at the H-19 hydropad (TerraTek 1996). Two claystone samples had effective porosities of 26.8 and 27.3 percent. One anhydrite sample had an effective porosity of 0.2 percent. The transmissivity values correspond to hydraulic conductivities of 1.5×10^{-11} m/sec (4.2×10^{-6} ft/day) and 1.2×10^{-11} m/sec (3.4×10^{-6} ft/day). Hydraulic conductivity in the lower portion of the ~~unnamed lower member~~ *Los Medaños* is believed by the DOE to increase to the west in and near Nash Draw, where dissolution at the underlying Rustler-Salado contact has caused subsidence and fracturing of the sandstone and siltstone.

The remainder of the *Los Medaños* ~~unnamed lower member~~ contains mudstones, anhydrite, and variable amounts of halite. The hydraulic conductivity of these lithologies is extremely low. It is for this reason the *Los Medaños* ~~unnamed lower member~~ is treated as a single hydrostratigraphic unit that overall acts as a confining unit. The conceptual model incorporating the ~~unnamed lower member~~ *Los Medaños* is discussed in Section 6.4.6.1. Important hydrologic model properties of the ~~unnamed lower member~~ are discussed in Section 6.4.6.1 and are summarized in Appendix PAR (Table PAR-31). *of the Los Medaños are summarized in Appendix PA.*

As described in Section 2.1.3.5, the Los Medaños contains two mudstone layers: one in the middle of the Los Medaños and one immediately below the Culebra. An anhydrite layer separates the two mudstones. The lower and upper Los Medaños mudstones have been given

the designations M1/H1 and M2/H2, respectively, by Holt and Powers (1988). This naming convention is used to indicate the presence of halite in the mudstone at some locations at and near the WIPP site. Powers (2002a) has mapped (Figure 2-15) the margins delineating the occurrence of halite in both mudstone layers. Whereas early researchers (e.g., Snyder 1985) interpreted the absence of halite west of these margins as evidence of dissolution, Holt and Powers (1988) interpreted it as reflecting changes in the depositional environment, not dissolution. However, Holt and Powers (1988) concluded that dissolution of Rustler halite may have occurred along the present-day margins. The presence of halite in the Los Medaños mudstones is likely to affect the conductivity of the mudstones, but its greater importance is the implications it has for the conductivity of the Culebra. As discussed in Section 2.2.1.4.1.2, the Culebra transmissivity in locations where halite is present in M2/H2 and M3/H3 (a mudstone in the lower Tamarisk Member of the Rustler) is assumed to be an order of magnitude lower than where halite does not occur (Holt and Yarbrough 2002).

Fluid pressures in the Los Medaños have been continuously measured at well H-16 since 1987. During this period, the fluid pressure has remained relatively constant at between 190 and 195 psi or a head of approximately 137 m (450 ft). Given the location of the pressure transducer (an elevation of 811.96 m amsl), the current elevation of the Los Medaños water level at H-16 is approximately 949 m amsl. No other wells in the WIPP monitoring network are completed to the Los Medaños. Thus, H-16 provides the only current head information for this member.

2.2.1.4.1.2 The Culebra *Dolomite Member*

The Culebra is of interest because it is the most transmissive *saturated* unit *above* at the WIPP *repository* site and hydrologic research has been concentrated on the unit for *nearly two* ~~over a~~ decades. Although it is relatively thin, it is an entire hydrostratigraphic unit in the WIPP hydrological conceptual model, and it is the most important conductive unit in this model. Implementation of the Culebra in the conceptual model is discussed in detail in Section 6.4.6.2. Model discussions cover groundwater flow and transport characteristics of the Culebra. These are supported by parameter values in Table 6-20, 6-21, 6-22, and 6-23. Additional background for the Culebra model is in *CCA* Appendix MASS, Sections MASS.14 and MASS.15.

The two primary types of field tests ~~that are being~~ used to characterize the flow and transport characteristics of the Culebra are hydraulic tests and tracer tests.

The hydraulic testing consists of pumping, injection, and slug testing of wells across the study area (for example, Beauheim 1987a, *p.* 3). The most detailed hydraulic test data exist for the WIPP hydropads (for example, H-19). The hydropads generally comprise a network of three or more wells located within a few tens of meters of each other. Long-term pumping tests have been conducted at hydropads H-3, H-11, and H-19 and at well WIPP-13 (Beauheim 1987b; 1987c; 1989; Beauheim et al. 1995; *Meigs et al. 2000*). These pumping tests provided transient pressure data at the hydropad and over a much larger area. Tests often included use of automated data-acquisition systems, providing high-resolution (in both space and time) data sets. In addition to long-term pumping tests, slug tests and short-term pumping tests have been conducted at individual wells to provide pressure data that can be used to interpret the transmissivity at that well (Beauheim 1987a). (Additional short-term pumping tests have been

conducted in the WQSP wells [*Beauheim and Ruskauff 1998* ~~Stensrud 1995~~]. Detailed cross-hole hydraulic testing has ~~recently~~ been conducted at the H-19 hydropad (~~Kloska et al. 1995~~ *Beauheim 2000*).

The hydraulic tests are designed to yield pressure data for the interpretation of such characteristics as transmissivity, permeability, and storativity. The pressure data from long-term pumping tests and the interpreted transmissivity values for individual wells are used for the generation of transmissivity fields in *PA* flow modeling (see Appendix *PA, Attachment TFIELD*, Sections ~~TFIELD-2~~ *5.0 and TFIELD-6.0*). Some of the hydraulic test data and interpretations are also important for the interpretation of transport characteristics. For instance, information about the vertical distribution of ~~the permeability values~~ interpreted from the hydraulic tests at a given hydropad ~~are~~ *is* needed for interpretations of tracer test data at that hydropad.

To evaluate transport properties of the Culebra, a series of tracer tests ~~has been~~ *were* conducted at six locations (the H-2, H-3, H-4, H-6, H-11, and H-19 hydropads) near the WIPP site. Tests at the first five of these locations consisted of two-well dipole tests and/or multiwell convergent flow tests and are described in detail in Jones et al. (1992). Tracer tests at the H-19 hydropad and additional tracer tests performed at the H-11 hydropad are described in ~~Beauheim et al. (1995)~~ *Meigs et al. (2000)*. The ~~more recent 1995-1996~~ tracer test program consisted of single-well injection-withdrawal tests and multi-well convergent flow tests (*Meigs and Beauheim 2001*). Unique features of this testing program include the single-well test at both H-19 and H-11, the injection of tracers into six wells during the H-19 convergent-flow test, the injection of tracer into upper and lower zones of the Culebra at the H-19 hydropad, repeated injections under different convergent-flow pumping rates, and the use of tracers with different free-water diffusion coefficients. The ~~1995-1996 recent~~ tracer tests were specifically designed to evaluate the importance of heterogeneity (both horizontal and vertical) and diffusion on transport processes.

The Culebra is a fractured dolomite with nonuniform properties both horizontally and vertically. Examination of core and shaft exposures has revealed that there are multiple scales of porosity within the Culebra including fractures ranging from microscale to potentially large, vuggy zones, and interparticle and intercrystalline porosity (*Holt 1997*). Porosity measurements made on core samples give porosity measurements ranging from 0.03 to 0.30 (Kelley and Saulnier 1990; *TerraTek 1996*). This large range in porosity for small samples is expected given the variety of porosity types within the Culebra. However, the effective porosity for flow and transport at larger scales will have a smaller range due to the effects of spatial averaging. The core measurements indicate that the Culebra has significant quantities of connected porosity.

Flow in the Culebra occurs within fractures, within vugs where they are connected by fractures, and to some extent within interparticle porosity where the porosity (and permeability) is high, such as chalky lenses. At any given location, flow will occur in response to hydraulic gradients in all places that are permeable. When the permeability contrast between different scales of connected porosity is large, the total porosity can effectively be conceptualized by dividing the system into advective porosity (often referred to as fracture porosity) and diffusive porosity (often referred to as matrix porosity). The advective porosity can be defined as the portion of the porosity where flow is the dominant process (for example fractures and to some extent vugs

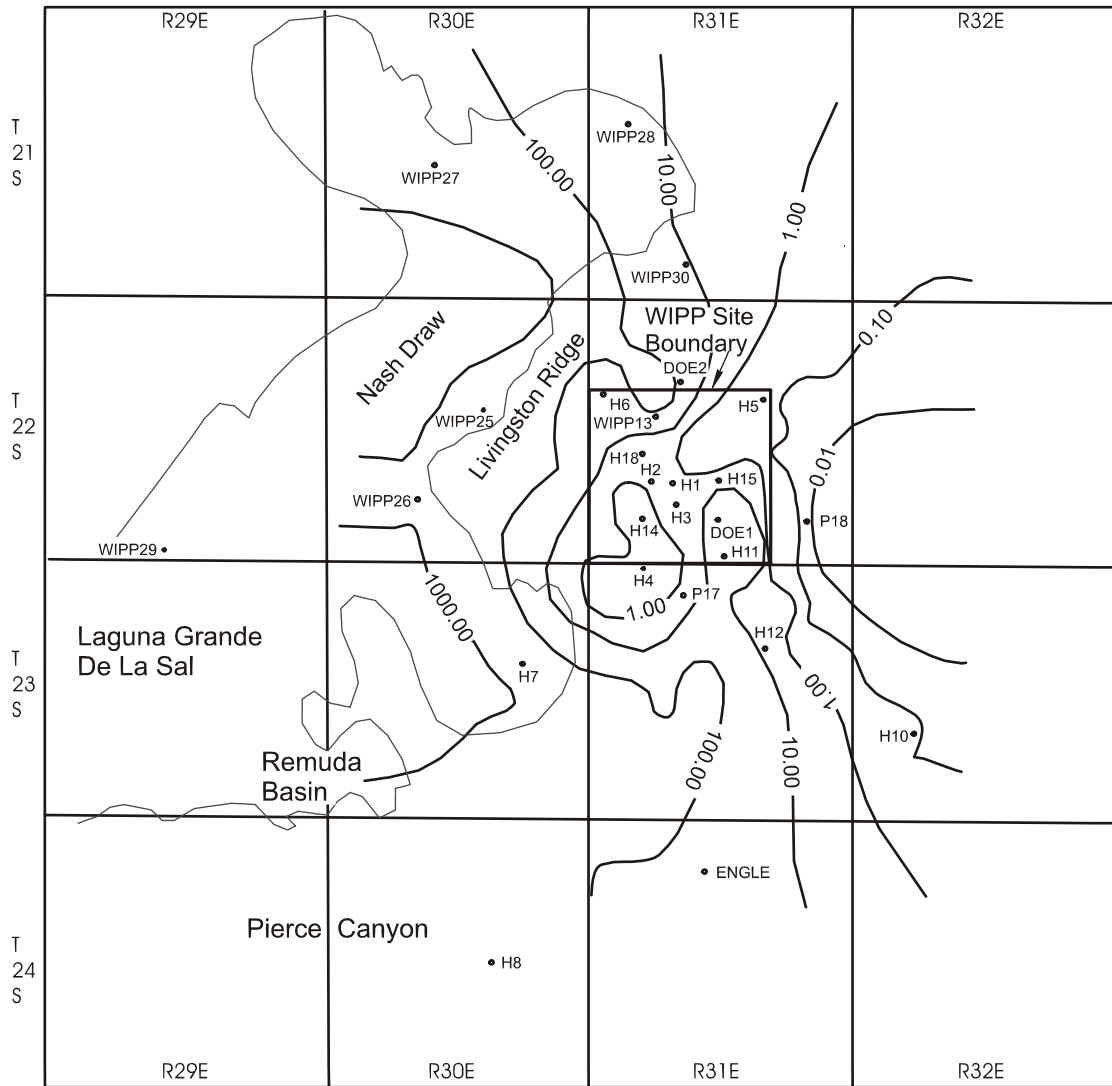
connected by fractures and interparticle porosity). Diffusive porosity can be defined as the portion of the porosity where diffusion is the dominant process (for example, intercrystalline porosity and to some extent microfractures, vugs and portions of the interparticle porosity.)

For the Culebra in the vicinity of the WIPP site, defining advective porosity is not a simple matter. In some regions the permeability of the fractures is inferred to be significantly larger than the permeability of the other porosity types, thus advective porosity can be conceptualized as predominantly fracture porosity (low porosity). In some regions, there appear to be no high permeability fractures. This may be due to a lack of large fractures or may be the result of gypsum fillings in a portion of the porosity. Where permeability contrasts between porosity types are small, the advective porosity can be conceptualized as a combination of fractures, vugs connected by fractures, and permeable portions of the interparticle porosity. In each case, the diffusive porosity can be conceptualized as the porosity where advection is not dominant.

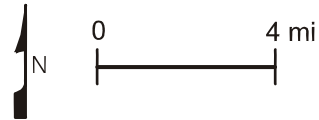
The major physical transport processes that affect actinide transport through the Culebra include advection (through fractures and other permeable porosity), diffusion from the advective porosity into the rest of the connected porosity (diffusive porosity) and dispersive spreading due to heterogeneity. Diffusion can be an important process for effectively retarding solutes by transferring mass from the porosity where advection (flow) is the dominant process into other portions of the rock. Diffusion into stagnant portions of the rock also provides access to additional surface area for sorption. ~~A further discussion of transport of actinides in the Culebra as either dissolved species or as colloids is given in Section 6.4.6.2. Parameter values determined from tests of the Culebra are given in CCA Appendix PAR and are described in Section 6.4.6.2.2. A summary of input values to the conceptual model is~~are in Tables 6-22 and 6-23.

Fluid flow in the Culebra is dominantly lateral and southward except in discharge areas along the west or south boundaries of the basin. Where transmissive fractures exist, flow is dominated by fractures but may also occur in vugs connected by microfractures and interparticle porosity. Regions where flow is dominantly through vugs connected by microfractures and interparticle porosity have been inferred from pumping tests and tracer tests. Flow in the Culebra may be concentrated along zones that are thinner than the total thickness of the Culebra. In general, the upper portion of the Culebra is massive dolomite with a few fractures and vugs, and appears to have low permeability. The lower portion of the Culebra appears to have many more vuggy and fractured zones and to have a significantly higher permeability (Meigs and Beauheim 2001).

There is strong evidence that the permeability of the Culebra varies spatially and varies sufficiently that it cannot be characterized with a uniform value or range over the region of interest to the WIPP. The transmissivity of the Culebra varies spatially over six orders of magnitude from east to west in the vicinity of the WIPP (Figure 2-30~~34~~). Over the site, Culebra transmissivity varies over three to four orders of magnitude. CCA Appendix TFIELD, Section TFIELD.2 contains the data used to develop Figure 2-30~~34~~, which shows variation in transmissivity in the Culebra in the WIPP region. *Attachment TFIELD to Appendix PA* Appendix MASS (Section MASS.15, including MASS Attachment 15-6) provides the modeling rationale and. ~~The discussion in Appendix TFIELD addresses how data collected over a number of years were correlated for the generations of transmissivity fields.~~



• Observation Well



Note: Transmissivities are given in square feet per day. Figure is modified from Cauffman et al. 1990 (Figure 5.22a). See Appendix TFIELD for details of the performance assessment implementation.

CCA-046-2

Figure 2-3034. Transmissivities of the Culebra

Transmissivities are from about $1 \times 10^{-9} \text{ m}^2/\text{sec}$ ($1 \times 10^{-3} \text{ ft}^2/\text{day}$) at well P-18 east of the WIPP site to about $1 \times 10^{-3} \text{ m}^2/\text{sec}$ ($1 \times 10^3 \text{ ft}^2/\text{day}$) at well H-7 in Nash Draw (see Figure 2-2 for the locations of these wells and see Figure 4-8 in CCA Appendix FAC for a Culebra isopach map).

Transmissivity variations in the Culebra are believed to be controlled by the relative abundance of open fractures rather than by primary (that is, depositional) features of the unit. Lateral

variations in depositional environments were small within the mapped region, and primary features of the Culebra show little map-scale spatial variability, according to Holt and Powers (CCA Appendix FAC). Direct measurements of the density of open fractures are not available from core samples because of incomplete recovery and fracturing during drilling, but observation of the relatively unfractured exposures in the WIPP shafts suggests that the density of open fractures in the Culebra decreases to the east. Qualitative correlations have been noted between transmissivity and several geologic features possibly related to open fracture density, including (1) the distribution of overburden above the Culebra, (2) the distribution of halite in other members of the Rustler, (3) the dissolution of halite in the upper portion of the Salado, and (4) the distribution of gypsum fillings in fractures in the Culebra (see Section 2.1.3.5.2 and Figure 2-12).

Recent investigations have made a significant contribution to the understanding of the large variability observed for Culebra transmissivity (e.g., Holt and Powers 1988; Beauheim and Holt 1990; Powers and Holt 1995; Holt 1997; Holt and Yarbrough 2002; Powers et al. 2003). The spatial distribution of Culebra transmissivity is believed to be due strictly to deterministic post-depositional processes and geologic controls (Holt and Yarbrough 2002). The important geologic controls include Culebra overburden thickness, dissolution of the upper Salado, and the occurrence of halite in the mudstone Rustler units (M2/H2 and M3/H3) above and below the Culebra (Holt and Yarbrough 2002). Culebra transmissivity is inversely related to thickness of overburden because stress relief associated with erosion of overburden (see Section 2.1.5.2) leads to fracturing and opening of preexisting fractures. Culebra transmissivity is high where dissolution of the upper Salado has occurred and the Culebra has subsided and fractured. Culebra transmissivity is observed to be low where halite is present in overlying and/or underlying mudstones. Presumably, high Culebra transmissivity leads to dissolution of nearby halite (if any). Hence, the presence of halite in mudstones above and/or below the Culebra can be taken as an indicator for low Culebra transmissivity. Details of the geologic-based transmissivity model for the Culebra are given in Attachment TFIELD (Section TFIELD-3.0) to Appendix PA and summarized below.

The Culebra has been tested hydraulically at 42 locations, yielding reliable transmissivity values. These values (log T) are plotted as a function of depth to Culebra (overburden thickness) in Figure 2-35. As shown, the Culebra transmissivities fall into two populations separated by a cutoff (termed 'high-T' cutoff) equal to -5.4 (log T [m²/s]). These data suggest a bimodal distribution for transmissivity with one population having high transmissivity and the other low transmissivity, with the difference attributed to open, interconnected fractures ("fracture interconnectivity") for the high-transmissivity population (Holt and Yarbrough 2002). Using these data, Holt and Yarbrough (2002) constructed a linear Culebra transmissivity model relating log T to the deterministic geologic controls described above. The linear model is expressed as follows:

$$Y(\mathbf{x}) = \beta_1 + \beta_2 d(\mathbf{x}) + \beta_3 I_f(\mathbf{x}) + \beta_4 I_D(\mathbf{x}), \quad (2.1)$$

where $Y(\mathbf{x})$ is log T (x), β_i ($i = 1$ to 4) are regression coefficients, \mathbf{x} is a two-dimensional location vector, $d(\mathbf{x})$ is the overburden thickness at \mathbf{x} (expressed in UTM coordinates and

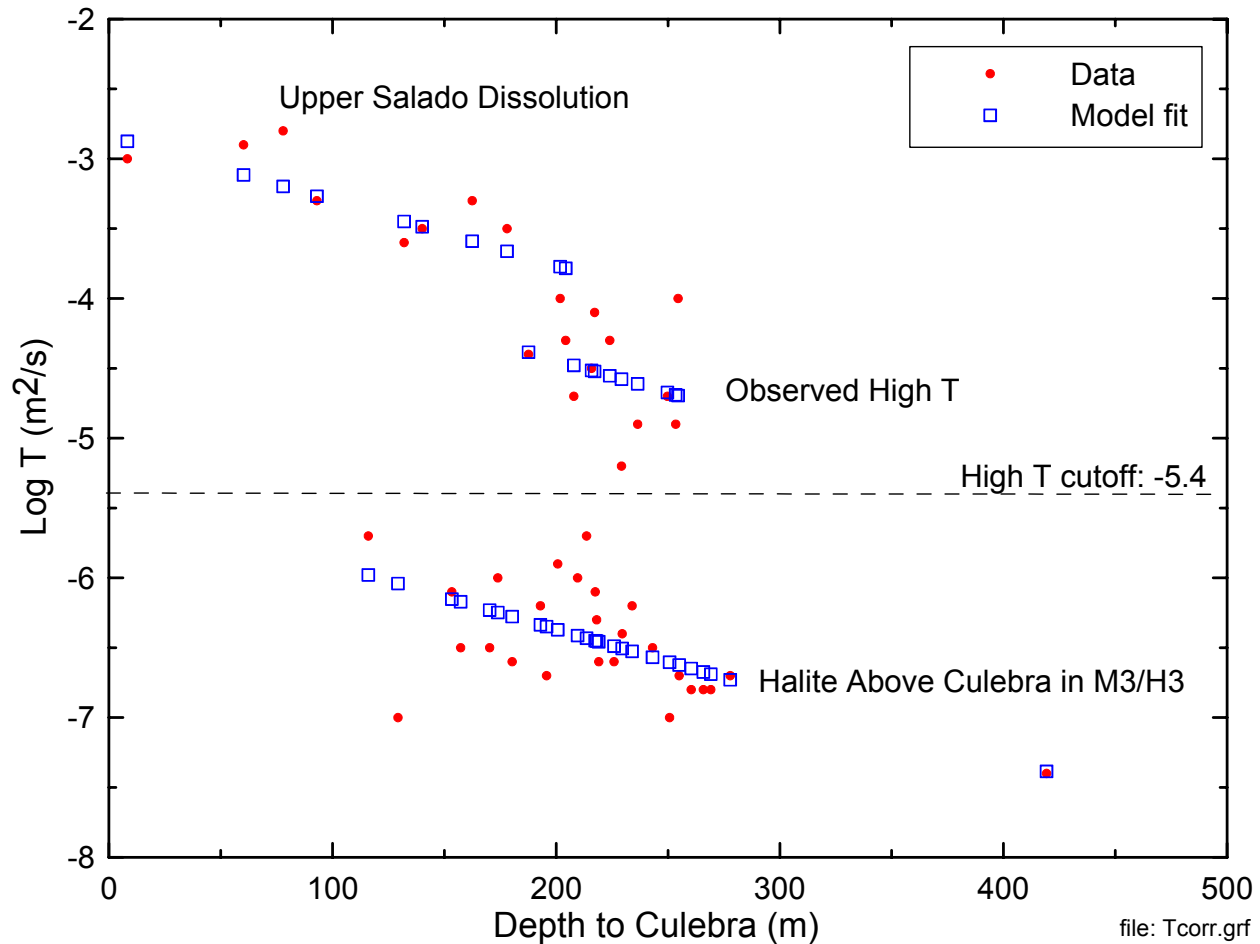


Figure 2-35. Correlation Between Culebra Transmissivity ($\log T$ (m^2/s)) and Overburden Thickness for Different Geologic Environments (after Holt and Yarbrough 2002)

meters), $I_f(x)$ is the fracture-interconnectivity indicator at x (equal to 1 when $\log T$ (m^2/s) > -5.4 or 0 when $\log T$ (m^2/s) < -5.4), and $I_D(x)$ is the dissolution indicator (equal to 1 when Salado dissolution has occurred at (x) and 0 when it has not). In this model, coefficient β_1 is the intercept value, β_2 is the slope of $Y(x)/d(x)$, and β_3 and β_4 represent adjustments to the intercept for the occurrence of open, interconnected fractures and Salado dissolution, respectively. Based on linear-regression analysis, Holt and Yarbrough (2002) estimated the coefficients in Equation (2.1). These estimates are summarized in Table 2-7. Predictions of the Culebra transmissivity model represented by Equation (2.1) are shown in Figure 2-35.

The regression model expressed by Equation (2.1) cannot adequately predict transmissivity in the regions where halite is present both in M2/H2 and M3/H3. In these regions, Culebra

Table 2-7. Estimates of Culebra Transmissivity Model Coefficients

β_1	β_2	β_3	β_4
-5.441	-4.636×10^{-3}	1.926	0.678

porosity is thought to be at least partially filled with halite, reducing transmissivity. For these regions, Equation (2.1) is modified as follows:

$$Y(\mathbf{x}) = \beta_1 + \beta_2 d(\mathbf{x}) + \beta_3 I_f(\mathbf{x}) + \beta_4 I_D(\mathbf{x}) + \beta_5 I_H(\mathbf{x}). \quad (2.2)$$

$I_H(x)$ is a halite indicator function equal to 1 in locations where halite occurs in both the M2/H2 and M3/H3 intervals and 0 otherwise. The coefficient β_5 is equal to -1 to assure that the model in Equation (2.2) reduces the predicted transmissivity values by one order of magnitude where halite occurs in both the M2/H2 and M3/H3 intervals.

In the region east of the upper Salado dissolution margin and west of the M2/H2 and M3/H3 margins, high transmissivity depends, in part, on the absence of gypsum fracture fillings. No method has yet been determined for predicting whether fractures will or will not be filled with gypsum at a given location, so the distribution of high and low transmissivity is treated stochastically in this region. Predictions of transmissivity in this region make use of an isotropic spherical variogram model. Fitted parameters for the variogram model are described in Attachment TFIELD (Section TFIELD-4.3) of Appendix PA.

Geochemical and radioisotope characteristics of the Culebra have been studied. There is considerable variation in groundwater geochemistry in the Culebra. The variation has been described in terms of different hydrogeochemical facies that can be mapped in the Culebra (see Section 2.4.2). A halite-rich hydrogeochemical facies exists in the region of the WIPP site and to the east, approximately corresponding to the regions in which halite exists in units above and below the Culebra (Figure 2-10) (Figure 2-15), and in which a large portion of the Culebra fractures are gypsum filled (Figure 2-17). An anhydrite-rich hydrogeochemical facies exists west and south of the WIPP site, where there is relatively less halite in adjacent strata and where there are fewer gypsum-filled fractures.

The Culebra groundwater geochemistry studies continue. Culebra water quality is evaluated semiannually at six wells, three north (WQSP-1, WQSP-2, and WQSP-3) and three south (WQSP-4, WQSP-5, and WQSP-6) (WIPP MOC 1995) of the surface structures area (see Figure 2-3 for well locations). Five rounds of semiannual sampling of water quality completed before the first receipt of waste at the WIPP were used to establish the initial Culebra water-quality baseline for major ion species including Na^+ , Ca^{2+} , Mg^{2+} , K^+ , Cl^- , SO_4^{2-} , and HCO_3^{2-} (Crawley and Nagy 1998). In 2000, this baseline was expanded to include five additional rounds of sampling that were completed before first receipt of RCRA-regulated waste (IT Corporation 2000). Table 2-8 gives the 95 percent confidence intervals presented in SNL (2001) for the major ion species determined from the 10 rounds (semiannual sampling for 5 years) of baseline sampling. Culebra water quality is extremely variable among the six sampling wells, as shown by the Cl^- concentrations that range from approximately 6,000 mg/L at WQSP-6 to 130,000 mg/L at WQSP-3.

Radiogenic isotopic signatures suggest that the age of the groundwater in the Culebra is on the order of 10,000 years or more (see, for example, Lambert 1987, Lambert and Carter 1987, and Lambert and Harvey 1987 in the bibliography). The radiogenic ages of the Culebra groundwater and the geochemical differences provide information potentially relevant to the groundwater flow directions and groundwater interaction with other units and are important constraints on

Table 2-8. Ninety-Five Percent Confidence Intervals for Culebra Water-Quality Baseline

<i>Well I.D.</i>	<i>Cl⁻ Conc. (mg/L)</i>	<i>SO₄²⁻ Conc. (mg/L)</i>	<i>HCO₃⁻ Conc. (mg/L)</i>	<i>Na⁺ Conc. (mg/L)</i>	<i>Ca²⁺ Conc. (mg/L)</i>	<i>Mg²⁺ Conc. (mg/L)</i>	<i>K⁺ Conc. (mg/L)</i>
<i>WQSP-1</i>	<i>31100-39600</i>	<i>4060-5600</i>	<i>45-54</i>	<i>15850-21130</i>	<i>1380-2030</i>	<i>940-1210</i>	<i>322-730</i>
<i>WQSP-2</i>	<i>31800-39000</i>	<i>4550-6380</i>	<i>43-53</i>	<i>14060-22350</i>	<i>1230-1730</i>	<i>852-1120</i>	<i>318-649</i>
<i>WQSP-3</i>	<i>113900-145200</i>	<i>6420-7870</i>	<i>23-51</i>	<i>62600-82700</i>	<i>1090-1620</i>	<i>1730-2500</i>	<i>2060-3150</i>
<i>WQSP-4</i>	<i>53400-63000</i>	<i>5620-7720</i>	<i>31-46</i>	<i>28100-37800</i>	<i>1420-1790</i>	<i>973-1410</i>	<i>784-1600</i>
<i>WQSP-5</i>	<i>13400-17600</i>	<i>4060-5940</i>	<i>42-54</i>	<i>7980-10420</i>	<i>902-1180</i>	<i>389-535</i>	<i>171-523</i>
<i>WQSP-6</i>	<i>5470-6380</i>	<i>4240-5120</i>	<i>41-54</i>	<i>3610-5380</i>	<i>586-777</i>	<i>189-233</i>	<i>113-245</i>

conceptual models of groundwater flow. Previous conceptual models of the Culebra (see for example, Chapman 1986, Chapman 1988, LaVenue et al. 1990, and Siegel et al. 1991 in the bibliography) have not been able to consistently relate the hydrogeochemical facies, radiogenic ages, and flow constraints (that is, transmissivity, boundary conditions, etc.) in the Culebra.

The groundwater basin modeling that ~~has been~~ **was** conducted, although it did not model solute transport processes, provides flow fields that can be used to develop the following concepts that help explain the observed hydrogeochemical facies and radiogenic ages. The groundwater basin model combines and tests three fundamental processes: (1) it calculates vertical leakage, which may carry solutes into the Culebra; (2) it calculates lateral fluxes in the Culebra (directions as well as rates); and (3) it calculates a range of possible effects of climate change. The presence of the halite-rich groundwater facies is explained by vertical leakage of solutes into the Culebra from the overlying halite-containing Tamarisk by advective or diffusive processes. Because lateral flow rates here are low, even slow rates of solute transport into the Culebra can result in high solute concentration. Vertical leakage occurs slowly over the entire model region, and thus the age of groundwater in the Culebra is old, consistent with radiogenic information. Lateral fluxes within the anhydrite zone are larger because of higher transmissivity, and where the halite and anhydrite facies regions converge, the halite facies signature is lost by dilution with relatively large quantities of anhydrite facies groundwater. Response of groundwater flow in the Culebra as the result of increasing recharge is modeled through the variation in climate, discussed in Section 6.4.9.

Groundwater levels in the Culebra in the WIPP region ~~have been~~ **were** measured continuously **prior to** for several decades ~~the CCA in numerous wells (Figure 2-2).~~ Water level rises have been observed in the WIPP region and are attributed to three causes as discussed below. The extent of water level rise observed at a particular well depends on several factors, but the proximity of the observation point to the cause of the water level rise appears to be a primary factor. **The Culebra monitoring wells as of the end of 2002 are shown in Figures 2-3 and 2-4; plugged and abandoned wells are not shown in these figures. Beginning in 1989, a general**

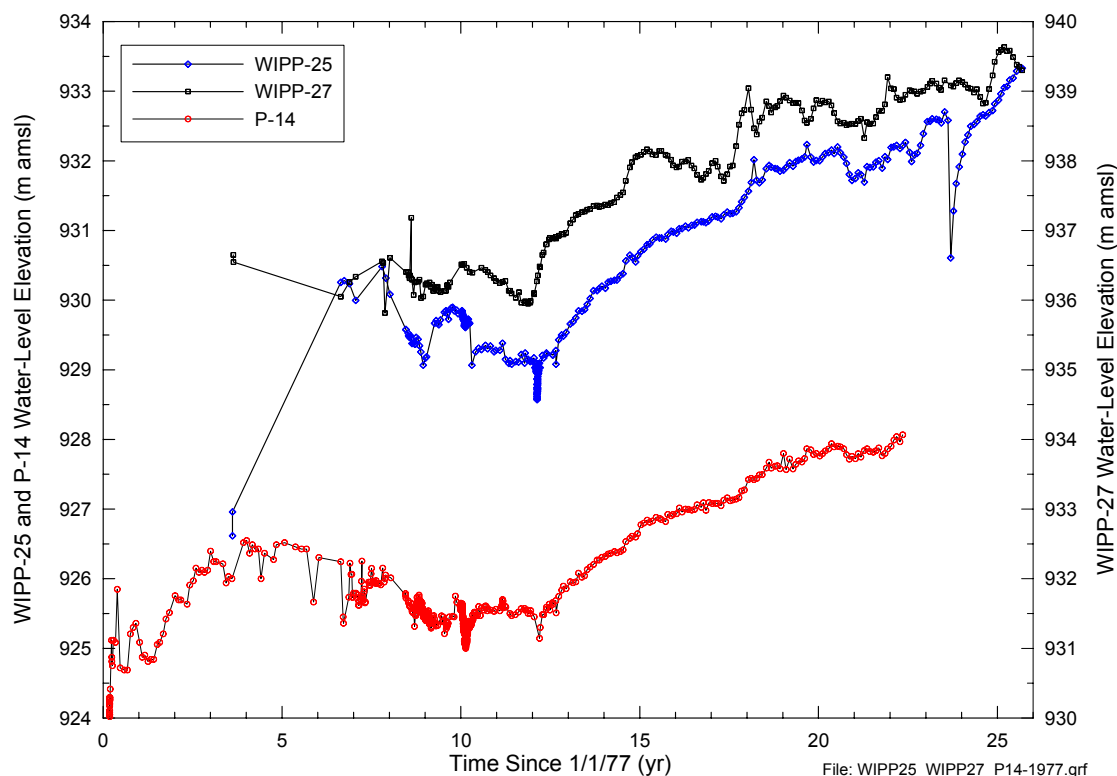


Figure 2-36. Water-level Trends in Nash Draw Wells and at P-14 (see Figure 2-2 for well locations)

long-term rise has been observed in both Culebra and Magenta water levels (Figure 2-36) over a broad area of the WIPP site including Nash Draw (SNL 2003a). At the time of the CCA this long-term rise was recognized, but was thought (outside of Nash Draw) to represent recovery from the accumulation of hydraulic tests that had occurred since the late 1970s and the effects of grouting around the WIPP shafts to limit leakage. Water levels in Nash Draw were thought to respond to changes in the volumes of potash mill effluent discharged into the draw (Silva 1996); however, correlation of these water levels with potash mine discharge cannot be proven because sufficient data on the timing and volumes of discharge are not available. As the rise in water levels has continued since 1996, observed heads have exceeded the ranges of uncertainty established for the steady-state heads in most of the 32 wells used in the calibration of the transmissivity fields described in CCA Appendix TFIELD. Although recovery from the hydraulic tests and shaft leakage has unquestionably occurred, the DOE has implemented a program to identify other potential causes for the water-level rises (SNL 2003b).

In the vicinity of the WIPP site, water level rises are unquestionably caused by recovery from drainage into the shafts. Drainage into shafts has been reduced by a number of grouting programs over the years, most recently in 1993 around the AIS. Northwest of the site, in and near Nash Draw, water levels appear to fluctuate in response to effluent discharge from potash mines. Correlation of water level fluctuation with potash mine discharge cannot be proven because sufficient data on the timing and volumes of discharge are not available.

1 *Although Culebra heads have been rising, the head* Head distribution in the Culebra (see
 2 *Figure 2-31) (see Figure 2-37)* is consistent with groundwater basin modeling results (discussed
 3 in Section 6.4.6 and Appendix *PA, Attachment* MASS, Section MASS.14.2) indicating that the
 4 generalized direction of groundwater flow *remains* north to south. However, caution should be
 5 used when making assumptions based on groundwater-level data alone. Studies in the Culebra
 6 have shown that fluid density variations in the Culebra can affect flow direction (Davies 1989, p.
 7 35). The fractured nature of the Culebra, coupled with variable fluid densities, can also cause
 8 localized flow patterns to differ from general flow patterns. Water-level rises in the vicinity of
 9 the H-9 hydropad, about 10.46 km (6.5 mi) south of the site, are not thought to be caused by
 10 either WIPP activities or potash mining discharge *and have been included in the DOE program*
 11 *to investigate Culebra water-level rises in general.* They remain unexplained. The DOE
 12 continues to monitor groundwater levels throughout the region, but only water-level changes at
 13 or near the site have the potential to affect performance *impact the prediction of disposal system*
 14 *performance.* The DOE has implemented water-level changes in its conceptual model through
 15 variations in climate as discussed in Section 6.4.9. These variations bring the water level *table* to
 16 the surface for some calculations. This modeling simplification bounds the possible effects of
 17 ~~anomalous water level changes regardless of their origin.~~ *The DOE has also used recent (late*
 18 *2000) Culebra heads in flow and transport calculations for this recertification application, as*
 19 *discussed in Appendix PA, Attachment TFIELD, Section TFIELD-6.2.*

20 Inferences about vertical flow directions in the Culebra have been made from well data collected
 21 by the DOE. Beauheim (1987a) reported flow directions towards the Culebra from both the
 22 ~~unnamed lower member~~ *Los Medaños* and the Magenta over the WIPP site, indicating that the
 23 Culebra acts as a drain for the units around it. This indication is consistent with results of
 24 groundwater basin modeling. A more detailed discussion of Culebra flow and transport can be
 25 found in *Appendix PA, Attachment TFIELD* Appendices (MASS [(Sections MASS.14 and
 26 MASS.15)] and TFIELD).

27 *In response to an EPA letter dated March 19, 1997 (Docket A-93-02, Item II-I-17),*
 28 *supplemental information to the CCA pertinent to groundwater flow and geochemistry within*
 29 *the Culebra was provided by the DOE in a letter dated May 14, 1997 (Docket A-93-02, Item II-*
 30 *I-31). In that letter, the DOE explained the conceptual model of Culebra groundwater flow*
 31 *used in the CCA. The CCA conceptual model, referred to as the groundwater basin model,*
 32 *offers a three-dimensional approach to treatment of supra-Salado rock units, and assumes*
 33 *that vertical leakage (albeit very slow) occurs between rock units of the Rustler (where*
 34 *hydraulic gradients exist). Flow in the Culebra is considered transient, but is not expected to*
 35 *change significantly over the next 10,000 years. This differs from previous interpretations,*
 36 *wherein no flow was assumed between the Rustler units.*

37 *In an attachment to the May 14, 1997 letter, the DOE concluded that the presence of anhydrite*
 38 *within the Rustler units did not preclude slow downward infiltration, as previously argued by*
 39 *the DOE, and that the observed geochemistry and flow directions can be explained with*
 40 *different recharge areas and Culebra travel paths. The EPA reviewed the groundwater flow*
 41 *and recharge conceptualization and concluded that it provides a realistic representation of site*
 42 *conditions.*

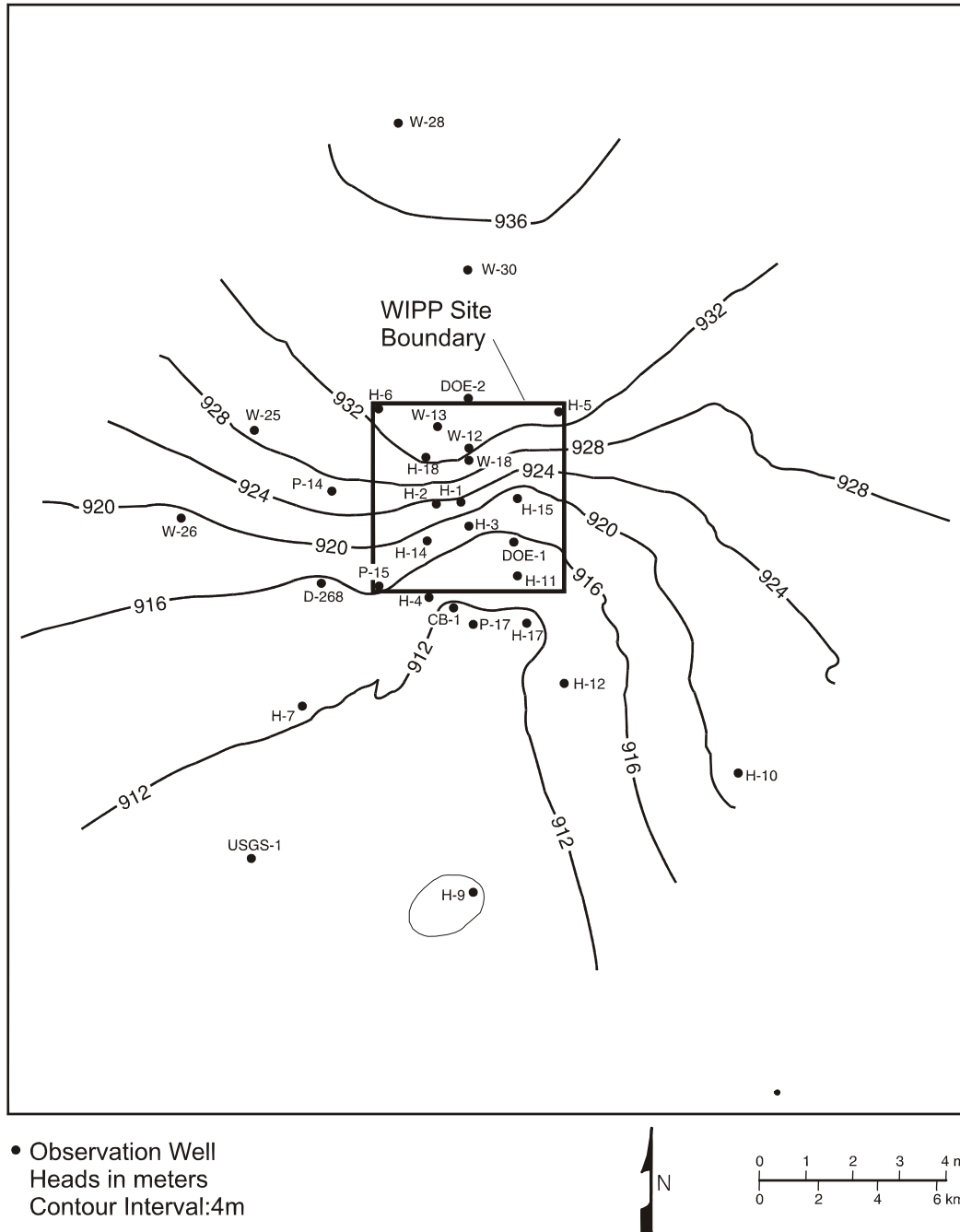


Figure 2-31. Hydraulic Heads in the Culebra

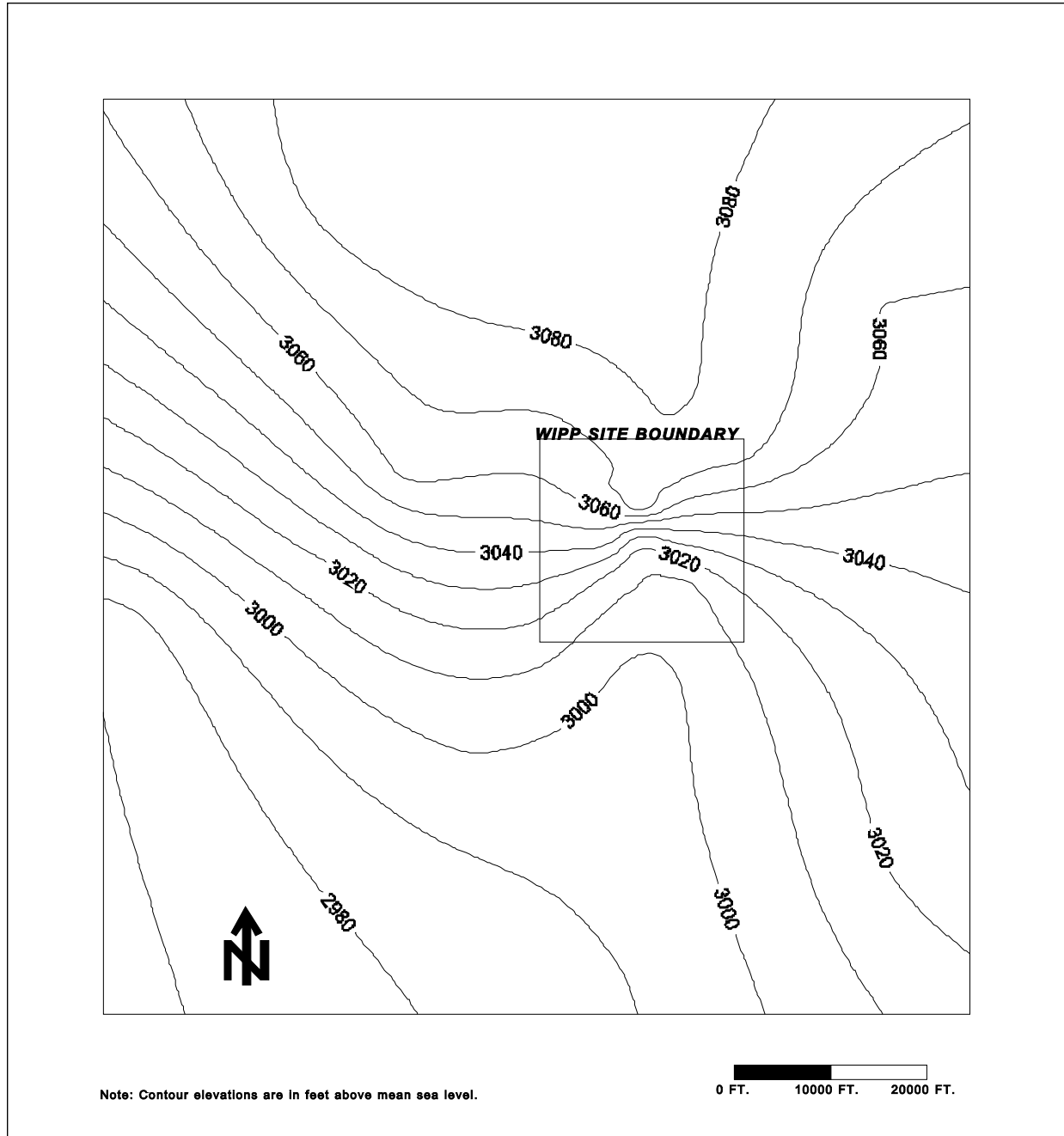


Figure 2-37. Hydraulic Heads in the Culebra

During the CCA review, the EPA found that information on the Culebra in the CCA lacked a detailed discussion on the origin of the transmissivity variations relative to fracture infill/dissolution, integration of climatic change, and loading/unloading events. These are important aspects to understanding not only current transmissivity differences, but also potential future transmissivity variations that could affect PA calculations. The EPA's review stated, however, that the determination of the specific origin of fractures was not necessary because conditions were not expected to change during the regulatory period.

The DOE provided supplemental information in letters in 1997 (Docket A-93-02, Items II-I-03, II-I-24, II-I-31, II-H-44, and II-H-46) indicating that dissolution of fracture fill (which has the potential to alter fracture permeability) is unlikely to occur. The EPA accepted the DOE's position that infiltrating waters would most likely become saturated with calcium sulfate and consequently would not dissolve anhydrite or gypsum fracture fill. Further information on the EPA review of anhydrite and gypsum fracture fill dissolution is contained in EPA Technical Support Document for Section 194.14: Content of Compliance Certification Application, Section IV.C (Docket A-93-02, Item V-B-3).

The Sandia National Laboratories Annual Compliance Monitoring Parameter Assessment reports the annual assessment of the Compliance Monitoring Parameters (COMPs) pursuant to the SNL Analysis Plan, AP-069. The first assessment, for calendar year 1998 (SNL 2000a), showed that changes in Culebra water levels were considered minor. During the assessment of the COMP 'changes in groundwater flow' for calendar year 2001 (SNL 2002), estimated freshwater Culebra heads in 15 wells were identified as above the ranges of uncertainty estimated for steady-state conditions at those wells. At 8 of the 15 wells, the measured water levels exceed the uncertainty range before being converted to freshwater head. In these cases, conversion to freshwater head using any feasible fluid density can only increase the deviation from the range. The freshwater head values from late 2000 were used to calibrate the Culebra transmissivity (T) fields used to simulate the transport of radionuclides through the Culebra (Appendix PA, Attachment TFIELD).

Because transport through the Culebra is a minor component of the total predicted releases from the repository, these changes in head values have little or no effect on the total releases to the accessible environment. The COMP assessment for the calendar year 2001 concluded that the current head values do not indicate a condition adverse to the predicted performance of the repository. However, because Culebra water levels are above expected values at most wells, work has been initiated to investigate the reason for the change and further evaluate the impact on performance.

Additional background for the Culebra model is in Appendix PA, Attachment TFIELD. Additional information on long-term pumping test data is documented in Meigs et al. (2000) and slug tests and short-term pumping tests are documented in Beauheim et al. (1991b) and Beauheim and Ruskauff (1998).

Several new publications on the Culebra updating the original CCA information have been released. Transport properties and tracer tests of the Culebra performed at the H-11 and H-19 hydropads are described in Meigs et al. (2000). The 1995-96 tracer test program, which consisted of single-well injection-withdrawal tests and multiwell convergent flow tests, is documented in Meigs and Beauheim (2001). The higher permeability of the lower Culebra has been addressed in Meigs and Beauheim (2001, p. 1116).

2.2.1.4.1.3 ~~The~~ Tamarisk

The Tamarisk acts as a confining layer in the groundwater basin model. Attempts were made in two wells, H-14 and H-16, to test a 2.4-m (7.9-ft) sequence of the Tamarisk that consists of claystone, mudstone, and siltstone overlain and underlain by anhydrite. Permeability was too

low to measure in either well within the time allowed for testing; consequently, Beauheim (1987a, *pp.* 108-110) estimated the transmissivity of the claystone sequence to be one or more orders of magnitude less than that of the tested interval in the unnamed lower member *Los Medaños* (that is, less than approximately $2.7 \times 10^{-11} \text{ m}^2/\text{sec}$ [$2.5 \times 10^{-5} \text{ ft}^2/\text{day}$]). The porosity of the Tamarisk was measured in 1995 as part of testing at the H-19 hydropad (TerraTek 1996). Two claystone samples had an effective porosity of 21.3 to 21.7 percent. Five anhydrite samples had effective porosities of 0.2 to 1.0 percent.

Fluid pressures in the Tamarisk have been measured continuously at well H-16 since 1987. From 1998 through 2002, the pressures increased approximately 20 psi, from 80 to 100 psi (185 to 230 ft of water), probably in a continuing recovery response to shaft grouting conducted in 1993 to reduce leakage. Given the location of the pressure transducer, the elevation of Tamarisk water level has increased from 899 to 913 m amsl (2,950 to 2,995 ft amsl) during this period. Currently, no other wells in the WIPP monitoring network are completed to the Tamarisk. Thus, H-16 provides the only information on Tamarisk head levels.

Similar to the Los Medaños, the Tamarisk includes a mudstone layer (M3/H3) that contains halite in some locations at and around the WIPP site. This layer is considered to be important because of the effect it has on the spatial distribution of transmissivity of the Culebra as described in Section 2.2.1.4.1.2. The M3/H3 margin is described in Section 2.1.3.5 and mapped in Figure 2-15.

The Tamarisk is incorporated into the conceptual model as discussed in Section 6.4.6.3. The role of the Tamarisk in the groundwater basin model is in *CCA* Appendix MASS, Section MASS.14.1. Tamarisk hydrological model parameters are in Appendix *PA, Attachment* PAR, Table PAR-2925.

2.2.1.4.1.4 The Magenta

The Magenta is a conductive hydrostratigraphic unit about 7.9 m (26 ft) thick at the WIPP. The Magenta is saturated except near outcrops along Nash Draw, and hydraulic data are available from 15 ~~22~~ wells *including 7 wells recompleted to the Magenta between 1995 and 2002 (SNL 2003a)*. According to Mercer (65 *CCA* Appendix HYDRO, *p.* 65), transmissivity ranges over five orders of magnitude from 1×10^{-9} to $4 \times 10^{-4} \text{ m}^2/\text{sec}$ (4×10^{-3} to $3.75 \times 10^2 \text{ ft}^2/\text{day}$). *A slug test performed in H-9c, a recompleted Magenta well (see Figure 2-5 for well location), yielded a transmissivity of $6 \times 10^{-7} \text{ m}^2/\text{s}$ ($0.56 \text{ ft}^2/\text{day}$), which is consistent with Mercer's findings (SNL 2003a).* The porosity of the Magenta was measured in 1995 as part of testing at the H-19 hydropad (*TerraTek 1996*). Four samples had effective porosities ranging from 2.7 to 25.2 percent.

The hydraulic transmissivities of the Magenta, based on sparse data, show a decrease in conductivity from west to east, with slight indentations of the contours north and south of the WIPP that correspond to the topographic expression of Nash Draw. In most locations, the hydraulic conductivity of the Magenta is one to two orders of magnitude less than that of the Culebra. The Magenta does not have hydraulically significant fractures in the vicinity of the

WIPP. Treatment of the Magenta in the model is discussed in Section 6.4.6.4 with modeling parameters in Table 6-224.

Based on Magenta water levels measured in the 1980s (Lappin et al. 1989) when a wide network of Magenta monitoring wells existed, the hydraulic gradient in the Magenta across the site varies from 3 to 4 m/km (16 to 20 ft/mi) on the eastern side, steepening to about 6 m/km (32 ft/mi) along the western side near Nash Draw (Figure 2-3238).

Regional modeling using the groundwater basin model indicates that leakage occurs into the Magenta from the overlying Forty-niner and out of the Magenta downwards into the Tamarisk. Regional modeling also indicates that flow directions in the Magenta are dominantly westward, similar to the slope of the land surface in the immediate area of the WIPP. This flow direction is different than the dominant flow direction in the next underlying conductive unit, the Culebra. This difference is consistent with the groundwater basin conceptual model, in that flow in shallower units is expected to be more sensitive to local topography.

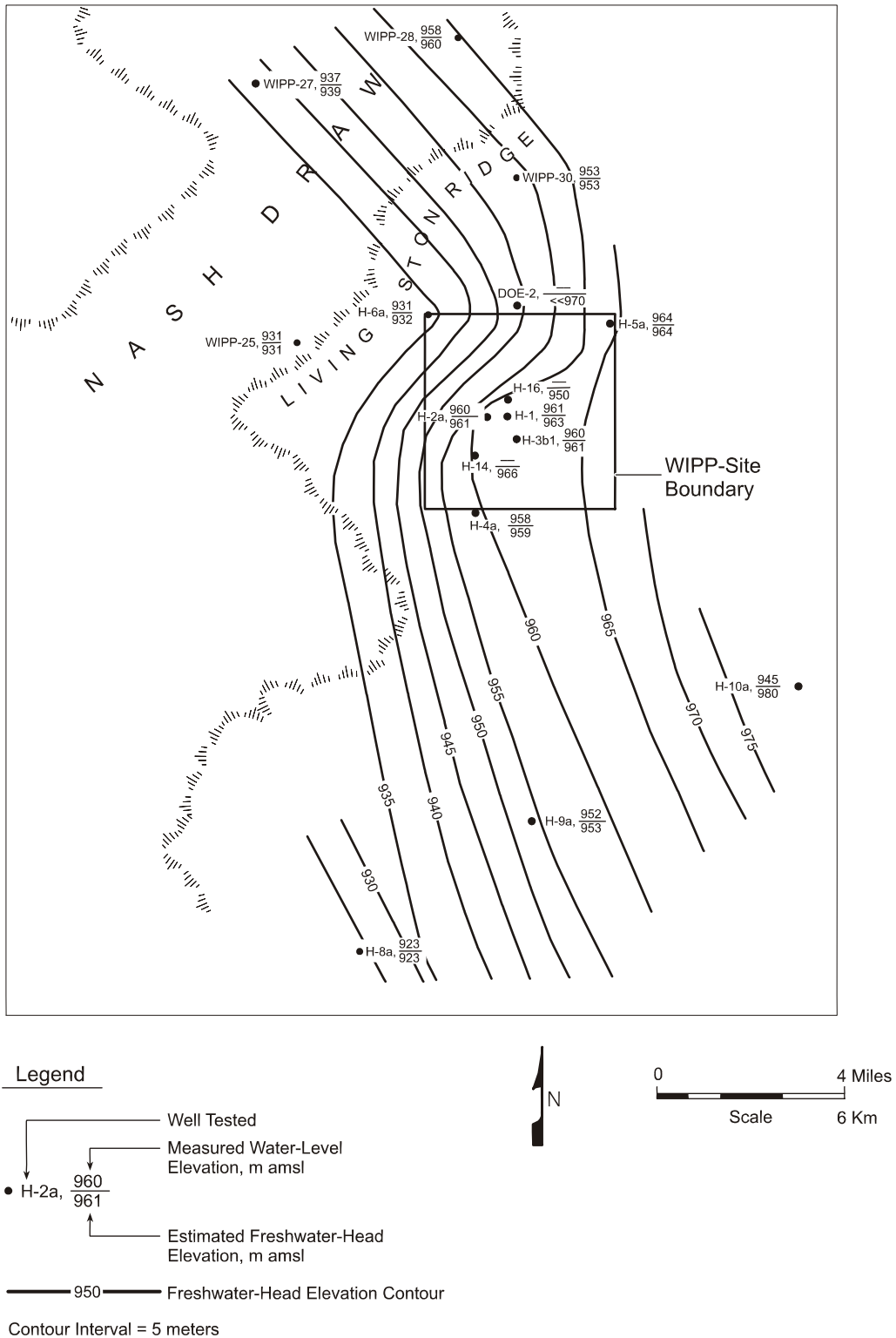
Inferences about vertical flow directions in the Magenta have been made from well data collected by the DOE. Beauheim (1987a, p. 137) reported flow directions downwards out of the Magenta over the WIPP site, consistent with results of groundwater basin modeling.

However, Beauheim (1987a, p. 139) concluded that flow directions between the Forty-niner and Magenta would be upward in the three boreholes from which reliable pressure data are available for the Forty-niner (H-3, H-14, and H-16), which is not consistent with the results of groundwater modeling. This inconsistency may be the result of local heterogeneity in rock properties that affect flow on a scale that cannot be duplicated in regional modeling.

As is the case for the Culebra, groundwater elevations in the Magenta have changed over the period of observation. The pattern of changes is similar to that observed for the Culebra (*see Section 2.2.1.4.1.2*), and is *being investigated under the current DOE hydrology program (SNL 2003b)*. ~~attributed to the same causes (see Section 2.2.1.4.1.2).~~

2.2.1.4.1.5 ~~The~~ Forty-niner

The Forty-niner is a confining hydrostratigraphic layer about 20 m (66 ft) thick throughout the WIPP area and consists of low-permeability anhydrite and siltstone. Tests by Beauheim (1987a, 119-123 and Table 5-2) in H-14 and H-16 yielded transmissivities of about 3×10^{-8} to 8×10^{-8} m²/sec (3×10^{-2} to 7×10^{-2} ft²/day) and 3×10^{-9} to 6×10^{-9} m²/sec (5×10^{-3} to 6×10^{-3} ft²/day), respectively, *for the medial siltstone unit of the Forty-niner. Tests of the siltstone in H-3d provided transmissivity estimates of 3.8×10^{-9} to 4.8×10^{-9} m²/s (3.5×10^{-3} to 4.5×10^{-3} ft²/day) (Beauheim et al. 1991b, Table 5-1). The porosity of the Forty-niner was measured as part of testing at the H-19 hydropad (TerraTek 1996). Three claystone samples had effective porosities ranging from 9.1 to 24.0 percent. Four anhydrite samples had effective porosities ranging from 0.0 to 0.4 percent. Model consideration of the Forty-niner is in Section 6.4.6.5. Modeling parameters are in CCA Appendix PAR, Table PAR-27.*



CCA-048-2

Figure 2-3238. Hydraulic Heads in the Magenta (1980s)

Fluid pressures in the Forty-niner have been measured continuously at well H-16, approximately 13.9 m (45.6 ft) from the well of the AIS, since 1987. The pressures cycle in a sinusoidal fashion on an annual basis. These cycles correlate with cycles observed in rock bolt loads in the WIPP shafts (DOE 2002c), and presumably reflect seasonal temperature changes causing the rock around the shafts to expand and contract. From 1998 through 2002, the pressures have cycled between 40 and 70 psi (90 and 160 ft of fresh water). Given the location of the pressure transducer, the elevation of Forty-niner water level has varied between 899 to 920 m (2,950 to 3,020 ft) amsl during this period. Through April 2002, Forty-niner water levels were also measured monthly at H-3d as part of the WIPP groundwater monitoring program. Measurements were discontinued after April 2002 because of an obstruction in the well. The April 2002 Forty-niner water level elevation determined at H-3d was 942 m (3,092 ft) amsl. Differences in Forty-niner water levels at H-16 and H-3d are probably due, in part, to differences in the densities of the fluids in the wells. No other wells in the WIPP monitoring network are completed to the Forty-niner.

2.2.1.4.2 Hydrology of the Dewey Lake and the Santa Rosa

The Dewey Lake and the Santa Rosa, and surficial soils, overlie the Rustler and are the uppermost hydrostratigraphic units considered by the DOE. The Dewey Lake and overlying rocks are more permeable than the anhydrites at the top of the Rustler. Consequently, basin modeling indicates that most (probably more than 70 percent) of the water that recharges the groundwater basin (that is, percolates into the Dewey Lake from surface water) flows only in the rocks above the Rustler. As modeled, the rest leaks vertically through the upper anhydrites of the Rustler and into the Magenta or continues downward to the Culebra. More flow occurs into the Rustler units at times of greater recharge. Even though it carries most of the modeled recharge, lateral flow in the Dewey Lake is slow because of its low permeability in most areas.

A saturated, perched-water zone has been identified in the lower Santa Rosa directly below the operational area of the WIPP (DOE 1999; INTERA 1997a; INTERA 1997b; DES 1997). The zone occurred at a location that previously had been dry or only partially saturated. Details are provided in Appendix DATA and a summary provided in Section 2.2.1.4.2.2.

2.2.1.4.2.1 The Dewey Lake

The Dewey Lake contains a productive zone of saturation, probably under water-table conditions, in the southwestern to south-central portion of the WIPP site and south of the site. Several wells operated by the J.C. Mills Ranch south of the WIPP site produce sufficient quantities of water from the Dewey Lake to supply livestock. Short-term production rates of 5.7 to 6.8 m³/hr (25 to 30 gpm) were observed in boreholes P-9 (Jones 1978, Vol. 1., pp. 167- 168), WQSP-6, and WQSP-6a (see CCA Appendix USDW). *Based on a single hydraulic test conducted at WQSP-6a (Figure 2-6), Beauheim and Ruskauff (1998) estimated the transmissivity of a 7.3-m (24-ft) fractured section of the Dewey Lake at 3.9×10^{-4} m²/s (360 ft²/day).* The productive zone is typically found in the middle of the Dewey Lake, 55 to 81 m (180 to 265 ft) below ground surface and appears to derive much of its transmissivity from open fractures. Where present, the saturated zone may be perched or simply underlain by less transmissive rock. Fractures below the productive zone tend to be completely filled with gypsum. Open fractures and/or moist (but not fully saturated) conditions have been observed at

similar depths north of the zone of saturation, at the H-1, H-2, and H-3 boreholes (CCA Appendix HYDRO, *p.* 69).

Under the groundwater monitoring program (Appendix MON-2004), water levels are measured in two Dewey Lake wells, WQSP-6a and H-3d, located south of the WIPP site center (Figure 2-6). Water levels in these two wells are currently 975 and 937 m (3,198 and 3,075 ft) amsl, respectively. Water levels at WQSP-6a remain relatively constant. Over the past several years, water levels at H-3d have risen about 0.3 m/yr (1 ft/yr). Future changes in the Dewey Lake water table due to wetter conditions are part of the conceptual model discussed in Sections 6.4.6 and 6.4.9.

Similar to the six Culebra WQSP wells (WQSP-1 through WQSP-6), Dewey Lake water quality is determined semiannually at WQSP-6a. Baseline concentrations for major ion species have also been determined from ten rounds of sampling. The 95 percent confidence intervals for the major ion species presented in SNL (2001) are shown in Table 2-9 and indicate the Dewey Lake water at this location is relatively fresh. Major ion concentrations have been stable within the baseline 95 percent confidence intervals for all 14 rounds of sampling conducted through May 2002 (Kehrman 2002).

Table 2-9. Ninety-Five Percent Confidence Intervals for Dewey Lake Water-Quality Baseline

<i>Well I.D.</i>	<i>Cl⁻ Conc. (mg/L)</i>	<i>SO₄²⁻ Conc. (mg/L)</i>	<i>HCO₃⁻ Conc. (mg/L)</i>	<i>Na⁺ Conc. (mg/L)</i>	<i>Ca²⁺ Conc. (mg/L)</i>	<i>Mg²⁺ Conc. (mg/L)</i>	<i>K⁺ Conc. (mg/L)</i>
<i>WQSP-6a</i>	<i>433-764</i>	<i>1610-2440</i>	<i>97-111</i>	<i>253-354</i>	<i>554-718</i>	<i>146-185</i>	<i>1.8-9.2</i>

Powers (1997) suggests that what distinguishes the low-transmissivity lower Dewey Lake from the high-transmissivity upper Dewey Lake is a change in natural cements from carbonate (above) to sulfate (below). Resistivity logs correlate with this cement change and show a drop in porosity across the cement-change boundary. Similarly, porosity measurements made on eight core samples from the Dewey Lake from well H-19b4 showed a range from 14.9 to 24.8 percent for the four samples from above the cement change, and a range from 3.5 to 11.6 percent for the four samples from below the cement change (TerraTek 1996). In the vicinity of the surface structures area of the WIPP, Powers (1997) proposed the surface of the cement change is at a depth of approximately 50 to 55 m (165 to 180 ft), is irregular, and trends downward stratigraphically to the south and west of the site center.

During site characterization and initial construction of the WIPP shafts, the Dewey Lake has ~~did~~ not produced water within the WIPP shafts or in boreholes in the immediate vicinity of the panels. However, since 1995, water has been observed leaking into the exhaust shaft at a depth of approximately 24.4 m (80 ft) at the location of the Dewey Lake/ Santa Rosa contact (Docket A-93-02, Item number 11-1-07, 1999; INTERA 1997a; INTERA 1997b). As described below in Section 2.2.1.4.2.2, the water is interpreted to be from an anthropogenic source, including infiltration from WIPP rainfall-runoff retention ponds and the WIPP salt storage

area and evaporation pond located at the surface. At the site center, thin cemented zones in the upper Dewey Lake retard, at least temporarily, downward infiltration of modern waters.

Saturation of the uppermost Dewey Lake was observed for the first time in 2001 as well C-2737 was being drilled (Powers 2002c). Well C-2811 was then installed nearby to monitor this zone (Powers and Stensrud 2003). Because of the proximity of these two wells to the WIPP surface structures area, and the absence of water at this horizon when earlier wells were drilled, the saturation is assumed to be an extension of the anthropogenic waters described in the following section.

For modeling purposes, the hydraulic conductivity of the Dewey Lake, assuming saturation, is estimated to be 10^{-8} m/sec (3×10^{-3} ft/day), corresponding to the hydraulic conductivity of fine-grained sandstone and siltstone (Davies 1989, *p.* 110). ~~The porosity of the Dewey Lake was measured as part of testing at the H-19 hydropad. Four samples taken above the gypsum-sealed region had measured effective porosities of 14.9 to 24.8 percent. Four samples taken from within the gypsum-sealed region had porosities from 3.5 to 11.6 percent.~~

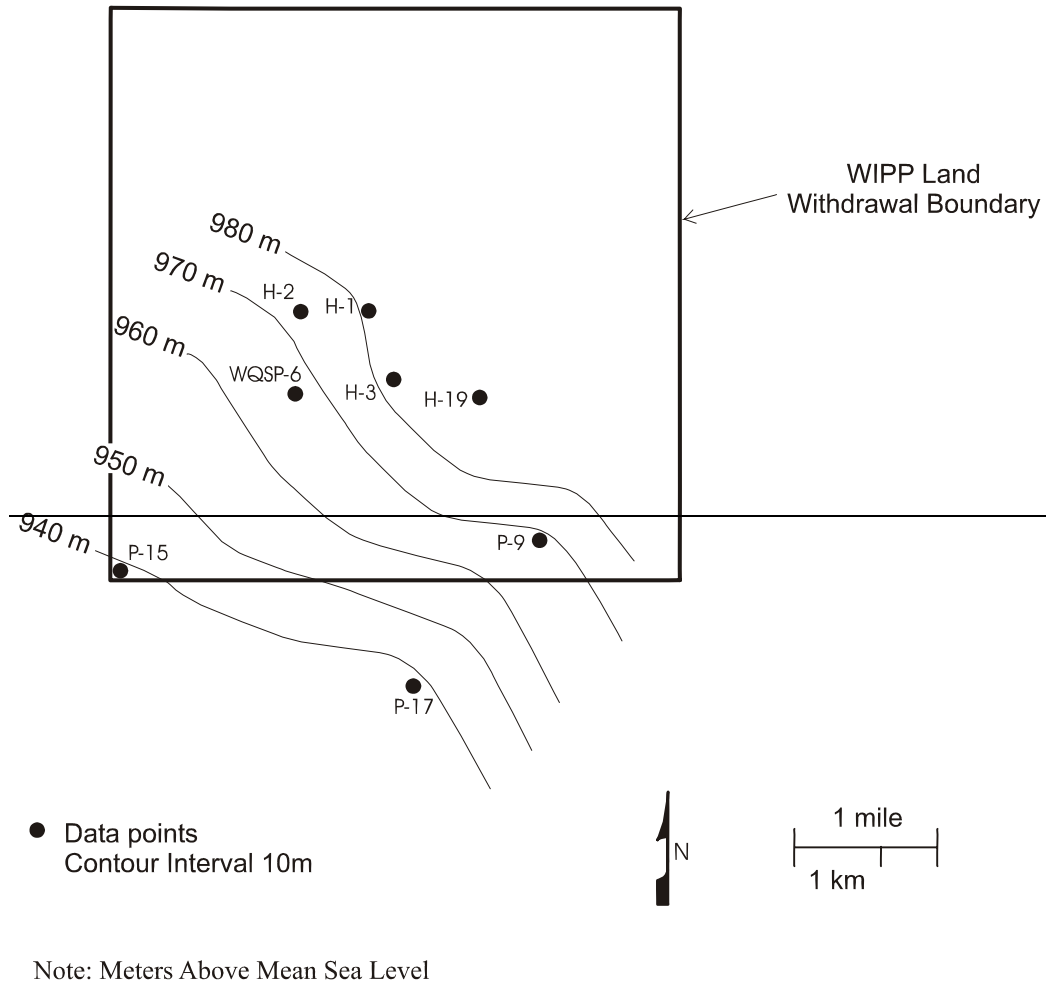
The Dewey Lake is the uppermost important layer in the hydrological model. Its treatment is discussed in Section 6.4.6.6 and Appendix **PA, Attachment MASS**, Section MASS.14.2. Model parameters are in Table 6-23**5 and in Appendix PA, Attachment PAR, Table PAR-22.**

~~The DOE has estimated the position of the water table in the southern half of the WIPP site from an analysis of drillers' logs from three potash exploration boreholes and five hydraulic test holes. These logs record the elevation of the first moist cuttings recovered during drilling. Assuming that the first recovery of moist cuttings indicates a minimum elevation of the water table, an estimate of the water table elevation can be made, and the estimated water table surface can be contoured. This method indicates that the elevation of the water table over the WIPP waste panels may be about 3,215 feet (980 meters) above sea level, as shown in Figure 2-33. Changes in this water table in the future, due to wetter conditions are part of the conceptual model discussed in Sections 6.4.6 and 6.4.9.~~

2.2.1.4.2.2 Santa Rosa

The Santa Rosa ranges from 0 to 91 m (0 to about 300 ft) thick and is present over the eastern half of the WIPP site. It is absent over the western portion of the site. It crops out northeast of Nash Draw. The Santa Rosa near the WIPP site may have a natural-water-saturated thickness of limited extent. It has a porosity of about 13 percent and a specific capacity of 0.029 to 0.041 L/s/m (0.14 to 0.20 **gallons per minute per foot** (gpm/ft) of drawdown, where it yields water in the WIPP region.

In May 1995, a scheduled inspection of the WIPP exhaust shaft revealed water emanating from cracks in the concrete liner at a depth of approximately 24.4 m (80 ft) below the shaft collar. Because little or no groundwater had been encountered at this depth interval previously (Bechtel 1979; DOE 1983; Holt and Powers 1984, 1986), the DOE implemented a program in early 1996 to investigate the source and extent of the water. The program included installation of wells and piezometers, hydraulic testing (pumping tests), water-quality



CCA-049-2

Figure 2-33. Interpreted Water Table Surface

sampling and analysis, and water-level and precipitation monitoring (Docket A-93-02, Item number 11-1-07, DOE 1999; INTERA 1997a; DES 1997; INTERA 1997b).

In the initial phases of the investigation, three wells (C-2505, C-2506, and C-2507) and 12 piezometers (PZ-1 through PZ-12) were installed within the surface structures area of the WIPP site (Figure 2-39). The three wells were located near the exhaust shaft and completed to the Santa Rosa/Dewey Lake contact (approximately 15 m [50 ft] below ground surface). Similarly, the piezometers were also completed to the Santa Rosa/Dewey Lake contact (approximately 16 to 23 m [55 to 75 ft] below ground surface). All wells and piezometers, with the exception of PZ-8, encountered a saturated zone just above the Santa Rosa/Dewey Lake contact, but water did not appear to have percolated significantly into the Dewey Lake. PZ-8, the piezometer located farthest to the east in the study area, was a dry hole.

Subsequent to the well and piezometer installations, water-level, water-quality, and rainfall data were collected. In addition, hydraulic tests were performed to estimate hydrologic

properties and water production rates. These data suggest that the water present in the Santa Rosa below the WIPP surface structures area represents an unconfined, water-bearing horizon perched on top of the Dewey Lake (DES 1997). Pressure data collected from instruments located in the exhaust shaft show no apparent hydrologic communication between the Santa Rosa and other formations located stratigraphically below the Santa Rosa.

A water-level-surface map of the Santa Rosa in the vicinity of the WIPP surface structures area indicates that a potentiometric high is located near the salt water evaporation pond and PZ-7 (Figure 2-40). The water level at PZ-7 is approximately 1 m (3.3 ft) higher than the water levels in any other wells or piezometers. Water is presumed to move radially from this potentiometric high. The areal extent of the water is larger than the 80-acre investigative area shown in Figure 2-39 (DES 1997) as evidenced by drilling records of C-2737 (Powers 2002c) located outside of and south of the WIPP surface structures area that indicate a Santa Rosa/Dewey Lake perched-water horizon at a depth of approximately 18 m (60 ft). The study of this water is ongoing.

Water-quality data for the perched Santa Rosa waters are highly variable and appear to be dominated by two anthropogenic sources: (1) runoff of rainfall into and infiltration from the retention ponds located to the south of the WIPP surface facilities, and (2) infiltration of saline waters from the salt storage area, the salt storage evaporation pond, and perhaps remnants of the drilling and tailings pit used during the construction of the WIPP salt shaft. The total dissolved solids (TDS) in the perched water range from less than 3,000 mg/L at PZ-10 to more than 160,000 mg/L at PZ-3 (DES 1997). Concentration contours are known to shift with time. For example, the high-TDS zone centered at PZ-3 moved observably to the northeast toward PZ-9 between February 1997 and October 2000 (DOE 2002b).

Hydraulic tests (Docket A-93-02, Item number 11-1-07, DOE; INTERA 1997a; DES 1997) conducted in the three wells and 12 piezometers indicate that the Santa Rosa behaves as a low-permeability, unconfined aquifer perched on the Dewey Lake. Hydraulic conductivity ranges from 2.6×10^{-8} to 5.5×10^{-5} m/s (7.4×10^{-3} to 16 ft/day). The wells are capable of producing at rates of about 0.3 to 1.0 gpm. The estimated storativity value for the Santa Rosa is 1×10^{-2} .

2.2.1.5 Hydrology of Other Groundwater Zones of Regional Importance

The groundwater regimes in the Capitan Limestone, which is generally regarded as the northern boundary of the Delaware Basin, and Nash Draw have been evaluated by the DOE as part of the WIPP project because of their importance in some processes, notably dissolution features, that the DOE has determined to be of low probability at the WIPP site.

2.2.1.5.1 Capitan Limestone

The Capitan *Limestone (hereafter referred to as the Capitan)*, which outcrops in the southern end of the Guadalupe Mountains, is a massive limestone unit that grades basinward into recemented, partly dolomitized reef breccia and shelfward into bedded carbonates and evaporites. A deeply incised submarine canyon near the Eddy-Lea county line has been identified (Hiss 1976). This canyon is filled with sediments of lower permeability than the Capitan and, according to Hiss (1975 *p.* 199), restricts fluid flow. The hydraulic conductivity of

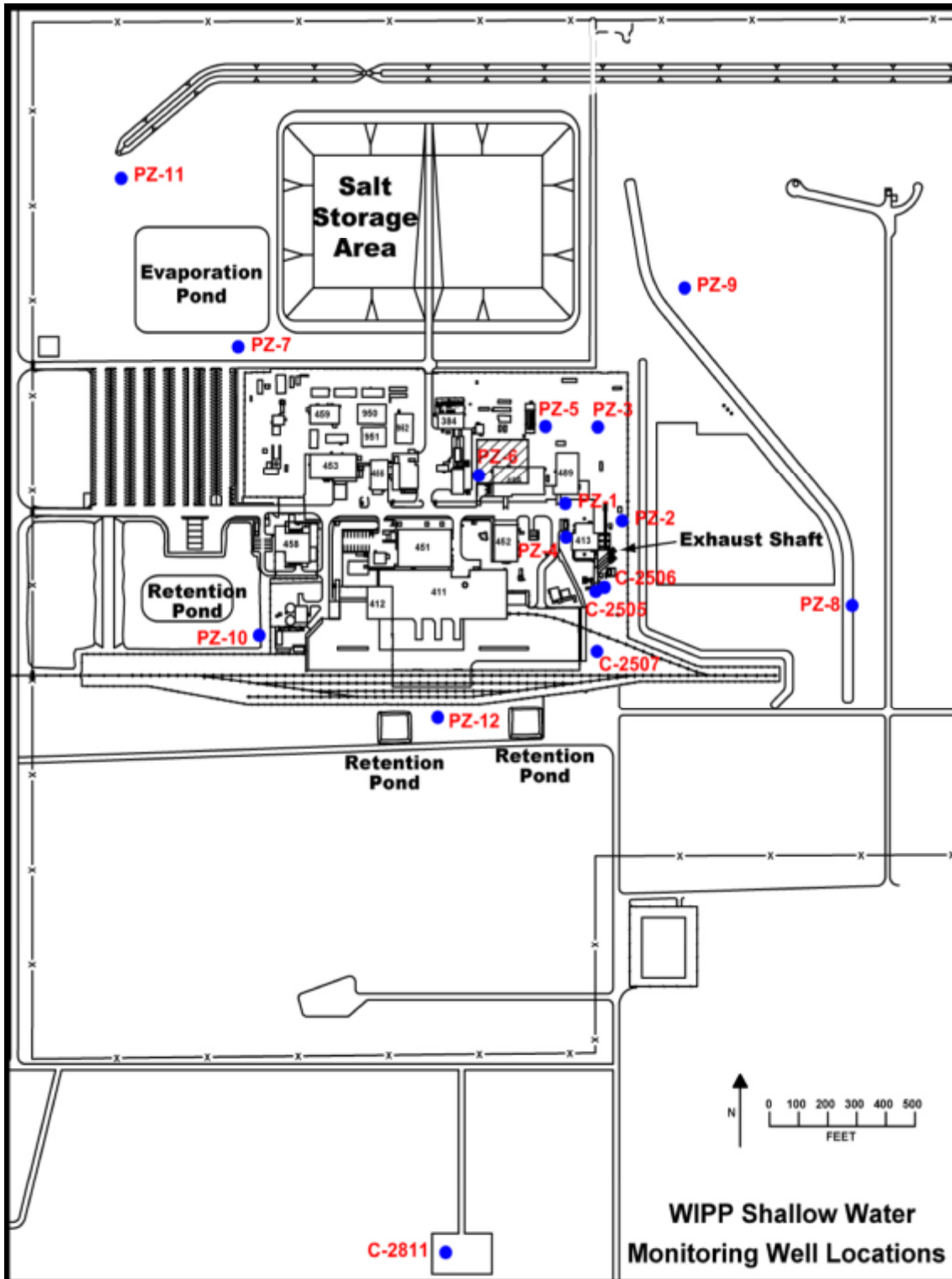


Figure 2-39. Site Map of WIPP Surface Structures Area Showing Location of Wells (e.g., C-2505) and Piezometers (e.g., PZ-1) (after INTERA 1997)

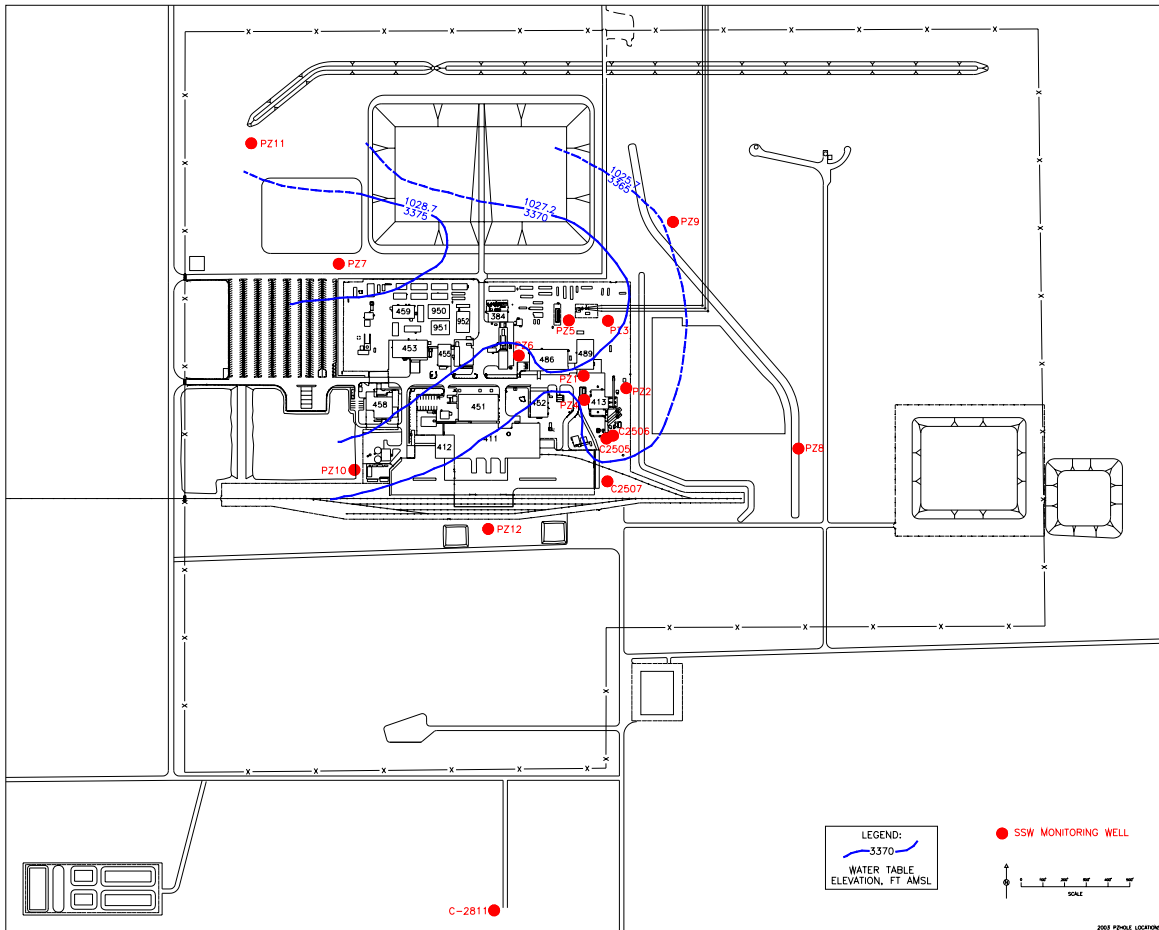


Figure 2-40. Santa Rosa Potentiometric Surface Map

the Capitan ranges from 3×10^{-6} to 9×10^{-5} m/sec (1 to 25 ft/day) in southern Lea County and is 1.7×10^{-5} m/sec (5 ft/day) east of the Pecos River at Carlsbad (CCA Appendix HYDRO, p. 34). Hiss (1975, p. 199) reported in 1975 that average transmissivities around the northern and eastern margins of the Delaware Basin are 0.01 m²/sec (10,000 ft²/day) in thick sections and 5.4×10^{-4} m²/sec (500 ft²/day) in incised submarine canyons. Water table conditions are found in the Capitan aquifer southwest of the Pecos River at Carlsbad; however, artesian conditions exist to the north and east. The hydraulic gradient to the southeast of the submarine canyon near the Eddy-Lea county line has been affected by large oil field withdrawals. The Capitan is recharged by percolation through the northern shelf aquifers, by flow from the south and west from underlying basin aquifers (see information on the Bell Canyon, Section 2.2.1.2.1), and by direct infiltration at its outcrop in the Guadalupe Mountains. The Capitan is important in the regional hydrology because breccia pipes in the Salado have formed over it, most likely in response to the effects of dissolution by groundwater flowing in the Castile along the base of the Salado. See CCA Appendix DEF, Section DEF.3.1 for a more thorough discussion of breccia pipe formation.

2.2.1.5.2 Hydrology of the Rustler-Salado Contact Zone in Nash Draw

As discussed in Sections 2.1.3.4 and 2.1.6.2.1, in Nash Draw the contact between the Rustler and the Salado is an unstructured residuum of gypsum, clay, and sandstone created by the dissolution of halite and has been known as the brine aquifer, Rustler-Salado residuum, and residuum. The residuum is absent under the WIPP site. It is clear that dissolution in Nash Draw occurred after deposition of the Rustler (see [CCA Appendix DEF, Section DEF.3.2](#) for a discussion of lateral dissolution of the Rustler-Salado contact). As described previously, the topographic low formed by Nash Draw is a groundwater divide in the groundwater basin conceptual model of the units above the Salado. The brine aquifer is shown in Figure 2-3441.

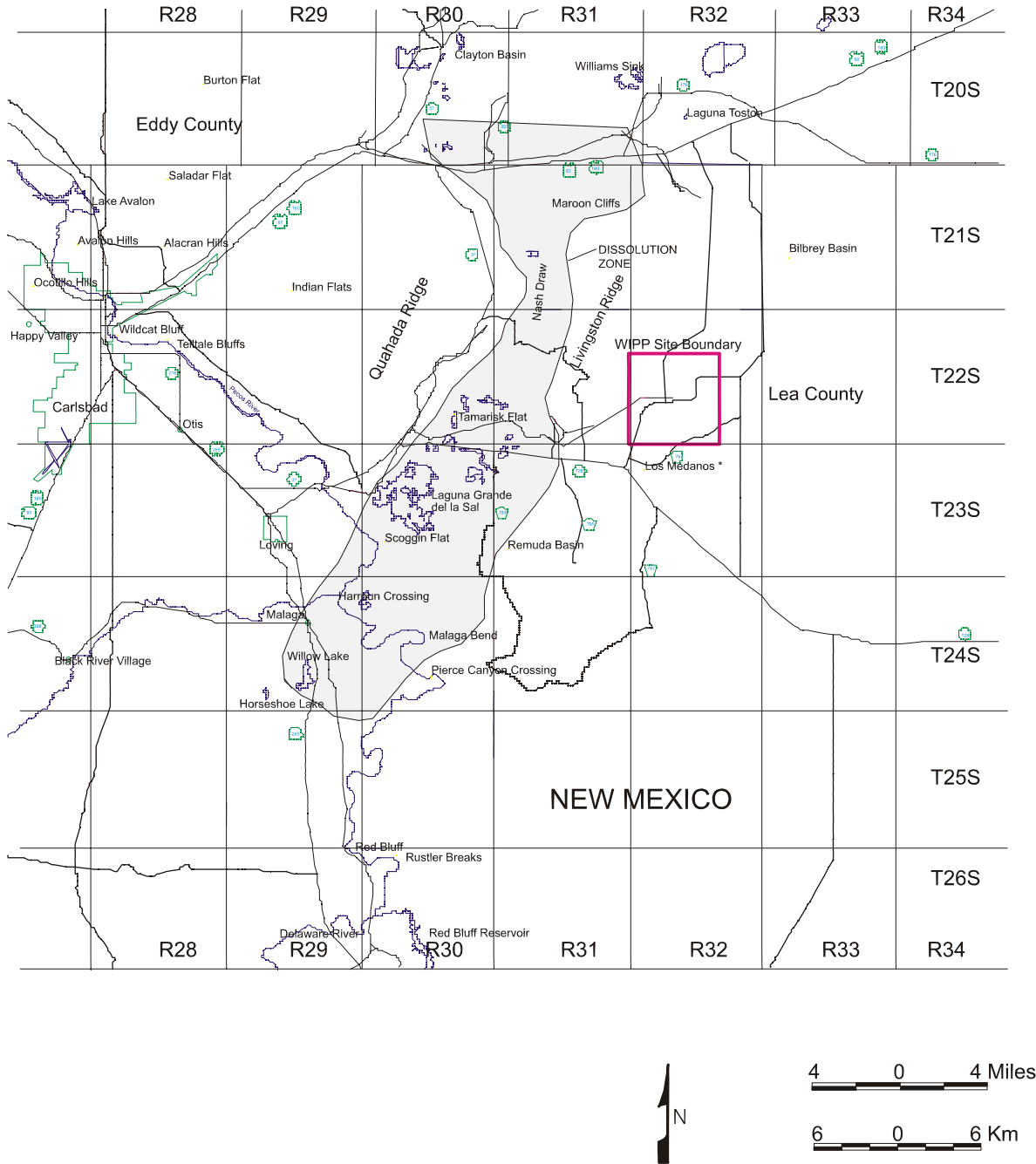
Robinson and Lang ([1938](#)) described the brine aquifer (Section 2.1.3.4) in 1938 and suggested that the structural conditions that caused the development of Nash Draw might control the occurrence of the brine; thus, the brine aquifer boundary may coincide with the topographic surface expression of Nash Draw, as shown in Figure 2-2933. Their studies show brine concentrated along a strip from 3.3 to 13 km (2 to 8 mi) wide and about 43 km (26 mi) long. Data from the test holes that Robinson and Lang ([1938](#)) drilled indicate that the residuum (containing the brine) ranges in thickness from 3 to 18 m (10.5 to 60 ft) and averages about 24 feet (7 meters).

In 1954, hydraulic properties were determined by Hale et al., ([1954](#)) primarily for the area between Malaga Bend on the Pecos River and Laguna Grande de la Sal. They calculated a transmissivity value of $8.6 \times 10^{-3} \text{ m}^2/\text{sec}$ (8,000 ft²/day) and estimated the potentiometric gradient to be 0.27 m/km (1.4 ft/mi). In this area, the Rustler-Salado residuum apparently is part of a continuous hydrologic system, as evidenced by the coincident fluctuation of water levels in the test holes (as far away as Laguna Grande de la Sal) with pumping rates in irrigation wells along the Pecos River.

In the northern half of Nash Draw, the approximate outline of the brine aquifer as described by Robinson and Lang in ([1938](#)) has been supported by drilling associated with the WIPP hydrogeologic studies. These studies also indicate that the main differences in areal extent occur along the eastern side where the boundary is very irregular and, in places (test holes P-14 and H-07), extends farther east than previously indicated by Robinson and Lang ([1938](#)).

Other differences from the earlier studies include the variability in thickness of residuum present in test holes WIPP-25 through WIPP-29. These holes indicate thicknesses ranging from 3.3 m (11 ft) in WIPP-25 to 33 m (108 ft) in WIPP-29 in Nash Draw, compared to 2.4 m (8 ft) in test hole P-14, east of Nash Draw. The specific geohydrologic mechanism that has caused dissolution to be greater in one area than in another is not apparent, although a general increase in chloride concentration in water from the north to the south may indicate the effects of movement down the natural hydraulic gradient in Nash Draw.

The average hydraulic gradient within the residuum in Nash Draw is about 1.9 m/km (10 ft/mi); in contrast, the average gradient at the WIPP site is 7.4 m/km (39 ft/mi) ([CCA Appendix HYDRO, p. 50](#)). This difference reflects the changes in transmissivity, which are as much as five orders of magnitude greater in Nash Draw. The transmissivity determined from aquifer tests in test holes completed in the Rustler-Salado contact residuum of Nash Draw ranges from



CCA-075-2

Figure 2-3441. Brine Aquifer in the Nash Draw (Redrawn from CCA Appendix HYDRO, Figure 14)

2.1 $\times 10^{-10}$ m²/see (2×10^{-4} ft²/day) at WIPP-27 to 8.6×10^{-6} m²/see (9.8×10^{-2} ft²/day) at WIPP-29. This is in contrast to the WIPP site proper, where transmissivities range from 3.2×10^{-11} m²/see (3×10^{-5} ft²/day) at test holes P-18 and H-5c to 5.4×10^{-8} m²/see (5×10^{-2} ft²/day) at test hole P-14 (CCA Appendix HYDRO, p. 50). Locations and estimated hydraulic heads of these wells based on water-level measurements made in the 1980s (Lappin et al. 1989) are illustrated in Figure 2-3542.

Hale et al. (1954) believed the Rustler-Salado contact residuum discharges to the alluvium near Malaga Bend on the Pecos River. Because the confining beds in this area are probably fractured because of dissolution and collapse of the evaporites, the brine (under artesian head) moves up through these fractures into the overlying alluvium and then discharges into the Pecos River.

According to Mereer-CCA Appendix HYDRO, p. 55, water in the Rustler-Salado contact residuum in Nash Draw contains the largest concentrations of dissolved solids in the WIPP area, ranging from 41,500 mg/L in borehole H-1 to 412,000 mg/L in borehole H-5c. These waters are classified as brines. The dissolved mineral constituents in the brine consist mostly of sulfates and chlorides of calcium, magnesium, sodium, and potassium; the major constituents are sodium and chloride. Concentrations of the other major ions vary according to the spatial location of the sample, are probably directly related to the interaction of the brine and the host rocks, and reflect residence time within the rocks. Residence time of the brine depends upon the transmissivity of the rock. For example, the presence of large concentrations of potassium and magnesium in water is correlated with minimal permeability and a relatively undeveloped flow system.

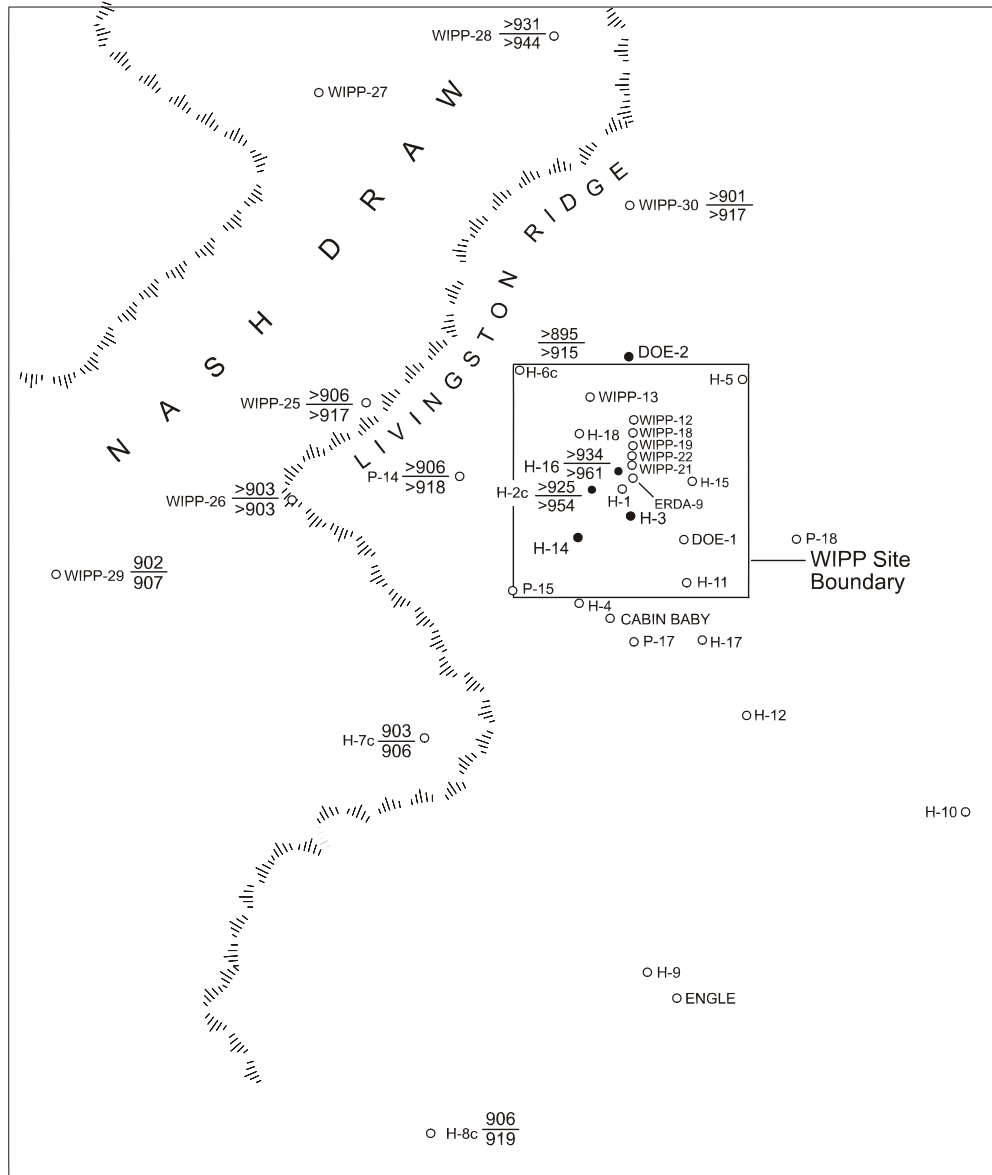
The EPA's initial review of the CCA found the discussion of the Rustler/Salado contact to require clarification, particularly with respect to the possibility of the continued development and characteristics of a dissolution front along this contact, and the impact that continued dissolution within the brine aquifer residuum would have on the overlying units of the Rustler. The DOE discussed the rate and extent of dissolution processes further in supplemental information provided in a letter dated June 13, 1997 (Docket A-93-02, II-H-44). Based upon this information, the EPA concluded that, while dissolution may occur along the Rustler/Salado contact, it would not affect the WIPP's containment capabilities during the regulatory time period. Further discussion of this topic is contained in EPA Technical Support Document for Section 194.14: Content of Compliance Certification Application, Section IV.C.3 (Docket A-93-02, Item V-B-3).

2.2.2 Surface-Water Hydrology

The WIPP site is in the Pecos River basin, which contains about 50 percent of the drainage area of the Rio Grande Water Resources Region. The Pecos River headwaters are northeast of Santa Fe, and the river flows to the south through eastern New Mexico and western Texas to the Rio Grande. The Pecos River has an overall length of about 805 km (500 mi), a maximum basin width of about 209 km (130 mi), and a drainage area of about 115,301 km² (44,535 mi²). (About 53,075 km² [20,500 mi²] contained within the basin have no external surface drainage and their surface waters do not contribute to Pecos River flows.) Figure 2-3643 shows the Pecos River drainage area.



Figure 2-35. Measured Water Levels of the Unnamed Lower Member and Rustler-Salado Contact Zone



CCA-050-2

Figure 2-42. Measured Water Levels of the Los Medaños and Rustler-Salado Contact Zone (1980s)

The Pecos River generally flows year-round, except in the reach below Anton Chico ~~and between Fort Sumner and Roswell~~, where the low flows percolate into the stream bed. The main stem of the Pecos River and its major tributaries have low flows, and the tributary streams are frequently dry. About 75 percent of the total annual precipitation and 60 percent of the annual flow result from intense local thunderstorms between April and September.

There are no perennial streams at the WIPP site. At its nearest point, the Pecos River is about 19 km (12 mi) southwest of the WIPP site boundary. A few small creeks and draws are the only westward flowing tributaries of the Pecos River within 32 km (20 mi) north or south of the site. Nash Draw, the largest surface drainage feature east of the Pecos River in the WIPP region, is a closed depression and does not provide surface flow into the Pecos. *Potash mining operations in and near Nash Draw likely contribute to the flow in Nash Draw. For example, the Mississippi Potash Inc. East operation located 11 to 13 km (7 to 8 mi) due north of the WIPP site disposes of mine tailings and refining-process effluent on its property and has done so since 1965. Records obtained from the New Mexico Office of the State Engineer show that since 1973, an average of $3 \times 10^6 \text{ m}^3$ (2,400 acre-feet [ac-ft]) of water per year has been pumped from local aquifers (Ogallala and Capitan) for use in the potash-refining process at that location (SNL 2003b). Based on knowledge of the potash refining process, approximately 90 percent of the pumped water is estimated to be discharged to the tailings pile. Geohydrology Associates (1978) estimated that approximately half of the brine discharged onto potash tailings piles in Nash Draw seeps into the ground annually, while the remainder evaporates.* The Black River (drainage area: 1,035 km² [400 mi²]) joins the Pecos from the west about 25 km (16 mi) southwest of the site. The Delaware River (drainage area: 1,812 km² [700 mi²]) and a number of small creeks and draws also join the Pecos River along this reach. The flow in the Pecos River below Fort Sumner is regulated by storage in Sumner Lake, Brantley Reservoir, Lake Avalon, and several other smaller irrigation dams.

Five major reservoirs are located on the Pecos River: Santa Rosa Lake, Sumner Lake, Brantley Reservoir, Lake Avalon, and the Red Bluff Reservoir, the last located just over the border in Texas (Figure 2-3643). The storage capacities of these reservoirs and the Two Rivers Reservoir in the Pecos River Basin are shown in Table 2-610.

With regard to surface drainage onto and off of the WIPP site, there are no major natural lakes or ponds within 8 km (5 mi) of the site. Laguna Gatuña, Laguna Tonto, Laguna Plata, and Laguna Toston are playas more than 16 km (10 mi) north and are at elevations of 1,050 m (3,450 ft) or higher. Thus, surface runoff from the site (elevation 1,010 m [3,310 ft] above sea level) would not flow toward any of them. To the northwest, west, and southwest, Red Lake, Lindsey Lake, and Laguna Grande de la Sal are more than 8 km (5 mi) from the site, at elevations of 914 to 1,006 m (3,000 to 3,300 ft). A low-flow investigation has been initiated by the USGS within the Hill Tank Draw drainage area, the most prominent drainage feature near the WIPP site. The drainage area is about 10.3 km² (4 mi²), with an average channel slope of 1 to 100, and the drainage is westward into Nash Draw. Two years of observations showed only four flow events. The USGS estimates that the flow rate for these events was under 0.057 m³/sec (2 ft³/sec) (DOE 1980, pp. 7- 74).

As discussed in Section 2.5.2.3, the mean annual precipitation in the region is 0.33 m (13 in.), and the mean annual runoff is 2.5 to 5 mm (0.1 to 0.2 in.). The maximum recorded 24-hour

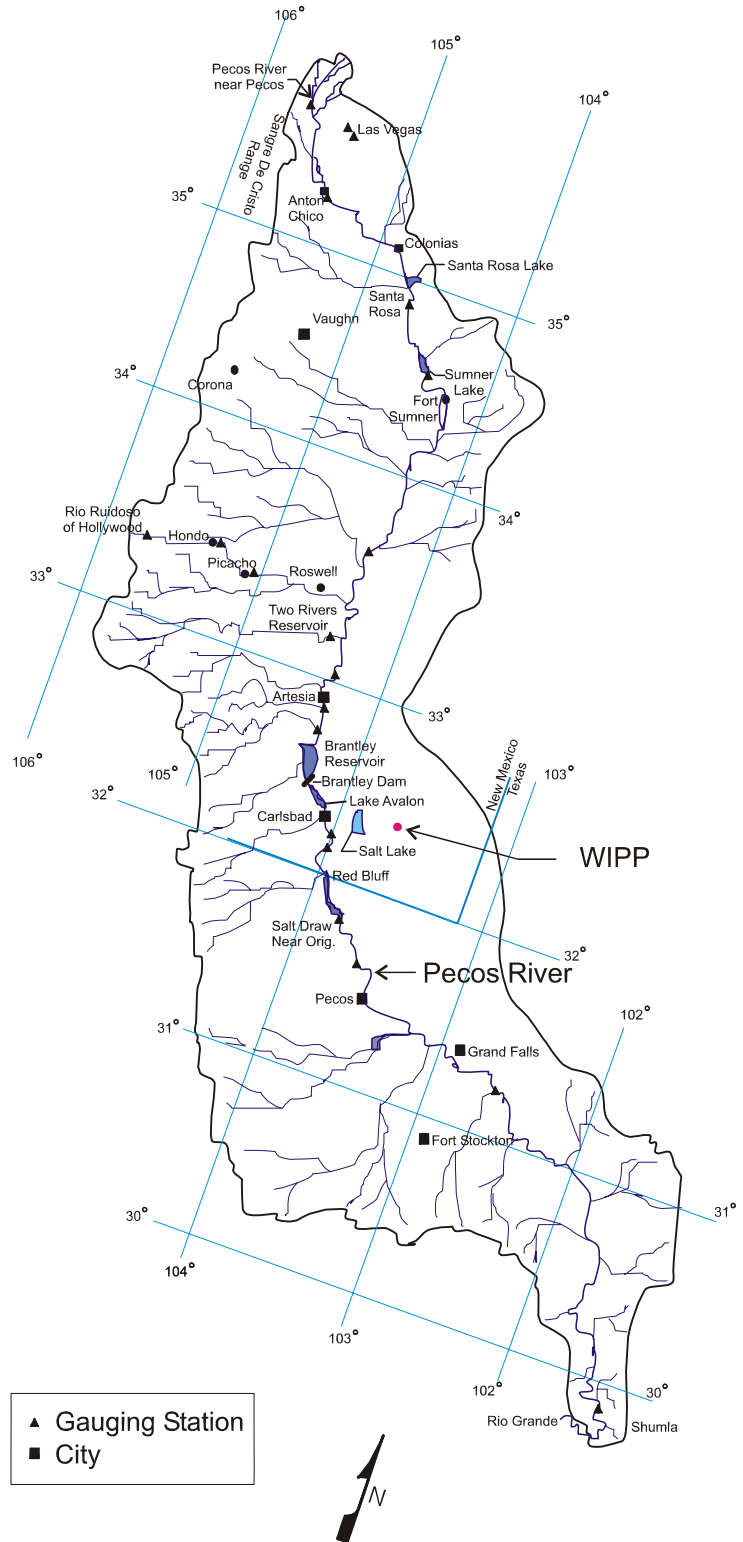


Figure 2-3643. Location of Reservoirs and Gauging Stations in the Pecos River Drainage Area

Table 2-610. Capacities of Reservoirs in the Pecos River Drainage

Reservoir	River	Total Storage Capacity ^a (<i>ac-ft</i>)	Use ^b
Santa Rosa	Pecos	282000	FC
Sumner	Pecos	122100	IR, R
Brantley	Pecos	42000	IR, R, FC
Avalon	Pecos	5000	IR
Red Bluff	Pecos	310000	IR, P
Two Rivers	Rio Hondo	167900	FC

^a Capacity below the lowest uncontrolled outlet or spillway.

^b Legend:

FC flood control
IR irrigation
R recreation
P hydroelectric

precipitation at Carlsbad was 130 mm (5.12 in.) in August 1916. The predicted maximum 6-hour, 100-year precipitation event for the site is 91 mm (3.6 in.) and is most likely to occur during the summer. The maximum recorded daily snowfall at Carlsbad was 254 mm (10 in.) in December 1923.

The maximum recorded flood on the Pecos River occurred near the town of Malaga, New Mexico, on August 23, 1966, with a discharge of 3,396 m³ (120,000 ft³) per second and a stage elevation of about 895 m (2,938 ft) *amsl*. The minimum surface elevation at the WIPP is over 91 m (300 ft) above the elevation of this maximum historic flood (DOE 1980, Section 7.4.1).

As discussed in the FEIS (DOE 1980, *pp.* 7- 71), more than 90 percent of the mean annual precipitation at the site is lost by evapotranspiration. On a mean monthly basis, evapotranspiration at the site greatly exceeds the available rainfall; however, intense local thunderstorms may produce runoff and percolation.

Water quality in the Pecos River basin is affected by mineral pollution from natural sources and from irrigation return flows (see Section 2.4.2.2 for discussion of surface-water quality). At Santa Rosa, New Mexico, the average suspended-sediment discharge of the river is about 1,497 metric tons/day (1,650 tons/day). Large amounts of chlorides from Salt Creek and Bitter Creek enter the river near Roswell. River inflow in the Hagerman area contributes increased amounts of calcium, magnesium, and sulfate; and waters entering the river near Lake Arthur are high in chloride. Below Brantley Reservoir, springs flowing into the river are usually submerged and difficult to sample; springs that could be sampled had TDS concentrations of 3,350 to 4,000 mg/L. Concentrated brine entering at Malaga Bend adds an estimated 64 metric tons/day (370 tons/day) of chloride to the Pecos River (*CCA* Appendix GCR, *pp.* 6-7).

2.3 Resources

At the outset of the repository program, the DOE understood the importance of resources in the vicinity of a disposal system. Several of the siting criteria emphasized avoidance of resources that would impact the performance of the disposal system. In this regard, the DOE selected a site that (1) maximized the use of federal lands, (2) avoided known oil and gas trends, (3) minimized the impacts on potash deposits, and (4) avoided existing drill holes. While the DOE could not meet all these criteria totally, ~~this application shows~~ *it is shown* that the favorable characteristics of the location compensate for any increased risks due to the presence of resources. Consequently, the DOE has prepared this section to discuss resources that may exist at or beneath the WIPP site. The topic of resources is used to broadly define both economic (mineral and nonmineral) and cultural resources associated with the WIPP site. These resources are important because they (1) provide evidence of past uses of the area and (2) indicate potential future use of the area with the possibility that such use could lead to disruption of the closed repository. Because of the depth of the disposal horizon, it is believed that only the mineral resources are of significance in predicting the long-term performance of the disposal system. However, the nonmineral and cultural resources are presented for completeness because they are included in the FEP screening discussions in Chapter 6 and Appendix *PA, Attachment* SCR. Information needed to make screening decisions includes natural resource distributions, including potable groundwaters, the distribution of drillholes, mines, excavations, and other man-made features that exploit these resources, the distribution of drillholes and excavation used for disposal or injection purposes, activities that significantly alter the land surface, agricultural activities that may affect the disposal system, archaeological resources requiring deep excavation to exploit, and technological changes that may alter local demographics. This information is presented here or is referenced.

With respect to minerals or hydrocarbons, reserves are the portion of resources that are economic at today's market prices and with existing technology. For hydrocarbons, proved (proven) reserves are an estimated quantity that engineering and geologic data analysis demonstrates, with reasonable certainty, is recoverable in the future from discovered oil and gas pools. Probable resources (extensions) consist of oil and gas in pools that have been discovered but not yet developed by drilling. Their presence and distribution can generally be surmised with a high degree of confidence. Probable resources (new pools) consist of oil and gas surmised to exist in undiscovered pools within existing fields. (Definitions are from NMBMMR 1995, V-2 and V-3.)

Mineral resource discussions are focused principally on hydrocarbons and potassium salts, both of which have long histories of development in the region. Development of either resource potentially could be disruptive to the disposal system. The information regarding the mineral resources concentrates on the following factors:

- number, location, depth, and present state of development, including penetrations through the disposal horizon,
- type of resource,
- accessibility, quality, and demand, and

- mineral ownership in the area.

The specific impacts of resource development are discussed in Section 6.4.6.2.3, where scenarios related to mineral development are included for evaluation of disposal system performance. This discussion uses information presented in [CCA](#) Appendices DEL and MASS as indicated in the following text. The discussion of cultural and economic resources is focused on describing past and present land uses unrelated to the development of minerals. The archaeological record supports the observation that changes in land use are principally associated with climate and the availability of forage for wild and domestic animals. In no case does it appear that past or present land use has had an impact on the subsurface beyond the development of shallow groundwater wells to water livestock.

2.3.1 Extractable Resources

The geologic studies of the WIPP site included the investigation of potential natural resources to evaluate the impact of denying access to these resources and other consequences of their occurrence. Studies were completed in support of the FEIS to ensure knowledge of natural resources, and the impacts of denying access were included in the decision-making process for WIPP. Of the natural resources expected to occur beneath the site, five are of practical concern: the two potassium salts sylvite and langbeinite, which occur in the McNutt; and the three hydrocarbons, crude oil, natural gas, and distillate liquids associated with natural gas, all three of which occur elsewhere in strata below the Castile. Other mineral resources beneath the site are caliche, salt, gypsum, and lithium; enormous deposits of these minerals near the site and elsewhere in the country are more than adequate (and more economically attractive) to meet future requirements for these materials. In 1995, the NMBMMR performed a reevaluation of the mineral resources at and within 1.6 km (1 mi) around the WIPP site. The following discussion is based in part on information from NMBMMR (1995).

2.3.1.1 Potash Resources at the WIPP Site

Throughout the Carlsbad Potash District, commercial quantities of potassium salts are restricted to the middle portion of the Salado, locally called the McNutt. A total of 11 zones (or distinct ore layers) have been recognized in the McNutt. Horizon Number 1 is at the base, and Number 11 is at the top. The 11th ore zone is not mined.

The USGS uses three standard grades—low, lease, and high—to quantify the potash resources at the site. The USGS assumes that the lease and high grades comprise reserves because some lease-grade ore is mined in the Carlsbad Potash District. Most of the potash that is mined, however, is better typified as high-grade. Even the high-grade resources may not be reserves, however, if properties such as high clay content make processing uneconomical. The analysis in the [NMBMMR \(1995\)](#) ~~NMBMMR report~~ distinguishes between lease-grade ore and economically mineable ore.

The [NMBMMR \(1995\)](#) study contains a comprehensive summary of all previous potash resource evaluations. ~~Griswold~~ (NMBMMR (1995, Chapter VII) used 40 existing boreholes drilled on and around the WIPP site to perform a reevaluation of potash resources. He selected holes that were drilled using brine so that the dissolution of potassium salts was inhibited. The conclusion

reached by Griswold is that only the 4th and 10th ore zones contain economic potash reserves. The quantities are summarized in Table 2-711.

Table 2-711. Current Estimates of Potash Resources at the WIPP Site

Mining Unit	Product	Recoverable Ore (10 ⁶ tons)	
		Within the WIPP site	One-Mile Strip Adjacent to the WIPP site
4th Ore Zone	Langbeinite	40.5 at 6.99%*	126.0 at 7.30%
10th Ore Zone	Sylvite	52.3 at 13.99%	105.0 at 14.96%

Source: NMBMMR 1995, Chapter VII.

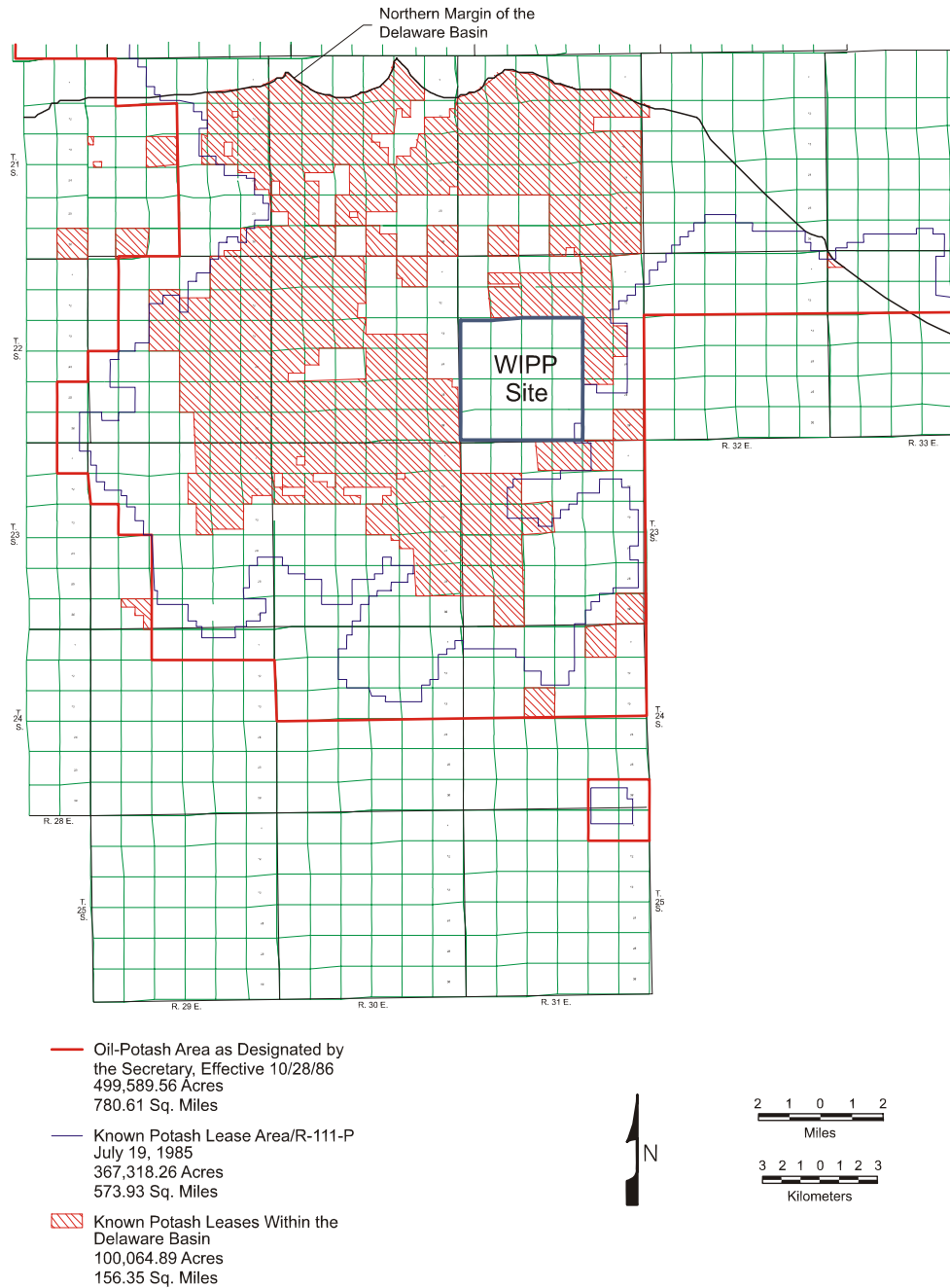
* For example, read as 40.5 × 106 tons of ore at a grade of 6.99 percent or higher.

Within the Carlsbad Known Potash Leasing Area, exploration holes have been drilled to evaluate the grade of the various ore zones. These are included in the drillhole database in CCA Appendix DEL. None of the economically minable reserves identified by the NMBMMR lies directly above the waste panels. The known potash leases within the Delaware Basin are shown in Figure 2-3744 and are detailed in CCA Appendix DEL, Figure DEL-8. From information in this figure and other data which is provided in CCA Appendix MASS, Attachment 15-5, DOE evaluates the extent of future mining outside the land withdrawal area. The extent of possible future mining within the controlled area is shown in Figure 2-3845. The DOE also addresses this subject with respect to PA in Section 6.4.6.2.3.

The EPA concluded that neither the DOE's nor the Department of Interior's (DOI) estimate shows the area above the WIPP waste panels as containing mineable reserves. The DOE provided supplemental information in a letter dated May 14, 1997, indicating that potash solution mining and brine extraction do not need to be considered for the PA, based on low consequence to the containment capability of the repository (Docket A-93-02, Item II-I-31). The EPA reviewed the supplemental data and concurred with the DOE's conclusion. To obtain further discussion on this topic, CARD 32-Section 32.B, CARD 33-Section 33A, and CARD 32-Section 32 F (Docket A-93-02, item III-B-2) may be referenced. Additional information is found in FEPs screening discussions for solution mining for potash and solution mining for other resources (FEPs H58 and H59) in Appendix PA, Attachment SCR.

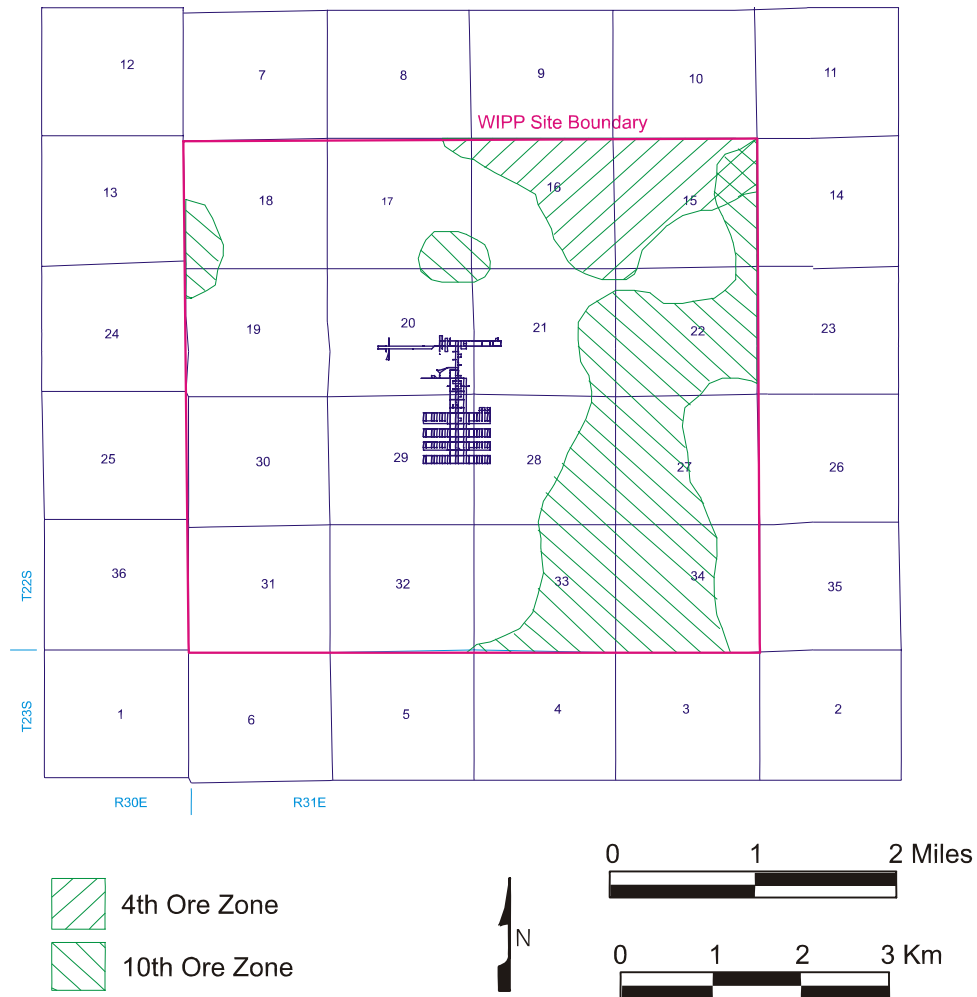
2.3.1.2 Hydrocarbon Resources at the WIPP Site

In 1974, Foster of the NMBMMR conducted a hydrocarbon resource study in southeastern New Mexico under contract to the ORNL. The study included an area of 3,914 km² (1,512 mi²). At the time of that study, the proposed repository site was about 8 km (5 mi) northeast of the current site. The 1974 NMBMMR evaluation included a more detailed study of a four-township area centered on the old site; the present site is in the southwest quadrant of that area. The 1974 NMBMMR hydrocarbon resources study (Foster 1974) is presented in more detail in the FEIS (DOE 1980, Section 9.2.3.5). The reader is referred to the FEIS or the original study for additional information.



CCA-074-2

Figure 2-3744. Known Potash Leases Within the Delaware Basin



CCA-077-2

Figure 2-3845. Extent of Economically Mineable Reserves Inside the Site Boundary (Based on NMBMMR Report)

The resource evaluation was based both on the known reserves of crude oil and natural gas in the region and on the probability of discovering new reservoirs in areas where past unsuccessful drilling was either too widely spread or too shallow to have allowed discovery. Potentially productive zones were considered in the evaluation; therefore, the findings may be used for estimating the total hydrocarbon resources at the site. A fundamental assumption in the study was that the WIPP area has the same potential for containing hydrocarbons as the

larger region studied for which exploration data are available. Whether such resources actually exist can be satisfactorily established only by drilling at spacings close enough to give a high probability of discovery.

The NMBMMR 1995 mineral resource reevaluation contains a comprehensive summary of all previous evaluations. Broadhead et al. (NMBMMR (1995, Chapter XI) provided a reassessment

of hydrocarbon resources within the WIPP site boundary and within the first mile adjacent to the boundary. Calculations were made for resources that are extensions of known, currently productive oil and gas resources that are thought to extend beneath the study area with reasonable certainty (called probable resources in the report). Qualitative estimates are also made concerning the likelihood that oil and gas may be present in undiscovered pools and fields in the area (referred to as possible resources). Possible resources were not quantified in the study. The results of the study are shown in Tables 2-8¹² and 2-9¹³.

Table 2-8¹². In-Place Oil within Study Area

Formation	Within WIPP Site (10 ⁶ bbl ^a)	1-Mile Strip Adjacent to the WIPP Site (10 ⁶ bbl)	Total (10 ⁶ bbl)
Delaware	10.33	20.8	31.13
Bone Spring	0.44	0.8	1.25
Strawn	0.4	0.4	0.8
Atoka	1.1	0.1	0.2
Total	12.3	22.9	35.3

Source: NMBMMR (1995, Chapter XI)

a bbl = barrel = 42 gallons

Table 2-9¹³. In-Place Gas within Study Area

Formation	Gas Reserves (Mcf) ^a	
	Within WIPP Site	1-Mile Strip Adjacent to the WIPP
Delaware	18176	32873
Bone Springs	956	1749
Strawn	9600	9875
Atoka	123336	94410
Morrow	32000	28780

Source: NMBMMR (1995, Chapter XI)

^a Mcf = thousand cubic feet

The DOE has compiled statistics on the historical development of hydrocarbon resources in the Delaware Basin and has included them in CCA Appendix DEL. For these purposes, the Delaware Basin is described as the surface and subsurface features that lie inside the boundary formed to the north, east, and west by the innermost edge of the Capitan Reef and formed to the south by a straight line drawn from the southeastern point of the Davis Mountains to the southwestern point of the Glass Mountains (see Figure 2-39⁴⁶).

Several important modeling parameters result from the study of hydrocarbon resources and the history of their exploitation. These include parameters related to the number of human intrusions, the size of boreholes, the operational histories of such holes, the plugging of these

holes, and the use of such holes for other purposes, such as liquid disposal. Each of these topics is discussed in detail in *CCA* Appendix DEL and Appendix *PA, Attachment MASS, Section MASS.16* (Section Appendix MASS.16) and is addressed in Sections 6.4.7 and 6.4.12. The distribution of existing boreholes is shown in Figure DEL-4 (*CCA Appendix DEL*) for the entire Delaware Basin and Figure 2-47 DEL-6 for the vicinity of the WIPP site. In addition, *CCA* Appendix DEL includes an assessment of current drilling and plugging practices in the Delaware Basin. *CCA* Appendix DEL also discusses the regulatory constraints placed on the use of wells for injection.

2.3.1.3 Other Resources

While the focus of studies at the WIPP has been on potash and hydrocarbon, other resources are known to occur within the Delaware Basin and are considered in the screening. For example, sulfur is produced in the vicinity of Orla, Texas. Sulfur wells are included in *CCA* Appendix DEL; however, no sulfur resources have been identified in the vicinity of the WIPP; therefore, there are no projected impacts. Another resource that is extensively produced is groundwater. Potable water occurs in numerous places within the Delaware Basin. Several communities rely solely on groundwater sources for drinking water. *CCA* Appendix DEL includes a distribution of groundwater wells in the Delaware Basin. All such wells in the vicinity of the WIPP are shallow, generally no deeper than the Culebra. An evaluation of underground sources of drinking water in the vicinity of the disposal system is presented in *CCA* Appendix USDW. Figure USDW-4 shows the distribution of groundwater wells in the vicinity of the disposal system. Sand, gravel, and caliche are produced in numerous areas within the Delaware Basin. In all cases, these are surface quarries that are generally shallow (10s of feet). No impact to the disposal system is expected from these activities.

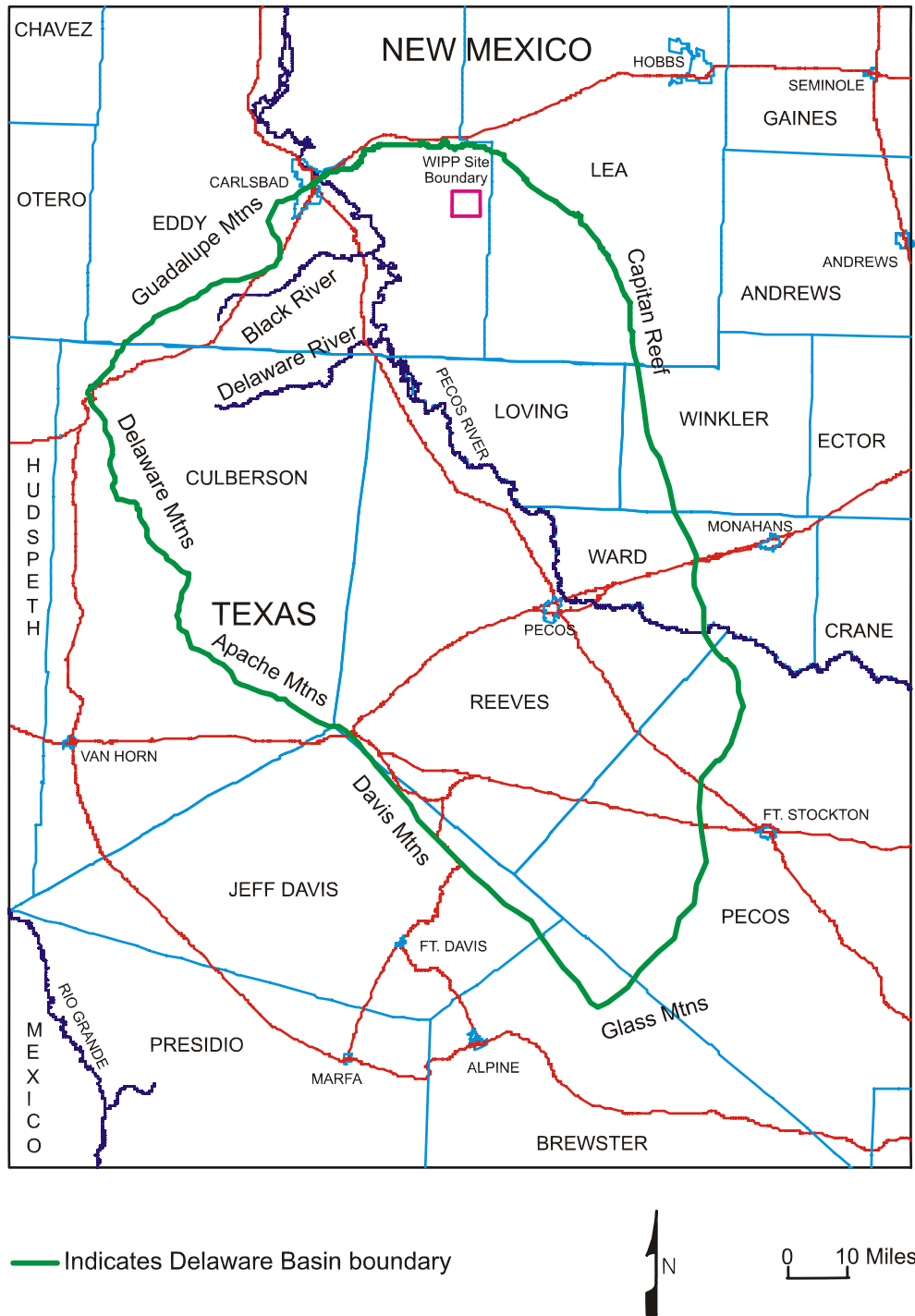
2.3.2 *Cultural and Economic Resources*

The demographics, land use, and history and archaeology of the WIPP site and its environs are characterized in the sections that follow.

2.3.2.1 Demographics

The WIPP facility is located 42 km (26 mi) east of Carlsbad in Eddy County in southeastern New Mexico and includes an area of 10,240 ac (approximately 41 km²) (16 mi²). The facility is located in a sparsely populated area with fewer than 30 permanent residents living within a 16-km (10-mi) radius of the facility. The area surrounding the facility is used primarily for grazing, potash mining, and hydrocarbon production. No resource development that would affect WIPP facility operations or the long-term integrity of the facility is allowed within the 10,240 ac that have been set aside for the WIPP project.

The permanent residence nearest to the WIPP site boundary is the J.C. Mills Ranch, which is 2 km (1.2 mi) to the south. The community nearest to the WIPP site is the town of Loving, New Mexico, 29 km (18 mi) west-southwest of the site center. The population of Loving decreased from 1,355 in 1980 to *increased from 1,243 in 1990 to 1,326 in 2000*. The nearest population center is the city of Carlsbad, New Mexico, 42 km (26 mi) west of the site. The population of



CCA-072-2

Figure 2-3946. Delaware Basin Boundary

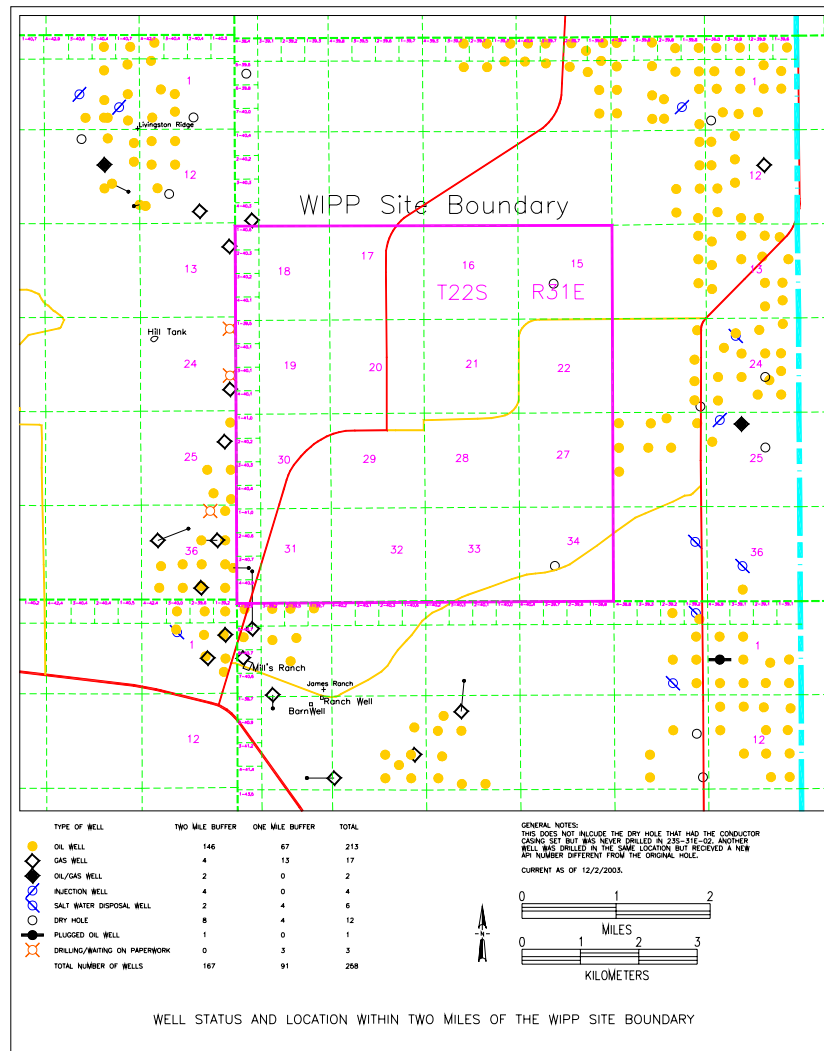


Figure 2-47. Distribution of Existing Petroleum Industry Boreholes Within Two Miles of the WIPP Site

Carlsbad has decreased **increased** from 25,496 in 1980 to 24,896 in 1990 **to 26,870 in 2000**. Hobbs, New Mexico, 58 km (36 mi) to the east of the site, had a 1980 population of 29,153 and a 1990 population decrease from of 29,115 **in 1990 to 28,657 in 2000**. Eunice, New Mexico, 64 km (40 mi) east of the site, had a 1980 population of 2,970 and a 1990 population of 2,731 **decrease to 2,562 in 2000**. Jal, New Mexico, 72 km (45 mi) southeast of the site, had a population of 2,575 in 1980 and of 2,153 in 1990 **decrease to 1,996 in 2000**.

The WIPP site is located in Eddy County near the border of Lea County, New Mexico. The Eddy County population increased from 47,855 in 1980 to 48,605 in 1990 **to 51,658 in 2000**. The Lea County population decreased from 55,993 in 1980 to 55,765 in 1990 **to 55,511 in 2000**. Population figures are taken from the 1980 and 1990 census (U.S. Department of Commerce, 1980, 1990) **and the 2000 census (U.S. Census Bureau, 2000)**.

2.3.2.2 Land Use

At present, land within 16 km (10 mi) of the site is used for potash mining operations, active oil and gas wells, activities associated with hydrocarbon production, and grazing.

The WIPP Land Withdrawal Act (LWA) (U.S. Congress 1992) withdrew certain public lands from the jurisdiction of the Bureau of Land Management (BLM). The law provides for the transfer of the WIPP site lands from the U.S. Department of the Interior (DOI) to the DOE and effectively withdraws the lands, subject to existing rights, from entry, sale, or disposition; appropriation under mining laws; *or* operation of the mineral and geothermal leasing laws. The LWA directed the Secretary of Energy to produce a management plan to provide for grazing, hunting and trapping, wildlife habitat, mining, and the disposal of salt and tailings.

Between 1978 and 1988, DOE acquired all active potash and hydrocarbon leases within the WIPP site boundary. These were acquired either through outright purchase or through condemnation. In one condemnation proceeding, the court awarded DOE the surface and top 1.82 km (6,000 ft) of Section 31 and allowed the leaseholder to retain the subsurface below 1.82 km (6,000 ft). This was allowed because analysis showed that wells developed within this lease below the 1.82-km (6,000-ft) limit would be too far away from the waste panels to be of consequence to the WIPP (see, for example, Brausch et al. 1982). This is corroborated by the results of *PA* discussed in Section 6.2.5.1; and Appendix *PA, Attachment SCR, FEP 56 SCR (Section SCR-3.3.1)*. Consequently, as the result of the DOE's acquisition activities, there are no producing hydrocarbon wells within the volumetric boundary defined by the land withdrawal (T22S, R31E, S15-22, 27-34). Two active wells were drilled to tap the oil and gas resources on the leases beneath Section 31. The James Ranch #13, drilled in 1982, is a gas well, and the James Ranch #27, drilled in 2000, is an oil well. Both wells are located on surface leases outside the WIPP site boundary. Both wells enter Section 31 below a depth of 1.82 km (6,000 ft) beneath ground level. Except for the leases in Section 31, the LWA prohibits all drilling into the controlled area unless such drilling is in support of the WIPP.

Grazing leases have been issued for all land sections immediately surrounding the WIPP facility. Grazing within the WIPP site lands occurs within the authorization of the Taylor Grazing Act of 1934, the Federal Land Policy and Management Act (FLPMA), the Public Rangelands Improvement Act of 1978, and the Bankhead-Jones Farm Tenant Act of 1973.

The responsibilities of DOE include supervision of ancillary activities associated with grazing (for example, wildlife access to livestock water development), tracking of water developments inside WIPP lands to ensure that they are configured according to the regulatory requirements, and ongoing coordination with respective allottees. Administration of grazing rights is in cooperation with the BLM according to the memorandum of understanding (MOU) and the coinciding Statement of Work through guidance established in the East Roswell Grazing Environmental Impact Statement. The WIPP site is composed of two grazing allotments administered by the BLM: the Livingston Ridge (No. 77027), and the Antelope Ridge (No. 77032) (*see Figure 7-2*).

2.3.2.3 History and Archaeology

From about 10,000 B.C. to the late 1800s, the WIPP site and surrounding region were inhabited by nomadic aboriginal hunters and gatherers who subsisted on various wild plants and animals. From about A.D. 600 onward, as trade networks were established with Puebloan peoples to the west, domesticated plant foods and materials were acquired in exchange for dried meat, hides, and other products from the Pecos Valley and Plains. In the late 1500s, the Spanish Conquistadors encountered Jumano and Apachean peoples in the region who practiced hunting and gathering and engaged in trade with Puebloans. After the Jumanos abandoned the southern Plains region, the Comanches became the major population of the area. Neighboring populations with whom the Comanches maintained relationships ranging from mutual trade to open warfare included the Lipan, or Southern Plains Apache, several Puebloan Groups, Spaniards, and the Mescalero Apaches.

The best documented indigenous culture in the WIPP region is that of the Mescalero Apaches, who lived west of the Pecos. The lifestyle of the Mescalero Apaches represents a transition between the full sedentism of the Pueblos and the nomadic hunting and gathering of the Jumanos. In 1763, the San Saba expedition encountered and camped with a group of Mescaleros in Los Medaños. Expedition records indicate the presence of both Lipan and Mescalero Apaches in the region.

A peace accord reached between the Comanches and the Spaniards in 1786 resulted in two historically important economic developments: (1) organized buffalo hunting by Hispanic and Puebloan ciboleros, and (2) renewal and expansion of the earlier extensive trade networks by Comancheros. These events placed eastern New Mexico in a position to receive a wide array of both physical and ideological input from the Plains culture area to the east and north and from Spanish-dominated regions to the west and south. Comanchero trade began to mesh with the Southwest American trade influence in the early nineteenth century. However, by the late 1860s, the importance of Comanchero trade was cut short by Texan influence.

The first cattle trail in the area was established along the Pecos River in 1866 by Charles Goodnight and Oliver Loving. By 1868, Texan John Chisum dominated much of the area by controlling key springs along the river. Overgrazing, drought, and dropping beef prices led to the demise of open-range cattle ranching by the late 1880s.

Following the demise of open-range livestock production, ranching developed using fenced grazing areas and production of hay crops for winter use. Herd grazing patterns were influenced by the availability of water supplies as well as by the storage of summer grasses for winter feeding.

The town of Carlsbad was founded as Eddy in 1889 as a health spa. In addition to ranching, the twentieth century brought the development of the potash, oil, and gas industries that have increased the population eightfold in the last 50 years.

Although technological change has altered some of the aspects, ranching remains an important economic activity in the WIPP region. This relationship between people and the land is still an important issue in the area. Ranch-related sites dating to the 1940s and 1950s are common in

parts of the WIPP area. These will be considered historical properties within the next several years, and thus will be treated as such under current law.

The National Historic Preservation Act (NHPA) (16 USC Part 470 et seq.) was enacted to protect the nation's cultural resources in conjunction with the states, local governments, Indian tribes, and private organizations and individuals. The policy of the federal government includes: (1) providing leadership in preserving the prehistoric and historic resources of the nation, (2) administering federally owned, administered, or controlled prehistoric resources for the benefit of present and future generations, (3) contributing to the preservation of nonfederally owned prehistoric and historic resources, and (4) assisting state and local governments and the national trust for historic preservation in expanding and accelerating their historic preservation programs and activities. The act also established the National Register of Historic Places (National Register). At the state level, the State Historic Preservation Officer (SHPO) coordinates the state's participation in implementing the NHPA. The NHPA has been amended by two acts: the Archeological and Historic Preservation Act (16 USC Part 469 et seq.), and the Archeological Resource Protection Act (16 USC Part 470aa et seq.).

To protect and preserve cultural resources found within the WIPP site boundary, the WIPP submitted a mitigation plan to the New Mexico SHPO describing the steps to either avoid or excavate archaeological sites. A site was defined as a place used and occupied by prehistoric people. In May 1980, the SHPO made a determination of "no adverse effect from WIPP facility activities" on cultural resources. The Advisory Council on Historic Preservation concurred that the WIPP Mitigation Plan is appropriate to protect cultural resources.

Known historical sites (more than 50 years old) in southeastern New Mexico consist primarily of early twentieth century homesteads that failed, or isolated features from late nineteenth century and early twentieth century cattle or sheep ranching, *or* military activities. To date, no Spanish or Mexican sites have been identified. Historic components are rare but are occasionally noted in the WIPP area. These include features and debris related to ranching.

Since 1976, cultural resource investigations have recorded 98 archaeological sites and numerous isolated artifacts within the 41-km² (16-mi²) area enclosed by the WIPP site. In the central 10.4-km² (4-mi²) area, 33 sites were determined to be eligible for inclusion on the National Register as archaeological districts. Investigations since 1980 have recorded an additional 14 individual sites outside the central 10.4-km² (4-mi²) area that are considered eligible for inclusion on the National Register. The following major cultural resource investigations to date are broken out in the list that follows. Additional information can be found in the bibliography *of CCA Chapter 2*.

1977. The first survey of the area was conducted for SNL by Nielson of the Agency for Conservation Archaeology (ACA). This survey resulted in the location of 33 sites and 64 isolated artifacts.

1979. MacLennan and Schermer of ACA conducted another survey to determine access roads and a railroad right-of-way for Bechtel, Inc. The survey encountered two sites and 12 isolated artifacts.

1980. Schermer conducted another survey to relocate the sites originally recorded by Nielson. This survey redescribed 28 of the original 33 sites.

1981. Hicks (1981a, 1981b) directed the excavation of nine sites in the WIPP core area.

1982. Bradley (Lord and Reynolds 1985) recorded one site and four isolated artifacts in an archaeological survey for a proposed water pipeline.

1985. Lord and Reynolds (1985) examined three sites within the WIPP core area that consisted of two plant-collecting and processing sites and one base camp used between 1000 B.C. and A.D. 1400. The artifacts recovered from the excavations are in the Laboratory of Anthropology at the Museum of New Mexico in Santa Fe.

1987. Mariah Associates, Inc.; identified 40 sites and 75 isolates in an inventory of 2,460 ac in 15 quarter-section units surrounding the WIPP site. In this investigation, 19 of the sites were located within the WIPP site's boundary. Sites encountered in this investigation tended to lack evident or intact features. Of the 40 new sites defined, 14 were considered eligible for inclusion in the National Register, 24 were identified as having insufficient data to determine eligibility, and 2 were determined to be ineligible for inclusion. The eligible and potentially eligible sites have been mapped and are avoided by DOE in its current activities at the WIPP site.

1988–1992. Several archaeological clearance reports have been prepared for seismic testing lines on public lands in Eddy County, New Mexico.

All archaeological sites are surface or near-surface sites, and no reasons exist (either geological or archeological) to suspect that deep drilling would uncover or investigate archaeological sites.

No artifacts were encountered during cultural resource surveys performed from 1992 until present. The following list provides examples of WIPP projects that required cultural resource surveys. All investigations were performed and reported in accordance with requirements established by the New Mexico Office of Cultural Affairs (OCA) and administered by the SHPO.

- *SPDV site investigation into status of a previously recorded site (#LA 33175) to determine potential impacts from nearby reclamation activity. Assessment included minor surface excavation.*
- *WIPP well bore C-2737. Cultural resource investigation for well pad and access road.*
- *WIPP well bores WQSP 1-6 and 6a. Individual cultural resource investigations conducted for construction of each respective well pad and access road.*
- *WIPP well bores SNL 1, 2, 3, 9 and 12. Cultural resource investigations conducted for construction of each respective well pad and access road.*
- *WIPP well bore WTS 4. Cultural resource investigation conducted in support of siting and constructing reserve pits for well drilling and development.*

- *North Salt Pile Expansion. Cultural resource investigation conducted in support of the expansion of the North Salt Pile, a project designed to mitigate surface water infiltration.*

All of the aforementioned archeological investigations received determinations of “No Adverse Affect” from the OCA and the SHPO. This determination serves as a clearance to proceed with work.

The Delaware Basin has been used in the past for an isolated nuclear test. This test, Project Gnome, took place in 1961 at a location approximately 13 km (8 mi) southwest of the WIPP. The primary objective of Project Gnome was to study the effects of an underground nuclear explosion in salt. The Gnome experiment involved the detonation of a 3.1-kiloton nuclear device at a depth of 361 m (1,200 ft) in the bedded salt of the Salado (Rawson et al. 1965). The explosion created a cavity of approximately 28,000 m³ (1,000,000 ft³) and caused surface displacements over an area of about a 360-m (1,200-ft) radius. Fracturing and faulting caused measurable changes in rock permeability and porosity at distances up to approximately 100 m (330 ft) from the cavity. No earth tremors were reported at distances over 40 km (25 mi) from the explosion. Project Gnome was decommissioned in 1979.

2.4 Background Environmental Conditions

Background environmental conditions at and near the WIPP site were characterized prior to the initiation of the operation of the facility and are described in CCA Section 2.4. Because background characterization focuses on environmental conditions existing prior to operations, it is not meaningful to redefine background environmental conditions after operations began. Accordingly, information presented in CCA Section 2.4 is not repeated and updated in this recertification application.

~~One of the criteria established for the selection of a repository site was that the impacts on the ecology from constructions and operations be minimal. Consequently, as the DOE assessed the geological and hydrological characteristics of the site, they also assessed the ecological characteristics. The result was a demonstration, documented in the FEIS, that the ecological impacts are minimal and within acceptable bounds. The FEIS concluded that adverse impacts on the ecology were expected to be slight for the following reasons:~~

- ~~1. No natural areas proposed for protection are present on or near the site,~~
- ~~2. No endangered species of plants or animals are known to inhabit the site or the vicinity of the site; nor are any critical habitats known to exist on or near the site,~~
- ~~3. Water requirements for the site are low,~~
- ~~4. The land contains soil types and vegetation associations that are common throughout the region, and~~
- ~~5. Access in the form of dirt roads is already available throughout the area; therefore, recreational use of the area is not likely to increase significantly.~~

The results of the DOE's assessment of background environmental conditions are provided in this application as part of the complete description of the WIPP and its vicinity. Background environmental conditions form the baseline for determining if releases to the environment have occurred during the operational period or during any postoperational monitoring period (Wolfe et al. 1977). For this reason, the EPA considers these are important criteria for certification as stated in 40 CFR § 194.14(g). The DOE routinely collects environmental information at and around the WIPP site in accordance with the WIPP Environmental Monitoring Plan (see Appendix EMP). The EMP satisfies the criteria of 40 CFR § 194.14(g) in that it provides programmatic specifications for implementing and operating the WIPP environmental monitoring program. Appendix EMP includes a description of sampling locations, sampling frequencies, sample management practices, and where appropriate, analytical procedures. Specific field procedures are maintained at the WIPP site in a separate Environmental Monitoring Procedures Manual. Emphasis is placed on ecological conditions, water quality, and air quality and includes the following.

Ecological Conditions

- Vegetation
- Mammals
- Reptiles and amphibians
- Birds
- Arthropods
- Aquatic ecology
- Endangered species.

Quality of Environmental Media

- Surface water
- Groundwater
- Air.

2.4.1 Terrestrial and Aquatic Ecology

The vegetation, mammals, reptiles and amphibians, birds, arthropods, aquatic ecology, and endangered species of the WIPP site and its environs are characterized in the sections that follow. Much of the information in this section was reported in the FEIS (DOE 1980). Where this information has been updated with more recent data, this update is noted.

2.4.1.1—Vegetation

The WIPP site is in an area characterized by stabilized sand dunes. The vegetation is dominated by shinny oak, mesquite, sand sage, dune yucca, smallhead snakeweed, three-awn, and numerous species of forbs and perennial grasses. The dominant shrubs are deep-rooted species with extensive root systems. The shrubs not only stabilize the dune sand but serve as food, shelter, and nesting sites for many species of wildlife inhabiting the area.

The vegetation in the vicinity of the WIPP site is not a climax vegetation, at least in part because of past grazing management. The composition of the plant life at the site is heterogeneous because of variations in terrain and in the type and depth of soil. Shrubs are conspicuous members of all plant communities. The site lies within a region of transition between the northern extension of the Chihuahuan Desert (desert grassland) and the southern Great Plains (short grass prairie); it shares the floral characteristics of both.

Grazing, primarily by domestic livestock, and fire control are largely responsible for the shrub-dominated seral communities of much of southeastern New Mexico. A gradual retrogression from the tall- and mid-grass-dominated vegetation of 100 years ago has occurred throughout the region. The cessation of grazing would presumably not alter the domination by shrubs, but it would result in an increase in grasses. Experimental exclosures have been established to study site-specific patterns of succession in the absence of grazing, but long-term results are not yet available.

The semiarid climate makes water a limiting factor in the entire region. The amount and timing of rainfall greatly influence plant productivity and, therefore, the food supply for wildlife and livestock. The seeds of desert plants are often opportunistic: they may lie dormant through long periods of drought to germinate in the occasional year of favorable rainfall. Significant fluctuations in the abundance and distribution of plants and wildlife are typical of this region. Several examples of such fluctuations have been documented in the area within 8.3 km (5 mi) of the center of the WIPP site, which has been intensively studied.

Two introduced species of significance in the region are the Russian thistle, or tumbleweed, a common invader in disturbed areas, and the Tamarisk, or salt cedar, which has proliferated along drainage ways.

Several distinct biological zones occur on or near the site: the mesa, the central dunes complex, the creosote bush flats, the Livingston Ridge escarpment, and the Tobosa Flats in Nash Draw west of the ridge. A low, broad mesa named the Divide lies on the eastern edge of the study area and supports a typical desert grassland vegetation. The dominant shrub and subshrub are mesquite and snakeweed, respectively. The most abundant grasses are black grama, bush muhly, ring muhly, and fluffgrass. Cacti, especially varieties of prickly pear, are present.

Where the ground slopes down from the Divide to the central dune plains, the soil becomes deep and sandy. Shrubs like shinny oak, mesquite, sand sagebrush, snakeweed, and dune yucca are dominant. In some places, all of these species are present; in others, one or more are either missing or very low in density. These differences appear to be caused by localized variations in the type and depth of soil. Thus, a number of closely related but distinct plant associations form

1 a patchwork complex, or mosaic, across the stabilized dunes in the central area. Hummocky,
2 partially stabilized sand dunes occur, and large, active dunes are also present. The former consist
3 of islands of vegetation, primarily mesquite, separated by expanses of bare sand. The mesquite-
4 anchored soil is less susceptible to erosion, mainly by wind, than is the bare sand. The result is a
5 series of valley-like depressions, or blowouts, between vegetated hummocks. Active dunes
6 running east to west are found 16 km (10 mi) south and east of the site.

7 To the west and southwest, the soil changes again, becoming more dense and shallow (less than
8 2.5 cm [10 in.] to caliche) than in the dune area. The composition of the plant life is radically
9 altered, and creosote bushes become dominant. Toward Livingston Ridge to the west and
10 northwest, creosote bushes gradually give way to an acacia-dominated association at the top of
11 the escarpment. The western face of the ridge drops sharply to a valley floor (flats) that is
12 densely populated with tobosa grass, which is rare elsewhere in the study area.

13 2.4.1.2 Mammals

14 The most conspicuous wild mammals at the site are the black-tailed jack rabbit and the desert
15 cottontail. Common small mammals found at the WIPP site include the Ord's kangaroo rat, the
16 Plains pocket mouse, and the northern grasshopper mouse. Big game species, such as the mule
17 deer and the pronghorn antelope, and carnivores, such as the coyote, are present in small
18 numbers.

19 2.4.1.3 Reptiles and Amphibians

20 Commonly observed reptiles in the study area are the side-blotched lizard, the western box turtle,
21 the western whiptail lizard, and several species of snakes, including the bullsnake, the prairie
22 rattlesnake, the western diamondback rattlesnake, the coachwhip, the western hognose, and the
23 glossy snake. Of these, only the side-blotched lizard is found in all habitats. The others are
24 mainly restricted to one or two associations within the central dunes area, although the western
25 whiptail lizard and the western diamondback rattlesnake are found in areas dominated by
26 creosote bush as well. The yellow mud turtle is found only in the limited number of aquatic
27 habitats in the study area (that is, dirt stock ponds and metal stock tanks), but it is common in
28 these locales.

29 Amphibians are similarly restricted by the availability of aquatic habitat. Stock-watering ponds
30 and tanks may be frequented by tiger salamanders and occasional frogs and toads. Fish are
31 sometimes stocked in the ponds and tanks.

32 2.4.1.4 Birds

33 Numerous birds inhabit the area either as transients or year-long residents. Loggerhead shrikes,
34 pyrrhuloxias, and black-throated sparrows are examples of common residents. Migrating or
35 breeding waterfowl species do not frequently occur in the area. Some raptors (for example,
36 Harris hawks) are residents. The density of large avian predators' nests has been documented as
37 among the highest recorded in the scientific literature.

2.4.1.5—Arthropods

About 1,000 species of insects have been collected in the study area. Of special interest are subterranean termites. Vast colonies of these organisms are located across the study area; they are detritivores and play an important part in the recycling of nutrients in the study area.

2.4.1.6—Aquatic Ecology

Aquatic habitats within a 8 km (5 mi) radius of the WIPP site are limited. Stock watering ponds and tanks constitute the only permanent surface waters. Ephemeral surface water puddles form after heavy thunderstorms. At greater distances, seasonally wet, shallow lakes (playas) and permanent salt lakes are found.

Laguna Grande de la Sal is a large, permanent salt lake at the south end of Nash Draw. Natural brine springs, effluent brine from nearby potash refineries, and surface and subsurface runoff discharge into the lake. One of the natural brine springs at the northern margin of the lake has been found to support a small population of the Pecos River pupfish. This species is among the species recognized as threatened by the state of New Mexico. The spring, now called Surprise Spring, is about 18 km (11 mi) west-southwest of the WIPP site.

Several marine organisms are present in the Lower Pecos River and in the Red Bluff Reservoir. They include small, shelled protozoans (Foraminifera), a Gulf Coast shrimp, an estuarine oligochaete and a dragonfly, and several species of marine algae. These species have presumably been introduced. Salt-tolerant species of insects, oligochaetes, and nematodes and unusual algal assemblages characterize this stretch of the river. The combination of high salinity, elevated concentrations of heavy metals, and salt-tolerant and marine fauna makes the Lower Pecos River a unique system (DOE 1980, Section 7.1.3.).

2.4.1.7—Endangered Species

The DOE consulted with the U.S. Fish and Wildlife Service (FWS) in 1979 to determine the presence of threatened and endangered species at the WIPP site. At that time the FWS listed the Lee pincushion cactus, the black-footed ferret, the American peregrine falcon, the bald eagle, and the Pecos gambusia as threatened or endangered and as occurring or having the potential to occur on lands within or outlying the WIPP site. In 1989, the FWS advised the DOE that the list of species provided in 1979 is still valid, with the exception of the black-footed ferret. The DOE believes that the actions described in the 1990 *Final Supplement Environmental Impact Statement* (SEIS, in the bibliography) will have no impact on any threatened or endangered species because these activities do not involve any ground disturbance that was not already evaluated in the FEIS. In addition, there is no critical habitat for terrestrial species identified as endangered by either the FWS or the New Mexico Department of Game and Fish (NMDG&F) at the site area.

Also in 1989, the DOE consulted with the NMDG&F regarding the endangered species listed by the state in the vicinity of the WIPP site. The NMDG&F currently lists (based on NMDG&F Regulation 657, dated January 9, 1988) seven birds and one reptile that are in one of two endangerment categories and that occur or are likely to occur at the site. The NMDG&F agreed in 1989 that the proposed WIPP activities would probably not have appreciable impacts on

endangered species listed by the state in the area. *A Handbook of Rare and Endemic Plants of New Mexico*, published by the University of New Mexico (UNM) (UNM 1984), lists the plants in New Mexico classified as threatened, endangered, or sensitive, and includes 20 species, representing 14 families, that are found in Eddy County and could occur at or near the WIPP site.

2.4.2 Water Quality

In this section, the DOE presents a discussion of the quality of groundwater and surface water in the WIPP area.

2.4.2.1 Groundwater Quality

Based on the major solute compositions described in Siegel et al. (1991, Section 2.3.2.1), four hydrochemical facies are delineated for the Culebra, as shown in Figure 2-40:

Zone A. A sodium chloride brine (approximately 3.0 molar) with a magnesium/calcium (Mg/Ca) mole ratio between 1.2 and 2.0 exists here. This water is found in the eastern third of the WIPP site. The zone is roughly coincident with the region of low transmissivity described by LaVenue et al. (1988, 6-1). On the western side of the zone, halite in the Rustler has been found only in the unnamed lower member. In the eastern portion of the zone, halite has been observed throughout the Rustler.

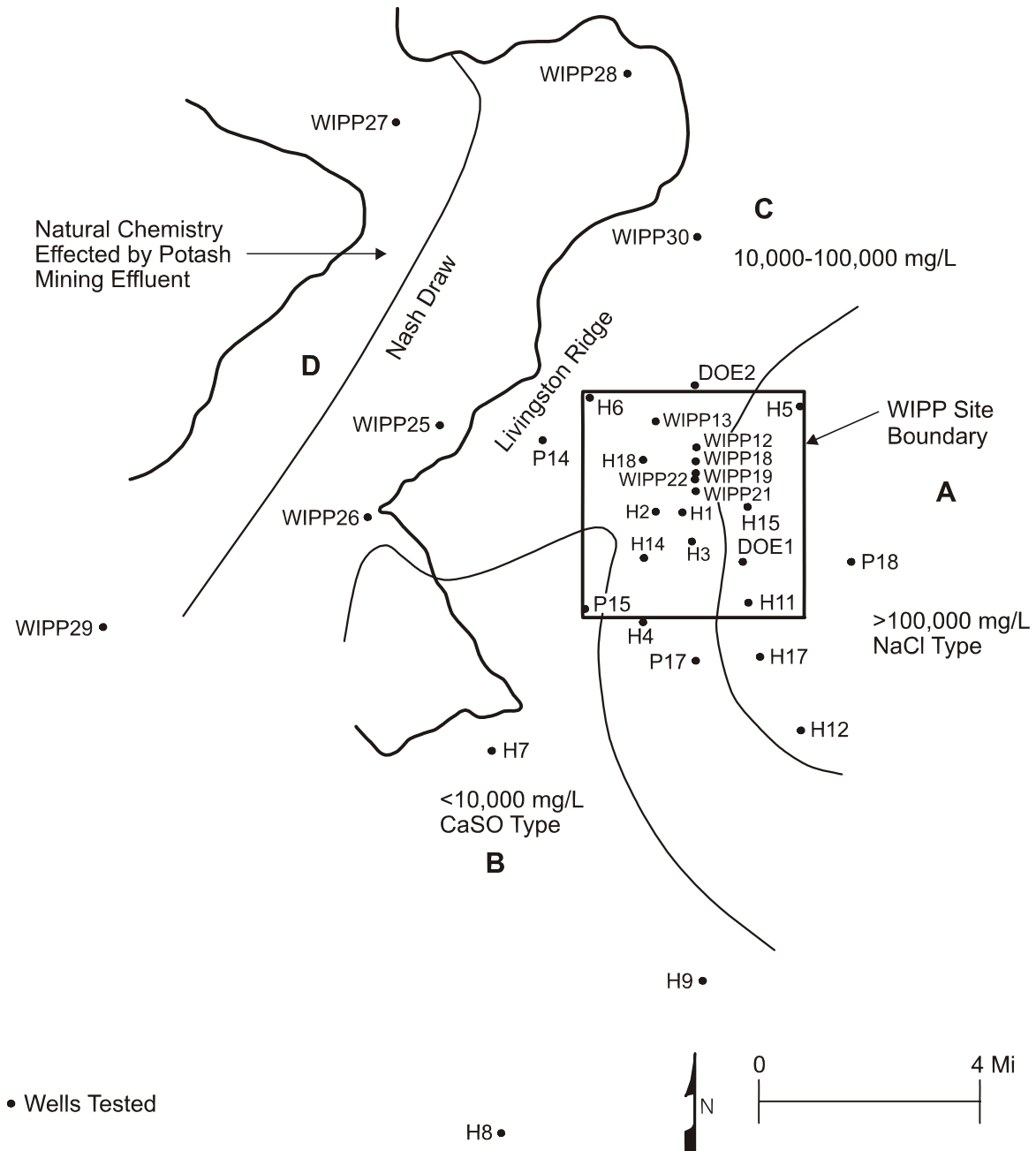
Zone B. A dilute anhydrite-rich water (ionic strength < 0.1 molar) occurs in the southern part of the site. The Mg/Ca mole ratios are uniformly low (0.0 to 0.5). This zone is coincident with a high-transmissivity region, and halite is not found in the Rustler in this zone.

Zone C. Waters of variable composition with low to moderate ionic strength (0.3 to 1.6 molar) occur in the western part of the WIPP site and along the eastern side of Nash Draw. Mg/Ca mole ratios range from 0.3 to 1.2. This zone is coincident with a region of variable transmissivity. In the eastern part of this zone, halite is present in the lower member of the Rustler. Halite is not observed in the formation on the western side of the zone. The most halite-rich water is found in the eastern edge of the zone, close to core locations where halite is observed in the Tamarisk Member.

Zone D. A fourth zone can be defined based on inferred contamination related to potash refining operations in the area. Waters from these wells have anomalously high solute concentrations (3 to 7 molar) and potassium/sodium (K/Na) weight ratios (0.2) compared to waters from other zones (K/Na = 0.01 to 0.09). In the extreme southwestern part of this zone, the composition of the Culebra well water has changed over the course of a seven-year monitoring period. The Mg/Ca mole ratio at WIPP-29 is anomalously high, ranging from 10 to 30 during the monitoring period (Siegel et al. 1991, Figure 2-19).

This zonation is consistent with that described by Ramey in 1985, who defined three zones. The fourth zone (D) was added by Siegel et al. in 1991 to account for the local potash contamination.

Together, the variations in solutes and the distribution of halite in the Rustler exhibit a mutual interdependence. Concentrations of solutes are lowest where Rustler halite is less abundant,



CCA-069-2

Figure 2-40. Hydrochemical Zones of the Culebra

consistent with the hypothesis that solutes in Rustler groundwaters are derived locally by dissolution of minerals (for example, halite, gypsum, and dolomite) in adjacent strata.

The TDS in the Magenta groundwater ranges in concentration from 3,240 to 222,000 milligrams per liter (Siegel et al. 1991, Table 4-6). This water is considered saline to briny. The transmissivity in areas of lower TDS concentrations is very low, thus greatly decreasing its usability, and the Magenta is not considered as a water supply. In general, the chemistry of

1 ~~Magenta water is variable. Groundwater types range from a predominantly sodium chloride type~~
2 ~~to a calcium magnesium sodium sulfate type chemistry. The water chemistry may indicate a~~
3 ~~general overall increase in TDS concentrations to the south and southwest, away from the WIPP~~
4 ~~site, and a potential change to a predominantly sodium chloride water in that area.~~

5 ~~In the WIPP area, the water quality of the Magenta is better than that of the Culebra. However,~~
6 ~~water from the Magenta is not used anywhere in the vicinity of the WIPP. The DOE has~~
7 ~~performed an analysis to determine whether there are underground source of drinking water~~
8 ~~(USDWs) in the vicinity of the WIPP. This analysis has resulted in a conclusion that there could~~
9 ~~be three USDWs as defined by 40 CFR Part 191 exist in the area, as given in Appendix USDW.~~
10 ~~The impact of the WIPP on USDWs is discussed in Chapter 8.0.~~

11 ~~2.4.2.2 — Surface Water Quality~~

12 ~~The Pecos River is the nearest permanent surface water source to the WIPP site. Natural brine~~
13 ~~springs, representing outfalls of the brine aquifers in the Rustler, feed the Pecos River at Malaga~~
14 ~~Bend, southwest of the site. This natural saline inflow adds approximately 370 tons of chloride~~
15 ~~per day to the Pecos River (Appendix GCR, 6-7). Return flow from irrigated areas above~~
16 ~~Malaga Bend further contributes to the salinity. The concentrations of potassium, mercury,~~
17 ~~nickel, silver, selenium, zinc, lead, manganese, cadmium, and barium also show significant~~
18 ~~elevations at Malaga Bend but tend to decrease downstream. The metals presumably are rapidly~~
19 ~~adsorbed onto the river sediments. Natural levels of certain heavy metals in the Pecos River~~
20 ~~below Malaga Bend exceed the water quality standards of the World Health Organization, the~~
21 ~~EPA, and the state of New Mexico. For example, the maximum level for lead is 50 parts per~~
22 ~~billion, and levels of up to 400 parts per billion have been measured in the Pecos River.~~

23 ~~As it flows into Texas south of Carlsbad, the Pecos River is a major source of dissolved salt in~~
24 ~~the west Texas portion of the Rio Grande Basin. Natural discharge of highly saline groundwater~~
25 ~~into the Pecos River in New Mexico keeps TDS levels in the water in and above the Red Bluff~~
26 ~~Reservoir very high. The TDS levels in this interval exceed 7,500 mg/L 50 percent of the time~~
27 ~~and, during low flows, can exceed 15,000 mg/L. Additional inflow from saline water bearing~~
28 ~~aquifers below the Red Bluff Reservoir, irrigation return flows, and runoff from oil fields~~
29 ~~continues to degrade water quality between the reservoir and northern Pecos County in Texas.~~
30 ~~Annual discharge weighted average TDS concentrations exceed 15,000 mg/L. Water use is~~
31 ~~varied in the southwest Texas portion of the Pecos River drainage basin. For the most part,~~
32 ~~water use is restricted to irrigation, mineral production and refining, and livestock. In many~~
33 ~~instances, surface water supplies are supplemented by groundwaters that are being depleted and~~
34 ~~are increasing in salinity.~~

35 ~~2.4.3 — Air Quality~~

36 ~~Measurements of selected air pollutants at the WIPP site began in 1976 and were reported by the~~
37 ~~DOE in the FEIS. Since the preparation of that document, a more extensive air quality~~
38 ~~monitoring program has been established. Seven classes of atmospheric gases regulated by the~~
39 ~~EPA have been monitored at the WIPP site between August 27, 1986, and October 30, 1994.~~
40 ~~These gases are carbon monoxide (CO), hydrogen sulfide (H₂S), ozone (O₃), nitrogen oxides~~
41 ~~(NO, NO₂, NO_x), and sulfur dioxide (SO₂). The total suspended particulates (TSPs) are~~

monitored in conjunction with the air monitoring programs of the WIPP. The results of the monitoring program are detailed in the annual reports for the WIPP Environmental Monitoring Program (see Appendix SER; Westinghouse 1991b, 1992, 1993, 1994, 1995 in the Bibliography).

2.4.4 Environmental Radioactivity

The background radiation conditions in the vicinity of the WIPP site are influenced by natural sources of radiation, fallout from nuclear tests, and one local research project (Project Gnome). Prior to the WIPP project, long term radiological monitoring programs were established in southeastern New Mexico to determine the widespread impacts of nuclear tests at the Nevada Test Site and to evaluate the effects of Project Gnome. As discussed in Section 2.3.2.3, Project Gnome resulted in the underground detonation of a nuclear device on December 10, 1961, at a site approximately 9 km (5.8 mi) southwest of the WIPP site.

The WIPP Radiological Baseline Program (RBP), which included the Radiological Environmental Surveillance Program, was initiated in July 1985 to describe background levels of radiation and radionuclides in the WIPP environment prior to the underground emplacement of radioactive waste. The RBP consisted of five subprograms: (1) atmospheric baseline; (2) ambient radiation (measuring gamma radiation); (3) terrestrial baseline (sampling soils); (4) hydrologic baseline (sampling surface water and bottom sediments and groundwater); and (5) biotic baseline (analyzing radiological parameters in key organisms along potential radionuclide migration pathways). The RBP has been succeeded by the Environmental Monitoring Plan (EMP). The final report on the RBP is included as Appendix RBP. This report summarizes the statistical approach used to analyze the RBP data. In addition, Appendix RBP discusses how values below detection limits are handled. The sampling locations for the RBP are the same as those reported on Figures 5-2 through 5-7 in Appendix EMP. This appendix discusses the statistical analyses used to support data.

2.4.4.1 Atmospheric Radiation Baseline

Historically, most gross alpha activity in airborne particulates has shown little variation and is within the range of from 1×10^{-15} to 3×10^{-15} microcuries per milliliter, which is equivalent to 3.7×10^{-11} to 11×10^{-11} becquerels per milliliter. Mean gross beta activity in airborne particulates fluctuates but is typically within the range of from 1×10^{-14} to 4×10^{-14} microcuries per milliliter (3.7×10^{-10} to 15×10^{-10} becquerels per milliliter). A peak of 3.5×10^{-13} microcuries per milliliter (1.2×10^{-8} becquerels per milliliter) in mean gross beta activity occurred in May 1986 and has been attributed to atmospheric fallout from the Chernobyl incident in the former Soviet Union. The average level of gamma radiation in the environment is approximately 7.5 microroentgens per hour, or approximately 66 millirem per year.

For 1995, the mean gross alpha concentrations show limited fluctuation throughout the year and range from 2.0×10^{-15} to 2.6×10^{-14} microcuries per milliliter (7.5×10^{-11} to 9.6×10^{-10} becquerels per milliliter). These fluctuations appeared to be consistent among all sampling locations. The mean gross beta concentrations fluctuate throughout the year within the range of 2.4×10^{-14} to 4.0×10^{-14} microcuries per milliliter (8.9×10^{-10} to 1.5×10^{-9} becquerels per

milliliter). Individual gross alpha and beta concentrations reported for each location are documented in Appendix SER.

2.4.4.2 Ambient Radiation Baseline

Using the average rate of 7.5 microroentgens per hour, the estimated annual dose is approximately 66 millirem. The fluctuations noted are primarily due to calibration of the system and meteorological events such as the high intensity thunderstorms that frequent this area in late summer. A seasonal rise in ambient radiation has been observed in the first and fourth quarters each year. It is speculated that this fluctuation may be due to variations in the emission and dispersion of radon-222 from the soil around the WIPP site. These variations can be caused by meteorological conditions, such as inversions, which would slow the dispersion of the radon and its progeny.

2.4.4.3 Terrestrial Baseline

Data were collected as part of the RBP at the WIPP in December 1985 and July 1987. Soil samples were collected and analyzed from a total of 37 locations within a 80-km (50-mi) radius of the WIPP (see Table 2-10). The soil samples were analyzed for 19 radionuclides: ^{40}K , ^{60}Co , ^{90}Sr , ^{137}Cs , two isotopes of radium, three isotopes of thorium, four isotopes of uranium, ^{237}Np , four isotopes of plutonium (^{239}Pu and ^{240}Pu were measured together), ^{241}Am , and ^{244}Cm . Four isotopes (^{40}K , ^{234}U , ^{235}U , and ^{238}U) exhibited significant differences among the three geographic groups, with samples from the outer sites having significantly higher levels of radioactivity than those from the 8-km (5-mi) ring sites (that is, 16 sampling sites in a ring around the WIPP with a 8-km [5-mi] radius). For ^{234}U , ^{235}U , and ^{238}U , the 8-km (5-mi) ring sites also showed higher levels than the WIPP sites. The isotopes ^{137}Cs , ^{226}Ra , ^{228}Th , and ^{230}Th exhibited differences between the outer sites and the other two groups, which were indistinguishable. Again, the outer sites had significantly higher levels of radioactivity than the other two groups. Measured mean values for ^{40}K , ^{137}Cs , ^{226}Ra , the three thorium isotopes, and the three uranium isotopes were above detection limits, as shown in Table 2-10. The mean values for ^{60}Co , ^{90}Sr , ^{228}Ra , ^{233}U , ^{237}Np , the plutonium isotopes, ^{241}Am , and ^{244}Cm fell below detection limits.

2.4.4.4 Hydrologic Radioactivity

The hydrologic radioactivity monitoring program is designed to establish characteristic radioactivity levels in surface water bodies, bottom sediments, and groundwater.

2.4.4.4.1 Surface Water and Sediment Background Radiation Levels

Samples of both surface water and groundwater were collected for the RBP. These samples were analyzed for 19 radionuclides (^3H , ^{40}K , ^{60}Co , ^{90}Sr , ^{137}Cs , two isotopes of radium, three isotopes of thorium, four isotopes of uranium, ^{237}Np , and four isotopes of plutonium [^{239}Pu and ^{240}Pu were measured together]). The resulting data from the sampling of surface water and groundwater were analyzed independently.

Table 2-10. Ranges of Mean Values Measured for Radioactive Isotopes In Soils at WIPP Site, 5 Miles from WIPP, and beyond 5 Miles from WIPP

Isotope	Range of Mean Values ^a	
	μCi/g	Bq/g
⁴⁰ K	4.9 to 9.3×10^{-6}	1.8 to 3.4×10^{-1}
⁶⁰ Co	-	0
⁹⁰ Sr	-	0
¹³⁷ Cs	1.3 to 2.2×10^{-7}	4.7 to 8.1×10^{-3}
²²⁶ Ra	2.6 to 5.4×10^{-7}	9.6 to 20×10^{-3}
²²⁸ Ra	-	b
²²⁸ Th	2.1 to 4.9×10^{-7}	7.8 to 18×10^{-3}
²³⁰ Th	2.5 to 52×10^{-7}	9.1 to 19×10^{-3}
²³² Th	3.0×10^{-7}	1.1×10^{-2}
²³³ U	-	b
²³⁴ U	1.5 to 3.3×10^{-7}	5.4 to 12×10^{-3}
²³⁵ U	4.4 to 17×10^{-9}	1.6 to 6.3×10^{-4}
²³⁸ U	1.6 to 3.0×10^{-7}	5.7 to 11×10^{-3}
²³⁷ Np	-	b
²³⁸ Pu	-	b
^{239/240} Pu	-	b
²⁴¹ Pu	-	b
²⁴¹ Am	-	b
²⁴⁴ Cm	-	b

Source: Appendix RBP, Table 4-1.

^a The ranges of mean values are expressed in terms of microcuries per gram of soil and becquerels per gram of soil.

^b Below minimum detection limit of 3.7×10^{-3} becquerels per gram.

2.4.4.4.1.1 Surface Water

Samples of surface water were collected from 12 locations over the course of the RBP. Sampling locations were divided into three groups for an initial analysis of geographic variability. Stock tanks represented the largest group, with five locations; they are located closest to WIPP. Stock tanks in this area are typically man-made earthen catchment basins with no surface outflow. The Pecos River represents the next major surface water group.

Four sampling locations were used along the Pecos River, from a northern (upriver) point near the town of Artesia to a southern (downriver) point near the town of Malaga, New Mexico. The third group, called Laguna Grande de la Sal, represents water from a series of playa lakes at the lower end of Nash Draw.

The sample mean radioactivity levels for most radionuclides were below their respective detection limits. Peak levels of ^{40}K from Laguna Grande de la Sal were 2.7×10^{-5} microcuries per gram (1.0 becquerels per gram), whereas the mean level at all other sampling locations was less than 2.7×10^{-7} microcuries per gram (0.01 becquerels per gram). All four isotopes of uranium exhibited significant differences among the three geographic groups. For all four isotopes, radionuclide levels in the tanks were at least one order of magnitude lower than levels found in the Pecos River and Laguna Grande de la Sal. Similar to ^{40}K , levels of uranium were highest in Laguna Grande de la Sal. Only ^{60}Co , ^{137}Cs , ^{228}Ra , ^{234}U , and ^{238}U were found to be above detection limits. (See Table 5-1 Appendix RBP for details.)

2.4.4.4.1.2 Sediments

Sediments were collected for the WIPP RBP from six locations: Hill Tank, Indian Tank, Noye Tank, Laguna Grande de la Sal, and two sites along the Pecos River. These samples were analyzed for 18 radionuclides (tritium was not analyzed in the sediments).

In all five cases where differences were found among location groups, the stock tanks had higher concentrations of radionuclides, possibly indicating an accumulation effect from the closed nature of the tanks. Laguna Grande de la Sal sediments contained significantly higher concentrations of ^{234}U than did the stock tanks and the Pecos River, which were indistinguishable.

2.4.4.4.2 Groundwater Radiological Characterization

Groundwater samples were collected from 37 wells: 23 completed by the DOE in the Culebra, four completed by the DOE in the Magenta, and 10 privately owned in various units. The samples were analyzed for the same 19 radionuclides as the surface water samples. Elevated levels of ^{40}K were found in the Magenta and private wells, and in the Culebra (2.0×10^{-7} to 5.4×10^{-7} microcuries per gram, or 7.3×10^{-3} to 20×10^{-3} becquerels per gram, respectively). The increased levels of ^{40}K can be attributed to the generally high levels of dissolved solids in groundwater in these formations. Only ^{60}Co , ^{137}Cs , ^{234}U , ^{238}U , and ^{226}Ra , which were found to have a distinct geographic pattern in the Culebra, were found above detection limits, as shown in Table 2-11. Means from individual wells show that levels of ^{226}Ra increase in concentration from west to east. Means of radionuclide concentrations from wells around the WIPP site are shown in Table 2-11.

Groundwater samples were collected in accordance with the EMP (Appendix EMP) and the Groundwater Monitoring Plan (Appendix GWMP) (Westinghouse 1991a). The primary objective of the WQSP is to obtain representative and repeatable groundwater quality data from selected wells under rigorous field and laboratory procedures and protocols. At each well site, the well is pumped and the groundwater serially analyzed for specific field parameters. Once the field parameters have stabilized, denoting a chemical steady state with respect to these parameters, a final groundwater sample is collected for analysis of radionuclides.

Table 2-11. Mean Values Measured for Radionuclides in Water Wells around the WIPP Site

Isotope	Mean Value (10^{-4} becquerels per gram)*
^3H	Below <MDL (56)
^{40}K	73 to 200
^{60}Co	12
^{90}Sr	<MDL (7.4)
^{137}Cs	7.2
^{226}Ra	6.9 to 52
^{228}Ra	9.6
^{228}Th	<MDL (3.7)
^{230}Th	<MDL (0.37)
^{232}Th	<MDL (0.37)
^{233}U	<MDL (0.37)
^{234}U	2.6
^{235}U	<MDL (N/S)
^{238}U	0.72
^{237}Np	<MDL (0.37)
^{238}Pu	<MDL (0.11)
$^{239/240}\text{Pu}$	<MDL (0.74)
^{241}Pu	<MDL (37)

Source: Appendix RBP, Table 5-4

* Units are becquerels per gram of sample.

Legend:

<MDL — Less than the minimum detection level (MDL is shown in parentheses)

N/S — MDL not specified

2.4.4.5 Biotic Baseline

This subprogram characterizes background radioactivity levels in key organisms along possible food chain pathways to man. Vegetation, rabbits, quail, beef, and fish are sampled, and palatable tissues are analyzed for concentrations of transuranics and common naturally occurring radionuclides. Because of the small sample sizes in this program, no attempt has been made to interpret these data. The results are presented in Appendix RBP, Section 7.

2.5 Climate and Meteorological Conditions

The DOE did not consider climate directly in its site selection process, although criteria such as low population density and large tracts of federally owned land tend to favor arid and semi-arid areas in the western United States. The semi-arid climate around the WIPP is beneficial since it is a direct cause of the lack of a near surface water table and the minimization of radiation exposure pathways that involve surface or groundwater. Data used to interpret paleoclimates in

the American southwest come from a variety of sources and indicate alternating arid and subarid to subhumid climates throughout the Pleistocene. The information in this section was taken from Swift (1992), and included in this application as CCA Appendix CLI and references therein.

2.5.1 *Historic Climatic Conditions*

Prior to 18,000 years ago, radiometric dates are relatively scarce, and the record is incomplete. From 18,000 years ago to the present, however, the climatic record is relatively well constrained by floral, faunal, and lacustrine data. These data span the transition from the last full-glacial maximum to the present interglacial period; given the global consistency of glacial fluctuations described below, they can be taken to be broadly representative of extremes for the entire Pleistocene.

Early and middle Pleistocene paleoclimatic data for the southwestern United States are incomplete and permit neither continuous reconstructions of paleoclimates nor direct correlations between climate and glaciation prior to the last glacial maximum, which occurred 22,000 to 18,000 years ago. Stratigraphic and soil data from several locations, however, indicate that cyclical alternation of wetter and drier climates in the Southwest had begun by the Early Pleistocene. Fluvial gravels in the Gatuña exposed in the Pecos River Valley of eastern New Mexico suggest wetter conditions 1.4 million years ago and again 600,000 years ago. The Mescalero caliche, exposed locally over much of southeastern New Mexico, suggests drier conditions 510,000 years ago, and loosely dated spring deposits in Nash Draw west of the WIPP imply wetter conditions occurring again later in the Pleistocene. The Blackwater Draw Formation of the southern High Plains of eastern New Mexico and western Texas, correlating in time to both the Gatuña Formation and the Mescalero caliche, contains alternating soil and eolian sand horizons that show at least six climatic cycles beginning more than 1.4 million years ago and continuing to the present.

Data used to construct the more detailed climatic record for the latest Pleistocene and Holocene come from six independent lines of evidence dated using carbon-14 techniques: plant communities preserved in packrat middens throughout the Southwest, including sites in Eddy and Otero counties, New Mexico; pollen assemblages from lacustrine deposits in western New Mexico and other locations in the Southwest; gastropod assemblages from western Texas; ostracod assemblages from western New Mexico; paleolake levels throughout the Southwest; and faunal remains from caves in southern New Mexico.

Prior to the last glacial maximum 22,000 to 18,000 years ago, evidence from faunal assemblages in caves in southern New Mexico, including the presence of species such as the desert tortoise that are now restricted to warmer climates, suggests hot summers and mild, dry winters. Lacustrine evidence confirms the interpretation of a relatively dry climate prior to and during the glacial advance. Permanent water did not appear in what was later to become a major lake in the Estancia Valley in central New Mexico until some time before 24,000 years ago, and water depths in lakes at higher elevations in the San Agustin Plains in western New Mexico did not reach a maximum until sometime between 22,000 and 19,000 years ago. Ample floral and lacustrine evidence documents cooler, wetter conditions in the southwest during the glacial peak. These changes were not caused by the immediate proximity of glacial ice. None of the Pleistocene continental glaciations advanced farther southwest than northeastern Kansas, and the

most recent, late-Wisconsinan ice sheet reached its limit in South Dakota, approximately 1,200 km (750 mi) from WIPP. Discontinuous alpine glaciers formed at the highest elevations throughout the Rocky Mountains, but these isolated ice masses were symptoms, rather than causes, of cooler and wetter conditions and had little influence on regional climate at lower elevations. The closest such glacier to WIPP was on the northeast face of Sierra Blanca Peak in the Sacramento Mountains, approximately 220 km (135 mi) to the northwest.

Global climate models indicate that the dominant glacial effect in the Southwest was the disruption and southward displacement of the westerly jet stream by the physical mass of the ice sheet to the north. At the glacial peak, major Pacific storm systems followed the jet stream across New Mexico and the southern Rocky Mountains, and winters were wetter and longer than either at the present or during the previous interglacial period.

Gastropod assemblages at Lubbock Lake in western Texas suggest mean annual temperatures 5 degrees-Celsius (9° F) below present values. Both floral and faunal evidence indicate that annual precipitation throughout the region was 1.6 to 2.0 times greater than today's values. Floral evidence also suggests that winters may have continued to be relatively mild, perhaps because the glacial mass blocked the southward movement of arctic air. Summers at the glacial maximum were cooler and drier than at present, without a strongly developed monsoon.

The jet stream shifted northward following the gradual retreat of the ice sheet after 18,000 years ago, and the climate responded accordingly. By approximately 11,000 years ago, conditions were significantly warmer and drier than previously, although still dominated by winter storms and still wetter than today. Major decreases in total precipitation and the shift toward the modern monsoonal climate did not occur until the ice sheet had retreated into northeastern Canada in the early Holocene.

By middle Holocene time, the climate was similar to that of the present, with hot, monsoon-dominated summers and cold, dry winters. The pattern has persisted to the present, but not without significant local variations. Soil studies show that the southern High Plains were drier from 6,500 to 4,500 years ago than before or since. Gastropod data from Lubbock Lake indicate the driest conditions from 7,000 to 5,000 years ago (precipitation, 0.89 times present values; mean annual temperature, 2.5° degrees-Celsius [4.5° F] higher than present values), with a cooler and wetter period 1,000 years ago (precipitation, 1.45 times present values; mean annual temperature, 2.5° degrees-Celsius [4.5° F] lower than present). Plant assemblages from southwestern Arizona suggest steadily decreasing precipitation from the middle Holocene to the present, except for a brief wet period approximately 990 years ago. Stratigraphic work at Lake Cochise (the present Willcox playa in southeast Arizona) shows two mid-Holocene lake stands, one near or before 5,400 years ago and one between or before 3,000 to 4,000 years ago; however, both were relatively short-lived, and neither reached the maximum depths of the Late Pleistocene high stand that existed before 14,000 years ago.

Inferred historical precipitation indicates that during the Holocene, wet periods were relatively drier and shorter in duration than those of the late Pleistocene. Historical records over the last several hundred years indicate numerous lower-intensity climatic fluctuations, some too short in duration to affect floral and faunal circulation. Sunspot cycles and the related change in the amount of energy emitted by the sun have been linked to historical climatic changes elsewhere in

1 the world, but the validity of the correlation is uncertain. Correlations have also been proposed
2 between volcanic activity and climatic change. In general, however, causes for past short-term
3 changes are unknown.

4 The climatic record presented here should be interpreted with caution because its resolution and
5 accuracy are limited by the nature of the data used to construct it. Floral and faunal assemblages
6 change gradually and show only a limited response to climatic fluctuations that occur at
7 frequencies that are higher than the typical life span of the organisms in question. For long-lived
8 species such as trees, resolution may be limited to hundreds or even thousands of years.
9 Sedimentation in lakes and playas has the potential to record higher-frequency fluctuations,
10 including single-storm events, but only under a limited range of circumstances. Once water
11 levels reach a spill point, for example, lakes show only a limited response to further increases in
12 precipitation.

13 With these observations in mind, three significant conclusions can be drawn from the climatic
14 record of the American southwest. First, maximum precipitation in the past coincided with the
15 maximum advance of the North American ice sheet. Minimum precipitation occurred after the
16 ice sheet had retreated to its present limits. Second, past maximum long-term average
17 precipitation levels were roughly twice the present levels. Minimum levels may have been
18 90 percent of the present levels. Third, short-term fluctuations in precipitation have occurred
19 during the present relatively dry, interglacial period, but they have not exceeded the upper limits
20 of the glacial maximum.

21 Too little is known about the relatively short-term behavior of global circulation patterns to
22 accurately predict precipitation levels over the next 10,000 years. The long-term stability of
23 patterns of glaciation and deglaciation, however, do permit the conclusion that future climatic
24 extremes are unlikely to exceed those of the late Pleistocene. Furthermore, the periodicity of
25 glacial events suggests that a return to full-glacial conditions is highly unlikely within the next
26 10,000 years.

27 **2.5.2 Recent Climatic Conditions**

28 Recent climatic conditions are provided to allow for the assessment of impacts of these factors
29 on the disposal unit and the site. Data are taken from the WIPP environmental monitoring
30 reports (see Westinghouse *WEC* 1991a, 1991b, 1992, 1993, 1994, 1995, 1996, 1997, 1998;
31 *WGESC 1999; ESRF 2000, 2001, 2002; and WRES 2003* in the Bibliography).

32 **2.5.2.1 General Climatic Conditions**

33 The climate of the region is semiarid, with generally mild temperatures, low precipitation and
34 humidity, and a high evaporation rate. Winds are mostly from the southeast and moderate. In
35 late winter and spring, there are strong west winds and dust storms. During the winter, the
36 weather is often dominated by a high-pressure system situated in the central portion of the
37 western United States and a low-pressure system located in north-central Mexico. During the
38 summer, the region is affected by a low-pressure system normally situated over Arizona.

2.5.2.2 Temperature Summary

Temperatures are moderate throughout the year, although seasonal changes are distinct. The mean annual temperature in southeastern New Mexico is 63° degrees Fahrenheit (17° C). In the winter (December through February), nighttime lows average near 23° degrees Fahrenheit (-5° C), and maxima average in the 50s. The lowest recorded temperature at the nearest Class-A weather station in Roswell was -29° degrees Fahrenheit (-34° C) in February 1905. In the summer (June through August), the daytime temperature exceeds 90°F (32° C) approximately 75 percent of the time. The National Weather Service recently documented 122° degrees Fahrenheit (50° C) at the WIPP site as the record high temperature for New Mexico. This temperature was recorded on June 27, 1994. Table 2-12 shows the annual average, maximum, and minimum temperatures from 1990 through 1994. Temperature data for 1995 are summarized in Appendix SER.

Table 2-12. Annual Average, Maximum, and Minimum Temperatures

Year	Annual Average Temperature		Maximum Temperature		Minimum Temperature	
	(°C)	(°F)	(°C)	(°F)	(°C)	(°F)
1990	17.8	64	46.1	115	-13.9	7
1991	17.2	63	42.8	109	-7.8	18
1992	17.2	63	42.8	109	-10	14
1993	17.8	64	42.8	109	-18.9	-2
1994	17.8	64	50	122	-14.4	6
Average	17.6	63.6	44.9	112.8	-13	8.6

Source: WIPP Annual Site Environmental Report for Calendar Years 1990 through 1994.

2.5.2.3 Precipitation Summary

Precipitation is light and unevenly distributed throughout the year, averaging 28.2 33 cm (11.1 13-in.) per year for the past five years from 1995 through 2002. Winter is the season of least precipitation, averaging less than 1.5 cm (0.6 in.) of rainfall per month. Snow averages about 13 cm (5 in.) per year at the site and seldom remains on the ground for more than a day. Approximately half the annual precipitation comes from frequent thunderstorms in June through September. Rains are usually brief but occasionally intense when moisture from the Gulf of Mexico spreads over the region. Monthly average, maximum, and minimum precipitations recorded at the WIPP site from 1990 through 1994 are summarized 2002 are summarized in Figure 2-48. 2-41. Precipitation data for 1995 are summarized in Appendix SER.

2.5.2.4 Wind Speed and Wind Direction Summary

The frequencies of wind speeds and directions are depicted by wind roses wind roses in in Figures 2-42 through 2-45 Figures 2-49 through 2-56 for the WIPP site and Figure 2-46 for Carlsbad, New Mexico.

1

Table 2-14. Annual Average, Maximum, and Minimum Temperatures

<i>Year</i>	<i>Annual Average Temperature</i>		<i>Maximum Temperature</i>		<i>Minimum Temperature</i>	
	<i>(°C)</i>	<i>(°F)</i>	<i>(°C)</i>	<i>(°F)</i>	<i>(°C)</i>	<i>(°F)</i>
<i>1990</i>	<i>17.8</i>	<i>64</i>	<i>46.1</i>	<i>115</i>	<i>-13.9</i>	<i>7</i>
<i>1991</i>	<i>17.2</i>	<i>63</i>	<i>42.8</i>	<i>109</i>	<i>-7.8</i>	<i>18</i>
<i>1992</i>	<i>17.2</i>	<i>63</i>	<i>42.8</i>	<i>109</i>	<i>-10</i>	<i>14</i>
<i>1993</i>	<i>17.8</i>	<i>64</i>	<i>42.8</i>	<i>109</i>	<i>-18.9</i>	<i>-2</i>
<i>1994</i>	<i>17.8</i>	<i>64</i>	<i>50</i>	<i>122</i>	<i>-14.4</i>	<i>6</i>
<i>1995</i>	<i>17</i>	<i>63</i>	<i>42</i>	<i>107</i>	<i>-7</i>	<i>19</i>
<i>1996</i>	<i>17</i>	<i>63</i>	<i>41</i>	<i>106</i>	<i>-7</i>	<i>19</i>
<i>1997</i>	<i>16.3</i>	<i>61.4</i>	<i>38.6</i>	<i>101.5</i>	<i>-11.4</i>	<i>11.4</i>
<i>1998</i>	<i>18.3</i>	<i>64.9</i>	<i>41.6</i>	<i>106.9</i>	<i>-10.8</i>	<i>12.6</i>
<i>1999</i>	<i>18.1</i>	<i>64.6</i>	<i>40.9</i>	<i>105.6</i>	<i>-7.9</i>	<i>17.8</i>
<i>2000</i>	<i>17.4</i>	<i>63.3</i>	<i>40.2</i>	<i>104.4</i>	<i>-6.8</i>	<i>19.7</i>
<i>2001</i>	<i>17.5</i>	<i>63.5</i>	<i>39.5</i>	<i>103.2</i>	<i>-7.8</i>	<i>18.0</i>
<i>2002</i>	<i>17.5</i>	<i>63.5</i>	<i>39.8</i>	<i>103.7</i>	<i>-8.9</i>	<i>16.0</i>
<i>Average</i>	<i>17.5</i>	<i>63.5</i>	<i>42.2</i>	<i>107.9</i>	<i>-0.2</i>	<i>13.9</i>

2 In general, the predominant wind direction in Carlsbad are from the south, southeast, and west.
3 Wind data for 1995 are summarized in Appendix SER.

4 **2.6 Seismology**

5 The DOE used tectonic activity as a siting criterion. The intent was to avoid tectonic conditions
6 such as faulting and igneous activity that would jeopardize waste isolation over the long term
7 and to avoid areas where earthquake size and frequency could impact facility design and
8 operations. The WIPP site met both aspects of this criterion fully. Long-term tectonic activity is
9 discussed in Section 2.1.5. The favorable results of the seismic (earthquake) studies are
10 discussed here. The purpose of the seismic studies is to build a basis from which to predict
11 ground motions that the WIPP repository may be subjected to in the near and distant future. The
12 concern about seismic effects in the near future, during the operational period, pertains mainly to
13 the design requirements for surface and underground structures for providing containment during
14 seismic events. The concern about effects occurring over the long term, after the repository has
15 been decommissioned and sealed, pertains more to relative motions (faulting) within the
16 repository and possible effects of faulting on the integrity of the salt beds and/or shaft seals.
17 *Updated seismic activity information is provided in Figures 2-57 and 2-58.* In this discussion,
18 the magnitudes are reported in terms of the Richter scale, and all intensities are based on the

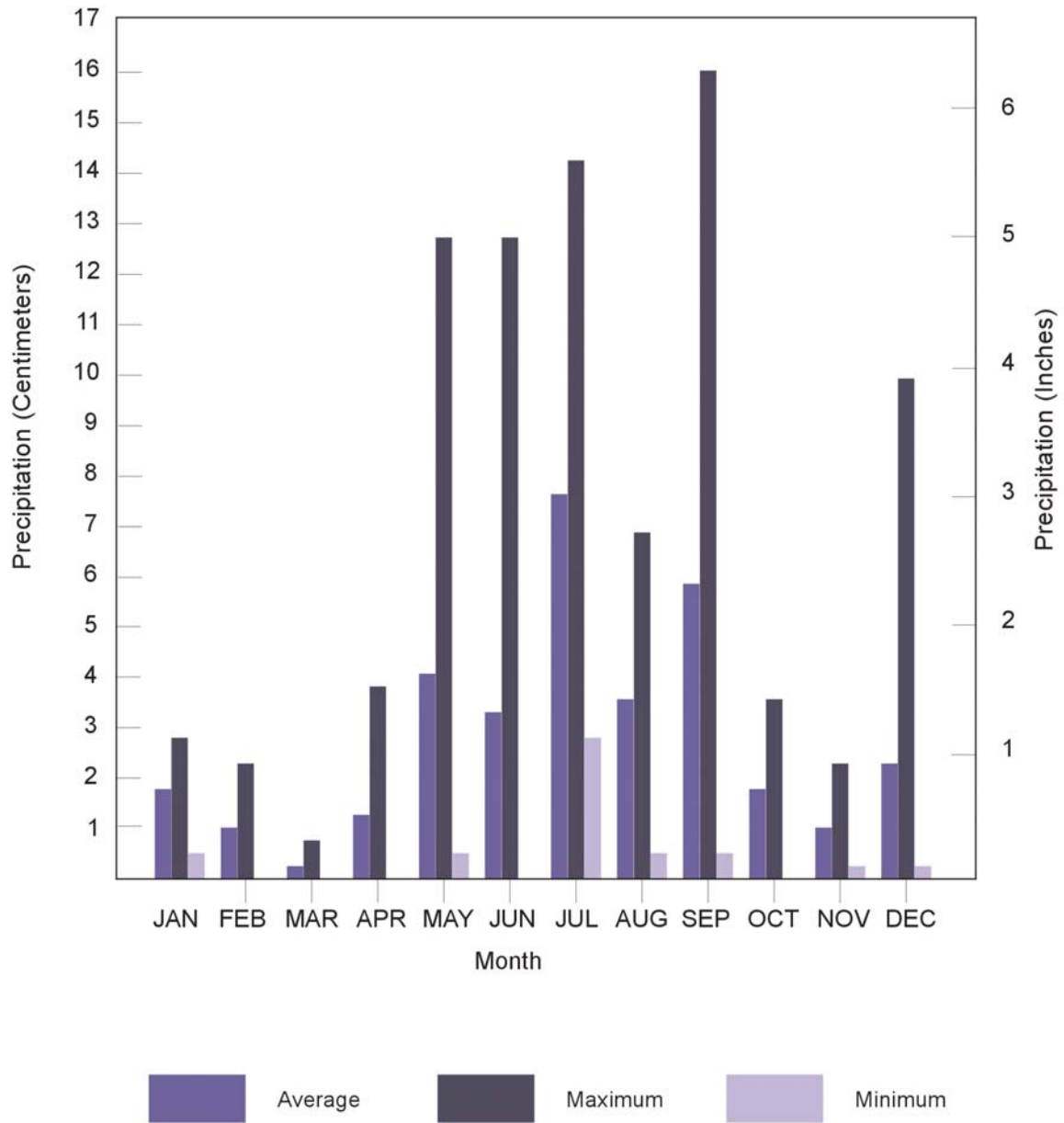


Figure 2-41. Monthly Precipitation for the WIPP Site from 1990 through 1994

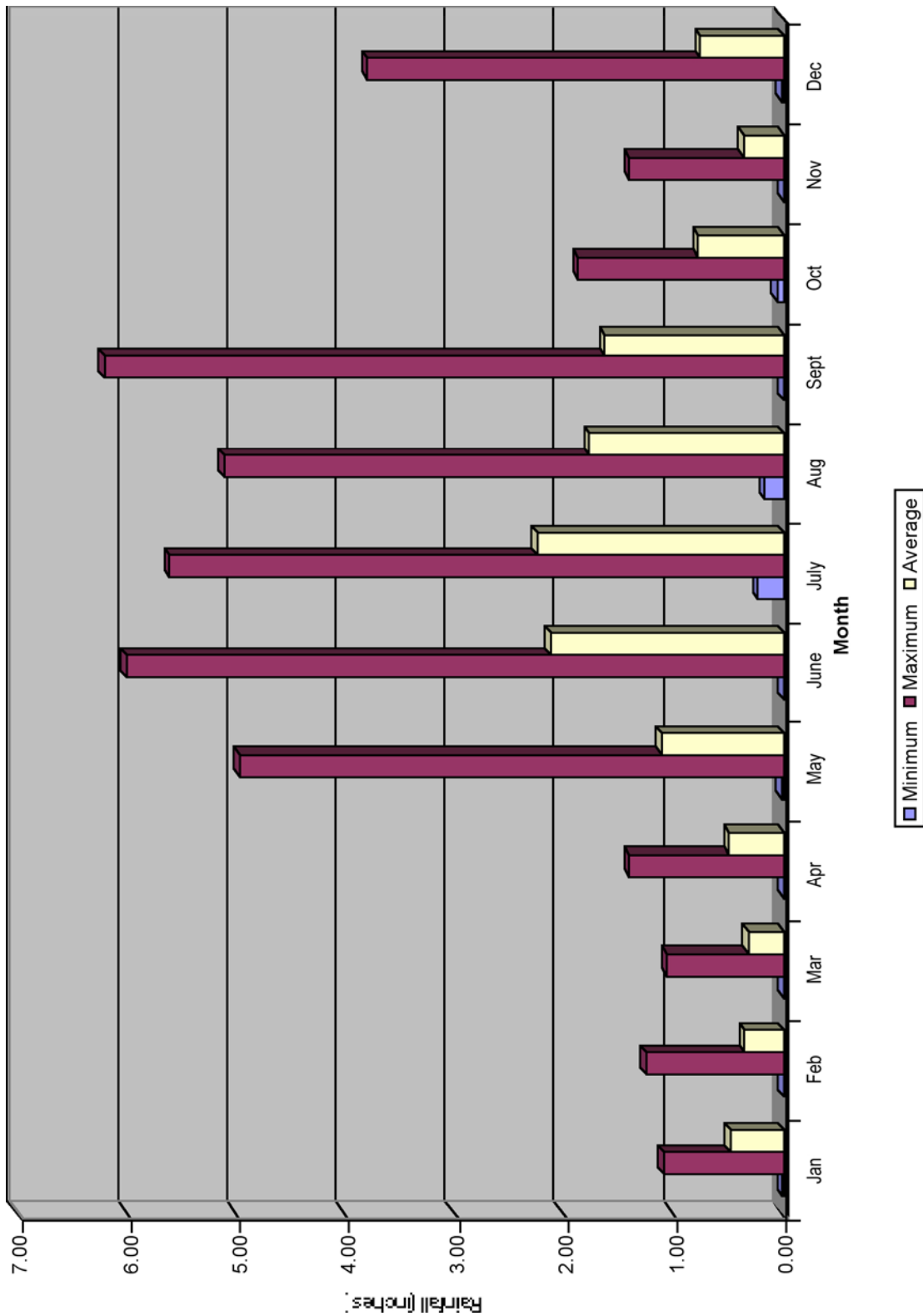
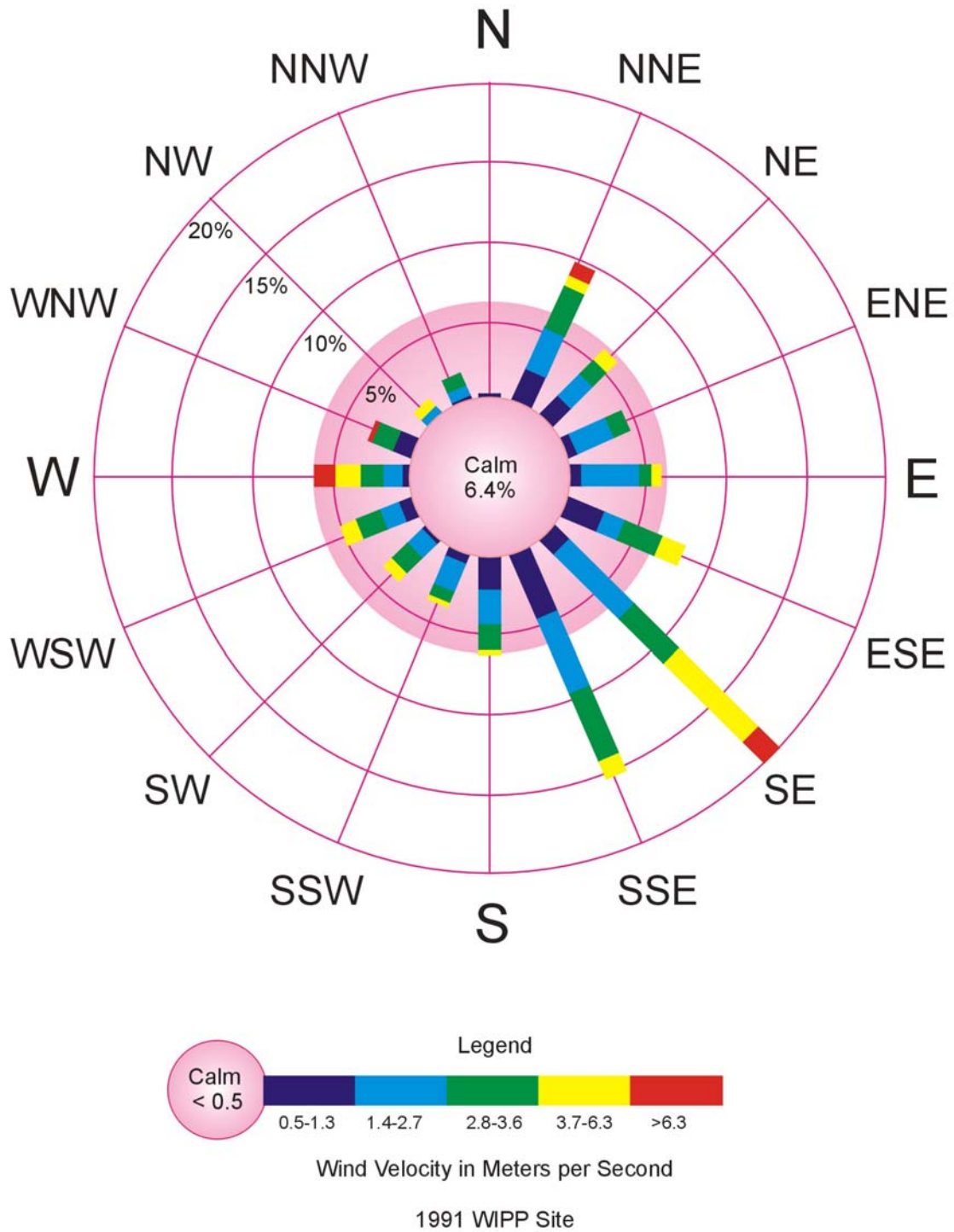


Figure 2-48. Monthly Precipitation for the WIPP Site from 1990-2002.

1
2
3

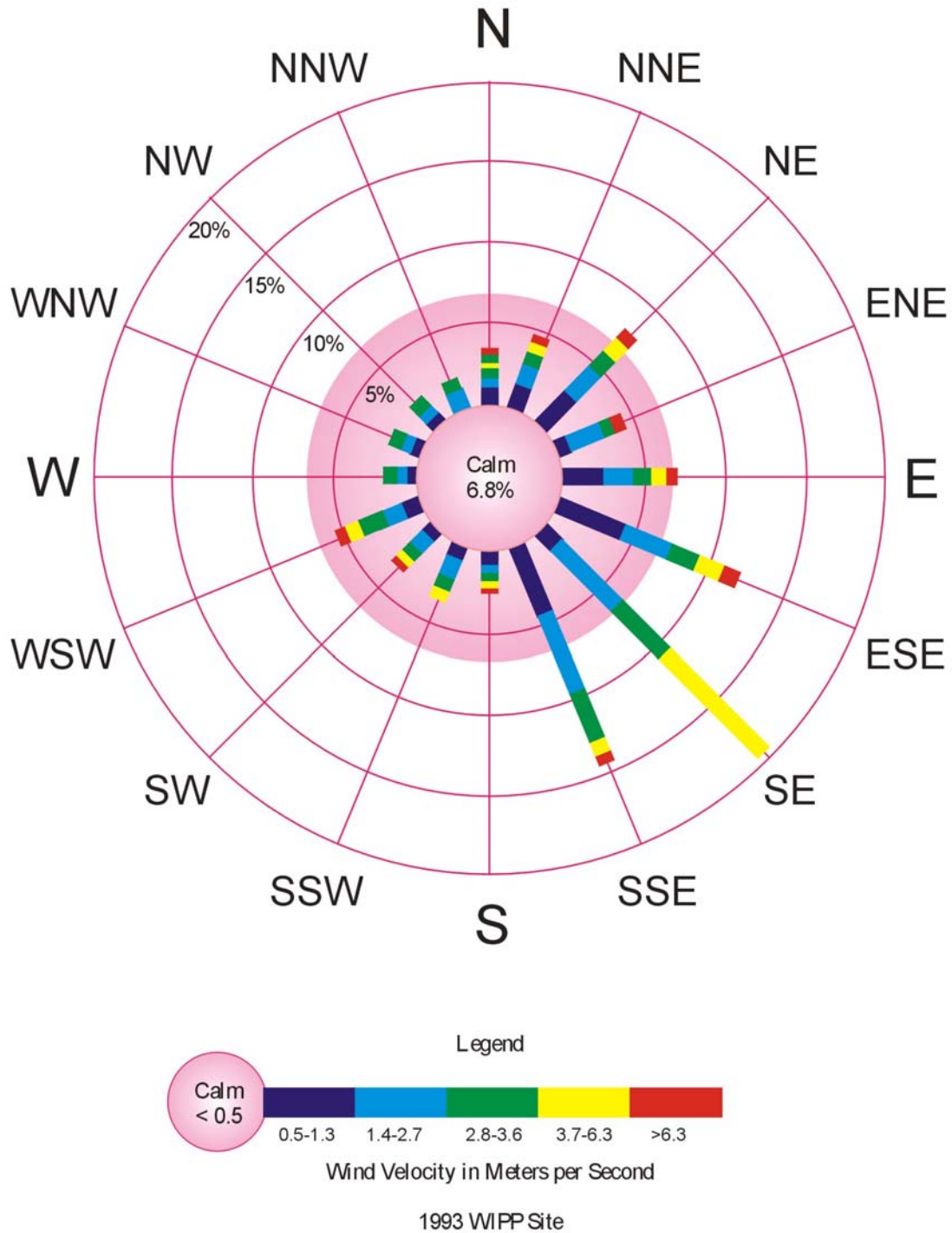


CCA-055-2

Figure 2-42. 1991 Annual Windrose—WIPP Site

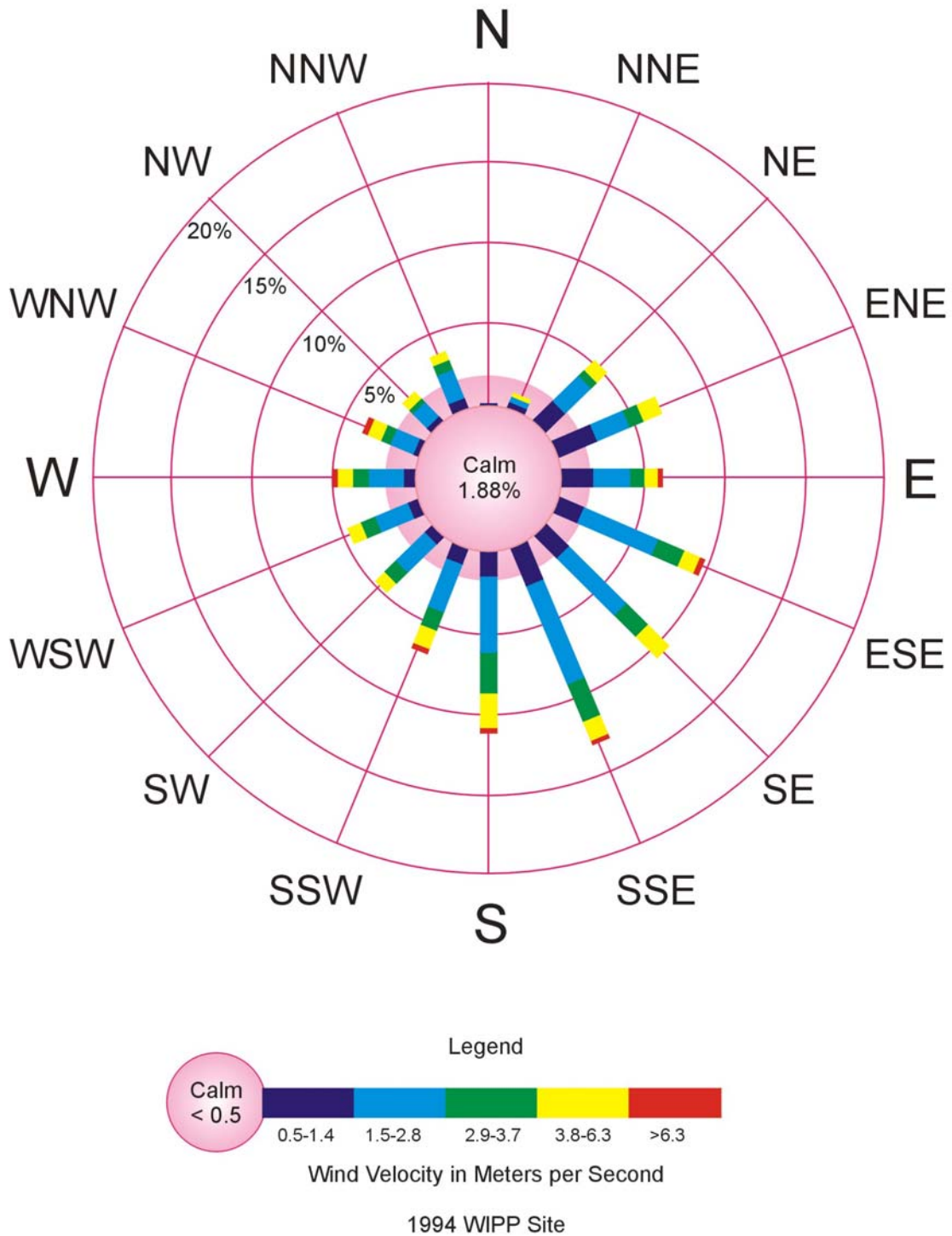


DOE/WIPP 2004-3231



CCA-057-2

Figure 2-44. 1993 Annual Windrose—WIPP Site



CCA-058-2

Figure 2-45. 1994 Annual Windrose—WIPP Site

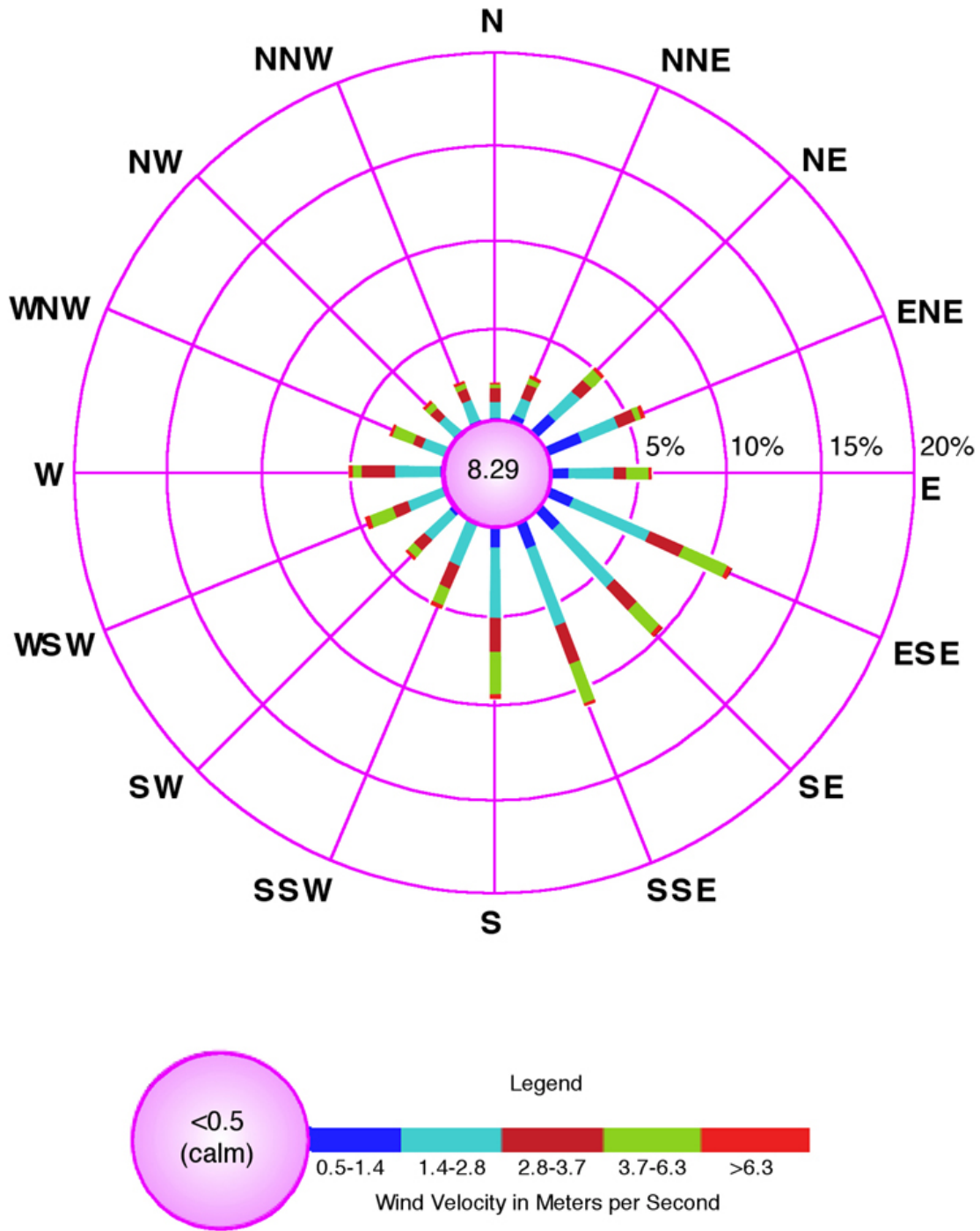


Figure 2-49. 1995 Annual Wind Rose at 10-m (33-ft.) Height at WIPP Site

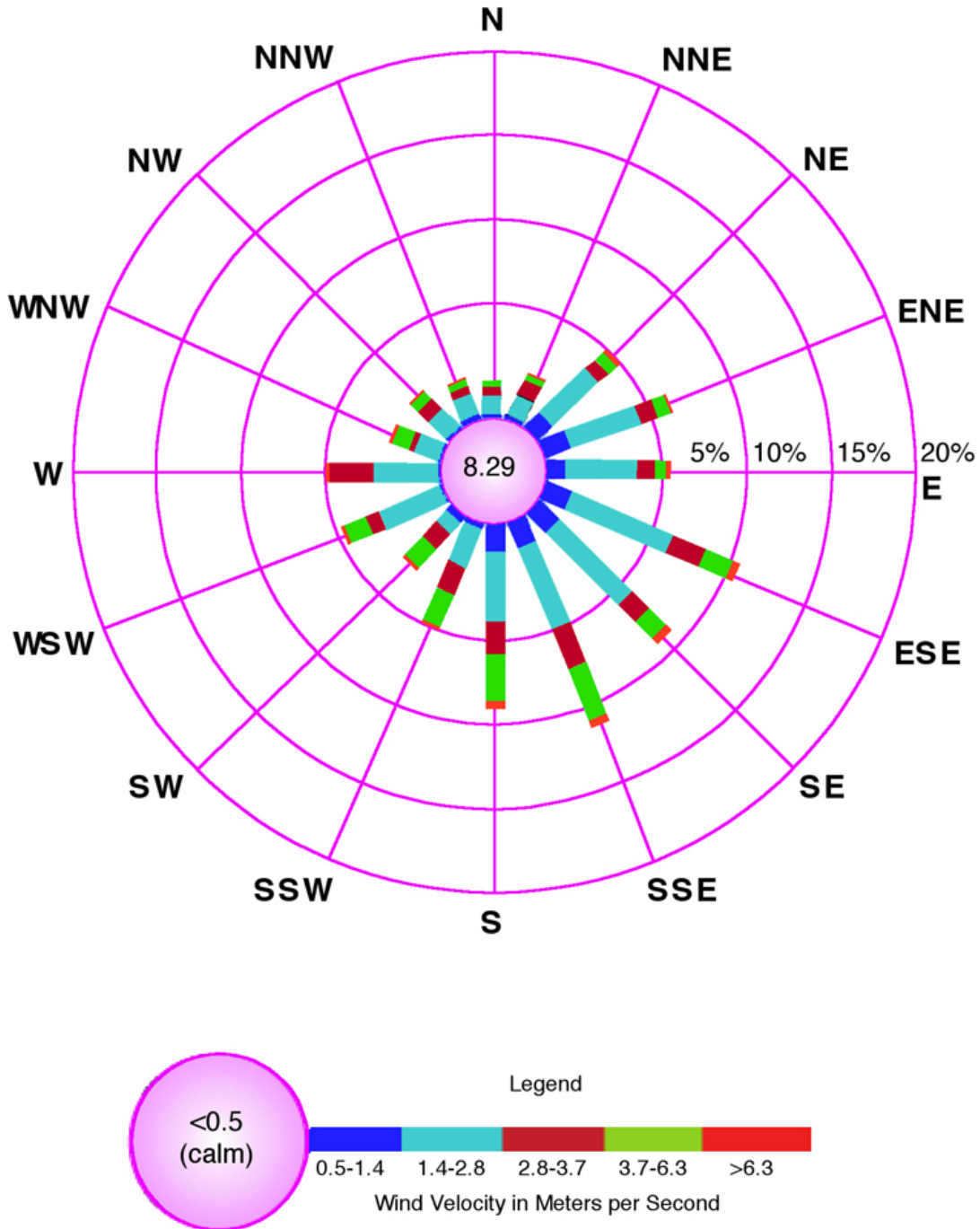


Figure 2-50. 1996 Annual Wind Rose at 10-m (33-ft.) Height at WIPP Site

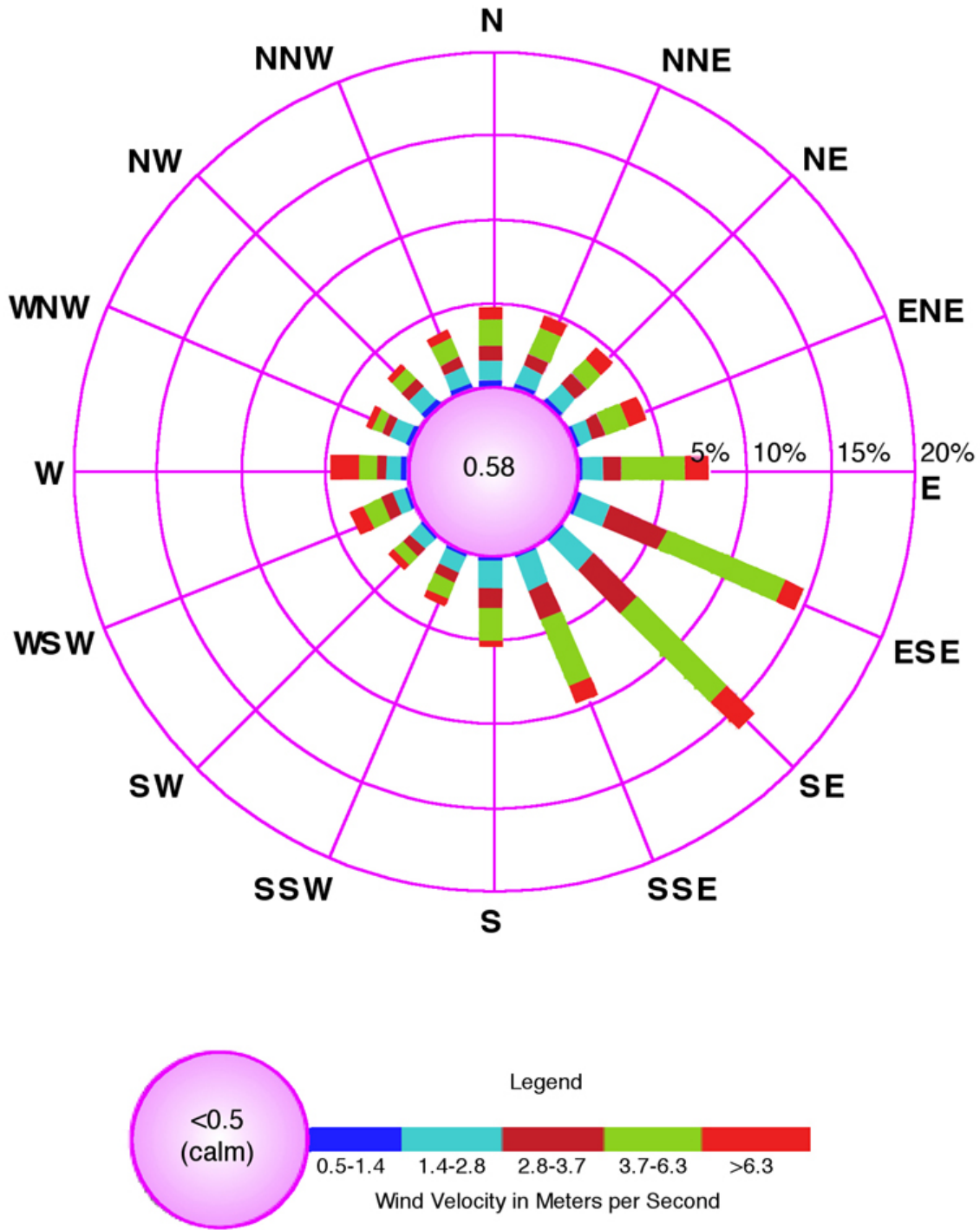


Figure 2-51. 1997 Annual Wind Rose at 10-m (33-ft.) Height at WIPP Site

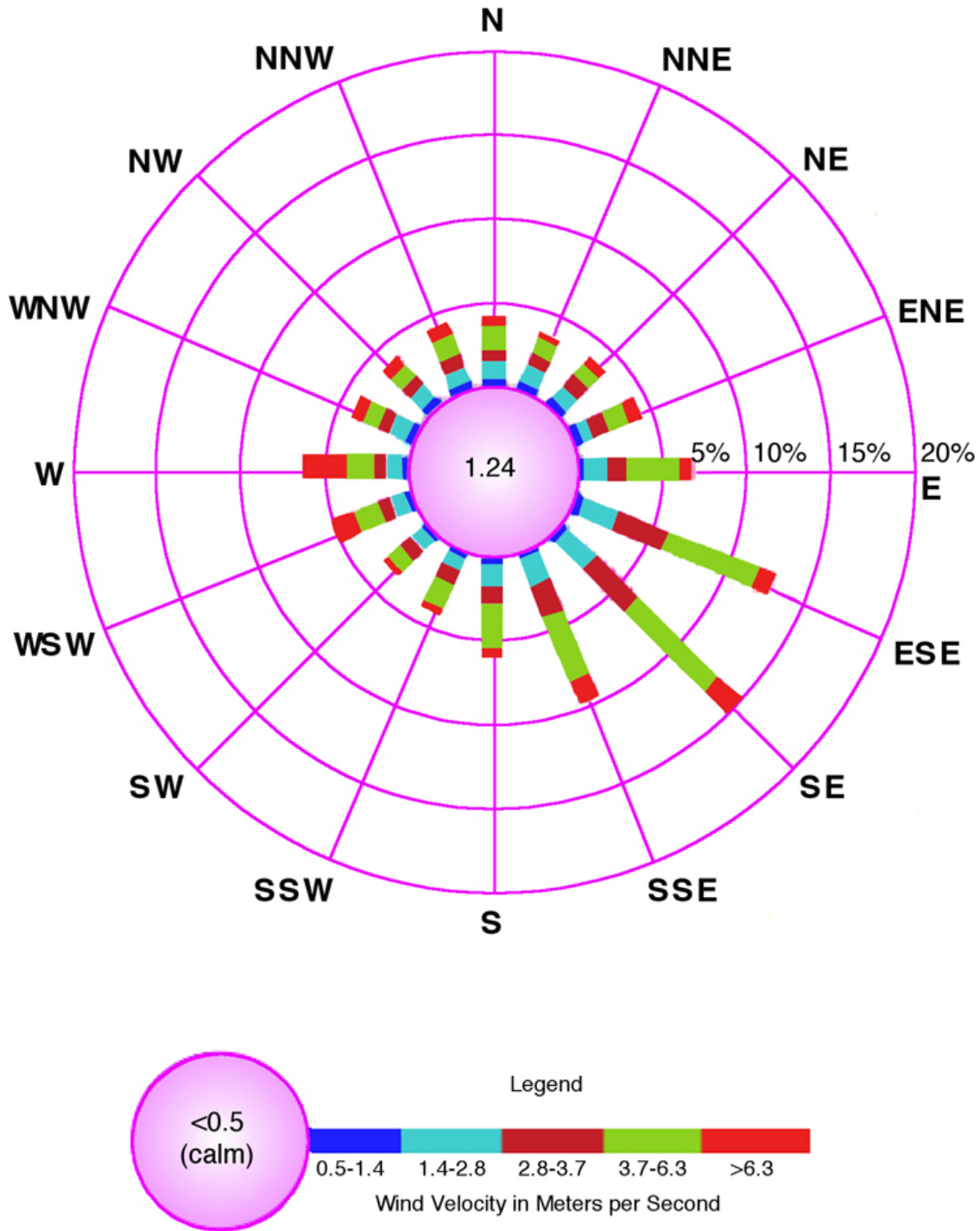


Figure 2-52. 1998 Annual Wind Rose at 10-m (33-ft.) Height at WIPP Site

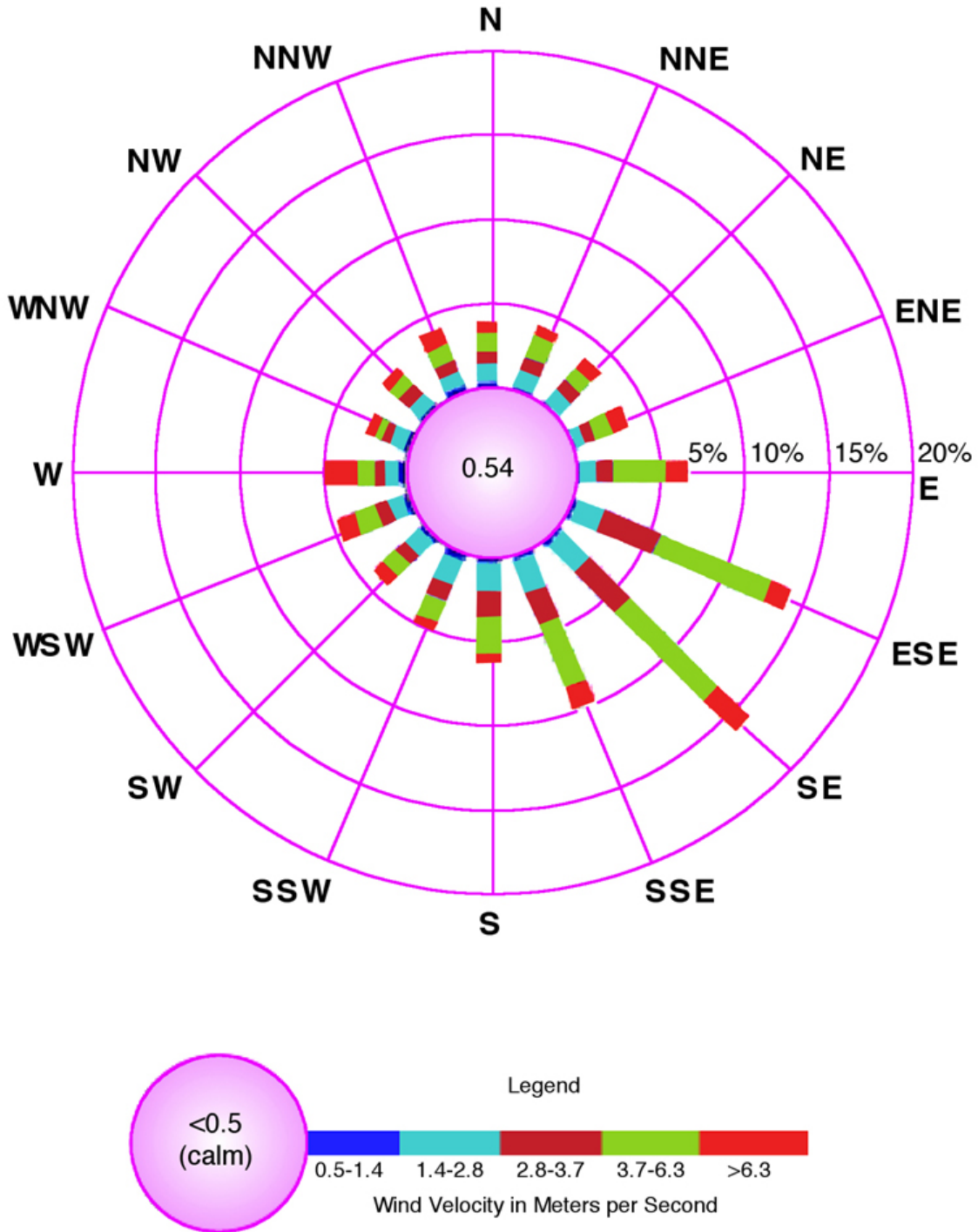


Figure 2-53. 1999 Annual Wind Rose at 10-m (33-ft.) Height at WIPP Site

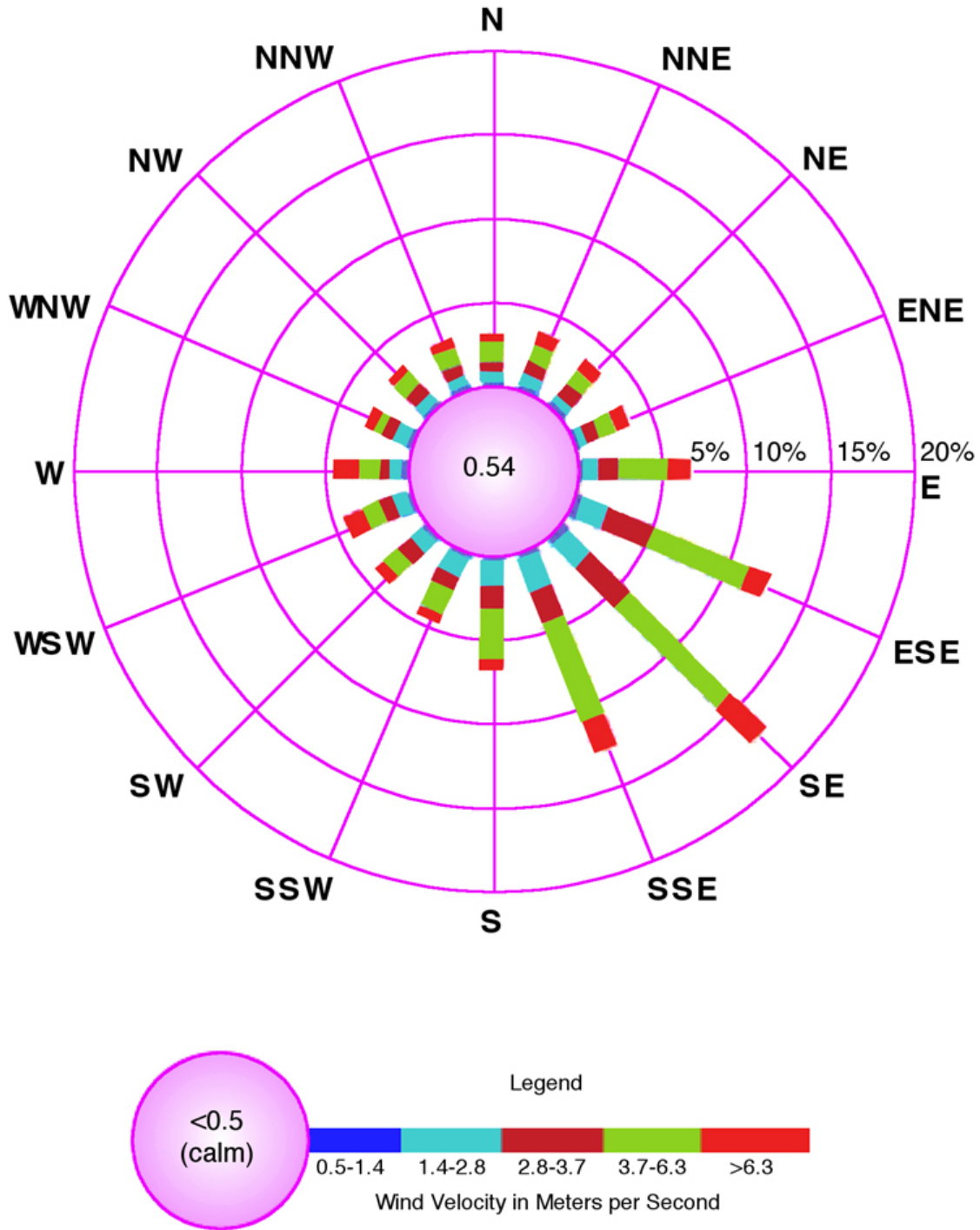


Figure 2-54. 2000 Annual Wind Rose at 10-m (33-ft.) Height at WIPP Site

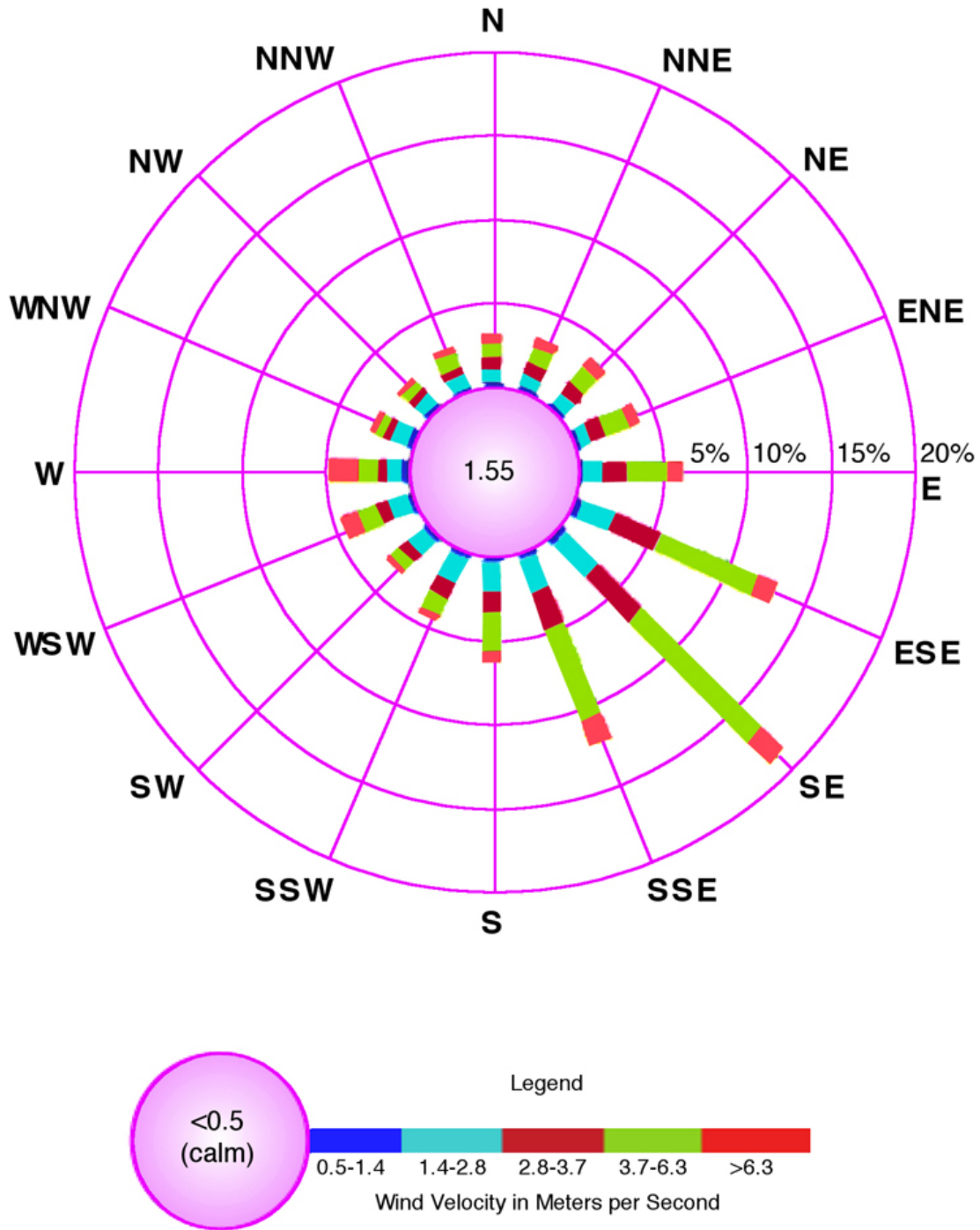


Figure 2-55. 2001 Annual Wind Rose at 10-m (33-ft.) Height at WIPP Site

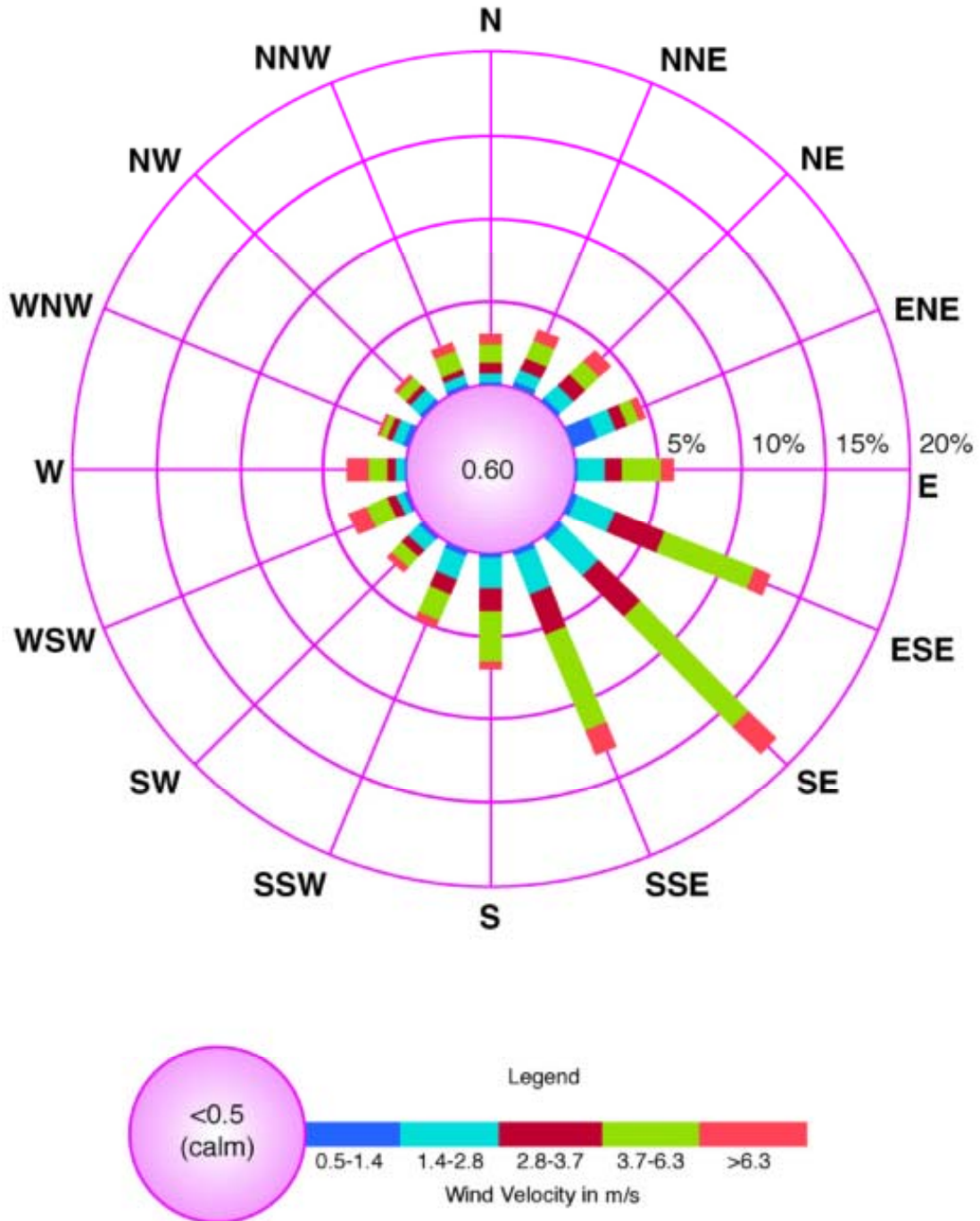
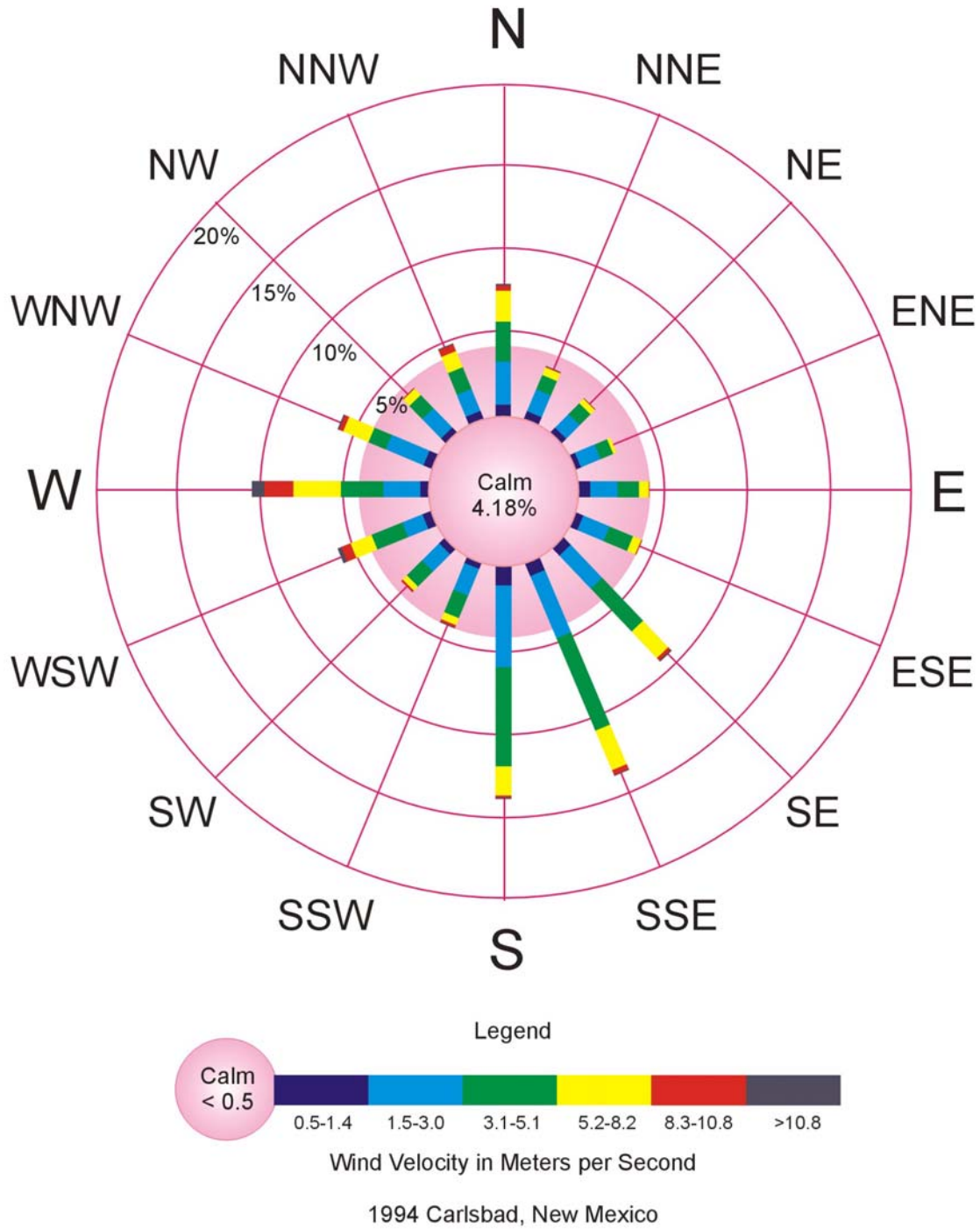


Figure 2-56. 2002 Annual Wind Rose at 10-m (33-ft.) Height at WIPP Site



CCA-059-2

Figure 2-46. 1994 Annual Wind Rose Carlsbad, NM

modified Mercalli intensity scale. Most of the magnitudes were determined by the New Mexico Institute of Mining and Technology or are described in [CCA](#) Appendix GCR and references therein.

2.6.1 Seismic History

Seismic data are presented in two time frames, before and after the time when seismographic data for the region became available. The earthquake record in southern New Mexico dates back only to 1923, and seismic instruments have been in place in the state since 1961. Various records have been examined to determine the seismic history of the area within 180 mi (288 km) of the site. With the exception of a weak shock in 1926 at Hope, New Mexico (approximately 64 km [40 mi] northwest of Carlsbad), and shocks in 1936 and 1949 felt at Carlsbad, all known shocks in the region before 1961 occurred to the west and southwest of the site more than 160 km (100 mi) away.

The strongest earthquake on record occurring within 288 km (180 mi) of the site was the Valentine, Texas earthquake of August 16, 1931. It has been estimated to have been of magnitude 6.4 on the Richter scale (Modified Mercalli Intensity of VIII). The Valentine earthquake was 208 km (130 mi) south-southwest of the site. Its Modified Mercalli Intensity at the site is estimated to have been V; this is believed to be the highest intensity felt at the site in this century.

In 1887, a major earthquake occurred in northeast Sonora, Mexico. Although about 536 km (335 mi) west-southwest of the site, it is indicative of the size of earthquakes possible in the eastern portion of the Basin and Range Province, west of the province containing the site. Its magnitude was estimated to have been 7.8 (VIII to IX in Modified Mercalli Intensity). It was felt over an area of 1.3 million km² (0.5 million mi²) (as far as Santa Fe to the north and Mexico City to the south); fault displacements near the epicenter were as large as 18 m (26 ft).

Since 1961, instrumental coverage has become comprehensive enough to locate most of the moderately strong earthquakes (local magnitude >3.5) in the region. Instrumentally determined shocks that occurred within 288 km (180 mi) of the site between 1961 and 1994 are shown in Figure 2-47⁵⁷. The distribution of these earthquakes may be biased by the fact that seismic stations were more numerous and were in operation for longer periods north and west of the site. Pre-1961 earthquakes can be found in [CCA](#) Appendix GCR, Figure 5.2-1.

Except for the activity southeast of the site, the distribution of epicenters since 1961 differs little from that of shocks before that time. There are two clusters, one associated with the Rio Grande Rift on the Texas-Chihuahua border and another associated with the Central Basin Platform in Texas near the southeastern corner of New Mexico. The latter activity was not reported before 1964. It is not clear from the record whether earthquakes were occurring in the Central Basin Platform before 1964, although local historical societies and newspapers tend to confirm their absence before that time.

The April 14, 1995, earthquake near Marathon, Texas, was located 240 km (150 mi) south of the WIPP site. The USGS estimated that moment magnitude for this event was 5.7. At a distance of

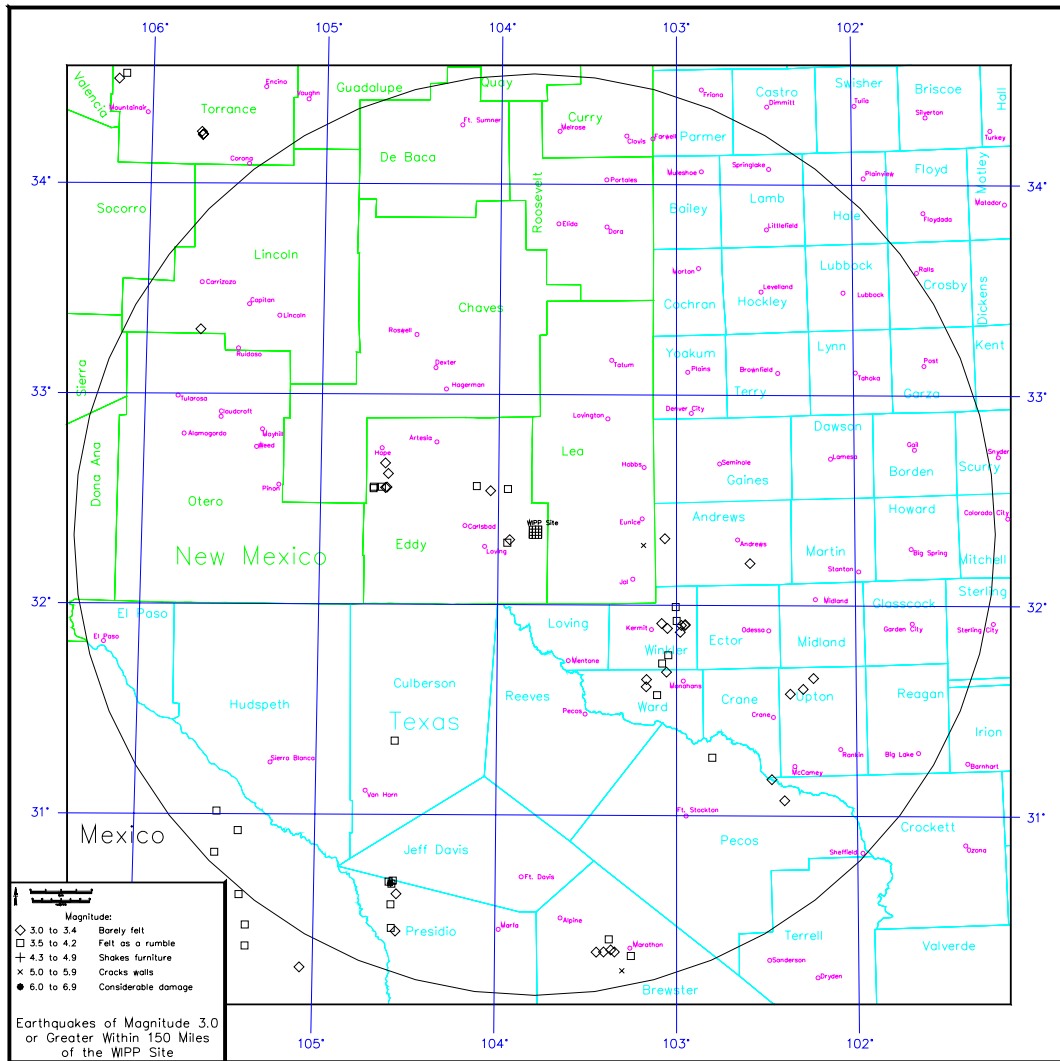


Figure 2-4757. Regional Earthquake Epicenters Occurring between 1961 and 2002

240 km (149 mi), an event of magnitude 5.7 would produce a maximum acceleration at the WIPP site of less than 0.01 g (*acceleration due to gravity*).

The Marathon earthquake should not be considered an unanticipated event. The shock occurred in the Basin and Range Province, a seismotectonic province with evidence for 24 Quarternary faults in West Texas and adjacent parts of Mexico. Two of these faults had recent surface-faulting events in the Holocene. Strong earthquakes have occurred within the West Texas part of the Basin and Range Province, most notably the $M_w = 6.4$ (Richter) Valentine, Texas earthquake on August 15, 1931.

The WIPP site is located within the Great Plains seismotectonic province, a region that has no evidence of Quarternary faulting, even above major buried structures such as the Central Basin Platform. Because the Great Plains seismotectonic province is geologically distinct from the Basin and Range Province and lacks evidence for recent faulting, the maximum possible or

credible earthquake for this region would be substantially smaller than that for the Basin and Range Province of West Texas.

2.6.2 *Seismic Risk*

Procedures exist that allow for formal determination of earthquake probabilistic design parameters. In typical seismic risk analyses of this kind, the region of study is divided into seismic source areas within which future events are considered equally likely to occur at any location. For each seismic source area, the rate of occurrence of events above a chosen threshold level is estimated using the observed frequency of historical events. The sizes of successive events in each source are assumed to be independent and exponentially distributed; the slope of the log number versus frequency relationship is estimated from the relative frequency of different sizes of events observed in the historical data. This slope, often termed the b value, is determined either for each seismic source individually or for all sources in the region jointly. Finally, the maximum possible size of events for each source is determined using judgement and the historical record. Thus, all assumptions underlying a measure of earthquake risk derived from this type of analysis are explicit, and a wide range of assumptions may be employed in the analysis procedure.

In this section, the particular earthquake risk parameter calculated is peak acceleration expressed as a function of annual probability of being exceeded at the WIPP site. The particular analysis procedure applied to the calculation of this probabilistic peak acceleration is taken from a computer program written by McGuire in (1976). In that program, the seismic source zones are modeled geometrically as quadrilaterals of arbitrary shape. Contributions to site earthquake risk from individual source zones are integrated into the probability distribution of acceleration, and the average annual probability of exceedence then follows directly.

In the analysis, the principal input parameters are as follows: site region acceleration attenuation, source zone geometry, recurrence statistics, and maximum magnitudes. Based on these parameters, several curves showing probabilistic peak acceleration are developed, and the conclusions that may be drawn from these curves are considered. The data treated in this way are used to arrive at a general statement of risk from vibratory ground motion at the site during its active phase of development and use.

2.6.2.1 Acceleration Attenuation

The first input parameters considered have to do with acceleration attenuation in the site region as a function of earthquake magnitude and hypocentral distance. The risk analysis used in this study employs an attenuation law of the form

$$a = b_1 \exp(b_2 M_L) R^{-b_3}, \quad (2.3)$$

where a is acceleration in cm/s^2 , M_L is Richter local magnitude, and R is the distance in km. The particular formula used in this study is based on a central United States model developed by Nuttli (1973). The formula coefficients $b_1 = 17$, $b_2 = 0.92$, and $b_3 = 1.0$ were selected. A justification for this assumption can be found in Section 5.3.2 of CCA Appendix GCR, Section 5.3.2.

2.6.2.2 Seismic Source Zones

Geologic, tectonic, and seismic evidence indicates that three seismic source zones may be used to adequately characterize the region. These are well approximated by the Basin and Range subregion, the Permian Basin subregion exclusive of the Central Basin Platform, and the Central Basin Platform itself. Specific boundaries are taken from a 1976 study by Algermissen and Perkins (1976) of earthquake risks throughout the United States. Additional details on this study are in CCA Appendix GCR, Section 5.3.2.

Site region seismic source zones are shown in Figure 2-48. Superposed on these zones are the earthquake epicenters of Figure 2-47. The zonation presented generally conforms with historical seismicity. The source zonation of Figure 2-48 has no explicit analog to the Permian Basin subregion exclusive of the Central Basin Platform. This is considered part of the broad background region.

For the purposes of this study, some minor modifications of the Algermissen and Perkins (1976) source zones were made. Geologic and tectonic evidence suggests that the physiographic boundary between the Basin and Range and Great Plains provinces provides a good and conservative approximation of the source zones (CCA Appendix GCR). In addition, information from the Kermit seismic array (Appendix to Rogers and Malkiel 1979) indicates that the geometry used to model the limits of the Central Basin Platform source zone may be modified somewhat from the original analogous Algermissen and Perkins (1976) zone. These modifications are shown in Figure 2-49 and constitute the preferred model for the WIPP site region seismic source zones in this study. This model is preferred because it more completely considers geologic and tectonic information, as well as seismic data, and because it results in a more realistic development of risks at the WIPP facility.

With regard to earthquake focal depth, there is little doubt that the focal depths of earthquakes in the WIPP facility region should be considered shallow. Early instrumental locations were achieved using an arc intersection method employing travel-time-distance curves calculated from a given crustal model, and the assumption of focal depths of 5 km (3.1 mi), 10 km (6.2 mi), or, for later calculations, 8 km (5 mi). Good epicentral locations could generally be obtained under these assumptions. For conservatism, a focal depth of 5 km (3.1 mi) is used in all source zones of this study including that of the site. For smaller hypocentral distances, the form of the

attenuation law adopted here severely exaggerates the importance of small, close shocks in the estimation of probabilistic acceleration at the WIPP site. Additional discussion is included in this application in Chapter 5 of CCA Appendix GCR, Chapter 5.

2.6.2.3 Source Zone Recurrence Formulas and Maximum Magnitudes

The risk calculation procedure used in this study requires that earthquake recurrence rates for each seismic source zone be specified. This is done formally by computing the constants a and b in the equation

$$\log N = a - bM, \quad (2.4)$$

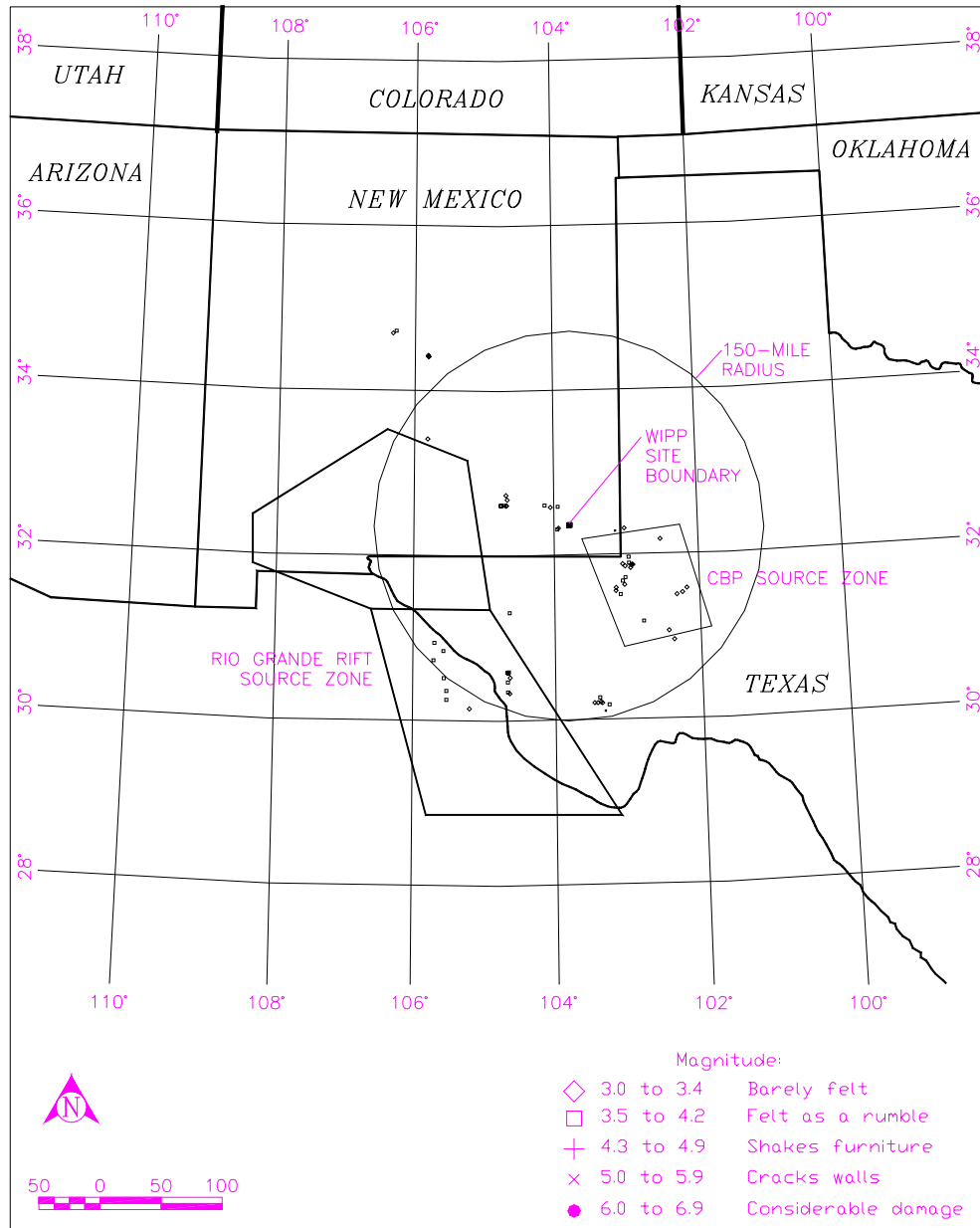
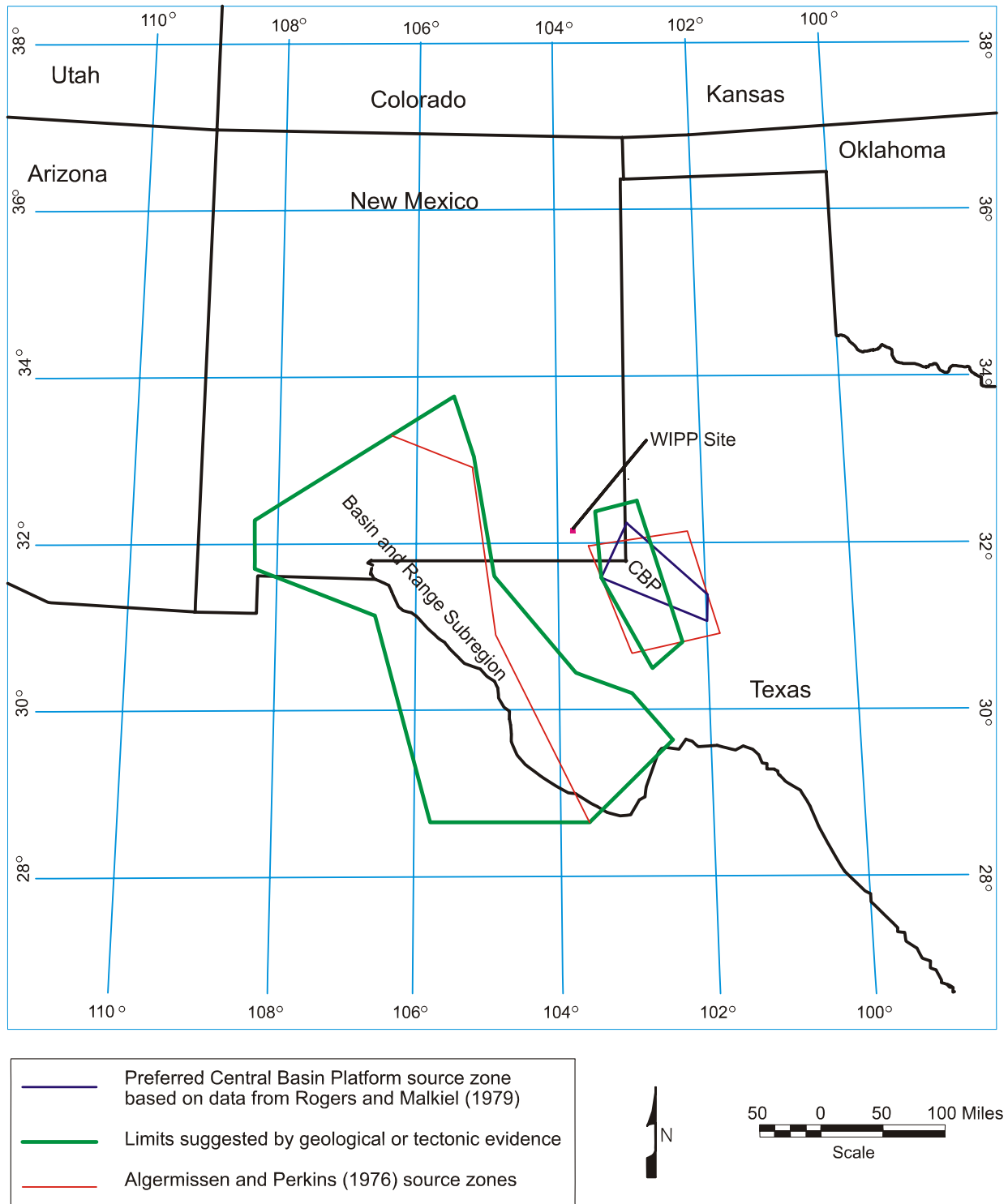


Figure 2-4858. Seismic Source Zones

where N is the number of earthquakes of magnitude greater than or equal to M within a specified area occurring during a specified period.

For the WIPP facility region, three formulas of this type are needed: one for the province west and southwest of the site (the Basin and Range subregion or Rio Grande **R**ift source zone), another for the province of the WIPP facility exclusive of the Central Basin Platform (the Permian Basin subregion or background source zone), and a final one for the Central Basin Platform. In practice, the difficulties in finding meaningful recurrence formulas for such small areas in a region of low historical earthquake activity are formidable.



CCA-062-2

Figure 2-4959. Alternate Source Geometries

The formulas have been determined to be

$$\bullet \log N = 2.43 - M_{\text{CORR}} \quad \text{Site source zone (background)} \quad (2.5)$$

$$\bullet \log N = 3.25 - M_{\text{CORR}} \quad \text{Basin and Range subregion} \quad (2.6)$$

$$\bullet \log N = 3.19 - 0.9 M_{\text{CORR}} \quad \text{Central Basin Platform} \quad (2.7)$$

The rationale for their development and the relationship used to determine M_{CORR} can be found in [CCA](#) Appendix GCR, Section 5.3.

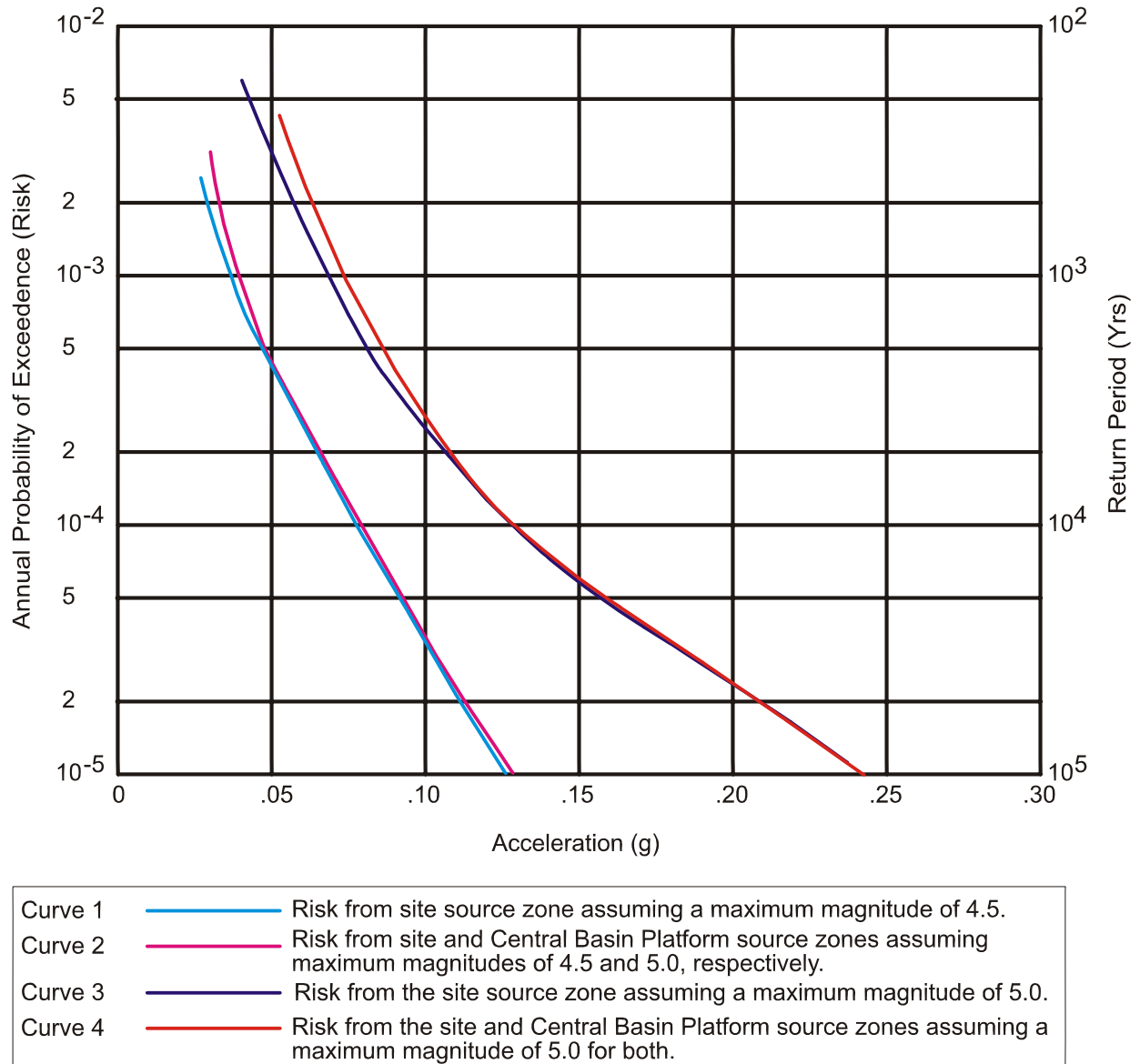
2.6.2.4 Design Basis Earthquake

The term Design Basis Earthquake (DBE) is used for the design of surface confinement structures and components at the WIPP facility. As used here, the DBE is equivalent to the design earthquake used in Regulatory Guide 3.24 (Nuclear Regulatory Commission [NRC] 1974). That is, in view of the limited consequences of seismic events in excess of those used as the basis, the DBE is such that it produces ground motion at the WIPP facility with a recurrence interval of 1,000 years. In practice, the DBE is defined in terms of the 1,000-year acceleration and design response spectra.

The generation of curves expressing probability of occurrence or risk as a function of peak WIPP facility ground acceleration is discussed in detail in [CCA](#) Appendix GCR, Section 5.3, for a number of possible characterizations of WIPP facility region source zones and source zone earthquake parameters. The most conservative (and the least conservative) risk curves are shown in Figure 2-5060.

From this figure, the most conservative calculated estimate of the 1,000-year acceleration at the WIPP facility is approximately 0.075 g. The geologic and seismic assumptions leading to this 1,000-year peak acceleration include the consideration of a Richter magnitude 5.5 earthquake at the site, a 6.0 magnitude earthquake on the Central Basin Platform, and a 7.8 magnitude earthquake in the Basin and Range subregion. These values, especially the first two, are considered quite conservative, as are the other parameters used in the 0.075-g derivation. For additional conservatism, a peak design acceleration of 0.1 g is selected for the WIPP facility DBE. The design response spectra for vertical and horizontal motions are taken from Regulatory Guide 1.60 (NRC 1973) with the high-frequency asymptote scaled to this 0.1-g peak acceleration value.

This DBE and the risk analysis that serves an important role in its definition are directly applicable to surface confinement structures and components at the WIPP facility. Underground structures and components are not subject to DBE design requirements because according to Pratt et al. (1979), mine experience and studies on earthquake damage to underground facilities show that tunnels are not damaged at sites having peak surface accelerations below 0.2 g.



Note: Risk curves generated by using worst and best case assumption from the parameter variation considered for site region source zones. See Appendix GCR, Figure 5.3-7 for further details.

CCA-063-2

Figure 2-5060. Total WIPP Facility Risk Curve Extrema

REFERENCES

- Adams, J.E. 1944. "Upper Permian Ochoa Series of the Delaware Basin, West Texas and Southeastern New Mexico." *American Association of Petroleum Geologists Bulletin*, Vol. 28, No. 11, 1596-1625.
- Algermissen, S.T., and Perkins, D.M. 1976. *A Probabilistic Estimate of Maximum Ground Acceleration in the Contiguous United States*. Open-file Report 76-416, pp. 1 – 45. U.S. Geological Survey.
- Anderson, R.Y. 1978. *Deep Dissolution of Salt, Northern Delaware Basin, New Mexico*. Report to Sandia National Laboratories, Albuquerque, NM. [ERMS #229530](#).
- Anderson, R.Y., and Kirkland, D.W. 1980. Dissolution of Salt Deposits by Brine Density Flow. *Geology*, Vol. 8, No. 2, pp. 66 – 69.
- Anderson, R.Y. 1981. "Deep-Seated Salt Dissolution in the Delaware Basin, Texas and New Mexico." In *Environmental Geology and Hydrology in New Mexico*, S.G. Wells and W. Lambert, eds., Special Publication No. 10, pp. 133 - 145. New Mexico Geological Society.
- Anderson, R.Y. 1993. "The Castile as a 'Nonmarine' Evaporite." In *Carlsbad Region, New Mexico and Texas, New Mexico Geological Society, Forty-Fourth Annual Field Conference, Carlsbad, NM, October 6-9, 1993*, D.W. Love et al., eds., pp. 12 - 13. New Mexico Geological Society, Socorro, NM.
- Anderson, R.Y., Dean, W.E., Jr., Kirkland, D.W., and Snider, H. I. 1972. "Permian Castile Varved Evaporite Sequence, West Texas and New Mexico." *Geological Society of America Bulletin*, Vol. 83, No. 1, pp. 59 - 85.
- Anderson, R.Y., and Powers, D.W. 1978. "Salt Anticlines in the Castile-Salado Evaporite Sequence, Northern Delaware Basin, New Mexico." In *Geology and Mineral Deposits of Ochoan Rocks in Delaware Basin and Adjacent Areas*, G.S. Austin, ed., Circular 159. pp. 79 - 83. New Mexico Bureau of Mines and Mineral Resources, Socorro, NM.
- Anderson, R.Y., Kietzke, K.K., and Rhodes, D.J. 1978. "Development of Dissolution Breccias, Northern Delaware Basin, New Mexico and Texas." In *Geology and Mineral Deposits of Ochoan Rocks in Delaware Basin and Adjacent Areas*, G.S. Austin, ed., Circular 159. New Mexico Bureau of Mines and Mineral Resources, Socorro, NM.
- Bachman, G.O. 1973. *Surficial Features and Late Cenozoic History in Southeastern New Mexico*. Open-File Report 4339-8. U.S. Geological Survey, Reston, VA.
- Bachman, G.O. 1974. *Geologic Processes and Cenozoic History Related to Salt Dissolution in Southeastern New Mexico*. Open-File Report 74-194. U.S. Geological Survey, Denver, CO.
- Bachman, G.O. 1976. "Cenozoic Deposits of Southeastern New Mexico and an Outline of the History of Evaporite Dissolution." *Journal of Research*, Vol. 4, No. 2, pp. 135 - 149. U.S. Geological Survey.

- 1 Bachman, G.O. 1980. *Regional Geology and Cenozoic History of Pecos Region, Southeastern*
2 *New Mexico*. Open-File Report 80-1099. U.S. Geological Survey, Denver, CO.
- 3 Bachman, G.O. 1981. *Geology of Nash Draw, Eddy County, New Mexico*. Open-File Report
4 81-31. U.S. Geological Survey, Denver, CO.
- 5 Bachman, G.O. 1984. *Regional Geology of Ochoan Evaporites, Northern Part of Delaware*
6 *Basin*. Circular 184, pp. 1 - 22. New Mexico Bureau of Mines and Mineral Resources, Socorro,
7 NM.
- 8 Bachman, G.O. 1985. *Assessment of Near-Surface Dissolution at and Near the Waste Isolation*
9 *Pilot Plant (WIPP), Southeastern New Mexico*. SAND84-7178. Sandia National Laboratories,
10 Albuquerque, NM. [**ERMS #224609**](#).
- 11 Barrows, L.J., Shaffer, S.E., Miller, W.B., and Fett, J.D. 1983. *Waste Isolation Pilot Plant*
12 *(WIPP) Site Gravity Survey and Interpretation*. SAND82-2922. Sandia National Laboratories,
13 Albuquerque, NM.
- 14 Beauheim, R.L., Hassinger, B.W., and Kleiber, J.A. 1983. *Basic Data Report for Borehole*
15 *Cabin Baby-1 Deepening and Hydrologic Testing, Waste Isolation Pilot Plant (WIPP) Project,*
16 *Southeastern New Mexico*. WTSD-TME-020. United States Department of Energy,
17 Albuquerque, NM.
- 18 Beauheim, R.L. 1986. *Hydraulic-Test Interpretations for Well DOE-2 at the Waste Isolation*
19 *Pilot Plant (WIPP) Site*. SAND86-1364. Sandia National Laboratories, Albuquerque, NM.
20 [**ERMS #227656**](#).
- 21 Beauheim, R.L. 1987a. *Interpretations of Single-Well Hydraulic Tests Conducted at and Near*
22 *the Waste Isolation Pilot Plant (WIPP) Site, 1983–1987*. SAND87-0039. Sandia National
23 Laboratories, Albuquerque, NM. [**ERMS #227679**](#).
- 24 Beauheim, R.L. 1987b. *Analysis of Pumping Tests of the Culebra Dolomite Conducted at the*
25 *H-3 Hydropad at the Waste Isolation Pilot Plant (WIPP) Site*. SAND86-2311. Sandia National
26 Laboratories, Albuquerque, NM.
- 27 Beauheim, R.L. 1987c. *Interpretation of the WIPP-13 Multipad Pumping Test of the Culebra*
28 *Dolomite at the Waste Isolation Pilot Plant (WIPP) Site*. SAND87-2456. Sandia National
29 Laboratories, Albuquerque, NM.
- 30 Beauheim, R.L. 1989. *Interpretation of H-141b4 Hydraulic Tests and the H-11 Multipad*
31 *Pumping Test of the Culebra Dolomite at the Waste Isolation Pilot Plant (WIPP) Site*. SAND89-
32 0536. Sandia National Laboratories, Albuquerque, NM.
- 33 [**Beauheim, R.L. 2002. "Analysis Plan for Evaluation of the Effects of Head Changes on**](#)
34 [**Calibration of Culebra Transmissivity Fields, AP-088, Rev. 1," ERMS #524785. Carlsbad,**](#)
35 [**NM: Sandia National Laboratories, WIPP Records Center.**](#)

- 1 ***Beauheim, R.L. 2000. "Appendix E, Summary of Hydraulic Tests Performed at Tracer-Test***
- 2 ***Sites," in Interpretations of Tracer Tests Performed in the Culebra Dolomite at the Waste***
- 3 ***Isolation Pilot Plant Site, Meigs, L.C., Beauheim, R.L., and Jones, T.L., eds. SAND97-3109.***
- 4 ***Albuquerque, NM: Sandia National Laboratories.***
- 5 Beauheim, R.L., and Holt, R.M. 1990. "Hydrogeology of the WIPP Site." In *Geological and*
- 6 *Hydrological Studies of Evaporites in the Northern Delaware Basin for the Waste Isolation Pilot*
- 7 *Plant (WIPP), New Mexico, Geologic Society of America 1990 Annual Meeting Field Trip #14*
- 8 *Guidebook*, pp. 131 -179. Dallas Geologic Society, Dallas, TX.
- 9 ***Beauheim, R.L., and Roberts, R.M. 2002. "Hydrology and Hydraulic Properties of a Bedded***
- 10 ***Evaporite Formation," Journal of Hydrology, v. 259, pp. 66-88.***
- 11 ***Beauheim, R.L., and Ruskauff, G.J. 1998. Analysis of Hydraulic Tests of the Culebra and***
- 12 ***Magenta Dolomites and Dewey Lake Redbeds Conducted at the Waste Isolation Pilot Plant***
- 13 ***Site. SAND98-0049. Albuquerque, NM: Sandia National Laboratories.***
- 14 Beauheim, R.L., Roberts, R.M., Dale, T.F., Fort, M.D., and Stensrud, W.A. 1993. *Hydraulic*
- 15 *Testing of Salado Formation Evaporites at the Waste Isolation Pilot Plant Site: Second*
- 16 *Interpretive Report. SAND92-0533. Sandia National Laboratories, Albuquerque, NM. ERMS*
- 17 ***#223378.***
- 18 Beauheim, R.L., Saulnier, G.J., ***JR.*** and Avis, J.D. 1991***a.*** *Interpretation of Brine-Permeability*
- 19 *Tests of the Salado Formation at the Waste Isolation Pilot Plant Site: First Interim Report.*
- 20 *SAND90-0083. Sandia National Laboratories, Albuquerque, NM.*
- 21 ***Beauheim, R.L., Dale, T.F., and Pickens, J.F. 1991b. Interpretations of Single-Well***
- 22 ***Hydraulic Tests of the Rustler Formation Conducted in the Vicinity of the Waste Isolation***
- 23 ***Pilot Plant Site, 1988-1989. SAND89-0869. Sandia National Laboratories, Albuquerque,***
- 24 ***NM.***
- 25 Beauheim, R.L., Meigs, L.C., Saulnier, G.J., ***JR.*** and Stensrud, W.A. 1995. *Culebra Transport*
- 26 *Program Test Plan: Tracer Testing of the Culebra Dolomite Member of the Rustler Formation*
- 27 *at the H-19 and H-11 Hydropads on the WIPP Site. ERMS #230156. Carlsbad, NM: Sandia*
- 28 ***National Laboratories, WIPP Records Center.***
- 29 ***Bechtel National Inc. 1979. "Soils Design Report – Volume 1 Plant Site Near-Surface***
- 30 ***Structures," Doc. No. Dr-22-V-01. San Francisco, CA: Bechtel National Inc.***
- 31 ***Becker, M.L., Rasbury, E.T., Meyers, W.J., and Hanson, G.N. 2002. U-Pb calcite age of the***
- 32 ***Late Permian Castile Formation, Delaware Basin: a constraint on the age of the Permian-***
- 33 ***Triassic boundary (?): Earth and Planetary Science Letters, v. 203, p. 681-689.***
- 34 Blackwell, D.D., Steele, J.L., and Carter, L.S. 1991. "Heat-Flow Patterns of the North
- 35 American Continent; A Discussion of the Geothermal Map of North America." In *Neotectonics*
- 36 *of North America*, D.B. Slemmons, E.R. Engdahl, M.D. Zoback, and D.D. Blackwell, eds., pp.
- 37 423 - 436. Geological Society of America, Boulder, CO.

- 1 Bodine, Jr., M.W. 1978. "Clay-Mineral Assemblages from Drill Core of Ochoan Evaporites,
2 Eddy County, New Mexico." In *Geology and Mineral Deposits of Ochoan Rocks in Delaware
3 Basin and Adjacent Areas*, G.S. Austin, ed., Circular 159. pp. 21 - 31. New Mexico Bureau of
4 Mines and Mineral Resources, Socorro, NM.
- 5 Borns, D.J. 1987. *The Geologic Structures Observed in Drillhole DOE-2 and Their Possible
6 Origins: Waste Isolation Pilot Plant*. SAND86-1495. Sandia National Laboratories,
7 Albuquerque, NM.
- 8 Borns, D.J., Barrows, L.J., Powers, D.W., and Snyder, R.P. 1983. *Deformation of Evaporites
9 Near the Waste Isolation Pilot Plant (WIPP) Site*. SAND82-1069. Sandia National
10 Laboratories, Albuquerque, NM.
- 11 Borns, D.J. 1985. *Marker Bed 139: A study of Drillcore from a Systematic Array*. SAND85-
12 0023. Sandia National Laboratories, Albuquerque, NM.
- 13 Borns, D.J., and Shaffer, S.E. 1985. *Regional Well-Log Correlation in the New Mexico Portion
14 of the Delaware Basin*. SAND83-1798. Sandia National Laboratories, Albuquerque, NM.
- 15 Brausch, L.M., Kuhn, A.K., and Register, J.K. 1982. *Natural Resources Study, Waste Isolation
16 Pilot Plant (WIPP) Project, Southeastern New Mexico*. TME 3156. Albuquerque, NM: U.S.
17 Department of Energy, Waste Isolation Pilot Plant.
- 18 Brokaw, A.L., Jones, C.L., Cooley, M.E., and Hays, W.H. 1972. *Geology and Hydrology of the
19 Carlsbad Potash Area, Eddy and Lea Counties, New Mexico*. Open-File Report 4339-1. U.S.
20 Geological Survey, Denver, CO.
- 21 Brookins, D.G. 1980. "Polyhalite K-Ar Radiometric Ages from Southeastern New Mexico." In
22 *Isochron/West*, No. 29, pp. 29 - 31.
- 23 Brookins, D.G. 1981. "Geochronologic Studies Near the WIPP Site, Southeastern New
24 Mexico." In *Environmental Geology and Hydrology in New Mexico*, S.G. Wells, and
25 W. Lambert, ed., Special Publication 10, pp. 147 - 152. New Mexico Geological Society.
- 26 Brookins, D.G., and Lambert, S.J. 1987. "Radiometric Dating of Ochoan (Permian) Evaporites,
27 WIPP Site, Delaware Basin, New Mexico, USA." *Scientific Basis for Nuclear Waste
28 Management X, Materials Research Society Symposia Proceedings, Boston, MA, December 1-4,
29 1986*, J.K. Bates and W.B. Seefeldt, eds., Vol. 84, pp. 771 - 780, Materials Research Society,
30 Pittsburgh, PA.
- 31 Brookins, D.G., Register, J.K., Jr., and Krueger, H.W. 1980. "Potassium-Argon Dating of
32 Polyhalite in New Mexico." *Geochimica et Cosmochimica Acta*, Vol. 44, No. 5, pp. 635 - 637.
- 33 ***Butcher, B.M. 1997. A Summary of the Sources of Input Parameter Values for the Waste
34 Isolation Pilot Plant Final Porosity Surface Calculations. SAND97-0796. Albuquerque, NM:
35 Sandia National Laboratories.***

- 1 Calzia, J.P., and Hiss, W.L. 1978. "Igneous Rocks in Northern Delaware Basin, New Mexico,
2 and Texas." In *Geology and Mineral Deposits of Ochoan Rocks in Delaware Basin and*
3 *Adjacent Areas*, G.S. Austin, ed., Circular 159, pp. 39 - 45. New Mexico Bureau of Mines and
4 Mineral Resources, Socorro, NM.
- 5 Cartwright, Jr., L.D. 1930. Transverse Section of Permian Basin, West Texas and Southeastern
6 New Mexico. *American Association of Petroleum Geologists Bulletin*, Vol. 14.
- 7 Casas, E., and Lowenstein, T.K. 1989. Diagenesis of Saline Pan Halite: Comparison of
8 Petrographic Features of Modern, Quaternary and Permian Halites. *Journal of Sedimentary*
9 *Petrology*, Vol. 59.
- 10 ***Chapman, J.B. 1986. Stable Isotopes in the Southeastern New Mexico Groundwater:***
11 ***Implications for Dating Recharge in the WIPP Area. EEG-35, DOE/AL/10752-35.***
12 ***Environmental Evaluation Group, Santa Fe, NM.***
- 13 ***Chapman, J.B. 1988. Chemical and Radiochemical Characteristics of Groundwater in the***
14 ***Culebra Dolomite, Southeastern NM. EEG-39. Environmental Evaluation Group,***
15 ***Santa Fe, NM.***
- 16 ***Chugg, J.C., Anderson, G.W., Kink, D.L., and Jones, L.H. 1952. Soil Survey of Eddy Area,***
17 ***New Mexico. U.S. Department of Agriculture.***
- 18 ~~Chugg, J.C., Anderson, G.W., Kink, D.L., and Jones, L.H. 1971. *Soil Survey of Eddy Area, New*~~
19 ~~*Mexico. Prepared by the U.S. Soil Conservation Service in cooperation with New Mexico*~~
20 ~~*Agricultural Experiment Station. For sale by the Superintendent of Documents, U.S.*~~
21 ~~*Government Printing Office, Washington, D.C.*~~
- 22 Claiborne, H.C., and Gera, F. 1974. *Potential Containment Failure Mechanisms and Their*
23 *Consequences at a Radioactive Waste Repository in Bedded Salt in New Mexico.* ORNL-TM
24 4639. Oak Ridge National Laboratories, Oak Ridge, TN.
- 25 Corbet, T.F. and Knupp, P.M. 1996. *The Role of Regional Groundwater Flow in the*
26 *Hydrogeology of the Culebra Member of the Rustler Formation at the Waste Isolation Pilot*
27 *Plant (WIPP), Southeastern New Mexico.* SAND96-2133. Sandia National Laboratories:
28 Albuquerque, NM.
- 29 ***Crawley, M.E., and Nagy, M. 1998. Waste Isolation Pilot Plant RCRA Background***
30 ***Groundwater Quality Baseline Report. DOE/WIPP 98-2285. Albuquerque, NM: IT***
31 ***Corporation for Westinghouse Electric Corporation.***
- 32 Davies, P.B. 1984. "Deep-Seated Dissolution and Subsidence in Bedded Salt Deposits." Ph.D.
33 Thesis. Stanford University, Palo Alto, CA.
- 34 Davies, P.B. 1989. *Variable-Density Ground-Water Flow and Paleohydrology in the Waste*
35 *Isolation Pilot Plant (WIPP) Region, Southeastern New Mexico.* Open-File Report 88-490. U.S.
36 Geological Survey, Albuquerque, NM.

- 1 Deal, D.E., and Case, J.B. 1987. *Brine Sampling and Evaluation Program Phase I Report*.
2 DOE-WIPP 87-008. Westinghouse Electric Corporation, Carlsbad, NM.
- 3 Deal, D.E., Case, J.B., Deshler, R.M., Drez, P.E., Myers, J., and Tyburski, J.R. 1987. *Brine*
4 *Sampling and Evaluation Program Phase II Report*. DOE-WIPP-87-010. Westinghouse
5 Electric Corporation, Carlsbad, NM.
- 6 Deal, D.E., Abitz, R.J., Belski, D.S., Case, J.B., Crawley, M.E., Deshler, R.M., Drez, P.E.,
7 Givens, C.A., King, R.B., Lauctes, B.A., Myers, J., Niou, S., Pietz, J.M., Roggenthen, W.M.,
8 Tyburski, J.R., and Wallace, M.G. 1989. *Brine Sampling and Evaluation Program, 1988*
9 *Report*. DOE-WIPP-89-015. Carlsbad, NM: Westinghouse Electric Corporation.
- 10 Deal, D.E., Abitz, R.J., Belski, D.S., Clark, J.B., Crawley, M.E., and Martin, M.L. 1991a. *Brine*
11 *Sampling and Evaluation Program, 1989 Report*. DOE-WIPP-91-009. Carlsbad, NM:
12 Westinghouse Electric Corporation.
- 13 Deal, D.E., Abitz, R.J., Myers, J. Case, J.B., Martin, M.L., Roggenthen, W.M., and Belski, D.S.
14 1991b. *Brine Sampling and Evaluation Program, 1990 Report*. DOE-WIPP-91-036. Prepared
15 for U.S. Department of Energy by IT Corporation and Westinghouse Electric Corporation.
16 Westinghouse Electric Corporation, Waste Isolation Division, Carlsbad, NM.
- 17 Deal, D.E., Abitz, R.J., Myers, J., Martin, M.L., Milligan, D.J., Sobocinski, R.W., Lipponer,
18 P.P.J., and Belski, D.S. 1993. *Brine Sampling and Evaluation Program, 1991 Report*. DOE-
19 WIPP-93-026. Carlsbad, NM: Westinghouse Electric Corporation.
- 20 *Deal, D.E., Abitz, R.J. Belski, D.S., Case, J. B., Crawley, M.E., Givens, C. A., James*
21 *Lipponer, P.P.J., Milligan, D.J., Myers, J., Powers, D. W., and Valdivia, M. A. 1995. Brine*
22 *Sampling and Evaluation Program, 1992-1993 Report and Summary of BSEP Data Since*
23 *1982, DOE-WIPP 94-011. Carlsbad, NM: Westinghouse Electric Corporation.*
- 24 Domski, P.S., Upton, D.T., and Beauheim, R.L. 1996. *Hydraulic Testing Around Room Q:*
25 *Evaluation of the Effects of Mining on the Hydraulic Properties of Salado Evaporites*. SAND96-
26 0435. Sandia National Laboratories, Albuquerque, NM.
- 27 *Duke Engineering and Services (DES). 1997. Exhaust Shaft: Phase 2 Hydraulic Assessment*
28 *Data Report Involving Drilling, Installation, Water-Quality Sampling, and Testing of*
29 *Piezometers 1-12. DOE/WIPP97-2278. Carlsbad, NM: Westinghouse Electric Corporation.*
- 30 Eager, G.P. 1983. Core from the Lower Dewey Lake, Rustler, and Upper Salado Formation,
31 Culberson County, Texas. In *Permian Basin Cores*, R.L. Shaw and B.J. Pollen, eds., P.B.S.-
32 S.E.P.M. Core Workshop No. 2, pp. 273 - 283. Permian Basin Section, Society of Economic
33 Paleontologists and Mineralogists, Midland, TX.
- 34 Earth Technology Corporation. 1988. *Final Report for Time Domain Electromagnetic (TDEM)*
35 *Surveys at the WIPP Site*. SAND87-7144. Albuquerque, NM: Sandia National Laboratories.

- 1 Elliot Geophysical Company. 1976. *A Preliminary Geophysical Study of a Trachyte Dike in*
2 *Close Proximity to the Proposed Los Medaños Nuclear Waste Disposal Site, Eddy and Lea*
3 *Counties, New Mexico.* Elliot Geophysical Company, Tucson, AZ.
- 4 *Environmental Science and Research Foundation (ESRF), Inc. 2000. Waste Isolation Pilot*
5 *Plant 1999 Site Environmental Report. DOE/WIPP 00-2225, ESRF-039. Idaho Falls, ID:*
6 *ESRF.*
- 7 *Environmental Science and Research Foundation (ESRF), Inc. 2001. Waste Isolation Pilot*
8 *Plant CY 2000 Site Environmental Report. DOE/WIPP 01-2225, ESRF-045. Idaho Falls, ID:*
9 *ESRF.*
- 10 *Environmental Science & Research Foundation (ESRF). 2002. Waste Isolation Pilot Plant*
11 *Site Environmental Report for Calendar Year 2001, DOE/WIPP 02-2225, Carlsbad, NM.*
- 12 *Ewing, T.E. 1993. "Erosional Margins and Patterns of Subsidence in the Late Paleozoic*
13 *West Texas Basin and Adjoining Basins of West Texas and New Mexico," New Mexico*
14 *Geological Society Guidebook, 44th Field Conference, Carlsbad Region New Mexico and*
15 *West Texas, D.W. Lowe et al., eds., pp. 155 - 166.*
- 16 Foster, R.W. 1974. *Oil and Gas Potential of a Proposed Site for the Disposal of High-Level*
17 *Radioactive Waste.* BNL/SUB-44231/1. Ridge National Laboratory, Oak Ridge, TN. Available
18 from NTIS. NTIS Accession number: ORNL/SUB-4423-1.
- 19 *Freeze, R.A., and Witherspoon, P.A. 1967. "Theoretical Analysis of Regional Groundwater*
20 *Flow: 2. Effect of Water-Table Configuration and Subsurface Permeability Variation,"*
21 *Water Resources Research. Vol. 3, No. 2, pp. 623 - 634.*
- 22 *FWS (U.S. Fish and Wildlife Service). 1989. Letter from John C. Peterson, Field Supervisor,*
23 *Albuquerque, NM, to Jack B. Tillman, Project Manager, U.S. DOE–Carlsbad, May 25, 1989.*
- 24 *Geohydrology Associates. 1978. Ground-Water Study Related to Proposed Expansion of*
25 *Potash Mining near Carlsbad, New Mexico. Contractor Report to Bureau of Land*
26 *Management, Denver, CO, Contract No. YA-512-CT7-217. Albuquerque, NM: Geohydrology*
27 *Associates.*
- 28 Hale, W.E., Hughes, L.S., and Cox, E.R. 1954. *Possible Improvement of Quality of Water of the*
29 *Pecos River by Diversion of Brine at Malaga Bend, Eddy County, NM.* Pecos River Commission
30 New Mexico and Texas, in cooperation with United States Department of the Interior,
31 Geological Survey, Water Resources Division, Carlsbad, NM.
- 32 *Harland, W.B., Armstrong, R.L., Cox, A.V., Craig, L.E., Smith, A.G., and Smith, D.G. 1989.*
33 *A Geologic Time Scale 1989. Cambridge Earth Science Series. Cambridge University Press.*
- 34 *Harms, J.C., and Williamson, C.R. 1988. "Deep-Water Density Current Deposits of Delaware*
35 *Mountain Group (Permian), Delaware Basin, Texas and New Mexico." American*
36 *Association of Petroleum Geologists Bulletin, Vol. 72.*

- 1 ***Haug, A., Kelley, V.A., LaVenue, A.M., and Pickens, J. F. 1987. Modeling of Ground-Water***
- 2 ***Flow in the Culebra Dolomite at the Waste Isolation Pilot Plant (WIPP) Site: Interim Report.***
- 3 ***SAND86-7167. Sandia National Laboratories, Albuquerque, NM.***
- 4 Hawley, J.W. 1993. "The Ogallala and Gatuña Formations in the Southeastern New Mexico
- 5 Region, a Progress Report." In *Carlsbad Region, New Mexico and West Texas, New Mexico*
- 6 *Geological Society, Forty-Fourth Annual Field Conference, Carlsbad, NM, October 6-9, 1993,*
- 7 *D.W. Love et al., eds., pp. 261 - 269. New Mexico Geological Society, Socorro, NM.*
- 8 Hayes, P.T., and Bachman, G.O. 1979. *Examination and Reevaluation of Evidence for the*
- 9 *Barrera Fault, Guadalupe Mountains, New Mexico.* Open-File Report 79-1520. U.S.
- 10 Geological Survey, Denver, CO.
- 11 ***Hazen, R.M., and Roedder, E. 2001. "How Old are Bacteria from the Permian Age?"***
- 12 ***Nature, v. 411, p. 155.***
- 13 Hills, J.M. 1984. Sedimentation, Tectonism, and Hydrocarbon Generation in Delaware Basin,
- 14 West Texas and Southeastern New Mexico. *American Association of Petroleum Geologists*
- 15 *Bulletin*, Vol. 68.
- 16 Hiss, W.L. 1975. "Stratigraphy and Ground-Water Hydrology of the Capitan Aquifer,
- 17 Southeastern New Mexico and Western Texas." PhD dissertation. University of Colorado,
- 18 Department of Geological Sciences, Boulder, CO.
- 19 Hiss, W.L. 1976. *Structure of the Premium Guadalupian Capitan Aquifer, Southeast New*
- 20 *Mexico and West Texas.* Resource Map. New Mexico Bureau of Mines and Mineral Resources,
- 21 Socorro, NM.
- 22 ***Holt, R.M. 1997. Conceptual Model for Transport Processes in the Culebra Dolomite***
- 23 ***Member, Rustler Formation. SAND97-0194. Albuquerque, NM: Sandia National***
- 24 ***Laboratories.***
- 25 Holt, R.M., and Powers, D.W. 1984. *Geotechnical Activities in the Waste Handling Shaft Waste*
- 26 *Isolation Pilot Plant (WIPP) Project Southeastern New Mexico.* WTSD-TME-038. U.S.
- 27 Department of Energy, Carlsbad, NM.
- 28 Holt, R.M., and Powers, D.W. 1986. *Geotechnical Activities in the Exhaust Shaft.* DOE-WIPP-
- 29 86-008. U.S. Department of Energy, Carlsbad, NM.
- 30 Holt, R.M., and Powers, D.W. 1988. *Facies Variability and Post-Depositional Alteration*
- 31 *Within the Rustler Formation in the Vicinity of the Waste Isolation Pilot Plant, Southeastern*
- 32 *New Mexico.* DOE/WIPP 88-004. U.S. Department of Energy, Carlsbad, NM. (This document
- 33 ~~is included as~~ **CCA** Appendix GCR.)
- 34 Holt, R.M., and Powers, D.W. 1990. *Geologic Mapping of the Air Intake Shaft at the Waste*
- 35 *Isolation Pilot Plant.* DOE/WIPP 90-051. U.S. Department of Energy, Carlsbad, NM.

- 1 **Holt, R.M., and Powers, D.W. 1990b. "Halite Sequences within the Late Permian Salado**
- 2 **Formation in the Vicinity of the Waste Isolation Pilot Plant," in Powers, D.W., Holt, R.M.,**
- 3 **Beauheim, R.L., and Rempe, N., eds., Geological and Hydrological Studies of Evaporites in**
- 4 **the Northern Delaware Basin for the Waste Isolation Pilot Plant (WIPP): Guidebook 14,**
- 5 **Geological Society of America (Dallas Geological Society), pp. 45-78.**
- 6 **Holt, R.M., and Powers, D.W. 2002. "Impact of Salt Dissolution on the Transmissivity of the**
- 7 **Culebra Dolomite Member or the Rustler Formation, Delaware Basin, Southeastern New**
- 8 **Mexico" Abstracts with Program, v. 34, no. 6, p. 215.**
- 9 **Holt, R.M. and Yarbrough, L. 2002. Analysis Report Task 2 of AP-088 – Estimating Base**
- 10 **Transmissivity Field. Sandia National Laboratories, WIPP Records Center. ERMS #523889.**
- 11 **WIPP Records Center.**
- 12 Howard, K.A., Aaron, J.M., Brabb, E.E., Brock, M.R., Gower, H.D., Hunt, S.J., Milton, D.J.,
- 13 Muehlberger, W.R., Nakata, J.K., Plafker, G., Prowell, D.C., Wallace, R.E., and Witkind, I.J.
- 14 1971 [reprinted 1991]. *Preliminary Map of Young Faults in the United States as a Guide to*
- 15 *Possible Fault Activity.* Miscellaneous Field Studies Map MF-916, 1:5,000,000. 4 maps on
- 16 2 sheets. U.S. Geological Survey, Denver, CO.
- 17 **Hubbert, M.K. 1940. "The Theory of Ground-Water Motion," The Journal of Geology. Vol.**
- 18 **48, no. 8, pt. 1., pp. 785 - 944.**
- 19 Hunter, R.L. 1985. *A Regional Water Balance for the Waste Isolation Pilot Plant (WIPP) Site*
- 20 *and Surrounding Area.* SAND84-2233. Sandia National Laboratories, Albuquerque, NM.
- 21 **INTERA. 1997a. Exhaust Shaft Hydraulic Assessment Data Report. DOE-WIPP 97-2219.**
- 22 **Carlsbad, NM: WIPP Management and Operating Contractor.**
- 23 **INTERA. 1997b. Exhaust Shaft Data Report: 72-Hour Pumping Test on C-2506 and 24-**
- 24 **Hour Pumping Test on C-2505. Carlsbad, NM: Waste Isolation Pilot Plant.**
- 25 **IT Corporation. 2000. Addendum 1, Waste Isolation Pilot Plant RCRA Background**
- 26 **Groundwater Quality Baseline Update Report. Prepared for Westinghouse Electric**
- 27 **Corporation, Carlsbad, NM.**
- 28 Izett, G.A., and Wilcox, R.E. 1982. *Map Showing Localities and Inferred Distribution of the*
- 29 *Huckleberry Ridge, Mesa Falls, and Lava Creek Ash Beds in the Western United States and*
- 30 *Southern Canada.* Misc. Investigations Map I-1325, scale 1:4,000,000. U.S. Geological Survey.
- 31 Jarolimek, L., Timmer, M.J., and McKinney, R.F. 1983. *Geotechnical Activities in the*
- 32 *Exploratory Shaft—Selection of the Facility Interval, Waste Isolation Pilot Plant (WIPP)*
- 33 *Project, Southeastern New Mexico.* TME 3178. U.S. Department of Energy, Albuquerque, NM.
- 34 Jones, C.L., Bowles, C.G., and Bell, K.G. 1960. *Experimental Drillhole Logging in Potash*
- 35 *Deposits of the Carlsbad District, New Mexico.* Open-File Report. U.S. Geological Survey,
- 36 Denver, CO.

- 1 Jones, C.L., Cooley, M.E., and Bachman, G.O. 1973. *Salt Deposits of Los Medaños Area, Eddy*
2 *and Lea Counties, New Mexico*. Open-File Report 4339-7. U.S. Geological Survey, Denver,
3 CO.
- 4 Jones, C.L. 1978. *Test Drilling for Potash Resources: Waste Isolation Pilot Plant Site, Eddy*
5 *County, New Mexico*. Open-File Report 78-592. Vols. 1 and 2. U.S. Geological Survey,
6 Denver, CO.
- 7 Jones, C.L. 1981. *Geologic Data for Borehole ERDA-6, Eddy County, New Mexico*. Open-File
8 Report 81-468. U.S. Geological Survey, Denver, CO.
- 9 Jones, T.L., Kelley, V.A., Pickens, J.T., Upton, D.T., Beauheim, R.L., and Davies, P.B. 1992.
10 *Integration of Interpretation Results of Tracer Tests Performed in the Culebra Dolomite at the*
11 *Waste Isolation Pilot Plant Site*. SAND92-1579. Sandia National Laboratories, Albuquerque,
12 NM.
- 13 Keesey, J. J. 1976. *Hydrocarbon Evaluation, Proposed Southeastern New Mexico Radioactive*
14 *Material Storage Site, Eddy County, New Mexico*. SAND71-7033. Vols. I and II. Sipes,
15 Williamson, and Aycock, Midland, TX.
- 16 ***Kehrman, R.F. 2002. Compliance Recertification Application Monitoring Data, Volume***
17 ***Two. Carlsbad, NM: Westinghouse TRU Solutions LLC. Copy on file in the Sandia WIPP***
18 ***Records Center under ERMS# 527193.***
- 19 Kelley, V.A. 1971. *Geology of the Pecos Country, Southeastern New Mexico*. Memoir 24.
20 New Mexico Bureau of Mines and Mineral Resources, Socorro, NM.
- 21 Kelley, V.A., and Saulnier, Jr., G.J. 1990. *Core Analyses for Selected Samples from the Culebra*
22 *Dolomite at the Waste Isolation Pilot Plant Site*. SAND90-7011. Sandia National Laboratories,
23 Albuquerque, NM.
- 24 King, P.B. 1948. *Geology of the Southern Guadalupe Mountains, Texas*. Professional Paper
25 215. U.S. Geological Survey, Washington, D.C.
- 26 ***Krumhansl, J.L., Kimball, K.M. and Stein, C.L. 1991. Intergranular Fluid Compositions***
27 ***from the Waste Isolation Pilot Plant (WIPP), Southeastern New Mexico. SAND90-0584.***
28 ***Albuquerque, NM: Sandia National Laboratories.***
- 29 Lambert, S.J. 1983a. *Dissolution of Evaporites in and around the Delaware Basin,*
30 *Southeastern New Mexico and West Texas*. SAND82-0461. Sandia National Laboratories,
31 Albuquerque, NM.
- 32 Lambert, S.J. 1983b. "Evaporite Dissolution Relevant to the WIPP Site, Northern Delaware
33 Basin, Southeastern New Mexico." In *Scientific Basis for Nuclear Waste Management VI,*
34 *Materials Research Society Symposia Proceedings, Boston, MA, November 1-4, 1982, SAND82-*
35 *1416C. D.G. Brookins, ed., pp. 291 - 298. Elsevier Science Publishing Company, New York,*
36 *NY.*

- 1 Lambert, S.J. 1987. *Feasibility Study: Applicability of Geochronologic Methods Involving*
2 *Radiocarbon and other Nuclides to the Groundwater Hydrogeology of the Rustler Formation,*
3 *Southeastern New Mexico.* SAND86-1054. Sandia National Laboratories, Albuquerque, NM.
- 4 ***Lambert, S.J. 1991. "Isotopic Constraints on the Rustler and Dewey Lake Groundwater***
5 ***Systems," in Siegel, M.D., Lambert, S.J., and Robinson, K.L., eds. Hydrogeochemical Studies***
6 ***of the Rustler Formation and Related Rocks in the Waste Isolation Pilot Plant Area,***
7 ***Southeastern New Mexico. SAND88-0196. Sandia National Laboratories, Albuquerque, NM.***
- 8 Lambert, S.J., and Carter, J.A. 1987. *Uranium-Isotope Systematics in Groundwaters of the*
9 *Rustler Formation, Northern Delaware Basin, Southeastern New Mexico. I. Principles and*
10 *Preliminary Results.* SAND87-0388. Sandia National Laboratories, Albuquerque, NM.
- 11 Lambert, S.J., and Harvey, D.M. 1987. *Stable-Isotope Geochemistry of Groundwaters in the*
12 *Delaware Basin of Southeastern New Mexico.* SAND87-0138. Sandia National Laboratories,
13 Albuquerque, NM.
- 14 ***Lang, W.B. 1935. "Upper Permian Formation of Delaware Basin of Texas and New***
15 ***Mexico." American Association of Petroleum Geologists Bulletin, Vol. 19, pp. 262 - 276.***
- 16 Lang, W.B. 1939. Salado Formation of the Permian Basin. *American Association of Petroleum*
17 *Geologists Bulletin, Vol. 23, pp. 1569 - 1572.*
- 18 Lang, W.B. 1942. Basal Beds of Salado Formation in Fletcher Potash Core Test near Carlsbad,
19 New Mexico. *American Association of Petroleum Geologists Bulletin, Vol. 26.*
- 20 ***Lang, W.B. 1947. "Occurrence of Comanche Rocks in Black River Valley, New Mexico,"***
21 ***American Association of Petroleum Geologists Bulletin, Vol. 31, pp. 1472 - 1478.***
- 22 ***Lappin, A.R., Hunter, R.L., Garber, D.P., and Davies, P.B., eds, 1989. Systems Analysis, Long***
23 ***-Term Radionuclide Transport, and Dose Assessments, Waste Isolation Pilot Plant (WIPP),***
24 ***Southeastern New Mexico; March 1989. SAND89-0462. Sandia National Laboratories,***
25 ***Albuquerque, NM.***
- 26 LaVenue, A.M., Haug, A., and Kelley, V.A. 1988. *Numerical Simulation of Ground-Water*
27 *Flow in the Culebra Dolomite at the Waste Isolation Pilot Plant (WIPP) Site: Second Interim*
28 *Report.* SAND88-7002. Sandia National Laboratories, Albuquerque, NM.
- 29 ***LaVenue, A.M., Cauffman, T.L., and Pickens, J.F. 1990. Ground-Water Flow Modeling of***
30 ***the Culebra Dolomite. Volume 1: Model Calibration. SAND89-7068/1. Sandia National***
31 ***Laboratories, Albuquerque, NM.***
- 32 ***Lee, W.T. 1925. "Erosion by Solution and Fill." In Contributions to Geography in the***
33 ***United States: USGS Bulletin, 760-C.***
- 34 Lord, K.J., and Reynolds, W.E., eds. 1985. *Archaeological Investigations of Three Sites within*
35 *the WIPP Core Area.* Prepared for the U.S. Army Corps of Engineers (COE), Albuquerque
36 District in NM. Eddy County, NM, Chambers Consultants and Planner, Albuquerque, NM.

- 1 Lowenstein, T.K. 1987. *Post Burial Alternation of the Permian Rustler Formation Evaporites,*
2 *WIPP Site, New Mexico: Textural Stratigraphic and Chemical Evidence.* EEG-36, New Mexico
3 Health and Environment Department, Santa Fe, New Mexico.
- 4 Lowenstein, T.K. 1988. "Origin of Depositional Cycles in a Permian Saline Giant: The Salado
5 (McNutt Zone) Evaporites of New Mexico and Texas." *Geological Society of America Bulletin,*
6 Vol. 100, No. 4, pp. 20 - 21, 592 - 608.
- 7 Lucas, S.G., and Anderson, O.J. 1993a. "Triassic Stratigraphy in Southeastern New Mexico and
8 Southwestern Texas." In *Carlsbad Region, New Mexico and West Texas, New Mexico*
9 *Geological Society, Forty-Fourth Annual Field Conference, Carlsbad, NM, October 6-9, 1993.*
10 D.W. Love et al., eds., pp. 231 - 235. New Mexico Geological Society, Socorro, NM.
- 11 Lucas, S.G., and Anderson, O.J. 1993b. "Stratigraphy of the Permian-Triassic Boundary in
12 Southeastern New Mexico and West Texas." In *Geology of the Carlsbad Region, New Mexico*
13 *and West Texas,* D.W. Love et al., eds., Forty-Fourth Annual Field Conference Guidebook. New
14 Mexico Geological Society, Socorro, NM.
- 15 Machette, M.N. 1985. "Calcic Soils of the Southwestern United States." In *Soils and*
16 *Quaternary Geology of the Southwestern United States,* D.L. Weide and M.L. Faber, eds.,
17 Special Paper Vol. 203, pp. 1 - 21. Geological Society of America, Denver, CO.
- 18 Madsen, B.M., and Raup, O.B. 1988. Characteristics of the Boundary between the Castile and
19 Salado Formations near the Western Edge of the Delaware Basin, Southeastern New Mexico.
20 *New Mexico Geology,* Vol. 10, No. 1.
- 21 *Maley, V.C., and Huffington, R.M. 1953. "Cenozoic Fill and Evaporite Solution in the*
22 *Delaware Basin, Texas and New Mexico." Geological Society of America Bulletin, Vol. 64.*
- 23 McGowen, J.H., and Groat, C.G. 1971. *Van Horn Sandstone, West Texas: An Alluvial Fan*
24 *Model for Mineral Exploration.* Report of Investigations No. 72. Bureau of Economic Geology,
25 Austin, TX.
- 26 McGuire, R.K. 1976. *FORTTRAN Computer Program for Seismic Risk Analysis.* Open-File
27 Report No. 76-67, pp. 1 - 68. U.S. Geological Survey.
- 28 *Meigs, L.C., and Beauheim, R.L. 2001. "Tracer Tests in a Fractured Dolomite, 1.*
29 *Experimental Design and Observed Tracer Recoveries," Water Resources Research, Vol. 25,*
30 *No. 5, pp. 1113-1128.*
- 31 *Meigs, L.C., Beauheim, R.L., and Jones, T.L. eds. 2000. Interpretation of Tracer Tests*
32 *Performed in the Culebra Dolomite at the Waste Isolation Pilot Plant. SAND97-3109.*
33 *Albuquerque, NM: Sandia National Laboratories.*
- 34 Mercer, J.W. 1983. *Geohydrology of the Proposed Waste Isolation Pilot Plant Site, Los*
35 *Medaños Area, Southeastern New Mexico.* Water Resources Investigation Report 83-4016. U.S.
36 Geological Survey, Albuquerque, NM. (*CCA* Appendix HYDRO.)

- 1 Mercer, J.W., Beauheim, R.L., Snyder, R.P., and Fairer, G.M. 1987. *Basic Data Report for*
2 *Drilling and Hydrologic Testing of Drillhole DOE-2 at the Waste Isolation Pilot Plant (WIPP)*
3 *Site*. SAND86-0611. Sandia National Laboratories, Albuquerque, NM.
- 4 Miller, D.N. 1955. *Petrology of the Pierce Canyon Formation, Delaware Basin, Texas and New*
5 *Mexico* [Ph.D. Dissertation]. University of Texas, Austin.
- 6 Miller, D.N. 1966. Petrology of Pierce Canyon Redbeds, Delaware Basin, Texas and New
7 Mexico. *American Association of Petroleum Geologists Bulletin*, Vol. 80.
- 8 ***Molecke, M.A. 1983. A Comparison of Brines Relevant to Nuclear Waste Experimentation.***
9 ***SAND83-0516. Albuquerque, NM: Sandia National Laboratories.***
- 10 Muehlberger, W.R., Belcher, R.C., and Goetz, L.K. 1978. Quaternary Faulting on Trans-Pecos,
11 Texas. *Geology*, Vol. 6, No. 6, pp. 337 - 340.
- 12 ***Neill, R.H., Channell, J.K., Chaturvedi, L., Little, M.S., Rehfeldt, K., and Spiegler, P. 1983.***
13 ***Evaluation of the Suitability of the WIPP Site. EEG-23. Environmental Evaluation Group,***
14 ***Santa Fe, NM.***
- 15 New Mexico Bureau of Mines and Mineral Resources (***NMBMMR***). 1995. *Final Report*
16 *Evaluation of Mineral Resources at the Waste Isolation Pilot Plant (WIPP) Site*. Vols. 1 to 4.
- 17 Nicholson, Jr., A., and Clebsch, Jr., A. 1961. *Geology and Ground-Water Conditions in*
18 *Southern Lea County, New Mexico*. Ground-Water Report 6. New Mexico Bureau of Mines and
19 Mineral Resources, Socorro, NM.
- 20 Nuttli, O.W. 1973. Design Earthquakes for the Central United States. Miscellaneous Paper S-
21 73-1, pp. 1 - 45. U.S. Army Waterways Experiment Station, Vicksburg, MS.
- 22 ***Olive, W.W. 1957. "Solution-Subsidence Troughs, Castile Formation of Gypsum Plain,***
23 ***Texas and New Mexico." Geological Society of America Bulletin, Vol. 68.***
- 24 ***O'Neill, J.R., Johnson, C.M., White, L.D., and Roedder, E. 1986. "The Origin of Fluid in the***
25 ***Salt Beds of the Delaware Basin, New Mexico and Texas," Applied Geochemistry, v. 1, pp.***
26 ***265-271.***
- 27 Palmer, A.R. 1983. "The Decade of North American Geology 1983 Geologic Time Scale."
28 *Geology*, Vol. 11, No. 9, pp. 503 -504.
- 29 Piper, A.M. 1973. *Subrosion in and about the Four-Township Study Area near Carlsbad, New*
30 *Mexico*. Report to Oak Ridge National Laboratories, Oak Ridge, TN.
- 31 Piper, A.M. 1974. *The Four-Township Study Area near Carlsbad, New Mexico: Vulnerability*
32 *to Future Subrosion*. Report to Oak Ridge National Laboratories, Oak Ridge, TN.
- 33 Popielak, R.S., Beauheim, R.L., Black, S.B., Coons, W.E., Ellingson, C.T., and Olsen, R.L.
34 1983. *Brine Reservoirs in the Castile Formation, Waste Isolation Pilot Plant (WIPP), Project*

- 1 *Southeastern New Mexico*. TME-3153. ~~Vols. 1 and 2.~~ Westinghouse Electric Corporation,
2 Carlsbad, NM.
- 3 *Powers, D.W. 1997. Geology of Piezometer Holes to Investigate Shallow Water Sources*
4 *under the Waste Isolation Pilot Plant, in INTERA, 1997, Exhaust Shaft Hydraulic Assessment*
5 *Data Report, DOE/WIPP 97-2219. Carlsbad, NM: US DOE*
- 6 *Powers, D.W. 2002a. Analysis Report for Task 1 of AP-088 – Construction of Geologic*
7 *Contour Maps: ERMS #522086. Carlsbad, NM: Sandia National Laboratories, WIPP Records*
8 *Center.*
- 9 *Powers, D.W. 2002b. “Addendum to Analysis Report Task 1 of AP-088 Construction of*
10 *Geologic Contour Maps.” ERMS #523886. Carlsbad, NM: Sandia National Laboratories,*
11 *WIPP Records Center.*
- 12 *Powers, D.W. 2002c. Basic Data Report for Drillhole C-2737 (Waste Isolation Pilot Plant –*
13 *WIPP): DOE/WIPP 01-3210. Carlsbad, NM: US DOE.*
- 14 *Powers, D.W. 2003a. Addendum 2 to Analysis Reports Task 1 of AP-088, Construction of*
15 *Geologic Contour Maps. ERMS #525199. Carlsbad, NM: Sandia National Laboratories,*
16 *WIPP Records Center.*
- 17 *Powers, D.W. 2003b. Geohydrological conceptual model for the Dewey Lake Formation in*
18 *the vicinity of the Waste Isolation Pilot Plant (WIPP). Test Plan TP02-05. ERMS# 526493.*
19 *Carlsbad, NM: Sandia National Laboratories, WIPP Records Center.*
- 20 *Powers, D.W., and Hassinger, B.W. 1985. “Synsedimentary Dissolution Pits in Halite of the*
21 *Permian Salado Formation, Southeastern New Mexico,” Journal of Sedimentary Petrology,*
22 *Vol. 55, pp. 769-773.*
- 23 Powers, D.W. and Holt, R. 1990. *Sedimentology of the Rustler Formation Near the Waste*
24 *Isolation Pilot Plant (WIPP) Site.* pp. 77 -106. GSA Field Trip #14. Geological Society of
25 America 1990 Annual Meeting. October 29 - November 1, 1990. Dallas, TX.
- 26 Powers, D.W., and Holt, R.M. 1993. “The Upper Cenozoic Gatuña Formation of Southeastern
27 New Mexico.” In *Carlsbad Region, New Mexico and West Texas, New Mexico Geological*
28 *Society, Forty-Fourth Annual Field Conference, Carlsbad, NM, October 6-9, 1993,* D.W. Love
29 et al., eds., pp. 271-282. New Mexico Geological Society, Roswell, NM.
- 30 Powers, D.W., and Holt, R.M. 1995. *Regional Geological Processes Affecting Rustler*
31 *Hydrogeology.* Prepared for U.S. Department of Energy by IT Corporation, Albuquerque, NM.
- 32 *Powers, D.W., and Holt, R.M. 1999. “The Los Medaños Member of the Permian Rustler*
33 *Formation,” New Mexico Geology, Vol. 21, No. 4, pp. 97-103.*
- 34 *Powers, D. W., and R. M. Holt. 2000. “The Salt That Wasn’t There: Mudflat Facies*
35 *Equivalents to Halite of the Permian Rustler Formation, Southeastern New Mexico,” Journal*
36 *of Sedimentary Research, Vol. 70, No. 1, pp. 29-36.*

- 1 ***Powers, D.W., and Stensrud, W.A. 2003. Basic Data Report for Drillhole C-2811 (Waste***
- 2 ***Isolation Pilot Plant–WIPP). DOE/WIPP 02-3223. Carlsbad, NM: US DOE.***
- 3 Powers, D.W., Lambert, S.J., Shaffer, S.E., Hill, L.R., and Weart, W.D., eds. 1978. *Geological*
- 4 *Characterization Report for the Waste Isolation Pilot Plant (WIPP) Site, Southeastern New*
- 5 *Mexico.* SAND78-1596, Vols. I and II. Sandia National Laboratories, Albuquerque, NM. (This
- 6 document is included as CCA Appendix GCR.)
- 7 Powers, D.W., Sigda, J.M., and Holt, R.M. 1996. “Probability of Intercepting a Pressurized
- 8 Brine Reservoir Under the WIPP.” ***ERMS #523414. Carlsbad, NM: Sandia National***
- 9 ***Laboatories. WIPP Records Center.***
- 10 ***Powers, D.W., Vreeland, R.H., and Rosenzweig, W.D. 2001. How Old are Bacteria from the***
- 11 ***Permian Age? Nature, Vol. 411, pp. 155-156.***
- 12 ***Powers, D.W., Holt, R.M., Beauheim, R.L., and McKenna, S.A. 2003. “Geological Factors***
- 13 ***Related to the Transmissivity of the Culebra Dolomite Member, Permian Rustler Formation,***
- 14 ***Delaware Basin, Southeastern New Mexico,” in Johnson, K.S., and Neal, J.T., eds., Evaporite***
- 15 ***karst and engineering/environmental problems in the United States: Oklahoma Geological***
- 16 ***Survey Circular 109, pp. 211-218.***
- 17 Pratt, H.R., Stephenson, D.E., Zandt, G., Bouchon, M., and Hustrulik, W.A. 1979. Earthquake
- 18 Damage to Underground Facilities. *Proceedings of the 1979 RETC*, Vol. 1. AIME, Littleton,
- 19 CO.
- 20 Ramey, D.S. 1985. *Chemistry of Rustler Fluids.* EEG-31. New Mexico Environmental
- 21 Evaluation Group, Santa Fe, NM.
- 22 Rawson, D., Boardman, C., and Jaffe-Chazan, N. 1965. *The Environment Created by a Nuclear*
- 23 *Explosion in Salt.* PNE-107F. U.S. Atomic Energy Commission Plowshare Program, Project
- 24 Gnome, Carlsbad, NM.
- 25 Register, J.K. 1981. *Rubidium-Strontium and Related Studies of the Salado Formation,*
- 26 *Southeastern New Mexico.* SAND81-7072. Sandia National Laboratories, Albuquerque, NM.
- 27 Register, J.K., and Brookins, D.G. 1980. “Rb-Sr Isochron Age of Evaporite Minerals from the
- 28 Salado Formation (Late Permian), Southeastern New Mexico.” *Isochron/West*, No. 29, pp. 39 -
- 29 42.
- 30 Reiter, M., Barroll, M.W., and Minier, J. 1991. “An Overview of Heat Flow in Southwestern
- 31 United States and Northern Chihuahua, Mexico.” In *Neotectonics of North America*, D.B.
- 32 Slemmons, E.R. Engdahl, M.D. Zoback, and D.D. Blackwell, eds., pp. 457 - 466. Geological
- 33 Society of America, Boulder, CO.
- 34 ***Renne, P.R., Sharp, W.D. and Becker, T.A. 1998. “⁴⁰Ar/³⁹Ar Dating of Langbeinite [K₂Mg₂***
- 35 ***(SO₄)₂] in Late Permian Evaporites of the Salado Formation, Southeastern New Mexico,***
- 36 ***USA,” Mineralogy Magazine, Vol. 62A, pp. 1253-1254***

- 1 ***Renne, P.R., Steiner, M.B., Sharp, W.D., Ludwig, K.R., and Fanning, C.M. 1996. “⁴⁰Ar/³⁹Ar***
- 2 ***and U/Pb SHRIMP Dating of Latest Permian Tephra in the Midland Basin, Texas,” Eos,***
- 3 ***Transactions, American Geophysical Union, Vol. 77, p. 794.***
- 4 Richardson, G.B. 1904. “Report of a Reconnaissance of Trans-Pecos Texas, North of the Texas
- 5 and Pacific Railway.” *Texas University Bulletin* 23. Var Boeckmann-Jones Company, Austin,
- 6 TX.
- 7 Richey, S.F. 1989. *Geologic and Hydrologic Data for the Rustler Formation Near the Waste*
- 8 *Isolation Pilot Plant, Southeastern New Mexico.* Open-File Report 89-32. U.S. Geological
- 9 Survey, Albuquerque, NM.
- 10 Richter, C.F. 1958. *Elementary Seismology.* W.H. Freeman & Co., San Francisco, CA.
- 11 ***Roberts, R.M., Beauheim, R.L., and Domski, P.S. 1999. Hydraulic Testing of Salado***
- 12 ***Formation Evaporites at the Waste Isolation Pilot Plant Site: Final Report. SAND98-2537.***
- 13 ***Sandia National Laboratories, Albuquerque, NM.***
- 14 Robinson, T.W., and Lang, W.B. 1938. “Geology and Ground-Water Conditions of the Pecos
- 15 River Valley in the Vicinity of Laguna Grande de la Sal, New Mexico, with Special Reference to
- 16 the Salt Content of the River Water.” *Twelfth and Thirteenth Biennial Reports of the State*
- 17 *Engineer of New Mexico for the 23rd, 24th, 25th, and 26th Fiscal Years, July 1, 1934 to July 30,*
- 18 *1938.* State Engineer, Santa Fe, NM.
- 19 Robinson, J.Q., and Powers, D.W. 1987. “A Clastic Deposit within the Lower Castile
- 20 Formation, Western Delaware Basin, New Mexico.” In *Geology of the Western Delaware Basin,*
- 21 *West Texas and Southeastern New Mexico,* D.W. Powers, and W.C. James, eds., El Paso
- 22 Geological Society Guidebook 18, pp. 66 -79. El Paso Geological Society, El Paso, TX.
- 23 ***Roedder, E. 1984. “The Fluids in Salt,” American Mineralogist, v. 69, pp. 413-439.***
- 24 Rogers, A.M., and Malkiel, A. 1979. A Study of Earthquakes in the Permian Basin of Texas–
- 25 New Mexico. *Bulletin of the Seismological Society of America,* Vol. 69, pp. 843 - 865.
- 26 Rosholt, J.N., and McKinney, C.R. 1980. *Uranium Series Disequilibrium Investigations*
- 27 *Related to the WIPP Site, New Mexico (USA), Part II. Uranium Trend Dating of Surficial*
- 28 *Deposits and Gypsum Spring Deposits Near WIPP Site, New Mexico.* Open-File Report 80-879.
- 29 U.S. Geological Survey, Denver, CO.
- 30 ***Salvador, A. 1985. “Chronostratigraphic and Geochronometric Scales in Colorado SUNA***
- 31 ***Stratigraphic Correlation Charts of the United States.” American Association of Petroleum***
- 32 ***Geologists Bulletin, Vol. 69.***
- 33 ***Sandia National Laboratories. 2000. “Sandia National Laboratories Annual Compliance***
- 34 ***Monitoring Parameter Assessment, WBS 1.3.5.2.1.1, Pkg. No. 510062.” ERMS #512733.***
- 35 ***Carlsbad, NM: Sandia National Laboratories, WIPP Records Center.***

- 1 *Sandia National Laboratories. 2001. "Sandia National Laboratories Annual Compliance*
- 2 *Monitoring Parameter Assessment, WBS 1.3.5.3.1, Pkg. No. 510062, October 2001." ERMS*
- 3 *#519620. Carlsbad, NM: Sandia National Laboratories, WIPP Records Center.*
- 4 *Sandia National Laboratories. 2002. "Sandia National Laboratories Annual Compliance*
- 5 *Monitoring Parameter Assessment for 2002, WBS 1.3.5.3.1, Pkg. No. 510062, November*
- 6 *2002." ERMS #524449. Carlsbad, NM: Sandia National Laboratories, WIPP Records Center.*
- 7 *Sandia National Laboratories. 2003a. "Sandia National Laboratories Technical Baseline*
- 8 *Reports, WBS 1.3.5.3, Compliance Monitoring; WBS 1.3.5.4, Repository Investigations,*
- 9 *Milestone RI 03-210, January 31, 2003." ERMS #526049. Carlsbad, NM: Sandia National*
- 10 *Laboratories, WIPP Records Center.*
- 11 *Sandia National Laboratories. 2003b. "Program Plan, WIPP Integrated Groundwater*
- 12 *Hydrology Program, FY03-FY09, Revision 0, March 14, 2003." ERMS #526671. Carlsbad,*
- 13 *NM: Sandia National Laboratories, WIPP Records Center.*
- 14 Sanford, A.R., Jaksha, L.H., and Cash, D.J. 1991. "Seismicity of the Rio Grand Rift in New
- 15 Mexico." In *Neotectonics of North America*, D.B. Slemmons, E.R. Engdahl, M.D. Zoback, and
- 16 D.D. Blackwell, eds., pp. 229 - 244. Geological Society of America, Boulder, CO.
- 17 ~~Saulnier, Jr., G.J., and Avis, J.D. 1988. *Interpretation of Hydraulic Tests Conducted in the*~~
- 18 ~~*Waste Handling Shaft at the Waste Isolation Pilot Plant (WIPP) Site. SAND88-7001. Sandia*~~
- 19 ~~*National Laboratories, Albuquerque, NM. WPO 24164.*~~
- 20 *Satterfield, C.L., Lowenstein, T.K., Vreeland, R, and Rosenzweig, W. 2002. "The Search for*
- 21 *Microorganisms in Brine Inclusions in Halite: an Update," Abstracts with Programs,*
- 22 *Geological Society of America, Annual Meeting, v. 34, no. 6, p. 19.*
- 23 Schiel, K.A. 1988. "The Dewey Lake Formation: End Stage Deposit of a Peripheral Foreland
- 24 Basin." Master's thesis. University of Texas at El Paso, El Paso, TX.
- 25 Schiel, K.A. 1994. "A New Look at the Age, Depositional Environment and Paleogeographic
- 26 Setting of the Dewey Lake Formation (Late Permian)." *West Texas Geological Society Bulletin*,
- 27 Vol. 33, No. 9, pp. 5 - 13.
- 28 *Sergent, Hauskins & Beckwith, 1979. *Subsurface Exploration & Laboratory Testing. Plant**
- 29 *Site: Waste Isolation Pilot Plant. Vols I & II. Phoenix, AZ: Sergent, Hauskins & Beckwith*
- 30 *(Copy on file at the U.S. Department of Energy, WIPP Information Center, Carlsbad, NM).*
- 31 Sowards, T., Williams, M.L., and Keil, K. 1991. *Mineralogy of the Culebra Dolomite Member*
- 32 *of the Rustler Formation. SAND90-7008. Sandia National Laboratories, Albuquerque, NM.*
- 33 Siegel, M.D., Lambert, S.J., and Robinson, K.L., eds. 1991. *Hydrogeochemical Studies of the*
- 34 *Rustler Formation and Related Rocks in the Waste Isolation Pilot Plant Area, Southeastern New*
- 35 *Mexico. SAND88-0196. Sandia National Laboratories, Albuquerque, NM.*

- 1 ***Silva, M.K. 1996. Fluid Injection for Salt Water Disposal and Enhanced Oil Recovery as a***
- 2 ***Potential Problem for WIPP: Proceedings of a June 1995 Workshop and Analysis. EEG-62.***
- 3 ***Albuquerque, NM: Environmental Evaluation Group.***
- 4 Snider, H.I. 1966. "Stratigraphy and Associated Tectonics of the Upper Permian Castile-
- 5 Salado-Rustler Evaporite Complex, Delaware Basin, West Texas and Southeast New Mexico."
- 6 Ph.D. dissertation. University of New Mexico, Albuquerque, NM.
- 7 Snyder, R.P. 1985. *Dissolution of Halite and Gypsum, and Hydration of Anhydrite to Gypsum,*
- 8 *Rustler Formation, in the Vicinity of the Waste Isolation Pilot Plant, Southeastern New Mexico.*
- 9 Open-File Report 85-229. U.S. Geological Survey, Denver, CO.
- 10 Snyder, R.P., Gard, Jr., L.M., and Mercer, J.W. 1982. *Evaluation of Breccia Pipes in*
- 11 *Southeastern New Mexico and Their Relation to the Waste Isolation Pilot Plant (WIPP) Site,*
- 12 *with Section on Drill-Stem Tests.* Open-File Report 82-968. U.S. Geological Survey, Denver,
- 13 CO.
- 14 ***Stein, C.L., and Krumhansl, J.L. 1988. "A Model for the Evolution of Brines in Salt from the***
- 15 ***Lower Salado Formation, Southeastern New Mexico," Geochimica et Cosmochimica Acta, v.***
- 16 ***52, pp. 1037-1046.***
- 17 ~~Stensrud, W.A. 1995. *Culebra Transport Program Test Plan: Hydraulic Tests at Wells WQSP-*~~
- 18 ~~*1, WQSP 2, WQSP 3, WQSP 4, WQSP 5, WQSP 6 and WQSP 6a at the Waste Isolation Pilot*~~
- 19 ~~*Plant (WIPP) Site. On file in the Sandia WIPP Central Files.*~~
- 20 Swift, P.N. 1992. *Long-Term Climate Variability at the Waste Isolation Pilot Plant,*
- 21 *Southeastern New Mexico, USA.* SAND91-7055. Sandia National Laboratories, Albuquerque,
- 22 NM. (This document is included as CCA Appendix CLI.)
- 23 ***TerraTek, Inc. 1996. "Physical Property Characterization of Miscellaneous Rock Samples,***
- 24 ***Contract AA-2896." Contractor Report TR97-03 to Sandia National Laboratories. ERMS***
- 25 ***#238234. Salt Lake City, UT.***
- 26 Thompson, G.A. and Zoback, M.L. 1979. Regional Geophysics of the Colorado Plateau.
- 27 *Tectonophysics*, Vol. 61, Nos. 1 - 3, pp. 149 - 181.
- 28 ***Tóth, J., 1963. "A Theoretical Analysis of Groundwater Flow in Small Drainage Basins,"***
- 29 ***Journal of Geophysical Research. Vol. 68, No. 16, pp. 4795 - 4812.***
- 30 UNM (University of New Mexico). 1984. *A Handbook of Rare and Endemic Plants of New*
- 31 *Mexico.* New Mexico Native Plants Protection Advisory Committee, eds. University of New
- 32 Mexico Press, Albuquerque, NM.
- 33 ***Urry, W.E. 1936. Post-Keweenawan Timescale. Exhibit 2, pp. 35 - 40. National Research***
- 34 ***Council, Report Committee on Measurement of Geologic Time 1935 -36.***
- 35 U.S. Congress. 1992. *Waste Isolation Pilot Plant Land Withdrawal Act.* Public Law 102-579,
- 36 October 1992. 102nd Congress, Washington, D.C.

- 1 ~~U.S. Department of Commerce. 1980. *Census of Population, General Population*~~
2 ~~*Characteristics of New Mexico.* Bureau of the Census.~~
- 3 ***U.S. Census Bureau. 2000. Census 2000 at <http://www.census.gov/main/www/access.html>.***
- 4 U.S. Department of Commerce. 1990. *Census of Population, General Population*
5 *Characteristics of New Mexico.* Bureau of the Census.
- 6 U.S. Department of Energy (DOE). 1980. *Final Environmental Impact Statement, Waste*
7 *Isolation Pilot Plant.* DOE/EIS-0026, Vols. 1 and 2. Office of Environmental Restoration and
8 Waste Management, Washington, D.C.
- 9 ***U.S. Department of Energy (DOE). 1983. Summary of the Results of the Evaluation of the***
10 ***WIPP Site and Preliminary Design Validation Program. WIPP-DOE-161. Carlsbad, NM:***
11 ***Waste Isolation Pilot Plant.***
- 12 ***U.S. Department of Energy (DOE). 1996. Title 40 CFR Part 191 Compliance Certification***
13 ***Application for the Waste Isolation Pilot Plant, DOE/CAO-1996-2184, October 1996, Carlsbad***
14 ***Field Office, Carlsbad, NM.***
- 15 ***U.S. Department of Energy (DOE). 1999. Exhaust Shaft: Phase III Hydraulic Assessment***
16 ***Data Report, October 1997 — October 1998. DOE-WIPP 99-2302. Carlsbad, NM: Waste***
17 ***Isolation Pilot Plant.***
- 18 ***U.S. Department of Energy (DOE). 2002a. Delaware Basin Monitoring Annual Report.***
19 ***DOE/WIPP-99-2308, Rev. 03. Carlsbad, NM: Department of Energy.***
- 20 ***U.S. Department of Energy (DOE). 2002b. Geotechnical Analysis Report for July 2000 -June***
21 ***2001. DOE/WIPP 02-3177, Vol. 1. Carlsbad, NM: Department of Energy.***
- 22 ***U.S. Department of Energy (DOE). 2003. Strategic Plan for Groundwater Monitoring at the***
23 ***Waste Isolation Pilot Plant. DOE/WIPP-03-3220, United States Department of Energy.***
24 ***Carlsbad, NM: February 2003.***
- 25 U.S. Environmental Protection Agency (EPA). 1988. “40 CFR Parts 124, 144, 146, and 148
26 Underground Injection Control Program: Hazardous Waste Disposal Injection Restrictions;
27 Amendments to Technical Requirements for Class 1 Hazardous Waste Injection Wells, and
28 Additional Monitoring Requirements Applicable to All Class 1 Wells.” *Federal Register*,
29 Vol. 53, 28188, July 26, 1988.
- 30 U.S. Environmental Protection Agency (EPA). 1993. 40 CFR Part 191 Environmental
31 Radiation Protection Standards for the Management and Disposal of Spent Nuclear Fuel, High-
32 Level and Transuranic Radioactive Wastes; Final Rule. *Federal Register*, Vol. 58, No. 242, pp.
33 66398 - 66416, December 20, 1993. Office of Radiation and Indoor Air, Washington, D.C.
- 34 U.S. Environmental Protection Agency (EPA). 1996. *40 CFR Part 194: Criteria for the*
35 *Certification and Re-Certification of the Waste Isolation Pilot Plant’s Compliance with the*
36 *40 CFR Part 191 Disposal Regulations; Final Rule. Federal Register*, Vol. 61, No. 28,

- 1 pp. 5224 - 5245, February 9, 1996. Office of Air and Radiation, Washington, D.C. In NWM
2 Library as KF70.A35.C751.
- 3 U.S. Environmental Protection Agency (EPA). 1996. Docket A-93-02, Item II-I-01, Enclosure
4 1, Letter from EPA to DOE, December 19, 1996 technical issues raised by EPA.
- 5 U.S. Nuclear Regulatory Commission (**NRC**). 1973. Design Spectra for Seismic Design of
6 Nuclear Power Plants, Revision 1. *Regulatory Guide* 1.60, December 1973.
- 7 Vine, J.D. 1963. "Surface Geology of the Nash Draw Quadrangle, Eddy County, New Mexico."
8 *U.S. Geological Survey Bulletin 1141-B*. U.S. Government Printing Office, Washington, DC.
- 9 ***Washington Regulatory & Environmental Services (WRES). 2003. Waste Isolation Pilot Plant***
10 ***Site Environmental Report for Calendar Year 2002, DOE/WIPP 03-2222, Carlsbad, NM.***
- 11 ***Waste Isolation Pilot Plant Management and Operating Contractor (WIPP MOC). 1995.***
12 ***Basic Data Report for WQSP 1, WQSP 2, WQSP 3, WQSP 4, WQSP 5, WQSP 6, WQSP 6a,***
13 ***DOE/WIPP 95-2154. WIPP MOC, Carlsbad, NM.***
- 14 Weart, W.D. 1983. *Summary Evaluation of the Waste Isolation Pilot Plant (WIPP) Site*
15 *Suitability*. SAND83-0450. Albuquerque, NM: Sandia National Laboratories.
- 16 Westinghouse Electric Corporation (**WEC**). 1991a. *Waste Isolation Pilot Plant Groundwater*
17 *Monitoring Program Plan and Procedures Manual*. WP02-1. Westinghouse Electric
18 Corporation, Waste Isolation Division, Carlsbad, NM.
- 19 Westinghouse Electric Corporation (**WEC**). 1991b. *Waste Isolation Pilot Plant Site*
20 *Environmental Report for Calendar Year 1990*. DOE/WIPP 91-008. Westinghouse Electric
21 Corporation, Waste Isolation Division, Carlsbad, NM.
- 22 Westinghouse Electric Corporation (**WEC**). 1992. *Waste Isolation Pilot Plant Site*
23 *Environmental Report for Calendar Year 1991*. DOE/WIPP 92-007. Westinghouse Electric
24 Corporation, Waste Isolation Division, Carlsbad, NM.
- 25 Westinghouse Electric Corporation (**WEC**). 1993. *Waste Isolation Pilot Plant Site*
26 *Environmental Report for Calendar Year 1992*. DOE/WIPP 93-017. Westinghouse Electric
27 Corporation, Waste Isolation Division, Carlsbad, NM.
- 28 Westinghouse Electric Corporation (**WEC**). 1994. *Waste Isolation Pilot Plant Site*
29 *Environmental Report for Calendar Year 1993*. DOE/WIPP 94-2003. Westinghouse Electric
30 Corporation, Waste Isolation Division, Carlsbad, NM.
- 31 Westinghouse Electric Corporation (**WEC**). 1995. *Waste Isolation Pilot Plant Site*
32 *Environmental Report for Calendar Year 1994*. DOE/WIPP 95-Draft-2094. Westinghouse
33 Electric Corporation, Waste Isolation Division, Carlsbad, NM.

- 1 *Westinghouse Electric Corporation (WEC). 1996. Waste Isolation Pilot Plant Site*
2 *Environmental Report for Calendar Year 1995, DOE/WIPP 96-2182, Westinghouse Electric*
3 *Corporation, Waste Isolation Division, Carlsbad, NM.*
- 4 *Westinghouse Electric Corporation (WEC). 1997. Waste Isolation Pilot Plant Site*
5 *Environmental Report for Calendar Year 1996, DOE/WIPP 97-2225, Westinghouse Electric*
6 *Corporation, Waste Isolation Division, Carlsbad, NM.*
- 7 *Westinghouse Electric Corporation (WEC). 1998. Waste Isolation Pilot Plant Site*
8 *Environmental Report for Calendar Year 1997, DOE/WIPP 98-2225, Westinghouse Electric*
9 *Corporation, Waste Isolation Division, Carlsbad, NM.*
- 10 *Westinghouse Government Environmental Services Company (WGESC), LLC. 1999. Waste*
11 *Isolation Pilot Plant Site Environmental Report for Calendar Year 1998, DOE/WIPP 99-2225,*
12 *Westinghouse Electric Corporation, Waste Isolation Division, Carlsbad, NM.*
- 13 Wolfe, H.G., et al., eds. 1977. *An Environmental Baseline Study of the Los Medaños Waste*
14 *Isolation Pilot Plant (WIPP) Project Area of New Mexico: A Progress Report.* SAND77-7017.
15 Sandia National Laboratories, Albuquerque, NM.
- 16 Wood, B.J., Snow, R.E., Cosler, D.J., and Haji-Djafari, S. 1982. *Delaware Mountain Group*
17 *(DMG) Hydrology—Salt Removal Potential, Waste Isolation Pilot Plant (WIPP) Project,*
18 *Southeastern New Mexico.* TME 3166. U.S. Department of Energy, Albuquerque, NM.
- 19 Zoback, M.L., and Zoback, M.D. 1980. “State of Stress in the Conterminous United States.”
20 *Journal of Geophysical Research*, Vol. 85, No. B11, pp. 6113 - 6156.
- 21 Zoback, M.L., Zoback, M.D., Adams, J., Bell, S., Suter, M., Suarez, G., Estabrook, C., and
22 Magee, M. 1991. *Stress Map of North America.* Continent Scale Map CSM-5, Scale
23 1:5,000,000. Geological Society of America, Boulder, CO.
- 24 Zoback, M.D., and Zoback, M.L. 1991. “Tectonic Stress Field of North America and Relative
25 Plate Motions.” In *Neotectonics of North America*, D.B. Slemmons, E.R. Engdahl, M.D.
26 Zoback, and D.D. Blackwell, eds., pp. 339 - 366. Geological Society of America, Boulder, CO.

INDEX

40 CFR Part 191	2-1
accessible environment	2-85, 2-87, 2-115
actinide	
<i>Culebra</i>	2-105
<i>transport</i>	2-105
advection	2-12, 2-45, 2-105, 2-110
analysis	
<i>probabilistic</i>	2-182, 2-186
anhydrite	2-22, 2-24, 2-29, 2-31, 2-32, 2-44, 2-45, 2-48, 2-51, 2-69, 2-74, 2-76, 2-85, 2-92, 2-95, 2-99, 2-102, 2-109, 2-112, 2-115, 2-117, 2-119
anthropogenic	2-120, 2-121, 2-123
archaeology	2-140, 2-145
area	
<i>controlled</i>	2-101, 2-136, 2-143
assurance requirements	2-85
barriers	2-11
<i>engineered</i>	2-2
<i>natural</i>	2-11
Bell Canyon	2-18, 2-21, 2-22, 2-24, 2-25, 2-26, 2-27, 2-71, 2-77, 2-80, 2-85, 2-91, 2-92, 2-93, 2-125
borehole ...	2-2, 2-13, 2-14, 2-15, 2-24, 2-27, 2-35, 2-39, 2-47, 2-56, 2-65, 2-71, 2-73, 2-76, 2-78, 2-80, 2-83, 2-85, 2-91, 2-92, 2-95, 2-117, 2-119, 2-128, 2-135, 2-139
boundary conditions	2-1, 2-110
breccia pipes	2-8, 2-74, 2-77, 2-80, 2-125
brine	2-2, 2-27, 2-31, 2-33, 2-35, 2-73, 2-77, 2-80, 2-85, 2-90, 2-92, 2-93, 2-96, 2-98, 2-101, 2-128, 2-133, 2-135
<i>aquifer</i>	2-33, 2-77, 2-126, 2-128
brine reservoirs	2-7, 2-28, 2-74, 2-91, 2-92, 2-93, 2-95
<i>volume</i>	2-92
calcite	2-28, 2-31
calibrate	2-115
Capitan Limestone	2-22, 2-24, 2-29, 2-59, 2-71, 2-73, 2-78, 2-80, 2-85, 2-92, 2-123, 2-131
carbonates	2-11, 2-21, 2-36, 2-39, 2-123
Castile	2-22, 2-24, 2-27, 2-28, 2-29, 2-31, 2-58, 2-71, 2-73, 2-74, 2-76, 2-77, 2-80, 2-85, 2-88, 2-90, 2-91, 2-92, 2-93, 2-95, 2-96, 2-98, 2-125, 2-135
Cenozoic	2-50, 2-63, 2-68, 2-80
Central Basin Platform	2-17, 2-63, 2-69, 2-180, 2-183, 2-184, 2-186
channeling	2-33, 2-51, 2-97
Cherry Canyon	2-22
climate	2-99, 2-110, 2-135, 2-162
colloid	2-105
Compliance Certification Application (CCA)	2-2, 2-10, 2-11, 2-12, 2-13, 2-17, 2-18, 2-21, 2-22, 2-24, 2-27, 2-28, 2-29, 2-31, 2-32, 2-33, 2-35, 2-39, 2-42, 2-44, 2-45, 2-47, 2-48, 2-50, 2-57, 2-58, 2-63, 2-69, 2-71, 2-73, 2-76, 2-78, 2-80, 2-85, 2-88, 2-89, 2-91, 2-93, 2-95, 2-97, 2-99, 2-101, 2-103, 2-105, 2-106, 2-107, 2-110, 2-111, 2-112, 2-114, 2-115, 2-116, 2-117,

1	2-119, 2-120, 2-125, 2-126, 2-127, 2-128, 2-133, 2-135, 2-136, 2-139, 2-140, 2-145, 2-147,	
2	2-160, 2-180, 2-182, 2-183, 2-186	
3	computational model.....	2-2, 2-12
4	conceptual model.....	2-1, 2-11, 2-12, 2-17, 2-28, 2-36, 2-44, 2-58, 2-78, 2-85, 2-93, 2-98, 2-101,
5	2-102, 2-103, 2-110, 2-116, 2-117, 2-126	
6	consequence analysis.....	2-58
7	controlled area.....	2-101, 2-136, 2-143
8	creep closure.....	2-36
9	Cretaceous.....	2-67
10	Culebra ..	2-11, 2-13, 2-16, 2-18, 2-33, 2-36, 2-42, 2-44, 2-45, 2-46, 2-47, 2-48, 2-66, 2-67, 2-68,
11	2-74, 2-81, 2-85, 2-87, 2-88, 2-90, 2-101, 2-102, 2-103, 2-105, 2-106, 2-108, 2-112, 2-116,	
12	2-119, 2-120, 2-140	
13	model.....	2-103, 2-115
14	cuttings	2-48
15	data	
16	quality	2-13
17	deformation	2-7, 2-11, 2-24, 2-27, 2-29, 2-32, 2-45, 2-51, 2-59, 2-65, 2-71, 2-74, 2-76, 2-92
18	Delaware Basin	2-11, 2-14, 2-21, 2-22, 2-24, 2-27, 2-28, 2-29, 2-31, 2-32, 2-35, 2-36, 2-63,
19	2-65, 2-69, 2-71, 2-76, 2-80, 2-85, 2-86, 2-87, 2-95, 2-98, 2-123, 2-125, 2-136, 2-139, 2-140,	
20	2-147	
21	Delaware Mountain Group.....	2-18, 2-22
22	demographics	2-134, 2-140
23	Devonian.....	2-21
24	Dewey Lake	2-51, 2-52, 2-53, 2-55, 2-58, 2-66, 2-68, 2-69, 2-71, 2-85, 2-87, 2-88, 2-89, 2-90,
25	2-91, 2-99, 2-119, 2-120, 2-121, 2-122, 2-123	
26	diapirism.....	2-7
27	diffusion.....	2-45, 2-104
28	dike.....	2-35, 2-69, 2-72
29	discharge.....	2-9, 2-89, 2-92, 2-99, 2-102, 2-105, 2-111, 2-128, 2-131
30	disposal system	
31	performance	2-11, 2-36, 2-58, 2-112
32	dissolution..	2-8, 2-9, 2-10, 2-11, 2-14, 2-24, 2-27, 2-29, 2-32, 2-34, 2-39, 2-44, 2-48, 2-50, 2-59,
33	2-62, 2-63, 2-69, 2-71, 2-74, 2-76, 2-78, 2-80, 2-90, 2-99, 2-102, 2-107, 2-114, 2-123, 2-125,	
34	2-126, 2-135	
35	disturbed rock zone (DRZ).....	2-2, 2-73, 2-87, 2-96, 2-98
36	Dockum Group.....	2-53, 2-66
37	double porosity	2-12
38	drainage.....	2-55, 2-59, 2-62, 2-83, 2-89, 2-99, 2-128, 2-133
39	drilling .	2-12, 2-13, 2-21, 2-24, 2-44, 2-48, 2-53, 2-55, 2-69, 2-73, 2-74, 2-77, 2-85, 2-96, 2-107,
40	2-123, 2-126, 2-134, 2-138, 2-143, 2-146	
41	engineered	
42	barriers	2-2
43	erosion	2-9, 2-10, 2-14, 2-17, 2-51, 2-57, 2-58, 2-59, 2-62, 2-63, 2-66, 2-81, 2-91, 2-107
44	exposure pathways	2-159
45	facility design.....	2-2, 2-55
46	fault.....	2-7, 2-24, 2-63, 2-73, 2-147, 2-164, 2-180, 2-181

1	<i>fauna</i>	2-10, 2-51, 2-160
2	<i>features, events, and processes (FEPs)</i>	2-1, 2-7, 2-13, 2-58, 2-136
3	<i>natural</i>	2-2, 2-7, 2-13
4	<i>fluvial</i>	2-9, 2-39, 2-51, 2-55, 2-160
5	<i>Forty-niner</i>	2-36, 2-39, 2-50, 2-88, 2-117
6	<i>fractures</i>	2-7, 2-28, 2-32, 2-42, 2-45, 2-46, 2-51, 2-66, 2-77, 2-92, 2-97, 2-101, 2-104, 2-114,
7	2-119, 2-128	
8	<i>future events</i>	2-182
9	<i>Gatuña</i>	2-50, 2-56, 2-59, 2-68, 2-71, 2-80, 2-160
10	<i>glaciation</i>	2-10, 2-160
11	<i>groundwater</i>	2-8, 2-9, 2-24, 2-32, 2-35, 2-45, 2-51, 2-58, 2-78, 2-91, 2-95, 2-99, 2-100, 2-101,
12	2-103, 2-109, 2-115, 2-117, 2-119, 2-120, 2-121, 2-125, 2-126, 2-134, 2-140, 2-159	
13	<i>monitoring</i>	2-85, 2-91, 2-111, 2-115, 2-119, 2-120
14	<i>Guadalupean Series</i>	2-22
15	<i>human intrusion</i>	2-14, 2-83, 2-85
16	<i>hummock</i>	2-57, 2-59
17	<i>hunting</i>	2-143, 2-144
18	<i>hydraulic</i>	
19	<i>potential</i>	2-98
20	<i>hydraulic conductivity</i>	2-87, 2-91, 2-99, 2-102, 2-116, 2-121, 2-123
21	<i>hydraulic gradient</i>	2-91, 2-92, 2-104, 2-112, 2-117, 2-125, 2-126
22	<i>potential</i>	2-99
23	<i>hydrostatic</i>	2-92, 2-98
24	<i>independent review</i>	2-13
25	<i>infiltration</i>	2-9, 2-51, 2-58, 2-83, 2-88, 2-89, 2-112, 2-120, 2-123, 2-125, 2-147
26	<i>interbed</i>	2-29, 2-36, 2-45, 2-97
27	<i>inventory</i>	2-146
28	<i>karst</i>	2-33, 2-59, 2-76, 2-78, 2-80, 2-101
29	<i>Lamar limestone</i>	2-22, 2-24
30	<i>Land Withdrawal Act (LWA)</i>	2-143
31	<i>land withdrawal area</i>	2-143
32	<i>Leonardian Series</i>	2-22
33	<i>lithofacies</i>	2-55
34	<i>Livingston Ridge</i>	2-33, 2-62, 2-143
35	<i>loading</i>	2-63, 2-67, 2-114
36	<i>Los Medaños</i>	2-36, 2-39, 2-44, 2-88, 2-102
37	<i>Magenta</i>	2-11, 2-17, 2-18, 2-36, 2-48, 2-50, 2-85, 2-88, 2-101, 2-111, 2-116, 2-117
38	<i>Malaga Bend</i>	2-99, 2-126, 2-133
39	<i>McNutt Potash Zone</i>	2-29, 2-135
40	<i>Mescalero Caliche</i>	2-55, 2-57, 2-59, 2-160
41	<i>metamorphic</i>	2-8, 2-14
42	<i>Mississippian</i>	2-21
43	<i>Mississippian Limestone</i>	2-21
44	<i>model</i>	
45	<i>computational</i>	2-2, 2-12

1	<i>conceptual</i>	2-1, 2-11, 2-12, 2-17, 2-28, 2-36, 2-44, 2-45, 2-47, 2-58, 2-78, 2-85, 2-93, 2-98,
2		2-101, 2-102, 2-110, 2-116, 2-117, 2-126
3	<i>Culebra</i>	2-103, 2-115
4	<i>numerical</i>	2-101
5	<i>monitoring</i>	2-13, 2-16, 2-17, 2-18, 2-85
6	<i>environmental</i>	2-122, 2-162
7	<i>groundwater</i>	2-91, 2-103, 2-110, 2-115, 2-116, 2-117, 2-119, 2-120
8	<i>mudstone</i>	2-32, 2-33, 2-48, 2-49, 2-102, 2-107, 2-115
9	<i>Nash Draw</i>	2-88, 2-99, 2-116, 2-121, 2-123, 2-126, 2-131, 2-160
10	<i>natural barriers</i>	2-11
11	<i>numerical model</i>	2-101
12	<i>Ochoan</i>	2-21, 2-24, 2-51, 2-63, 2-78
13	<i>Ogallala Formation</i>	2-55, 2-59, 2-62, 2-65, 2-68, 2-69, 2-76, 2-131
14	<i>oil and gas</i>	2-24, 2-69, 2-134, 2-139, 2-143, 2-144
15	<i>Ordovician</i>	2-21, 2-63
16	<i>Paleozoic</i>	2-18, 2-21, 2-63
17	<i>parameter</i> ... 2-1, 2-11, 2-14, 2-18, 2-28, 2-36, 2-44, 2-63, 2-81, 2-97, 2-109, 2-116, 2-117, 2-121,	
18		2-139, 2-182, 2-186
19	<i>value</i>	2-2, 2-47, 2-48, 2-53, 2-93, 2-103, 2-105
20	<i>Pecos River</i>	2-55, 2-59, 2-62, 2-69, 2-83, 2-99, 2-125, 2-126, 2-128, 2-133, 2-144, 2-160
21	<i>Pennsylvanian</i>	2-21, 2-63
22	<i>performance assessment (PA)</i>	2-1, 2-2, 2-11, 2-12, 2-14, 2-36, 2-53, 2-85, 2-88, 2-93, 2-95,
23		2-97, 2-99, 2-101, 2-104, 2-114, 2-136, 2-143
24	<i>permafrost</i>	2-10
25	<i>permeability</i>	2-87
26	<i>Permian</i>	2-21, 2-57
27	<i>Basin</i>	2-63, 2-64, 2-183, 2-184
28	<i>Period</i>	2-35, 2-63
29	<i>plugging</i>	2-139
30	<i>polyhalite</i>	2-29, 2-31, 2-32, 2-35, 2-71
31	<i>possible futures</i>	2-136
32	<i>potash resources</i>	2-12, 2-77
33	<i>Precambrian</i>	2-14, 2-21, 2-69
34	<i>precipitation</i>	2-10, 2-58, 2-83, 2-89, 2-122, 2-131, 2-133, 2-161, 2-162, 2-166
35	<i>pressure</i>	
36	<i>gradient</i>	2-90
37	<i>probabilistic analysis</i>	2-182, 2-183, 2-186
38	<i>probability</i>	2-28, 2-58, 2-63, 2-74, 2-93, 2-123, 2-138, 2-182, 2-186
39	<i>Project Gnome</i>	2-147
40	<i>quality assurance (QA)</i>	2-12
41	<i>Quaternary</i>	2-57, 2-63, 2-69, 2-80
42	<i>ranching</i>	2-144
43	<i>recharge</i>	2-9, 2-78, 2-88, 2-89, 2-99, 2-110, 2-112, 2-119, 2-125
44	<i>records packages</i>	2-13
45	<i>resources</i>	2-2, 2-76, 2-143
46	<i>potash</i>	2-12, 2-77

1	<i>Richter scale</i>	2-164, 2-180
2	<i>risk</i>	2-134, 2-182, 2-183, 2-186
3	<i>Rustler</i>	2-11, 2-28, 2-31, 2-33, 2-36, 2-38, 2-39, 2-41, 2-42, 2-43, 2-44, 2-48, 2-49, 2-50, 2-51,
4		2-53, 2-58, 2-69, 2-71, 2-73, 2-77, 2-78, 2-80, 2-85, 2-87, 2-88, 2-90, 2-99, 2-101, 2-102, 2-
5		103, 2-107, 2-112, 2-119, 2-126, 2-128
6	<i>Salado</i>	2-10, 2-22, 2-24, 2-27, 2-30, 2-31, 2-33, 2-34, 2-35, 2-36, 2-42, 2-44, 2-58, 2-63, 2-71,
7		2-73, 2-74, 2-77, 2-78, 2-80, 2-81, 2-83, 2-85, 2-87, 2-88, 2-89, 2-90, 2-91, 2-92, 2-95, 2-96,
8		2-97, 2-98, 2-99, 2-101, 2-102, 2-107, 2-108, 2-109, 2-112, 2-125, 2-126, 2-128, 2-135, 2-147
9	<i>San Simon Sink</i>	2-77
10	<i>San Simon Swale</i>	2-62
11	<i>Santa Rosa</i>	2-51, 2-54, 2-55, 2-68, 2-69, 2-88, 2-90, 2-99, 2-119, 2-120, 2-121, 2-125
12	<i>scarps</i>	2-59, 2-69
13	<i>scenarios</i>	2-1, 2-85, 2-135
14	<i>seals</i>	2-164
15	<i>seismic</i>	2-7, 2-8, 2-27, 2-63, 2-73, 2-146, 2-164, 2-180, 2-183, 2-186
16	<i>shafts</i>	2-36, 2-48, 2-74, 2-87, 2-107, 2-111, 2-119, 2-120
17	<i>siliciclastic</i>	2-32, 2-39, 2-44
18	<i>siltstone</i>	2-33, 2-48, 2-51, 2-102, 2-115, 2-117, 2-121
19	<i>Silurian</i>	2-21
20	<i>Simpson</i>	2-21
21	<i>site characterization</i>	2-1, 2-11, 2-13, 2-59, 2-120
22	<i>sorption</i>	2-105
23	<i>stratigraphy</i>	2-36, 2-38
24	<i>subsidence</i>	2-7, 2-59, 2-62, 2-63, 2-77, 2-80, 2-102
25	<i>surface</i>	
26	<i>drainage</i>	2-89, 2-128
27	<i>structures</i>	2-13, 2-88, 2-109, 2-120, 2-121, 2-122, 2-123
28	<i>water</i>	2-9, 2-83, 2-89, 2-119, 2-147, 2-159
29	<i>sylvite</i>	2-31, 2-32, 2-35, 2-135, 2-136
30	<i>syndeposition</i>	2-33, 2-35, 2-45, 2-48, 2-51, 2-74, 2-77
31	<i>Tamarisk</i>	2-36, 2-39, 2-47, 2-48, 2-78, 2-88, 2-103, 2-110, 2-115
32	<i>tectonic</i>	2-7, 2-58, 2-68, 2-69, 2-71, 2-78, 2-164, 2-181, 2-183
33	<i>threshold pressure</i>	2-97
34	<i>time-domain electromagnetic (TDEM)</i>	2-93
35	<i>transmissivity</i>	2-12, 2-85, 2-87, 2-88, 2-90, 2-102, 2-114, 2-116, 2-117, 2-119, 2-126
36	<i>Culebra</i>	2-42, 2-103, 2-106, 2-108, 2-116
37	<i>transport</i>	2-10, 2-12, 2-39, 2-45, 2-50, 2-81, 2-87, 2-89, 2-95, 2-103, 2-110, 2-112, 2-115
38	<i>transuranic (TRU) waste</i>	2-80
39	<i>Triassic</i>	2-28, 2-51, 2-53, 2-66, 2-80
40	<i>uncertainty</i>	2-1, 2-42, 2-111, 2-115
41	<i>underground</i>	2-12, 2-164, 2-186
42	<i>facilities</i>	2-87, 2-164, 2-186
43	<i>source of drinking water (USDW)</i>	2-88, 2-140
44	<i>undisturbed performance (UP)</i>	2-83
45	<i>unloading</i>	2-63, 2-67, 2-114
46	<i>unnamed lower member</i>	2-29, 2-36, 2-44, 2-102

1	<i>uplift</i>	2-63, 2-68, 2-69
2	<i>Upper Devonian Woodford Shale</i>	2-21
3	<i>vug</i>	2-44, 2-45, 2-104
4	<i>Wolfcampian Series</i>	2-21
5		